The use of induced pluripotent stem cells (iPSCs) and mesenchymal stem cells (MSCs) to study the genetic basis of human diseases

Thesis submitted in accordance with the requirements

of Chulalongkorn University, Thailand, and

the University of Liverpool, UK,

for the degree of Doctor of Philosophy by

Susama Chokesuwattanaskul, M.D.

Joint Ph.D. Programme in Biomedical Sciences and Biotechnology

(Chulalongkorn University and University of Liverpool)

September 2016

I declare that this thesis entitled:

"**The use of induced pluripotent stem cells (iPSCs) and mesenchymal stem cells (MSCs) to study the genetic basis of human diseases"**

is entirely my own work.

Candidate: **Susama Chokesuwattanaskul, M.D.**

Supervisors: **Professor Steven W. Edwards**

Institutive of Integrative Biology
University of Liverpool, UK

Professor Kanya Suphapeetiporn

Head of Division of Medical Genetics and Metabolism
Department of Paediatrics
Faculty of Medicine
Chulalongkorn University, Thailand

Dr. Helen L. Wright

Institutive of Integrative Biology
University of Liverpool, UK

Co-supervisor: **Assisted Professor Nipan Israsena**

Head of Centre of Stem Cells and Cell Therapies
Faculty of Medicine
Chulalongkorn University, Thailand

Table of contents

Acknowledgements

First of all, I would like to thank my supervisors in Liverpool, Prof. Steven W. Edwards and Dr. Helen L. Wright. I could not expect anything more from you.

Prof. Steve, I would like to thank you for always being there for me and having faith that I would be able to complete this thesis and Ph.D. I could not imagine my Ph.D. without your help and support. You are brilliant.

Helen, I would like to thank you my lovely supervisor. Even though, you were the last to join my supervisor team, you have mentored me long before that. Thank you for always be there whenever I needed your help and advice. Thank you for always supporting me. You are amazing!

Prof. Suthiluk Pathumraj, who inspired me to pursue my Ph.D. study, I would like to thank you that you always had faith that I was going to complete this Ph.D. Thank you for all your support and advice, without which I could not complete this thesis and Ph.D. Prof. Apiwat Mutirangura and Dr. Amornpan Sereemaspun, I would also like to thank you for all your advice and support.

Dr. Steve Hill and Dr. Caroline Dart, thank you very much for being with me for the whole Ph.D., your keen questions always helped me to improve my research project.

I would like to thank Prof. Vorasuk Shotelersuk. Your advice and support are always appreciated. I could not pursue my Ph.D. without you. Thank you very much indeed.

Prof. Kanya Suphapeetiporn and Dr. Nipan Israsena, I would like to thank you for teaching me to be a strong and independent Ph.D. student. You have given me many precious opportunities to learn and grow up as a scientist.

My colleagues and friends at University of Liverpool and Chulalongkorn University, I would like to thank you for all your support and the techniques you have taught me. Without you all, I would not have known how to use the pipette!

Special thanks also to Dr. Marie M. Phelan for her help, support and enthusiasm in teaching me about metabolomics.

I would like to thank you everyone who always love and care for me. Your companionships either academically or leisurely, really contributed to the success of my thesis and Ph.D.

Thank you Chulalongkorn University and the 100th anniversary Chulalogkorn University Fund for Doctoral Scholarship for facilitating my Ph.D. study and to the University of Liverpool for this Joint Ph.D. Programme in Biomedical Sciences and Biotechnology.

Thank you my family, Dr. Payap, Dr. Vacharee, Dr. Ronpichai and Dr. Peerapat Chokesuwattanaskul, for all your love and support. Without you, I could not complete this Ph.D. I know you will be with me whenever I need you. Thank you indeed. Additionally, I would like to thank you my family and relatives. I always appreciate any kind of your love and support.

Abstract

Objectives: The aim of this thesis was to evaluate the potential of new technologies, including two stem cell technologies, mesenchymal stem cells (MSCs) and induced pluripotent stem cells (iPSCs), to understand the molecular basis of human diseases. These technologies were evaluated for their ability to restore diabetes-induced defects in wound tissue repair (MSCs) and to generate mature neutrophils after *in vitro* differentiation of iPSCs. The latter used iPSCs from a patient with abnormal function due to impaired WASp (Wiskott Aldrich syndrome protein) signalling. Other techniques evaluated were differentiation of the myeloid cell line, PLB-985 (expressing exogenous genes) into mature neutrophils and new advances in metabolomics, to identify altered neutrophil function in human diseases.

Methods: The potential of MSCs and oral vitamin C to generate factors that could promote healing of diabetic wounds, was measured by RT-PCR for eight genes associated with either angiogenesis or extracellular matrix production, after incubation under normoglycaemic and hyperglycaemic conditions with and without vitamin C. The angiogenic effects of the MSC secretome on wound healing was measured using a tubular formation assay (*in vitro*) and a nude mice diabetic wound model (*in vivo*). The bilateral full-skin thickness wounds were created in an *in vivo* wound model using diabetic nude mice. Oral vitamin C (1.5 g/L) was administered in combination with topical MSC treatment (MSCs 1x 10^6 cells per wound). Diabetic wound models were divided into five groups; control (CON; n=6), diabetes (DM; n=12), diabetes treated with MSCs (DM+MSCs; n=12), diabetes treated with VitC (DM+VitC; n=6), and diabetes treated with MSCs and VitC (DM+MSCs+VitC; n=12). The capillary density was measured under *in vivo* fluorescent microscopy, and the tissue VEGF levels were measured. WAS dermal fibroblasts were reprogrammed using retrovirus transfection, and the corrected-WAS-iPSCs were differentiated into the neutrophil-like cells *via* the formation of iPS-sacs (the sac-like structure containing haematopoietic progenitor cells derived from iPSCs). Neutrophil (from WAS patients and healthy controls) chemotaxis was measured using transwell migration towards N-formylmethionine-leucyl-phenylalanine (fMLP). PLB-985 and KCL-22 cells were differentiated into neutrophil-like cells using RPMI-1640 media containing N,N-dimethyl formamide, sodium pyruvate, all-trans retinoic acid, human AB serum and dimethyl sulfoxide

(with penicillin/streptomycin). Morphology was assessed by cytospin. PLB-985 cells were transduced with *enhanced green fluorescent protein (EGFP)*-tagged *Myeloid Cell Leukaemia-1 (Mcl-1)*, sub-cloned into a pLVX-TetOne-Puro system. ^{1}H NMR metabolomics was carried out using protocols optimised for neutrophils as part of this thesis. An intracellular metabolite extraction method was developed to minimise the loss of neutrophil metabolites and to avoid contaminants arising during the extraction procedure. The NMR analyses were also optimised to identify neutrophil metabolites and allow the comparison from resting and activated states and in health and disease (rheumatoid arthritis patients).

Results: Upregulation of angiogenic genes, *vascular endothelial growth factor-α (mVEGF-α)* and *platelet-derived growth factor-BB* (*mPDGF-BB*), in response to TGF-β1 in MSCs was lower following incubation under hyperglycemia (compared to normoglycaemic controls), but vitamin C treatment re-sensitised the MSC response to TGF-β1. A diabetic mouse model showed that administration of oral vitamin C, as an adjunct to MSC therapy, resulted in accelerated wound healing that was associated with increased capillary density. Preliminary experiments with WAS neutrophils showed significantly lower rates of chemotaxis towards fMLP compared to healthy controls. iPSCs from WAS fibroblasts were cultured and differentiated into neutrophil-like cells. The efficiency of both PLB-985 and KCL-22 cells to differentiation into neutrophil-like cells was evaluated and PLB-985 cells differentiated more efficiently into neutrophil-like cells than the KCL-22 cells. PLB-985 cells, transfected with *Mcl-1:EGFP* in pLVX-TetOne-Puro system were generated. Nuclear magnetic resonance (NMR) metabolomics identified metabolites and pathways altered during *in vitro* activation with PMA (including metabolites of NADPH synthesis and inhibitors of reactive oxygen species (ROS)) and *in vivo* activation in rheumatoid arthritis identified metabolites of the ketosis pathway, citrullination pathway and tryptophan metabolism.

Conclusions: A number of technologies have been evaluated to study the molecular basis of human disease, including metabolic (diabetes mellitus) and genetic (WAS) diseases. Vitamin C modulated the secretome of MSCs, increasing angiogenesis and accelerating wound healing, providing a potential new approach for designing adjuncts to existing therapies. Neutrophils from WAS patients demonstrated chemotactic defects, and the potential of WAS-iPSCs to differentiate into neutrophil-like cells was

demonstrated. The approach could be applied in further studies to study genetic defects of leukocyte function. PLB-985 cells transduced with *EGFP*-tagged *Mcl-1* in an inducible expression vector, was developed as a cell-line model of neutrophil differentiation, to facilitate further studies into the role of the *Mcl-1* gene in regulating neutrophil survival. Protocols for human neutrophil metabolomics, using ^{1}H NMR spectroscopy were developed and applied to the study of *in vitro* and *in vivo* activated neutrophils. The results demonstrated the potential of metabolomics for future studies of human diseases.

Abstracts and Publications

Publications

Chokesuwattanaskul S et al. (2016) Oral vitamin C accelerates diabetic wound healing *via* increased angiogenic effects on the mesenchymal stem cell secretome. *Under review, Scientific Reports*

Anderson J, Chokesuwattanaskul S et al. (2016) Synovial fluid metabolite profiles in inflammation. *In Preparation*

Chokesuwattanaskul S et al. (2016) Metabolomic analysis of human neutrophils during *in vivo* and *in vitro* inflammation. *In Preparation*

Chokesuwattanaskul S et al. (2016) *ETFDH* mutation in a case of riboflavin responsive multiple acetyl-coA dehydrogenase deficiency at King Chulalongkorn Memorial Hospital. *In preparation*. (Included as a supplementary document)

Abstracts

2016 "Optimising Protocols for NMR Metabolomic Analyses of Human Neutrophils in Health and Disease", a poster presentation at Genomes to Systems (G2S) Theme away day, University of Liverpool, UK.

2016 "Oral vitamin C accelerates diabetic wound healing *via* increased angiogenic effects on the mesenchymal stem cell secretome", a poster presentation at School of Life Sciences poster day, University of Liverpool, UK.

Abbreviations

ACR	American College of Rheumatology
ADA	Adenosine deaminase
ANLL	Acute nonlymphocytic leukaemia
APC	Allophycocyanin
Arp2/3	Actin-related protein 2/3
ATRA	All-trans retinoic acid
Bak	B-cell leukaemia-2 homologous antagonist/killer protein
BAL	Bronchoalveolar lavage
Bcl-2	*B-cell lymphoma 2*
Bcl-X_L	B-cell lymphoma-extra large protein
BH domain	Bcl-2 homology domain
Bim	B-cell leukaemia-2 like protein-11
BM-MSC	Bone marrow-derived mesenchymal stem cell
Cas9	CRISPR-associated protein-9 nuclease
CD	Cluster of differentiation
cDNA	Complementary DNA
CGD	Chronic granulomatous disease
CON	Control
CRISPR	Clustered Regularly Interspaced Short Palindromic Repeats

CRP	C-reactive protein
CV	Capillary vascularity
% CV	Percentage of capillary vascularity
DAG	Diacylglycerol
DM	Diabetes mellitus
DMEM	Dulbecco's Modified Eagle Medium
DMF	N,N-dimethyl formamide
DMSO	Dimethyl sulfoxide
DNA	Deoxyribonucleic acid
Dox	Doxycyclin
DSB	Double-strand break
EB	Embryoid body
ECG	Electrocardiogram
EDTA	Ethylenediaminetetraacetic acid
EGFP	Enhanced green fluorescent protein
ESC	Embryonic stem cell
EULAR	European League Against Rheumatism
FACS	Fluorescence activated cell sorting
FBS	Fetal bovine serum
FcγR	Fcγ receptor
FITC	Fluoresceinisothiocyanate

fMLP	formyl-Met-Leu-Phe, N-formylmethionine-leucyl-phenylalanine
G-CSF	Granulocyte colony-stimulating factor
GM-CSF	Granulocyte Macrophage colony-stimulating factor
GDM	Gestational diabetes mellitus
GLUT	Glucose transporter
GOI	Gene of interest
GWAS	Genome-Wide Association Study
HEK	Human embryonic kidney
HR	Homologous recombination
HSC	Haematopoietic stem cell
HUVEC	Human umbilical vein endothelial cell
HyperCM	Conditioned media derived from MSCs cultured under hyperglycaemia
IA	Non-RA inflammatory arthritis
ICAM-1	Intercellular adhesion molecule 1
IL-8	Interleukin 8
IMDM	Iscove's modified Dulbecco's medium
Ins 1,4,5-P3	Inositol 1,4,5-triphosphate
iPSC	induced pluripotent stem cell
iPSC-Neu	induced pluripotent stem cell-derived neutrophil
iPS-sac	induced pluripotent stem cell–derived sac

JAM	Junctional adhesion molecule
JIA	Juvenile idiopathic arthritis
kDa	kilo Dalton
LAD	Leukocyte adhesion deficiency
LB	Luria-Bertani
LFA-1	Lymphocyte function-associated antigen 1
LPS	Lipopolysaccharide
LTB_4	Leukotriene B4
M	Molarity
mAB	Mouse antibody
MAC-1	Macrophage-1 antigen
MADCAM-1	Mucosal vascular addressin cell adhesion molecule 1
mANGPT-1	*Mus musculus Angiopoietin 1*
Mcl-1	*Myeloid cell leukaemia 1*
MEM	Minimum essential medium
mFN-1	*Mus musculus Fibronectin 1*
mGADPH	*Mus musculus Glyceraldehyde-3-phosphate dehydrogenase*
mHGF-1	*Mus musculus Hepatocyte growth factor 1*
mIGF-1	*Mus musculus Insulin-like growth factor 1*
MOI	Multiplicity of infection
mPDGF-BB	*Mus musculus Platelet-derived growth factor BB*

MRI	Magnetic resonance imaging
MSC	Mesenchymal stem cell
mSDF-1	*Mus musculus Stromal cell-derived factor 1*
MTG	α-Monothioglycerol
mTNC	*Mus musculus Tenascin C*
mVEGF-α	*Mus musculus Vascular endothelial growth factor α*
NAD+	Nicotinamide adenine dinucleotide (oxidised)
NADH	Nicotinamide adenine dinucleotide (reduced)
NADP+	Nicotinamide adenine dinucleotide phosphate (oxidised)
NADPH	Nicotinamide adenine dinucleotide phosphate (reduced)
NBT	Nitroblue tetrazolium
NET	Neutrophil extracellular trap
NETosis	Neutrophil extracellular trap formation
NHEJ	Non-homologous end joining
NMR	Nuclear magnetic resonance
NormoCM	Conditioned media derived from MSCs cultured under normoglycaemia
NS	Number of scans
OGTT	Oral glucose tolerance test
OKSM	*OCT4*, *KLF4*, *SOX2*, and *cMYC* transcription factors
PAD4	Protein arginine deiminase 4

PBMC	Peripheral blood mononuclear cell
PCA	Principal component analysis
PECAM-1	Platelet endothelial cell adhesion molecule 1
PerCP	Peridinin Chlorophyll Protein Complex
PEST	Proline (P), Glutamic acid (E), Serine (S), and Threonine (T)
PHOX	Phagocyte oxidase
PI	Propidium iodide
PIP_2	Phosphatidylinositol 4,5-bisphosphate
PKC	Protein kinase C
PLC	Phospholipase C
PMA	Phorbol-12-miristate-13-acetate
PMN	Polymorphonuclear
pVSV-G	Vesicular stomatitis virus-G envelope protein
RIPA	Radio-immuno-precipitation assay buffer
RNA	Ribonucleic acid
ROS	Reactive oxygen species
RT-PCR	Reverse transcription-polymerase chain reaction
SCID	Severe combined immunodeficiency
SD	Standard deviation
SF	Synovial fluid
SLE	Systemic Lupus Erythematosus

SOC	Super optimal broth with catabolite repression
SSN	Site specific nuclease
TALENs	Transcription activator-like effector nucleases
TCA	Tricarboxylic acid
TGF-β1	Transforming growth factor beta 1
TNF	Tumor necrosis factor
TSP/TMSP	Trimethylsilylpropanoic acid
VCAM-1	Vascular cell adhesion molecule 1
VEGF	Vascular endothelial growth factor
VLA-4	Very late antigen 4
WAS	Wiskott-Aldrich syndrome
WAS-iPSC	Wiskott-Aldrich syndrome-induced pluripotent stem cell
WASp	Wiskott-Aldrich syndrome protein
WC	Wound closure
% WC	Percentage of wound closure
WHO	World Health Organisation
XLN	X-linked neutropaenia
ZFNs	Zinc finger nucleases

CHAPTER 1 INTRODUCTION

Scope of this thesis

This thesis sets out to evaluate the usefulness of a number of emerging new technologies to understand or correct the molecular basis of human diseases. Recent technological developments in stem cells and –omics based technologies have provided unprecedented insights in the fine structure and detailed composition of human cells and tissues, and how these become dysregulated or mutated in human disease. Many of these also have therapeutic or diagnostic potential. For example, stem cell technologies can be successfully used to treat degenerative diseases or promote tissue repair, and some of these approaches, using autologous stem cells, have the potential to correct for human conditions that arise from inherited genetic defects. Many –omics-based technologies can also be used to obtain detailed molecular "fingerprints" of human cells and tissues to identify particular genes, transcripts or metabolites that may be altered in disease. Such changes can often be used diagnostically, and the sensitivity of such techniques is now sufficient to profile individual patients and inform specific therapeutic strategies, *via* "personalised" or "precision" medicine approaches.

This thesis first explores the potential of two stem cell technologies to understand the molecular basis of human conditions. The first of these is the use of mesenchymal stem cells (MSCs), which have the potential to differentiate into a variety of cell types, including osteoblasts, chondrocytes and myocytes, but these cells can also secrete important growth factors and angiogenic molecules. Chapter 3 of this thesis explores the potential of MSCs to promote wound healing in an animal model of diabetes mellitus. A second stem cell technology was also evaluated for its ability to generate a mature blood cell, the neutrophil. This approach, using induced pluripotent stem cells derived from fibroblasts (iPSCs), has the advantage in that it can, potentially, be used to correct genetic diseases. Identification and correction of the genetic lesion in stem cells, should in theory, enable the generation of mature, differentiated cells with a corrected phenotype. In Chapter 4, preliminary experiments are described in which iPSCs from a patient with impaired signalling *via* WASp (which results in impairments in neutrophil function) were isolated, the genetic defect corrected and differentiated into cells that morphologically resembled mature

neutrophils. These preliminary experiments provide "proof of principle" that this approach can be used to generate functionally-mature blood cells during *in vitro* differentiation.

Another approach that is commonly-used to explore the function of human genes and proteins is to transfect mature tissues or cells with exogenous genes to probe the function of that gene (or mutations thereof) with the ultimate aim of *in vivo* manipulation of that gene. However, cells such as mature human neutrophils are notoriously difficult to transfect with exogenous genes or proteins because they do not divide and have a very short half life. One approach to overcome these problems, is to use immature myeloid cell lines that can be transfected and then induced to differentiate *in vitro*. However, many of these cell lines lead to the differentiation of cells with only some of the properties of mature neutrophils: hence they can at best be termed "neutrophil-like" cells. Another major problem with this approach is that as the cultured cells mature into neutrophils, they undergo spontaneous apoptosis, making their experimental usefulness rather limited. Chapter 4 describes experiments in which the human *Mcl-1* gene (which is the major cell survival gene in human neutrophils) was cloned into a lentiviral vector for the generation of transfectants of PLB-985 cells. Recently-modified culture conditions result in the generation of mature PLB-985 cells which morphologically resemble neutrophils, in particular possession of a "late stage" differentiation marker; a multi-lobed nucleus.

Finally, this thesis explores the potential of a new –omics technology, namely nuclear magnetic resonance (NMR) metabolomics, to profile the metabolome of human neutrophils stimulated *in vitro* with a number of activating agents. The experiments in Chapter 5 describe the optimisation of this new technology for human neutrophil studies and also some preliminary experiments on the analysis of the metabolites present in diseased synovial fluid or in neutrophils isolated from the blood of patients with rheumatoid arthritis. The results of this Chapter confirm the usefulness of this technique to profile the metabolomes of neutrophils activated *in vitro* but also its potential to identify metabolic changes that may occur in disease.

1.1 New approaches to understanding and correcting human diseases

1.1.1 The study of human diseases

1.1.1.1 Clinical studies

The diagnosis of a human disease requires a clinical examination and evaluation of a patient's signs and symptoms, and is based initially on the physical examination and patient history. These physical examinations usually prompt the physician to request a range of suitable diagnostic laboratory tests (e.g. assays of blood or urinary metabolites or antibodies) or physical procedures (e.g. ECG, MRI scan, X-ray) to confirm diagnosis and prompt interventions, such as prescription of medicines. An appropriate response of a patient to a particular medicine may also help to confirm diagnosis.

1.1.1.1.1 Clinical studies: Current approaches and their limitations

Understanding the underlying genetic, environmental or metabolic defect that is responsible for the symptoms of the disease usually requires more detailed investigative procedures. For example: haematological disorders may require specific measurements or assays on isolated blood or marrow samples; solid cancers may require measurements on biopsy or resected materials; inflammatory disorders may require measurements on cells or fluids isolated from the inflamed sites (e.g. lung or synovial joints). Sometimes, tissue materials from these disease sites can be cultured *ex vivo*, for short times in the case of blood cells or for longer times if the isolated cell retains its proliferative potential, as a result of either *in vitro* or *in vivo* transformation. Such approaches have resulted in the generation of a vast range of human (and animal) cell lines that can be used in *in vitro* experiments to "model" the disease from which the cell or tissue was isolated and to understand the genetic or biochemical defects responsible for the disease phenotype. It is also possible to use such cell lines in drug screening programmes to identify potential new therapeutic agents prior to consideration of their development for clinical use as new drugs.

1.1.1.2 Use of *ex vivo* cells or cell lines

These approaches have led to great advances in our understanding of human disease and have provided a platform for drug discovery programmes, many of which have found their way into clinics to successfully treat human diseases (e.g. the tyrosine kinase inhibitors, typified by imatinib to treat chronic myeloid leukaemia). Such approaches have many advantages. For example: (a) the cell lines can be shared amongst researchers across the globe so that multiple groups can work on the same biological materials; (b) there are few ethical issues to consider when working on such cell lines, that have been derived from isolated somatic cells, either *via* blood samples, biopsy or surgery; (c) toxic effects of exploratory medicines are not problematic and indeed cell lines are highly suited for high throughput screening assays; (d) specific genes or sets of genes may be "knocked in", "knocked out" or mutated, and their effects on the disease phenotype measured, again, with few ethical issues to consider.

1.1.1.2.1 Use of *ex vivo* cells or cell lines: Current approaches and their limitations

However, a disadvantage of the use of such cell lines is that they can lose their particular disease phenotype or properties the longer they are cultured after isolation from the patient or donor. If they change their properties (which they inevitably do) then their usefulness as disease models may be compromised. Another disadvantage is that these cells could never be re-introduced into a patient to correct the disease. Also, there is a limit to their usefulness in toxicology studies because it is not possible to extrapolate the effects of a particular concentration of drug on an isolated, homogenous cell population, to the effects of that concentration of a particular molecule on "off target" cells or tissues or after the molecule has undergone biochemical modification in the body.

Another consideration of using *ex vivo* cells or tissues from a diseased patient, is that some cells cannot be cultured and do not replicate in the laboratory. For example, human neutrophils are terminally-differentiated cells that have lost their proliferative properties and have a short half life *ex vivo* of a few hours, even in the presence of survival-enhancing cytokines. Because of this short half life and lack of proliferation, genetic manipulation of human neutrophils is not possible. There are a

few reports describing the introduction of exogenous proteins, genes or antisense molecules into human neutrophils, but such approaches are highly variable, lack reproducibility and are not without criticisms of the experimental validity (1). One approach to genetically modifying neutrophils is to use myeloid cell lines that can proliferate *in vitro*, but that can also be induced to terminally differentiate e.g. following genetic manipulation. Such myeloid cell lines include those isolated from the blood or peritoneal fluid of patients with haematological disorders (such as HL-60, U-937 and PLB-985 cells). These cell lines (discussed in more detail in Chapter 5) proliferate *in vitro* and can be genetically modified to express *EGFP*-tagged genes or mutated genes. The addition of specific agents can induce differentiation into more mature cells, but is questionable if these differentiated "neutrophil-like" cells acquire all of the properties of mature blood neutrophils (2,3). Furthermore, neutrophil-like cells will undergo apoptosis (4) and therefore there is a finite time in which to study the properties of these differentiated cells.

1.1.1.3 Animal models

To overcome many of these above limitations in the use of *ex vivo* cells from patients with particular diseases or human cell lines, a number of model systems have been studied. These include animal, insect, non-vertebrate or microbial models. For toxicology testing of new pharmaceuticals, cell lines have very limited use (see above) and whole animal testing is required to determine "off target" effects or effects on development. Many species can be used for such studies, but with varying degrees of suitability. Ultimately, toxicological testing on humans is the only definitive method of determining toxic effects of new drugs, although genetic diversity can result in varying responses of individual humans to particular drugs. This diversity forms the basis of new "precision medicine" approaches to find the right drug for the right patient. Toxicological testing of new medicines on primates is also of value, but this approach is highly legislated and very controversial.

1.1.1.3.1 Animal models: Current approaches and their limitations

There are many advantages to the use of animal models to understand the genetic and molecular basis of human disease, ranging from the use of insects (e.g. *Drosophila*), worms (e.g. *Caenorhabditis elegans)*, yeast (e.g. *Saccharomyces*

cerevisiae) and fish (e.g. zebrafish, *Danio rerio*). The use of such model systems has led to many landmark discoveries and several Nobel prizes, for example identification of genes regulating apoptosis (*Bcl-2* and *caspase* family genes in *C. elegans* (5)), development (e.g. homeobox genes in *Drosophila* (6,7)) and cell cycle genes (in yeast (8)). A major advantage to the use of such model systems is the relative ease with which specific genes can be mutated, "knocked out", "knocked in" or "humanised". New technologies based around Clustered Regularly Interspaced Short Palindromic Repeats/CRISPR-associated protein-9 nuclease (CRISPR/cas9) allow for very subtle, specific and rapid gene editing (9). Mutations can be animal-wide or conditional, such that only specific cells or tissues carry the genetic change.

An additional advantage to the use of animal models is that human diseases or conditions can be experimentally induced and the underlying mechanisms explored or therapeutically manipulated. For example: the MRL*/lpr* mouse strain spontaneously develops lupus-like symptoms (10); adjuvants or serum transfer can induce inflammatory joint disease in rodents (11) and diabetes mellitus can be induced in animals by the administration of streptozotocin which destroys pancreatic β-cell (12) (see Chapter 3). The ability to induce such human-like diseases, coupled with the ability to genetically modify specific genes and administer new therapeutic agents, has again led to many major advances in human biology and understanding and treatment of human diseases.

There are a number of disadvantages, however, in the use of such animal models. Firstly, experiments with mice or other vertebrates requires specialised, highly-regulated animal facilities that are expensive to maintain to the appropriate legal requirements within different countries. Consequently, such experiments (which require appropriate project- and personal-licenses) are usually performed in dedicated, specialised animal handling units. Secondly, there are a number of ethical issues to consider in such animal experiments, and much interest in approaches that minimise the use of animals in such experiments and decrease the pain and suffering that an animal experiences in these studies. Finally, there is an emerging debate developing on the appropriateness of some animal models to study human diseases. For example, many experimental approaches assume that genetic manipulations in mice are accurate representations of human gene function. However, there is a growing acceptance that

many genes, particularly those of the immune system, have sufficient structural and functional differences in mice and humans (13). Therefore, it may not always be possible to extrapolate observations of mouse experiments to human processes and disease.

1.2 Stem cells and their use in human diseases

Technologies based on the use of stem cells offer great potential to both understand and then correct for specific genetic or cellular defects that underpin human diseases. Stem cells can be derived from many sources, including embryonic stem cells, mesenchymal stem cells and induced pluripotent stem cells. Each of these has particular advantages and disadvantages, and there a number of ethical and technical issues to consider before such technologies will become routinely used to treat human diseases. Among the stem cell technologies, mesenchymal stem cell (MSC) and induced pluripotent stem cell (iPSC) have been used in this thesis and so these systems will be described here in detail. These two technologies have particular advantages. First, they can be derived from adult cells (e.g. bone marrow for MSCs or fibroblasts for iPSCs) thus overcoming some of the moral issues that have been raised with the use of embryonic stem cells. Second, they can be derived from patients with particular diseases. Such stem cells can be analysed *in vitro* to identify any genetic defect, and this genetic defect can often be corrected *in vitro*. The use of CRISPR-cas9 technology can now provide relatively rapid and highly-selective changes in the genome of stem cells to correct such genetic defects (14). This approach therefore has the potential to re-introduce genetically-corrected stem cells back into the same patients to generate new cells that have the correct function. Such an approach is particularly attractive to genetic diseases that involve blood cells. The aberrant cells and their progenitors can be eliminated by radiotherapy or chemotherapy, and then the bone marrow restored with corrected stem cells.

1.3 Mesenchymal Stem Cells (MSCs)

1.3.1 Background

Mesenchymal stem cells (MSCs) are multipotent stem cells, originally derived from bone marrow (15). MSCs were first defined as a subset of fibroblast-like cells from the bone marrow stroma that can generate bone, fat cells, cartilage and reticular cells following bone marrow transplantation. Since then, MSCs have been discovered in the stromal fraction of many adult tissues, including adipose tissue and skin. However, there is no equivocal identification of MSCs from different tissues. In practice, MSCs are defined by their ability to differentiate into osteoblasts, adipocytes and chondrocytes, with self-renewal capacity. Some studies have reported the ability of these cells to differentiate into multiple other cell types, including cells of both of mesodermal (for example, hepatocytes (16)) and non-mesodermal origins (for example, endothelial cells (17), neural cells (18)).

1.3.2 MSC characterisation

Currently, no unique surface marker unequivocally distinguishes MSCs from other cells. Therefore, the International Society for Cell Therapy has established the minimum criteria to characterise MSCs (19). First, MSCs must adhere to a plastic dish in standard culture conditions. Second, the cells must express the surface molecules CD105, CD73 and CD90, in the absence of CD45, CD34, CD14, CD11b, CD79a or CD19 and HLA-DR surface molecules. Third, MSCs must be able to differentiate into osteoblasts, adipocytes and chondroblasts *in vitro*.

1.3.3 Limitations and Concerns

There is great heterogeneity in MSCs depending on the tissue from which they were derived. For example, the single-cell derived clones of MSCs from human umbilical cord display varying degrees of *in vitro* multi-differentiation (20) and proliferative capacities (21). The *in vivo* localisation and identification of MSCs in tissues are largely unknown due to the low frequency of these cells in tissues, and the lack of a distinct MSC-specific immune-phenotype to enable their identification and isolation. Therefore, in order to compare the properties of MSCs, including their therapeutic potential, their biological properties must be thoroughly characterised.

1.4 Induced Pluripotent Stem Cells (iPSCs)

1.4.1 Background

Induced pluripotent stem cell (iPSC), a newly-developed stem cell technology, provides a promising new model system to study the molecular biology of cellular development (such as neutrophil development) and to probe the mechanisms of genetic diseases.

iPSCs were discovered in 2008 (22). These stem cells are derived by re-programming adult, somatic cells into a pluripotent stem cell state, or embryonic stem cell-like state. Embryonic stem cells (ESCs) are derived from the inner cell mass of a blastocyst (a human embryo 4-5 days after fertilisation), which is an early-stage pre-implantation embryo. Therefore, ESCs have the potential to be maintained indefinitely in their undifferentiated state, while sustaining their capability to differentiate into cells of three germ layers, including haematopoietic cells. One limitation, however, is that their genetic background is unique to the donor and this must be considered if they are to be used to treat a recipient with a different genetic background with a specific disease. In addition to the ethical considerations of using human embryonic materials, this genetic diversity (and possible genetic incompatibility) is a major consideration that limits their applications as either a disease model or a therapeutic option (23).

iPSCs have the equivalent capability of ESCs to differentiate into three germ layers while still possessing the potential to be expanded in culture indefinitely. These cells offer many new possibilities for studying the genetics of human disease processes (24). Additionally, as they can be derived, for example from the skin of patients with a particular genetic disease, they may be genetically-corrected and re-introduced back into the donor patient. This circumvents many of the ethical issues and technical constraints (e.g. tissue rejection) associated with the use of embryonic stem cells.

1.4.2 iPSC as a disease model e.g. in genetic diseases

iPSCs contain the patient's own genetic background and possess full stem cell capacities (24). Therefore, the major advantages of iPSC technology result from the opportunity to generate disease- or patient-specific iPSCs through the reprogramming of somatic cells from patients with specific diseases. However, major considerations

for the use of iPSCs as disease models include the development of effective methods for differentiating iPSCs into mature somatic cells, and ensuring that the properties of iPSC-derived cells match those of mature tissue cells. Furthermore, while both genetic and environmental factors may contribute to disease mechanisms, only genetic factors can be effectively manipulated when iPSCs are used as a disease model.

1.4.3 Limitations and Concerns

As iPSCs are obtained through reprogramming adult somatic cells with pluripotent transcription factors, the epigenetic traits from the cell of origin are somehow retained (25,26). This could result in an obstacle for the iPSCs to differentiate towards the required cell lineage. Moreover, the differentiation of iPSCs towards mature somatic cells requires a mimicking of natural development in humans, therefore, the efficiency of the differentiation protocols and the functions of the resulting differentiated cells require proper evaluation.

1.5 Diabetes Mellitus (DM)

Diabetes mellitus (DM) is a chronic metabolic condition characterised by hyperglycaemia (high blood glucose) resulting from either insulin resistance (inability of cells to effectively respond to insulin) and/or insufficient pancreatic insulin production (27). Diabetes mellitus can be classified into four categories: type 1 DM; type 2 DM; gestational DM (GDM); and DM due to other specified causes. However, all patients with diabetes mellitus share common clinical characteristics of chronic hyperglycaemia that is responsible for increasing the risks of long-term microvascular and macrovascular complications. In the general population, type 1 DM (due to pancreatic β-cell destruction) and type 2 DM (due to insulin resistance and insufficient pancreatic insulin production) are the most common, and hence will be discussed in more detail in this thesis.

1.5.1 Epidemiology

In 2015, 415 million people worldwide were reported to have a form of diabetes mellitus (approx. 4 million in Thailand and approx. 3 million in the UK) (28). It has been estimated that by 2040, approx. 642 million adults worldwide will have diabetes mellitus. In the UK, men aged 35 - 54 (8.4% of men) are almost twice as likely to have diabetes mellitus compared to females (4.8% of women) (29). Over the last decade in the UK, the incidence of diabetes mellitus in men aged 35 - 54 has risen faster compared to women in the same age group. These statistics are consistent with the fact that more men are overweight than women. Among these forms of the disease, type 2 DM is responsible for the majority (approx. 90%) of cases, the major risk factors of which are related to obesity and physically inactive lifestyles.

1.5.2 Diagnosis

Patients are usually diagnosed with diabetes mellitus when their blood glucose is abnormally high, with or without any symptoms of hyperglycaemia (for example, polyuria, polydipsia, and excessive weight loss) or hyperglycaemic complications (including acute and chronic complications). The diagnostic criteria for diabetes mellitus proposed by the WHO recommendation (2006) (30) are shown in Table 1.1.

Table 1.1: Diagnosis of diabetes mellitus by World Health Organisation (WHO) (2006)

Diagnostic criteria for diabetes mellitus (WHO 2006)
1. Diabetes mellitus symptoms (e.g. polyuria, polydipsia and unexplained weight loss for Type 1) plus:
- A randomly-sampled venous plasma glucose concentration ≥ 11.1 mmol/L or
- A fasting plasma glucose concentration ≥ 7.0 mmol/L (whole blood ≥ 6.1 mmol/L) or
- A plasma glucose concentration ≥ 11.1 mmol/L, measured 2 h after ingestion of 75 g anhydrous glucose in an oral glucose tolerance test (OGTT)
2. When no symptoms are evident, diagnosis should not be based on a single glucose determination but requires confirmatory venous plasma measurements. At least one **additional glucose test result on another day** with a value in the diabetic range is essential, either fasting, from a random sample or from the 2 h post-glucose load. If the fasting random values are not diagnostic, the 2 h value post-glucose test should be used.

1.5.3 Clinical manifestations

Clinical presentation may vary in the different categories of diabetes mellitus, and also at the time of presentation. However, symptoms include: polyuria (frequent urination); polydipsia (feeling very thirsty); polyphagia (feeling very hungry); extreme fatigue; blurry vision; impaired wound healing; excessive weight loss (type 1), and numbness in the extremities (type 2).

1.5.4 Pathophysiology

In type 1 DM, autoimmunity is generally considered as the major underlying pathophysiology. The β-cells of the islets of Langerhans in the pancreas are destroyed, and so insulin production is inadequate to maintain normal blood glucose levels (31).

Type 2 DM is a metabolic disturbance, comprised of insulin resistance, impaired insulin secretion, and inappropriate glucagon secretion (32). Patients with type 2 DM usually have accompanying metabolic conditions, including lipid dysfunction, obesity and high blood pressure.

1.5.5 Laboratory Findings

The high values of blood glucose levels seen in diabetes mellitus are described in Table 1.1. Either fasting or random blood glucose concentrations are routinely measured in diabetes mellitus. However, for monitoring and controlling long-term blood glucose levels, the glycated proteins, including haemoglobin A1c (HbA1c) and fructosamine, are measured to indicate cumulative blood glucose levels. HbA1c is a glycosylated form of haemoglobin, formed from haemoglobin and glucose, and is used to estimate an average measurement of blood glucose levels during the previous 2 - 3 months. HbA1c is widely used in clinical assays as an indicator for monitoring and controlling blood glucose levels. Fructosamine, formed from glucose and an amine group on proteins, is another glycated protein used for monitoring and controlling blood glucose levels, but is less commonly used.

Moreover, there are numerous other laboratory findings are used to either detect or follow-up the possible diabetic complications that may occur, including damage to kidneys, retina, and other cardiovascular problems.

1.5.6 Treatment

Current clinical care and management of diabetes mellitus includes lifestyle modifications (diet and exercise) and medical interventions aimed at preventing and controlling hyperglycaemia (33). When blood glucose levels of diabetic patients are controlled such that they remain in the normal range, the risks for developing either short-term or long-term complications are markedly decreased. Medications are aimed

at lowering blood glucose levels. Oral hypoglycemic drugs normally involve either mechanisms that result in insulin sensitisation or increased insulin secretion (insulin secretogogues). Otherwise, exogenous insulin is injected to control blood glucose levels to control the most severe forms of diabetes mellitus (usually type 1).

There are also treatments for some of the complications that arise as a consequence of diabetes mellitus. However, for some diabetic complications, and diabetic wound in particulars, there are no specific treatments (see Chapter 3).

1.5.7 Prognosis

Currently, there is no cure for either type 1 or type 2 DM. Therefore, diabetes mellitus is still a chronic disease for which life-long medications are usually needed. The major goal for management of the disease is to control blood glucose levels to those within the normal range, as morbidity and mortality, and microvascular and macrovascular complications in particular, are associated with the persistently high blood glucose levels in uncontrolled disease. Cardiovascular complications remain the major cause of death in diabetic patients (34).

1.5.8 Complications

In general, diabetic complications are classified as microvascular (neuropathy, retinopathy and nephropathy) and macrovascular complications (coronary artery disease, peripheral artery disease and stroke) (33). Prolonged hyperglycaemic conditions disturb the physiologic conditions of the vessels through different mechanisms, including the pathologic effects of advanced glycation end product accumulation, impaired vasodilatory response attributable to nitric oxide inhibition, smooth muscle cell dysfunction, overproduction of endothelial growth factors, chronic inflammation, hemodynamic dysregulation, impaired fibrinolytic ability, and enhanced platelet aggregation (35). Thus, prolonged hyperglycaemia results in microvascular complications and, at the same time, induces to the formation and acceleration on atherosclerotic plaque formation, which are major contributing factors of macrovascular complications.

1.6 New approaches to the treatment of diabetic wounds and enhanced diabetic wound healing

1.6.1 Diabetes mellitus and diabetic wound

Diabetes mellitus is a leading cause of non-traumatic lower limb amputation, which is often a consequence of an impaired wound healing process. Many physiological factors, including cytokines and other compounds that contribute to normal wound healing are impaired in the diabetic wound microenvironment, including growth factors (36–38), angiogenic factors (38,39), extracellular matrix components (40) and immunologic responses (38,41). Moreover, current therapeutic approaches to improve healing of diabetic wounds are not specific to the underlying pathologic condition that is responsible for the defect and this can contribute to ineffective therapy.

Wound healing is a complex process that requires an intricate orchestration of multiple cellular functions. During wound healing, affected tissues undergo phases of inflammation, proliferation and remodeling, which require regulated expression of inflammatory cytokines, angiogenic factors and extracellular matrix proteins. However, prolonged hyperglycaemia alters the inflammatory response and disrupts the microvasculature (38). Therefore, delayed and impaired wound healing is often clinically observed in diabetic patients, sometimes leading to infections or more severely, amputations. New approaches are therefore needed to address the problem of non-healing of chronic wounds to prevent morbidity and mortality, particularly in diabetic patients.

1.6.2 Current clinical management in diabetic wound

Current clinical management regimens for the care of diabetic wounds mainly centre around moisture, tissue debridement and epithelial edge advancement (42), but these frequently fail to address the pathologic characteristics of diabetic wounds, in particular poor perfusion and persistent inflammation. Therefore, outcomes for diabetic wound management are still relatively poor. Recently, research has focused on identifying novel modes of intervention, including the use of cell therapy and exogenous growth factors to modulate angiogenesis and inflammation (43). Among

the growth factors tested clinically, platelet-derived growth factor (PDGF) has shown promise as it has an important role in the formation of connective tissue during wound healing (44). However, despite FDA approval, topical PDGF-BB has only shown limited effects on ischemic wounds, which are characteristic of diabetic wounds (45–48).

1.6.3 Possible role of MSCs in diabetic wound healing

More recently, the potential for cell therapy to address this important issue, including the use of MSCs, has been trialled, exploiting the ability of these cells to generate paracrine factors that can promote wound healing (49–51). Several clinical studies using bone marrow-derived MSCs (BM-MSCs) for the treatment of chronic non-healing wounds, including diabetic wounds, have shown that application of MSCs to the wound can promote normal wound healing by facilitating re-epithelialisation and angiogenesis (49,52), and in effect, decreasing wound closure times (53). However, when used as a single therapy, MSCs usually show only limited beneficial effects on diabetic wounds compared to normal wound healing. Of interest, many MSC functions, including angiogenesis, are impaired by the chronic hyperglycaemic conditions associated with diabetes mellitus (54,55). It is believed that an underlying mechanism of MSCs in tissue repair is *via* the secretion of soluble factors that alter the tissue microenvironment. These factors may enhance regeneration of injured cells, stimulate proliferation and differentiation of endogenous stem-like progenitors found in most tissues, decrease inflammatory and immune reactions, rather than to induce transdifferentiation of the stem cells into epithelial or endothelial cells (56,57). Thus, compounds that can stimulate MSCs to secrete growth factors or alter the wound microenvironment, have the potential to promote more effective wound healing by MSCs in diabetes mellitus.

The mechanisms that have been proposed to be regulated by MSCs in the wound healing process, include secretion of soluble factors associated with angiogenesis (51), immunomodulation (58), and extracellular matrix production (59,60). Support for the involvement of soluble factors comes from the fact that conditioned media from MSCs can enhance wound healing (61,62). However, MSC treatment in a genetic mouse model of diabetes mellitus actually delayed wound closure time compared to their effects in non-diabetic mice (53). It was suggested that

hyperglycaemic conditions in diabetic wounds impair MSC function through induction of replicative senescence and apoptosis, as well as decreasing paracrine signalling (63,64). Therefore, research is needed to identify new ways to restore the wound healing activities of MSCs under hyperglycaemic conditions.

1.6.4 Other supplements in diabetes mellitus and regulation of MSC functions in wound healing

Vitamin C, a natural compound that is an essential dietary component, has been shown in a number of studies (65) to stimulate MSC proliferation without a reciprocal loss of their phenotype or differentiation ability: this mechanism may be related to both the antioxidant and non-antioxidant properties of vitamin C (65–68). Vitamin C also enhances cell survival by inhibiting cell senescence and may prolong MSC function in the wound. Additionally, the effect of vitamin C on extracellular matrix production may be to provide a more suitable microenvironment for MSCs to function appropriately. Consequently, oral vitamin C may be suitable as a synergystic treatment with MSCs in diabetic wound healing. Vitamin C is a micronutrient that facilitates wound healing, mainly through promotion of collagen synthesis and its antioxidative effects (69,70). In some conditions including diabetes mellitus, relatively low levels of vitamin C in either cells or serum have been proposed to contribute to ineffective wound healing (71,72). Apart from its antioxidative effects, vitamin C might play other roles in regulation of cellular metabolism. In this thesis, both *in vitro* and *in vivo* wound healing models have been used to investigate the effects of vitamin C on MSC function during wound healing under hyperglycaemic conditions (see Chapter 3).

1.7 Neutrophil Defects

1.7.1 Neutrophil

Neutrophils are the most abundant white blood cells in the circulation and much of the activity of the bone marrow is to generate and release mature neutrophils. In the circulation, neutrophils represent approximately 60 - 70% of white blood cells in the resting state, but only remain in the circulation for 6 - 9 h before undergoing apoptosis or migrating into tissues such as the lung, liver and spleen (73). In response to infection and inflammation, blood neutrophils become activated to stimulate their specific antimicrobial activity, and in parallel their numbers in the circulation increase (*via* mobilisation of mature cells from the bone marrow) and their lifespan is increased (73). Because of these mechanisms, processes and functions, neutrophils are the prominent innate immune cells that are responsible for the clearance of bacterial and fungal infections (74). Neutrophil activation requires coordinated activation of multiple cellular mechanisms: identification of chemotactic gradients *via* chemoattractant receptors; the mobilisation of secretory granules and vesicles; reorganisation of the actin cytoskeleton to allow for chemotaxis and phagocytosis (rolling and adhesion); penetration of the endothelial basement membrane and directional movement towards the infection or inflammation site (diapedesis). At the inflammation/ infection site, the transmigrated neutrophils phagocytose microbes which are subsequently killed by mechanisms that involve the reactive oxygen species (ROS) producing NADPH oxidase and granule proteins (such as myeloperoxidase, proteases and defensins). Once the neutrophil has completed its role in inflammation or infection, the cell undergoes apoptosis, which is required for the resolution of inflammation (75) (Figure 1.1). Consequently, patients with neutrophil defects in one or more of these mechanisms suffer from infections that are often life-threatening.

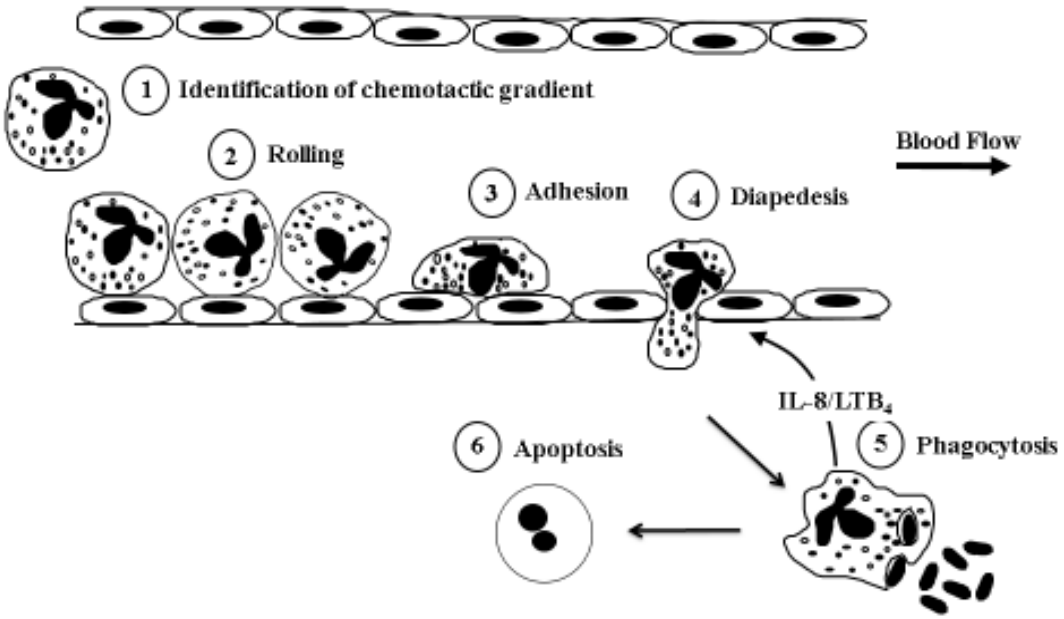

Figure 1.1: Regulation of inflammation and infection. (1) **The identification of chemotactic gradients**, for example interleukin 8 (IL-8) and Leukotriene B4 (LTB_4), *via* chemoattractant receptors and the mobilisation of secretory granules and vesicles. (2, 3) **Rolling and adhesion**: reorganisation of the actin cytoskeleton to allow for chemotaxis and phagocytosis. Neutrophils roll on and off the endothelial walls of capillaries, sensing changes in their surface properties *via* interactions between selectins (P-Selectin on neutrophils and E-Selectin on endothelial cells). During adhesion, changes in the surface properties of endothelial cells, such as increased E-selectin and P-selectin expression triggers L-selectin shedding on neutrophils and upregulation of adhesion molecules (VLA-4, LFA-1 and MAC-1 on neutrophils and ICAM-1, VCAM-1 and MADCAM-1 on endothelial cells). (4) **Diapedesis**: the penetration of the endothelial basement membrane and directional movement towards the infection or inflammation site. Surface ligands such as ICAM-2, PECAM-1 and JAM family proteins facilitate neutrophil migration through gaps in the endothelial cells and into the tissue. (5) **Phagocytosis**: at the inflammation/ infection site, the transmigrated neutrophils phagocytose the microbes which are then killed by mechanisms that involve the reactive oxygen species (ROS) producing NADPH oxidase and granule proteins (such as myeloperoxidase, proteases and defensins). (6) **Apoptosis**: once the neutrophil has completed its role in inflammation or infection, neutrophil apoptosis is required for the resolution of inflammation (75).

1.7.2 Neutrophils: Health and Disease

Many haematological diseases affect the differentiation of neutrophils and other myeloid cells, leading to defects in neutrophil number or function. Although several genetic mutations in key neutrophil genes have been identified in these haematological diseases, detailed understanding of the pathophysiology of many conditions is still unclear in many cases. Identifying the genetic lesion underlying altered neutrophil function has been important for understanding the clinical symptoms, but has also been important for understanding of the function of normal, healthy neutrophils.

One of the most studied genetic disease of human neutrophils is chronic granulomatous disease (CGD), in which circulating neutrophils have an impaired ability to generate reactive oxidants *via* the respiratory burst that requires activation of a normally dormant NADPH oxidase (76). The disease can be X-linked (more severe and often fatal) or autosomal recessive (milder disease), and the phenotype is an impaired ability to generate reactive oxygen species, defective killing of certain types of bacterial or fungal pathogens and increased morbidity and mortality from infections (77). Molecular characterisation of the biochemical defects responsible for this life threatening condition have been extremely important in defining the components of the NADPH oxidase and the ways in which this oxidase is activated (76). These studies have shown that the X-linked form of the disease is characterised by defective expression or absence of the membrane bound cytochrome b of the oxidase ($gp91^{phox}$ and $gp22^{phox}$) (78), while the autosomal recessive form of the disease arises *via* defective activation or expression of the cytosolic components, $gp47^{phox}$ (79) or $gp67^{phox}$ (80). These discoveries have been invaluable in identifying the mechanisms for activation and assembly of the oxidase, in particular identification of polymorphisms in the gene structure of the defective components has been instrumental in identifying structure: function relationships and the mapping of key amino acid residues that control oxidase function (81). Importantly, identification of these genetic lesions led to some of the first clinical trials for gene therapy to correct this defect in CGD patients with the most severe (X-linked) form of the disease (81).

Other neutrophil genetic defects that have been identified include leukocyte adhesion deficiency (LAD) (83) and myeloperoxidase deficiency (84). LAD-1 results

from impaired expression of CD18, the common ß2 subunit of the lymphocyte function-associated antigen (LFA) family of integrins (85). Many leukocytes express LFA with CD18 forming a heterodimer with CD11a, CD11b or CD11c. Human neutrophils have high expression of the CD11b/CD18 heterodimer (Mac-1 or CR3) (86). Patients with this condition suffer from life threatening infections as neutrophils fail to adhere to the endothelial wall of the capillaries in their attempts to migrate into the site of infection (85). Myeloperoxidase deficiency may be complete (rare) or partial (more common) and only patients with the complete deficiency show severe clinical symptoms, such as impaired killing of *Candida albicans* or *Aspergillus* (87), particularly against a background of diabetes (88). Partial myeloperoxidase-deficiency is usually asymptomatic because the enzyme is normally present in the granules of mature neutrophils at very high concentrations, representing ~5% of the total neutrophil protein content (88).

There are, however, many limitations in current models and systems that can be used to explore the molecular basis of diseases associated with neutrophil defects. There are a number of "neutrophil"-like or myeloid cell lines available, but even following *in vitro* differentiation, these lines do not possess all of the properties of mature neutrophils (89). Furthermore, as discussed above (Section 1.1.1.3.1), there are significant differences in the properties of human immune cells and murine cells, particularly neutrophils. The two major sources of cells for studies of human neutrophils are CD34+ cells (that can be induced to mature *in vitro*) and mature cells isolated from the peripheral blood (of patients with diseases or controls). While there has been some success in genetic modification of CD34+ cells and their maturation into mature neutrophils *in vitro*, results are highly variable and there have been only a few reports of the re-introduction of genetically-corrected CD34+ into patients. In previous studies, Haematopoietic stem cells (HSCs), or CD34+, gene therapy for adenosine deaminase (ADA)–deficient severe combined immunodeficiency (SCID) has shown the limited clinical efficiency due to the small proportion of engrafted genetically corrected HSCs (90). Therefore, new approaches are needed to correct human diseases and conditions associated with defective neutrophil function, and to design new ways to re-introduce genetically-corrected cells back into the patients to improve the disease symptoms.

1.8 Wiskott-Aldrich syndrome (WAS)

Wiskott-Aldrich syndrome (WAS) is caused by mutations in the *WAS* gene resulting in either the absence of, or expression of, a truncated Wiskott-Aldrich syndrome protein (WASp) (91). WAS patients are characterised by microthrombocytopaenia, eczema and recurrent infections. Currently, more than 160 mutations in the *WAS* gene have been discovered (92). However, the role of WASp in haematopoietic cells is not fully characterised. WASp is a 502-amino acid, proline-rich protein, which is constitutively expressed in the cytoplasm of all non-erythroid haematopoietic cells. This protein is involved in signal transduction pathways that are important for responses to cellular growth factors and in cytoskeleton reorganisation events of haematopoietic cells, possibly in response to cellular activation (93). Clinical manifestations of defective *WAS* are caused by loss-of-function mutations in the *WAS* gene. Most WAS patients suffer from severe infections that are normally associated with neutrophil dysfunction, although the absolute neutrophil count is not affected. As a result, infection represents the leading cause of death, along with bleeding in WAS patients (94) (Table 1.2). Early studies of WAS neutrophils demonstrated a chemotaxis impairment that could be corrected by addition of endotoxin-activated serum (95). However, until now, the role of WASp in neutrophil differentiation and function has not been elucidated.

Constitutive expression of WASp results in a clinically-distinct WASp-associated disorder, an X-linked neutropaenia (XLN). The clinical presentations are mainly the consequences of low numbers of neutrophils, which leads to proneness to bacterial infections (96). The XLN patients may also suffer from myelodysplasia and other cytopaenias (Table 1.2).

The purpose of the studies in this Thesis was to use WAS-iPSCs as a disease model. WAS is a monogenic disease that mainly affects haematopoietic cells. In addition, WAS is an early onset and non-developmental disease. Consequently, it may be possible to reproduce cellular phenotypes experimentally by generating iPSCs from WAS patients, defining their genetic defects and then differentiating the cells *in vitro* into mature neutrophils. Furthermore, it may be possible to correct the genetic defect in the iPSCs from these patients and then determine if normal neutrophil functions are restored after *in vitro* differentiation. While some functions of WASp are defined in

normal cells, the role of this protein in the pathophysiology of disease needs further studies. Therefore, this thesis aimed to investigate the use of iPSC-derived neutrophils as a WAS disease model.

Table 1.2: Comparison between loss-of-function and gain-of-function mutations in *WAS*

	Loss-of-function mutation	**Gain-of-function mutation**
Genotypes	Xp11.23, *WAS*	Xp11.23, *WAS*
***WAS* mutations**	Nonsense; frameshift caused by deletions, insertions; splicing defects	Missense in the Cdc42-binding site of *WAS* gene (97,98)
Phenotypes	Wiskott-Aldrich syndrome (WAS)	X-linked neutropaenia (XLN)
WASp expression	Absent or truncated	Present
Clinical features	Eczema, microthrombocytopaenia, proneness to infection, bloody diarrhoea	Recurrent major bacterial infections; severe congenital neutropaenia; monocytopaenia; predisposition to myelodysplasia in the absence of thrombocytopaenia and T-cell immunodeficiency; maturation arrest at the promyelocyte/ myelocyte stage in bone marrow

	Loss-of-function mutation	Gain-of-function mutation
Neutrophil count	Normal	Low (neutropaenia)
Pathogenesis	Absence of WASp, a key regulator of actin polymerisation in haematopoietic cells; five well-defined domains have been identified in WASp that are involved in signalling, cell locomotion and immune synapse formation (93,99).	Loss of *WAS* autoinhibition; the Leu270Pro mutation in the *WAS* gene encoding the conserved GTPase binding domain (100)
Animal model	WASp-deficient mice are not as severely affected as WAS patients. WASp may be a candidate for involvement in 'scurfy' (101), a T cell-mediated fatal lymphoreticular disease of mice that had previously been proposed as a mouse homolog of Wiskott-Aldrich syndrome (102).	Mutations in the mouse *WAS* gene corresponding to the human Leu270Pro mutation (L270P; 300392.0012) and Ile294Thr (I294T; 300392.0025) mutations; interfered with normal lymphocyte activation by inducing a marked increase in polymerised actin; decreased cell spreading and increased apoptosis, associated with increased genomic instability

1.9 New approaches to the use of iPSCs to understand and correct neutrophil genetic defects

1.9.1 Genetic manipulation of iPSCs to understand and correct human disease

Targeted double-strand breaks in DNA enables precise genome editing. In nature, a double-strand break (DSB) can be repaired through two main mechanisms, the endogenous homology-mediated repair machinery using an exogenous provided repair template and the non-homologous end joining (NHEJ)-DNA repair pathway (103). The introduction of gene-targeting DSB into iPSCs results in homologous recombination as a DNA-repair mediated genome editing including genetic correction. The genome editing technologies have been developed from the use of site specific nucleases (SSNs) such as zinc finger nucleases (ZFNs) and transcription activator-like effector nucleases (TALENs), to the use of bacteria adaptive immune systems, Clustered regularly interspaced short palindromic repeats (CRISPR)/ CRISPR-associated protein-9 nuclease (Cas-9), as a SSN. Zinc finger nucleases (ZFNs) will be described in details as the technique was applied in this thesis.

1.9.1.1 Genetic manipulations to reverse abnormal cellular phenotypes: Zinc finger nucleases (ZFNs) technique

Zinc finger nucleases (ZFNs) technique (104)*:* Zinc finger nuclease (ZFN)–facilitated homologous recombination–mediated gene targeting in iPSC-derived haematopoietic progenitors and iPSC-derived neutrophils could allow for precise genomic modifications. ZFNs induce a sequence-specific double-strand DNA break, enhancing site-specific homologous recombination. Previous studies of iPSCs have shown that the *AAVS1* locus lies within the first intron of the *PPP1R12C* gene on chromosome 19, and this can be used as a non-pathogenic "safe harbour", with persistent and strong transgene expression, to target a function-correcting minigene. The *AAVS1* locus resides in an open chromatin structure, flanked by insulator elements preventing the integrated cassette from trans-activation or repression. Gene insertion at the *AAVS1* locus may affect *PPP1R12C* gene expression. However, disruption of one *AAVS1* allele in human iPSCs appears to have no adverse effects.

1.9.2 The potential use of genetically-corrected iPSCs as a potential therapy

The derivation of patient-specific pluripotent cells with genetically-corrected fibroblasts allows the generation of corrected iPSCs (105). The differentiation of genetically-corrected iPSCs into adult somatic cells, including haematopoietic cells, establishes new pathways for implementing iPSC therapy. Moreover, the differentiation protocols have been developed to generate the functional adult somatic cells including haematologic cells, for example, neutrophils (106). iPSCs, therefore, may become a personalised medicine by allowing the autologous cells as the therapeutic sources, including haematopoietic stem cells.

1.10 Aims of this thesis

The overall aim of this thesis is to explore the potential of several new technologies to understand the molecular basis of human diseases. These technologies, their potential uses and the experimental approaches used in this study are shown in Table 1.3.

Table 1.3: Experimental design and approach of this thesis

Technology evaluated	Potential application	Experimental approach used in this thesis	Chapter
Mesenchymal Stem Cells (MSCs)	Tissue repair/regeneration	Generation of growth/angiogenic factors from cultured MSCs; use of MSCs to promote wound healing in a murine model of diabetes mellitus and effects of vitamin C supplementation	3
Induced Pluripotent Stem Cells	Correction of genetic defects: generation of mature blood cells	Isolation of iPSCs from a patient with Wiskott-Aldrich syndrome; generation of mature neutrophil-like cells after *in vitro* differentiation of iPSCs	4
Transfected cultured cell lines	Generation of mature neutrophils expressing exogenous gene(s)	Cloning of *EGFP*-tagged human *Mcl-1* into a lentivrus vector;	5

	and with extended lifespan	transfection of PLB-985 cells and differentiation *in vitro*	
^{1}H NMR metabolomics	Identification of neutrophil metabolites in health and disease	Development of new protocols to extract, identify and quantify the metabolome of human neutrophils; changes in composition of the neutrophil metabolome after *in vitro* activation and activation *in vivo* in disease	6

Objectives:

- to investigate the potential of mesenchymal stem cells (MSCs) and vitamin C
- supplementation in the treatment of diabetic wounds using the diabetic nude mouse model
- to investigate the ability of induced pluripotent stem cells (iPSCs) isolated from a patient with Wiskott-Aldrich syndrome to differentiate into mature neutrophils *in vitro*
- to develop a cell-line model of neutrophil differentiation using PLB-985 cells and to produce clones expressing *EGFP*-tagged *Myeloid Cell Leukaemia-1 (Mcl-1),* an anti-apoptotic protein that plays a key role in regulating neutrophil survival
- to develop protocols to profile of metabolome of human neutrophils from healthy individuals and patients with inflammatory disease, using ^{1}H NMR spectroscopy

CHAPTER 2: METHODS

2.1 MSC experiments

2.1.1 Mesenchymal stem cell (MSC) isolation and culture

MSCs were selected from adult mouse bone marrow (BM)-derived cells by their lack of surface antigen markers of haematopoiesis, in particular CD34 and CD45, using Fluorescence Activated Cell Sorting (FACS). BM-MSCs were further characterised by having a spindle-like shape with self-renewal capability, and ability to differentiate into osteoblasts (data not shown). MSCs at early passage (usually 20 - 40 passages) were cultured in 3 different conditions: (i) basal media (α-MEM with 20% FBS); (ii) normoglycaemic (D-Glucose 5.56 mmol/L (100 mg/dL)); (iii) hyperglycaemic (D-Glucose 55.56 mmol/L (1,000 mg/dL)). MSCs were cultured for one month under these latter conditions to study the effects of chronic hyperglycaemia on MSC function. Cells were seeded at a density of 2 x 10^4 cells/well (6-well plate) and counted (after culture as indicated in the text) using a haemocytometer.

2.1.2 *Real-time* reverse transcription-polymerase chain reaction (RT-PCR)

Mouse BM-MSCs were routinely cultured under normoglycaemic conditions. After 24 h incubation with and without TGF-β1, (a key inflammatory cytokine generated during cutaneous wound healing) at 20 ng/mL, RNA was isolated using TRIzol reagent (Invitrogen, USA). Subsequently, *real-time* RT-PCR was used to measure expression levels of mRNA of genes associated with (a) **angiogenesis**: *vascular endothelial growth factor-α (mVEGF-α)*; *angiopoietin-1 (mANGPT-1)*; *platelet-derived growth factor-BB (mPDGF-BB)*; *hepatocyte growth factor-1 (mHGF-1)*; or (b) **the extracellular matrix production**: *insulin-like growth factor-1 (mIGF-1)*; *fibronectin-1 (mFN-1)*; *stromal cell-derived factor 1 (mSDF-1)*; *tenascin C (mTNC)*. The primer sequences, obtained from other published studies (107–115), are listed in Table 2.1. Expression levels were normalised to those of the house-keeping gene, *glyceraldehyde-3-phosphate dehydrogenase (mGADPH*).

Four genes (*mVEGF-α*, *mPDGF-BB*, *mFN-1*, and *mTNC*) were selected for further studies, and their expression levels were compared in MSCs cultured under

normoglycaemia and hyperglycaemia after 24 h culture in the presence or absence of TGF-β1 (20 ng/mL) and/or vitamin C (100 μg/mL).

Table 2.1: Primer Sequences for *real-time* RT-PCR of genes associated with either angionesis or the extracellular matrix production

Genes	Primers	Sequences (5´→3´)	Products (bp)
mVEGF-α	Forward	CAGAAGGAGAGCAGAAGTCC	188
	Reverse	CTCCAGGGCTTCATCGTTA	
mANGPT-1	Forward	GCAAATGCGCTCTCATGCTA	146
	Reverse	GGAGTAACTGGGCCCTTTGAA	
mPDGF-BB	Forward	AGCAGAGCCTGCTGTAATCG	315
	Reverse	GGACTTCTAGTCACAGGCCG	
mHGF-1	Forward	CCCCTATGCAGAAGGACAGAA	159
	Reverse	GCCCTGTTCCTGATACACC	
mIGF-1	Forward	CTGAGCTGGTGGATGCTCT	118
	Reverse	CACTCATCCACAATGCCTGT	
mFN-1	Forward	TACCAAGGTCAATCCACACCCC	366

Genes	Primers	Sequences (5′→3′)	Products (bp)
	Reverse	CAGATGGCAAAAGAAAGCAGAGG	
mSDF-1	Forward	GTCCTCTTGCTGTCCAGCTC	192
	Reverse	AGATGCTTGACGTTGGCTCT	
mTNC	Forward	GTTTGGAGACCGCAGAGAAGAA	344
	Reverse	TGTCCCCATATCTGCCCATCA	

2.1.3 Proliferation assay

Mouse BM-MSCs were cultured under three different conditions: control (α-MEM + 20% fetal bovine serum); normoglycaemia (α-MEM + 20% fetal bovine serum + 5.56 mmol/L (100 mg/dL) D-glucose**)**; hyperglycaemia (α-MEM + 20% fetal bovine serum + 55.56 mmol/L (1,000 mg/dL) D-glucose**)**, for more than one month. At day 0, the cells were seeded at 2 x 10^4 cells in each 6-well plate. The cells were counted at day 3 and day 5 after seeding using haemocytometer. The culture medium was replaced every 2 days.

2.1.4 Tubular formation assay

Tubular formation by human umbilical vein endothelial cells (HUVECs) was used as a model of angiogenesis (116). HUVEC medium (Endothelial cell growth medium, Lonza, USA) was used to maintain HUVEC cultures, that were seeded at 3 x 10^4 cells/500 μL in each well of a 24-well plate covered with matrigel. Cells were incubated in the presence and absence of conditioned medium from MSCs and the effects of angiogenic cytokines secreted into the conditioned medium by the MSCs were assessed by measurements of tubular formation. Conditioned media was prepared from serum-free basal media (M199) derived from 80% confluence of MSCs after

overnight culture in different conditions (as detailed in the text and figure legends), such as hyperglycaemia (HyperCM) or normoglycaemia (NormoCM). After 6 h incubation, tubular formation was evaluated using ImagePro software and Pipeline software (Madison, USA).

Image analysis of tubular formation, such as area density, tubular length, number of branch points and tubular thickness, was evaluated by two separate investigators in a blinded manner.

2.1.5 Animals model of induced diabetes mellitus

Male BALB/C nude mice (7 - 8 week-old, weight 20 – 25 g), from the National Laboratory Animal Center, Salaya Campus, Bangkok, were housed according to the guidelines for the use of experimental animals by The National Research Council of Thailand. All experimental procedures were approved by the Ethics Committee, Faculty of Medicine, Chulalongkorn University. The mice were allowed to acclimatise for 1 - 2 weeks in the animal house after delivery, and then streptozotocin (Sigma Chemical Co., USA.) at 45 mg per kg body weight in citrate buffer pH 4.5 (Sigma Chemical Co., USA.), was intraperitoneally injected once a day for 5 continuous days to induce diabetes mellitus. Control nude mice were injected with citrate buffer pH 4.5. The induction of diabetes mellitus was confirmed by measuring tail-venous plasma glucose levels ($\geq$ 11.11 mmol/L (200 mg/dL)) at the 2^{nd} and 3^{rd} weeks after induction (Figure 2.1). To ensure that this diabetic state was stable, these treated mice were used 4 - 6 weeks after the diagnosis of diabetes mellitus in the wound model experiments.

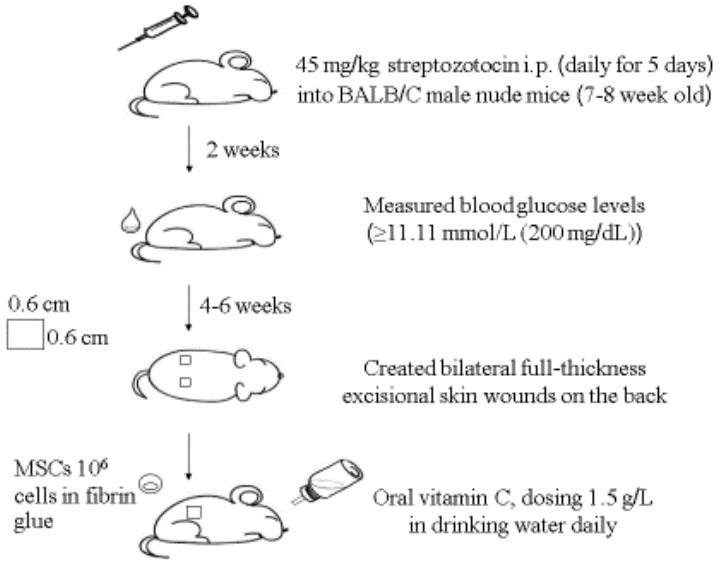

Figure 2.1: Schematic representation of the generation of diabetic mice and the diabetic wound model. 7 - 8 week old BALB/C male nude mice were intraperitoneally injected by Streptozotocin, once daily for 5 continous days. Two weeks after the injection, the tail-venous blood glucose was measured. Only the mice with the blood glucose level of 11.11 mmol/L (≥ 200 mg/dL) on two separate occasions were included into the diabetic groups. After 4 - 6 weeks of diabetes mellitus, full-skin thickness wounds were created bilaterally on the backs of the mice. Treatments were either MSCs, vitamin C or the combinations of the two.

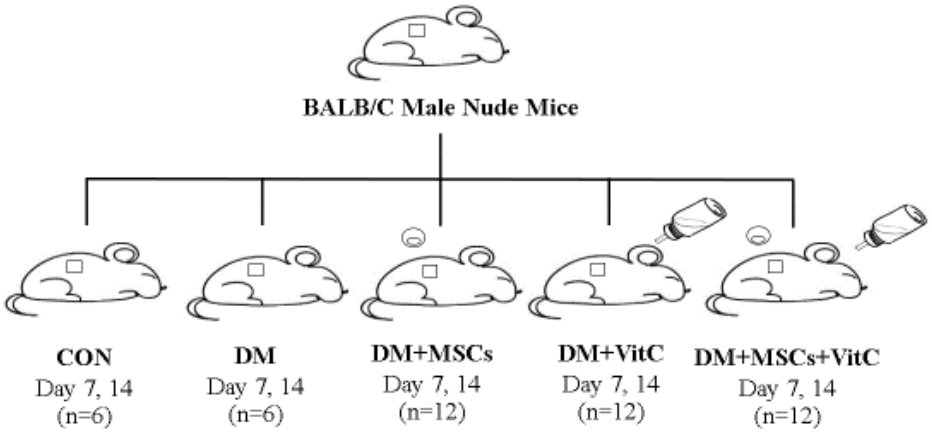

Figure 2.2: The diabetic wound model. Mice were divided into five groups; control (CON; n = 6), diabetes mellitus (DM; n = 12), diabetes mellitus treated with MSCs (DM+MSCs; n = 12), diabetes mellitus treated with VitC (DM+VitC; n = 6), and diabetes mellitus treated with MSCs and VitC (DM+MSCs+VitC; n = 12). For the MSC treatment groups (DM+MSCs and DM+MSCs+VitC), MSCs (1×10^6 cells) were applied in combination with fibrin glue topically on the first day of wound. Oral vitamin C, at 1.5 g/L, was supplemented daily into the drinking water in the vitamin C treatment groups (DM+VitC and DM+MSCs+VitC).

2.1.6 Generation of wounds in diabetic mice

Bilateral full-thickness excisional skin wounds (0.6 x 0.6 cm^2), were created on the backs of nude mice under intraperitoneal pentobarbital anesthesia (55 mg per kg body weight). For all experimental groups, the wounds were treated with fibrin glue (fibrinogen and thrombin, Shanghai RAAS Blood Products Co., China) and then covered by tegaderm (3M, USA). MSCs (1 x 10^6 cells) were applied in combination with fibrin glue topically on the first day of wound. Oral vitamin C, at 1.5 g/L, was supplemented daily into the drinking water, as indicated in the text and figures. The mice were examined at 7 and 14 days after wounding. For this wound model, mice were divided into five groups; control (CON; n = 6) (non-diabetic nude mice with the fibrin glue applied on the wound), diabetes mellitus (DM; n = 12) (diabetic nude mice with the fibrin glue applied on the wound), diabetes mellitus treated with MSCs (DM+MSCs; n = 12) (diabetic nude mice with MSC treatment in combination with the fibrin glue on the wound), diabetes mellitus treated with VitC (DM+VitC; n = 6) (diabetic nude mice with the fibrin glue applied on the wound and the oral vitamin C treatment), and diabetes mellitus treated with MSCs and VitC (DM+MSCs+VitC; n = 12) (diabetic nude mice with the MSC treatment in combination with the fibrin glue on the wound and oral vitamin C treatment) (Figure 2.2).

2.1.7 Measurement of wound area closure

Digital image software analysis (Image Pro II 6.1) was used to measure the percentage of wound closure (% WC) which was quantified using the equation (117,118):

$$\frac{\text{(Area of original wound at day 0 - Area of actual wound at day 7 (or day 14))} \times 100}{\text{Area of original wound at day 0}}$$

Each image was analysed by two separate investigators, in a blinded method. Briefly, the images of wounds were given a code. The images were then randomly distributed between four research staff and the mean values of the two measured wound values were recorded and used in the above equation.

2.1.8 Capillary vascularity (CV) of the wound

At day 7 and 14 post-wounding, mice were cannulated (after anesthetisation with pentobarbital), and 0.2 mL 5% fluoresceinisothiocyanate (FITC)-labeled dextran (MW. 150,000, Sigma Chemical Co., USA) was injected through the jugular vein. The degree of capillary vascularity (CV) was examined by intravital fluorescence video microscopy using a 10x objective lens. The percentage of capillary vascularity (% CV) was quantified using digital image software (Image Pro II 6.1). Images were analysed in a blinded manner. Histopathological study of the wound was conducted to confirm re-epithelialisation, rather than wound shrinkage, in the area of wound closure.

2.1.9 Tissue vascular endothelial growth factor (VEGF) levels

After the *in vivo* studies of wounds at day 7 and 14, wound biopsies from the area of the original wound were performed by needle punch. Skin tissues were homogenised using mechanical agitation and then ultra-sonication on ice at 90% amplitude (10 cycles of 30 s sonication followed by 30 s rest) to generate cell-free homogenates that were analysed for tissue VEGF levels by ELISA (Sigma Aldrich, USA).

2.1.10 Statistical analysis

All data are presented as mean ± standard deviation (SD), using one-way ANOVA and Tukey *post-hoc* multiple comparison tests. Statistical significance was considered at $\leq$ 5% (p value $\leq$ 0.05). The R project (version 3.2.3) for statistical computing were used (From: https://www.r-project.org/).

2.2 iPSC Experiments

2.2.1 Generation of Wiskott-Aldrich syndrome (WAS) induced pluripotent stem cell lines for use as a disease model

Studies using human cells were approved by the Institutional Review Board of the Faculty of Medicine of Chulalongkorn University and were conducted in accordance with the Declaration of Helsinki.

Previous work in this laboratory established protocols to generate iPSCs from skin fibroblasts and WAS-iPSCs were generated from skin fibroblasts of WAS patients (119). Skin fibroblasts were derived from punch skin biopsies, which were dissected into 4-mm round pieces, before being placed on an inverted glass slide and cultured in 0.1% gelatin-coated 6-well plates. The culture media was DMEM (Dulbecco's Modified Eagle Medium, Thermo Fisher Scientific, USA) with 20% FBS, and replaced every 2 days until confluence. The derived fibroblasts (WAS fibroblasts) were further characterised by immunostaining using Anti-SERPHIN-1 (Anti-rabbit, mAB, Sigma Aldrich, USA).

To generate Retrovirus-iPSCs (ReV-iPSCs), 6×10^6 GP-293 cells (a HEK 293-based retroviral packaging cell, Clontech, USA) were transfected with 13 μg of each of the following retroviral vectors (Addgene, USA): pMIG-OCT4 (clone 17225); pMIG-SOX2 (clone 17226); pMIG-KLF4 (clone 17227); pMXS-cMYC (clone 13375), and 5 μg of pVSV-G (vesicular stomatitis virus-G envelope protein) (Clontech, USA) using X-tremeGENE HP DNA Transfection Reagent (Roche, USA). 48 h after transfection, the media were collected and filtered through a 0.45-μm pore-size filter. Virus-containing supernatants were collected, filtered, and centrifuged at 25,000 g for 90 min. Viral pellets were resuspended in Opti-MEM (Invitrogen, USA), to generate an OKSM (*OCT4*, *KLF4*, *SOX2*, and *cMYC* transcription factors) retrovirus cocktail, which was supplemented with 6 μg/mL polybrene prior to the transduction of the WAS fibroblasts.

Five days after transduction, transduced WAS fibroblasts were seeded onto mitotically inactivated (using mitomycin-C treatment), human foreskin fibroblasts (as feeder cells) and cultured with iPS media (mTeSR™1 Medium, STEMCELL

Technologies, USA) until iPSC colonies were visible under the microscope as microcolonies.

2.2.2 Characterisation of WAS-iPSC line

After transduction, only WAS-iPSC lines generated compact colonies with morphology and cell-cycle profiles similar to those of embryonic stem cell (ESC) controls were then selected for further characterisation (120–122).

2.2.2.1 Immunofluorescence staining

Human iPSCs were fixed with 4% formaldehyde for 15 min at room temperature and then permeabilised with 1xPBS supplemented with 0.3% Triton X-100 for 15 min at room temperature. Human iPSCs were then blocked in blocking solution (10% goat serum and 0.3% Triton X-100 in PBS) for 30 min at room temperature and stained with primary antibodies for expression of the following transcription factors: *Oct4*, *Nanog*, *Tra-1–60* and *Tra-1–181* (StemLiteTM-Pluripotency Immunofluorescence (IF) kit, Cell Signalling, Danvers, MA, USA) at 4 °C overnight. Cells were stained with the Alexa Fluor conjugated secondary antibody (Molecular Probes, Invitrogen) for 1 h.

All fluorescence images were obtained by using Axio Observer fluorescence microscope (Carl Zeiss, Jena, Germany).

2.2.2.2 Tri-lineage differentiation *in vitro* and *in vivo*

The tri-lineage differentiation potential of iPSCs was tested *in vitro* by embryoid body (EB) formation assays. iPSCs were collected by enzymatic passaging using collagenase (to detach the iPSC colonies from the plate), dissected and resuspended in 10% fetal bovine serum (FBS) containing Knockout Dulbecco's Modified Eagle Medium (Knockout DMEM, with no L-Glutamine, used as a basal medium optimised for growth of undifferentiated induced pluripotent stem cells). Embryoid body (EB) formation was continued for up to 2 weeks, and cystic formation was observed as early as 6 days. Then, the EBs were disrupted into smaller clumps before passaging onto gelatin-coated plates for an additional 2 days, followed by fixing and staining for the three embryonic germ layers. *In vivo* differentiation was tested by

teratoma formation assays. iPSCs were collected using a cell-scraper, centrifuged and the cell pellet resuspended on ice in 400 mL of a 1:1 mixture of matrigel and Knockout DMEM, with no L-Glutamine. The suspension was injected intramuscularly into the hind limb of an immunodeficient mouse. Teratoma formation was observed at 6 weeks and the presence of tissues of three germ layers was confirmed by histopathological studies.

2.2.2.3 *Real-time* reverse transcription-polymerase chain reaction (RT-PCR)

Total RNA was extracted by using TRI reagent (Molecular Research Center, Cincinnati, OH, USA) and reverse transcribed with RevertAid™ H Minus M-MuLV (Fermentas, Glen Burnie, MD, USA). *Real-time* PCR was performed by using Maxima SYBR Green/ROX qPCR Master Mix (2x) (Fermentas, USA) on ABI 7500 Fast *Real-Time* PCR System. The expression of pluripotency marker genes, including *OCT3/4*, *NANOG*, *SOX2*, *cMYC* and *Nodal*, were studied to confirm the differential expression of the genes which were absent in the original fibroblasts, but should be expressed in their pluripotent state, iPSCs. The primer sequences, obtained from other published studies (123–125), are listed in Table 2.2.

Table 2.2: The primer lists of pluripotency marker genes

Genes	Primers	Sequences (5´→ 3´)	Products (bp)
OCT3/4	Forward	GACAGGGGGAGGGGAGGAGCTAGG	144
	Reverse	CTTCCCTCCAACCAGTTGCCCCAAAC	
NANOG	Forward	CAGCCCCGATTCTTCCACCAGTCCC	391
	Reverse	CGGAAGATTCCCAGTCGGGTTCACC	
SOX2	Forward	GGGAAATGGGAGGGGTGCAAAAGAGG	151
	Reverse	TTGCGTGAGTGTGGATGGGATTGGTG	
cMYC	Forward	GCGTCCTGGGAAGGGAGATCCGGAGC	328
	Reverse	TTGAGGGGCATCGTCGCGGGAGGCTG	
Nodal	Forward	GGGCAAGAGGCACCGTCGACATCA	234
	Reverse	GGGACTCGGTGGGGCTGGTAACGTTTC	

2.2.3 Western blot for WASp expression

5 x 10^6 WAS-iPSCs were collected and resuspended with cold PBS. The cell suspension was centrifuged at 3,000 g for 5 min, and the supernatant was discarded. 1 mL cold radio-immuno-precipitation assay (RIPA) buffer, with freshly-added protease inhibitors, was added into the pellet. The mixture, WAS-iPSCs:RIPA, was incubated on ice for 30 min, with vortexing every 10 min, and then centrifuged at 14,000 g for 15 min at 4 ^{o}C. The supernatant was collected as the protein lysates. 40 μg of total protein lysates were mixed with 6x loading dye, Laemmli sample buffer, boiled at 95 °C for 5 min, and loaded onto 10% sodium dodecylsulfate polyacrylamide gels. A mouse anti-WASp monoclonal antibody raised against a recombinant protein corresponding to the N-terminal region of human WASp (B-9; Santa Cruz Biotechnology, USA) and a goat anti-mouse IgG2a-HRP (sc-2005; Santa Cruz Biotechnology, USA) were used as primary and secondary antibodies, respectively. GAPDH was used as a control for protein loading. In the antibody staining step, milk protein (in 5% non-fat milk in wash buffer (Tris-buffered saline (TBS, 10mM Tris, 150 mM NaCl, pH 8.0) with 0.1% Tween20) was applied to block non-specific binding sites.

2.2.4 Cell culture and differentiation of multipotent haematopoietic progenitors from human WAS-iPSCs *via* "iPS-sacs"

OP9 stromal cells (as feeder cells in a co-culture system) were treated with mitomycin and plated onto gelatin-coated 10-mL dishes. Small clumps of human WAS-iPSCs (suspended in PBS containing 0.25% trypsin, 1 mM $CaCl_2$ and 20% knockout serum replacement) were transferred onto OP9 cells and cultured in iPSC differentiation medium (Iscove's modified Dulbecco's medium (IMDM) supplemented with 10 μL/mL, Insulin/ transferrin/ selenite (ITS) 100x stock solution, 2 mM L-glutamine, 0.45 μM α-Monothioglycerol (MTG), 50 μg/mL ascorbic acid and 15% fetal bovine serum (FBS)), which was refreshed every 3 days. For the first 7 days, iPSCs were cultured under hypoxic conditions, to allow the generation of haematopoietic stem cells in the form of induced pluripotent stem cell–derived sacs (iPS-sacs). On day 14 to 15 of culture, iPS-sacs were collected into a 50-mL tube, gently crushed with a pipette, and passed through a 40-μm cell strainer to obtain haematopoietic progenitors (126,127).

2.2.4.1 Flow cytometry analysis

Progenitor cells isolated from iPS-sacs were stained with allophycocyanin (APC)-conjugated anti-human CD34 (BD Biosciences, USA) and Peridinin Chlorophyll Protein Complex (PerCP)–conjugated anti-human CD45 (BD Biosciences, USA) for haematopoietic cell analysis on day 14 of differentiation. Stained cells were analysed by using BD FACSAria II (Becton Dickinson, Franklin Lakes, USA).

2.2.4.2 iPS-sac formation and terminal differentiation to mature neutrophils

iPSCs were dissociated into small clumps of approx. 100 cells using collagenase, which were then transferred onto mitotically-activated OP9 cells in a haematopoietic cell differentiation medium (IMDM supplemented with a cocktail of 10 μg/mL human insulin, 5.5 μg/mL human transferrin, 5 ng/mL sodium selenite, 2 mM L-glutamine, 0.45 mM α-monothioglycerol, 50 μg/mL ascorbic acid, 15% FBS and 20 ng/mL human vascular endothelial growth factor (VEGF; R&D Systems, USA)). The sac-like structures, called iPS-sacs, were observed 5 - 7 days after seeding. At 14 days, the sac membrane was gently opened by a pipette and the contents were filtered through a 40-μm cell strainer to discriminate haematopoietic progenitors from the membranous structure which was discarded.

The haematopoietic progenitors were transferred onto newly mitomycin-treated OP9 cells, with terminal differentiation medium (IMDM supplemented with 10% FBS, 0.1 mM 2-mercaptoethanol, 100 U/mL penicillin, 100 μg/mL streptomycin, and 50 ng/mL granulocyte colony-stimulating factor (G-CSF)). The culture medium was replaced with fresh medium on day 3. This terminal differentiation phase was continued for 6 - 7 days.

2.2.5 Neutrophil morphology (128,129)

Cell morphology and granule characteristics of iPSC-derived neutrophils were assessed by Wright-Giemsa staining, in particular examining nuclear morphology (multi-lobed nucleus) and granular cytoplasm. Myeloperoxidase and alkaline-phosphatase staining were performed by immunohistochemistry.

2.2.6 Functional studies of mature neutrophils (128,129)

Chemotaxis assay: Neutrophil chemotaxis was determined using a modified Boyden chamber method. First, 800 µL of the reaction medium (RPMI-1640, Thermo Fisher Scientific, USA) with or without 0.01 µM formyl-Met-Leu-Phe (fMLP) was placed into each well of a 24-well plate. A cell culture hanging insert (3.0-µm pores) was use to separate the well into upper and lower chambers (Figure 2.3). Neutrophils were suspended in reaction medium at 5 X 10^6 cells/mL and 200 µL cells (1 X 10^6 cells) were added to the upper well. After 120 min incubation at 37 °C to allow the migration of neutrophils, the number of neutrophils that migrated through the membrane were counted using a microscope with a high-power lens (X400) in 3 different fields selected at random. The percentage of migrating cells were calculated using the following equation:

$$\text{Percentage of migrating cells} = \frac{\text{Number of cells in lower chamber x 100}}{\text{Total cell number in upper and lower chambers}}$$

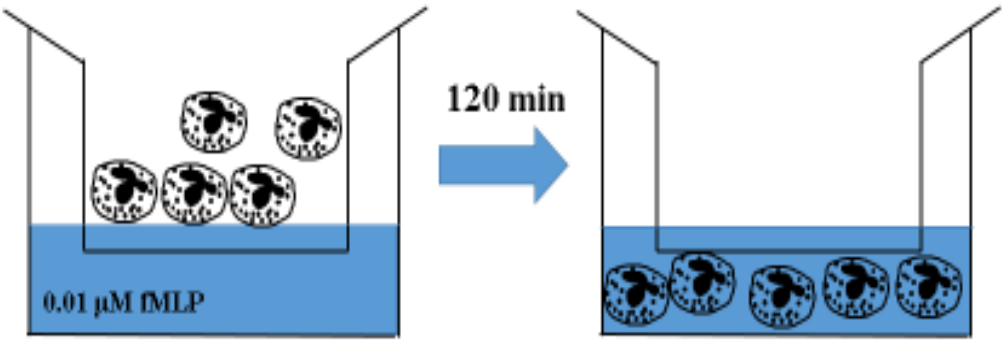

Figure 2.3: Schematic diagram of chemotaxis assay. 10^6 neutrophils were placed in the upper chamber, in either the presence (experiment) or absence (negative control, to observe random migration) of 0.01 µM fMLP in lower chambers. The upper and lower chambers were created by placing a 3.0-µm hanging insert into each well. After 120 min, the cells in both chambers were counted using a haemocytometer.

2.3 Culture and Differentiation of Myeloid Cell Lines

2.3.1 Differentiation of PLB-985 cells towards neutrophils

Exponentially growing PLB-985 cells, were seeded at a concentration of 2×10^5 cells/mL, and cultured in either differentiation medium or maintenance medium. The maintenance medium comprised RPMI-1640/glutamine medium with 10% fetal bovine serum (FBS) and 1% penicillin/streptomycin, while in the differentiation medium, FBS concentration was decreased to 5% plus the addition of the following differentiating agents: 0.5% N,N-dimethyl formamide (DMF), 1% sodium pyruvate and 0.1 µM all-trans retinoic acid (ATRA).

The cells were analysed twice daily for 5 continuous days to assess cell density, morphology and viability.

2.3.2 Differentiation of KCL-22 cells towards neutrophils

Exponentially growing KCL-22 cells, at a concentration of 2×10^5 cells/mL, were cultured in either differentiation medium or maintenance medium. The maintenance medium consisted of RPMI-1640/glutamine medium with 10% fetal bovine serum (FBS) and 1% penicillin/streptomycin, while in the differentiation medium, FBS was decreased to 5% with the addition of differentiating agents including 0.5% N,N-dimethyl formamide (DMF), 1% sodium pyruvate and 0.1 µM all-trans retinoic acid (ATRA). Different differentiation media and culture conditions were tested (see Table 2.3) to determine the conditions that resulted in optimal differentiation into neutrophil-like cells.

The cells were collected once daily for 7 continuous days to assess cell density, morphology and viability. (see Section 2.3.3; 2.3.4)

Table 2.3: Culture conditions used to optimise the differentiation of KCL-22 cells to neutrophils

Conditions	Differentiation media	Media changed
Differentiation media 1	RPMI-1640/glutamine medium + 5% FBS + 0.5% DMF + 1% sodium pyruvate + 0.1 µM ATRA	No
Differentiation media 2	RPMI-1640/glutamine medium + 5% FBS + 0.5% DMF + 1% sodium pyruvate + 0.1 µM ATRA	Day 2 and 5
Differentiation media 3	RPMI-1640/glutamine medium + 5% FBS + 0.5% DMF + 1% sodium pyruvate + 0.1 µM ATRA + 5 ng/mL GM-CSF	Day 2 and 5
Differentiation media 4	RPMI-1640/glutamine medium + 5% human AB serum + 0.5% DMF + 1% sodium pyruvate + 0.1 µM ATRA	Day 2 and 5
Differentiation media 5	RPMI-1640/glutamine medium + 5% FBS + 0.5% DMF + 1% sodium pyruvate + 0.1 µM ATRA + 1.2% DMSO	Day 2 and 5

(**Abbreviations**: FBS = Fetal bovine serum, DMF = N,N-dimethyl formamide, ATRA = All-trans retinoic acid, DMSO = Dimethyl sulfoxide, GM-CSF = Granulocyte Macrophage-colony stimulating factor)

2.3.3 Morphological studies and nuclear characteristics

10^5 cells were prepared for microscopy using a cytospin. Rapid Romanowsky staining was used to visualise nuclear morphology and sub-cellular components. Using morphological criteria, cells were categorised into three groups in accordance with their nuclear, cytoplasmic and granular appearance, as follows: non-differentiated cells (mononuclear cells with deep blue cytoplasm and no granules); partially-differentiated cells (partially-segmented nucleus with light blue or pink cytoplasm and no granules); differentiated cells (polysegmented nucleus with pink cytoplasm, with or without granules) (Table 2.4; Figure 2.4).

Table 2.4: Morphological criteria for differentiated PLB-985 and KCL-22 cells

	Non-differentiated cell	**Partially differentiated cell**	**Differentiated cell**
Nucleus	Mononuclear	Partially segmented nucleus or Band form	Polysegmented
Cytoplasm	Deep blue	Light blue/ pink	Pink
Cytoplasmic granule	None	None	Appearance of granules

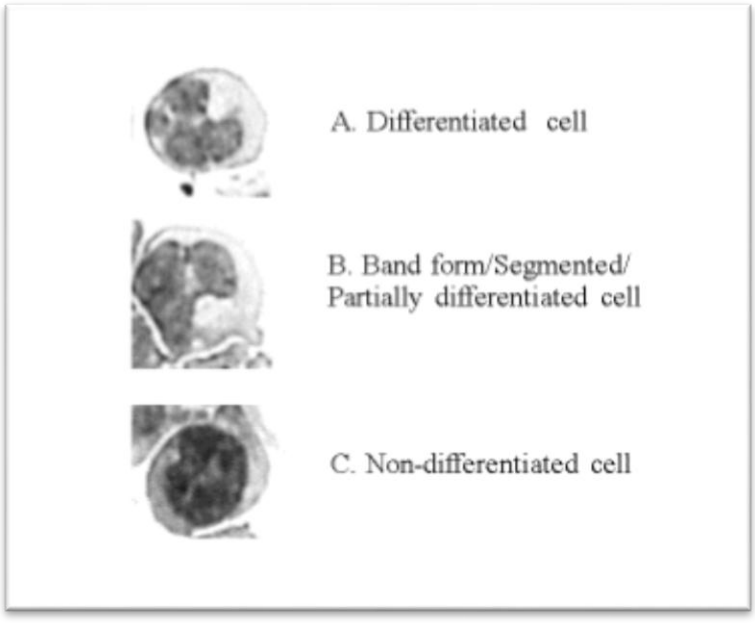

Figure 2.4: Morphological criteria for differentiated PLB-985 and KCL-22 cells. The cells are classified into three groups: A) Differentiated cells, B) Band form/Segmented/Partially differentiated cells and C) Non-differentiated cells.

2.3.4 Cell count and cell viability

Cell viability was evaluated by flow cytometry using Guava ViaCount® reagent (Merck Millipore, USA). This commercial reagent comprises two DNA-binding dyes: a nuclear stain (membrane permeable) and a viability stain (impermeable to live cells). It is capable of distinguishing viable, apoptotic and dead cells, based on differential permeabilities of the DNA-binding dyes. Dead cells exhibit high fluorescence with the viability stain, while apoptotic cells exhibit medium fluorescence and viable cells do not stain with this dye. The nuclear stain shows high fluorescence for all three groups of cells. Cell debris is excluded by gating out cells that stain negatively with the nuclear dye.

2.4 Sub-cloning *Mcl-1:EGFP* cDNA into pLVX-TetOne-Puro system and the transduced PLB-985 cells

2.4.1 Isolating *Mcl-1:EGFP* cDNA from the pEGFP-C3 vector

The *Mcl-1* gene was originally cloned into the pEGFP-C3 vector and ligated into the pEGFP-C3 vector between the restriction sites, HindIII and BamHI. The *Mcl-1* and *EGFP* sequences were amplified from the original vector, pEGFP-C3 by PCR, using primers that were designed to be used with the linearised pLVX-TetOne-Puro vector. The 5′ end of the primers contained the 15 bases complementary to the specific linearisation sites (**Bold** letters in Table 2.5) on the linearised vector and the 3′ end of the primers must contain sequences of 18 - 25 bases specific to the *Mcl-1:EGFP* cDNA (Table 2.5). Because the pLVX-TetOne-Puro vector did not contain complimentary cloning sites, a EcoRI site was engineered into the *Mcl-1:EGFP* cDNA using the primers (**Bold** and *Italic* letters in Table 2.5). The GC-content of the primers was between 40 – 60%, giving the primers a melting temperature of 58 - 65 ^{o}C ± 4 ^{o}C.

Table 2.5: The primers used to obtain the *Mcl-1:EGFP* sequences for cloning into pLVX-TetOne-Puro vector. Restriction sites in the primers are shown in **Bold** and *Italic*.

Primers	Sequences (5′→3′)
Forward	**CCCTCGTAAA*GAATTC***ATGGTGAGCAAGGGCGAGGAG
Reverse	**GAGGTGGTCT*GGATCC***TCTTGCCACTTGCTTTTCTGGCTA

2.4.2 Cloning the *Mcl-1:EGFP* cDNA into the pLVX-TetOne-Puro system using In-Fusion HD® (Clontech, USA)

After amplification, the PCR products contained restriction sites for EcoRI (*GAATTC*) and BamHI (*GGATCC*) which were essential for the subsequent cloning of the *Mcl-1:EGFP* construct into the pLVX-TetOne-Puro system using In-Fusion HD (Clontech, USA). The PCR products were amplified using CloneAmp^{TM} DNA

polymerase, and the size of the product (1,937 bp for *Mcl-1:EGFP* chimera) verified on an agarose gel. The PCR products were isolated by gel purification. At the same time, the pLVX-TetOne-Puro vector was linearised by double restriction enzyme digestion (EcoRI-HF and BamHI-HF) (New England BioLabs (NEB) Inc., USA). Using the online programme, Double Digest Finder (From: http://www.neb.com/tools-and-resources/interactive-tools/double-digest-finder, NEB Inc., USA) the optimal restriction endonuclease conditions were determined as: 10 units of each restriction enzyme, 1 µg *Mcl-1:EGFP* PCR product, 5 µL 10X CutSmart® Buffer and dH_2O to give a total reaction volume of 50 µL. The mixture was incubated at 37 °C for 6 h. The linearised vector was verified on an agarose gel and purified (gel purification) for the next In-Fusion cloning step on the same day.

To clone the *Mcl-1:EGFP* gene (1,937 bp) into the pLVX-TetOne-Puro vector (9,227 bp), a 3:1 molar ratio of insert:vector was used, with the minimal amount of linearised vector as 10 ng (Figure 2.5). Therefore, the amount of *Mcl-1:EGFP* DNA was 6.3 ng. To set up the In-Fusion cloning reaction, 2 µL of 5X In-Fusion HD Enzyme Premix, 10 ng of linearised pLVX-TetOne-Puro vector (9,227 bp) and 6.3 ng of *Mcl-1:EGFP* PCR product were mixed with dH_2O to a total reaction volume of 10 µL. The reaction was incubated at 50 °C for 15 min and immediately placed on ice. After an overnight incubation at 4 °C, the reaction mixture was ready to transform competent cells.

$$\frac{\text{Kb of insert x molar ratio (insert:vector)}}{\text{ng of insert}} = \frac{\text{Kb of vector}}{\text{ng of vector}}$$

Figure 2.5: Formula for calculating the amounts of insert and vector for efficient ligation

2.4.3 Transforming competent cells to transfect with the pLVX-TetOne-Puro vector

2.5 µL of the In-Fusion HD cloning reaction was used to transform Stellar competent cells (ClonTech, USA). The competent cells were thawed on ice (approx. 20 - 30 min). 2.5 µL of the ligation mixture was added into 50 µL of competent cells

in a 1.5 mL centrifuge tube. Then, the competent cell/In-Fusion cloning reaction mixture was placed on ice for 20 - 30 min. The mixture was immediately heated shock at 42 ^{o}C for 45 s, then was put on ice for 2 min. 500 µL of pre-warmed Super Optimal broth with Catabolite repression (SOC) medium was added into the mixture and incubated at 37 ^{o}C for 45 min with shaking. The transformation mixture was spread onto a 10-cm Luria-Bertani (LB) agar plate containing 100 µg/mL ampicillin to select for transformants.

2.4.4 Sequence analyses of the *Mcl-1:EGFP* in pLVX-TetOne-Puro vector

Two primers were designed to cover the junctional area (between the insertion and the vector) and the *Mcl-1* gene (Figure 5.6). The first primer to cover the junctional area was designed to confirm the *Mcl-1* in conjunction with *EGFP* genes in the vector. The second primer was designed to sequence the *Mcl-1* gene, to confirm the presence and the correctness of the *Mcl-1* gene in the vector (Table 2.6). After PCR, the products were sent for sequencing to Macrogen, Korea. The interpretation of Sanger sequencing was described in details in Chapter 5.

Table 2.6: The primers used to confirm the sequence of the *Mcl-1:EGFP* in pLVX-TetOne-Puro vector

	Sequence (5′ → 3′)
Primer to sequence the junctional area	TATGCAGACTTTACTCCCT
Primer to sequence the *Mcl-1* gene	GAGGTCCCCGACGTCACC

2.4.5 Production of lentiviral supernatants using Lenti-X Packaging Single Shots (VSV-G) (Clontech, USA)

4 – 5 x 10^6 Lenti-X 293T cells (a subclone of human embryonic kidney (HEK) 293T cell line that is highly transfectable and facilitates high-level viral protein expression), seeded in 10-cm plate with 8 mL of growth media (90% Dulbecco's Modified Eagle's Medium (DMEM) with 10% FBS), were incubated at 37 °C, 5% CO_2

for 24 h before transfection. 7.0 μg of the lentiviral vector plasmid DNA was diluted in 600 μL sterile water, and mixed by vortexing. The diluted DNA was added in a tube of Lenti-X Packaging Single Shots (Clontech, USA), and the tube was vortexed at a high speed for 20 s. The mixture was incubated for 10 min at room temperature to allow the formation of nanoparticle complex, then centrifuged at 500 g for 2 s. The nanoparticle complex solution were gently dropped on the Lenti-X 293T cell culture, with 80% confluence. The cells were incubated at 37 °C supplied with 5% CO_2. After 4 h, 6 mL of fresh complete growth medium was added and incubated for an additional 24 - 48 h. At 48 h after the transfection, the lentiviral supernatant was collected, and centrifuged at 500 g for 10 min, to remove the cell debris. The lentivirus production was now ready to transduce target cells, PLB-985 cells, or stored at –80°C for the transduction.

Before the transduction, the viral titre was determined to adjust the multiplicity of infection (MOI) for the proper transduction conditions. The Lenti-X p24 Rapid Titre Kit (Clontech, USA) was performed to quantify the viral titre. Briefly, lentiviral (HIV-1) p24 core protein in packaging cell supernatants is bound to wells of a microtitre plate coated with HIV-1 p24 capture antibody. The presence of bound p24 in the wells is detected using a biotinylated secondary anti-p24 antibody, a streptavidin-horseradish peroxidase conjugate, and a color-producing substrate. Quantitation was performed by comparing test samples to a p24 standard curve.

2.4.6 Transduce PLB-985 cells with pLVX-TetOne-Puro vector

PLB-985 cells, at 70 - 80% confluence, were cultured in RPMI-1640 with 10% FBS before the transduction. Polybrene was added to the cell culture to obtain the final concentration of 4 μg/mL. The PLB-985 cells were transduced at an MOI of 1-10, and make sure that the total volume of viral supernatant, *Mcl-1:EGFP* in pLVX-TetOne-Puro lentiviral stock was less than 1/3 the culture medium. The cultures were centrifuged at 1,200 g for 90 min at 32 °C to improve transduction efficiency. After 8 - 24 h, the virus-containing medium was discarded and the fresh growth medium was added.

2.4.7 Clonal selection of PLB-985 cells transduced with *Mcl-1:EGFP* in pLVX-TetOne-Puro vector

The transduced PLB-985 cells were cultured in 6 well-plate containing complete growth medium supplemented with 0.1 - 1 μg/mL puromycin. The cultures were maintained for 2 weeks with the antibiotic replacement every 48 h, the puromycin-resistant clones were selected. The clonal selection was performed by a serial dilution in a 96 well-plate.

2.4.8 Confirmation of expression in cells using flow cytometry and fluorescent microscopy

Approximately 20 clones of transduced PLB-985 cells were added with 100 ng/mL doxycycline to induce gene expression. *Mcl-1* was tagged with *EGFP* gene, therefore, the gene expression was confirmed by the combination of the visualisation by a fluorescent microscopy and the flow cytometry detection of a green fluorescence.

2.5 Methods: Metabolomics

2.5.1 Neutrophil Isolation

The study of neutrophils from healthy control was approved by the University of Liverpool Committee on Research Ethics, and the study of neutrophils from RA patients was approved by the NRES Committee North West (Greater Manchester West, UK). All participants gave written, informed consent. Whole blood was collected into lithium-heparin vacutainers (the use of EDTA as an anticoagulant was avoided because extra resonance signals can be observed in the NMR spectrum *via* the formation of complexes between EDTA and the Ca^{2+} and Mg^{2+} ions that are present in plasma) (130), and neutrophils were isolated within 15 min of blood collection. HetaSep solution (STEM CELL Technologies, USA) was added to the blood at a ratio of 1:5 (i.e. 1 mL HetaSep to 5 mL blood), then mixed and incubated at 37 ^{o}C for 30 min, to aggregate the erythrocytes. The erythrocyte-free phase containing all nucleated blood cells was collected, and carefully layered on top of Ficoll-Paque solution (GE Healthcare, USA) at a ratio of 1:1, and then centrifuged at 500 g for 30 min. The peripheral blood mononuclear cells (PBMC) layer, plasma, and Ficoll-Paque solution, were carefully removed, leaving a pellet of polymorphonuclear (PMN) cells (> 97% neutrophils). The PMN pellet was resuspended in RPMI-1640 media with 25 mM phosphate buffer pH 7.4. Note that the use of HEPES was avoided because it interferes with the NMR signal. Ammonium chloride solution (8.02 g NH_4Cl (ammonium chloride), 0.84 g $NaHCO_3$ (sodium bicarbonate) and 0.37 g EDTA (ethylenediaminetetraacetic acid, disodium) in 1 L Millipore H_2O) was added to the media at a ratio of 1:9 (i.e. 1 mL RPMI-1640 media to 9 mL ammonium chloride) to lyse the remaining erythrocytes. The mixture was left at room temperature for 3 min, and then centrifuged at 400 g for 3 min. The supernatant was removed, and the PMN pellet was then suspended in RPMI-1640 with 25 mM phosphate buffer pH 7.4 for further analyses.

2.5.2 Neutrophil metabolomics in response to stimulation

Neutrophils, at 2 – 10 x 10^6 cells/mL, were divided into two groups: one group was incubated with PMA (100 ng/mL), while the other was untreated and served as a

control. The cells at baseline were collected first at 0 h (time zero, no additions) and then at 5 and 15 min afterwards. All samples were collected as technical triplicates.

2.5.3 Sample preparation for intracellular metabolite extraction

After incubation as described above, neutrophils were centrifuged at 1,000 g, at room temperature for 2 min. The supernatants were collected and heated at 100 ^{o}C for 1 min (to inhibit any further reactions), and then snap-frozen in liquid nitrogen. The cell pellets were resuspended with cold PBS, then centrifuged at 1,000 g, at room temperature for 2 min. The supernatant was discarded, and the pellets were heated at 100 ^{o}C for 1 min (to inhibit any further reactions), and then were snap-frozen in liquid nitrogen. All samples were kept at -80 ^{o}C prior to intracellular metabolite extraction.

2.5.4 Intracellular metabolite extraction

Ice-cold solvent solution (50% HPLC grade acetonitrile, 50% double distilled water (ddH_2O)), was prepared freshly each day. 500 µL of the solution was added into the pelleted cells. The cell pellets were sonicated on ice (maximum frequency) in 3 x 30 s bursts (with 30 s off-period in-between to prevent heating). The samples were vortexed for 15 s before centrifugation at 12,000 g for 10 min at 4 ^{o}C. The supernatants were collected and snap-frozen in liquid nitrogen. The samples were lyophilised at -55 ^{o}C overnight. After this step, lyophilised samples were stored at -80 ^{o}C prior to NMR analyses.

2.5.5 Extraction at soluble metabolites (lyophilisation)

On the day of NMR analyses, the lyophilised samples were extracted. 1 mL of extraction buffer was prepared from 898 µL 100% D_2O, 100 µL 1 mM sodium phosphate pH 7.4 in 100% D_2O and 1 µL 100 mM Trimethylsilylpropanoic acid (TMSP or TSP) (a chemical compound used as an internal reference in NMR) in 100% D_2O. 200 µL of this solution was added into the lyophilised samples. The samples were centrifuged at 12,000 g for 2 min at room temperature. The supernatants were collected and then transferred into 3-mm tubes for NMR analyses.

2.5.6 Synovial fluid sample preparation

Synovial fluid (SF) samples from patients with inflammatory arthritis were obtained from Dr. Helen L Wright (Institute of Integrative Biology, University of Liverpool), and from patients with osteoarthritis from Dr. Mandy Peffers and Dr. James Anderson (Institute of Ageing and Chronic Disease, University of Liverpool). RA patients fulfilled the 1987 American College of Rheumatology (ACR) criteria for RA (131). Non-RA inflammatory arthritis (IA) patients with joint effusions included adults (over the age of 18) with gout/crystal arthropathy (n = 4), reactive arthritis (n = 2), and n = 1 each of Systemic Lupus Erythematosus (SLE), Juvenile Idiopathic Arthritis (JIA), Behçets disease, ulcerative colitis, ankylosing spondylitis, palindromic arthritis and inflammatory monoarthritis. RA and IA SF was aspirated into heparinised tubes and processed within 1 h. Aliquots of whole SF were centrifuged at 2,000 g for 5 min and cell-free SF was decanted and frozen at -20°C. The SF samples were thawed on ice and 100 μL of SF were aliquoted. 20 μL of 1 M sodium phosphate buffer pH 7.4 in D_2O, 80 μL of H_2O and 0.5 μL 1.2 M sodium azide (NaN_3, as a preservative) were added into the samples. The samples were vortexed for 1 min prior to centrifugation at room temperature at 13,000 g for 5 min. 200 μL of the supernatants were collected and then transferred into 3-mm NMR tubes for further analyses.

2.5.7 Spectral acquisition, Quality assessment of NMR spectrum, and Spectral analyses

The samples were analysed using an NMR-based metabolomic method using a 700 MHz NMR machine (see Chapter 6 for detailed experiments)

2.5.8 Statistical analyses

Principal component analysis is the statistical technique to simplify a set of observations. In the principal component analysis (PCA), the directions of the original variables were identified as the principal components, new variables, using mathematical algorithms (an orthogonal transformation) to decrease the dimensionality of the data. Each principal component includes different ranges of variance in the original variables (see details in Chapter 6).

For the statistical analysis, the spectral data in the peak intensity tables, were analysed *via* the Metaboanalyst® online programme which uses R-based statistics. In the time-point experiments, e.g. samples collected at different times after PMA treatment), a fold-change analysis was selected. For the spectral data of neutrophils from healthy controls and patients with disease, e.g. rheumatoid arthritis, either ANOVA or T-test with *post-hoc* analyses were applied with regards to the number of different groups: ANOVA for three groups or more, and T-test to compare two groups. The p value for the spectral analyses was set at 0.01.

2.5.9 Experiments to optimise protocols for neutrophil metabolomics

2.5.9.1 Optimal neutrophil cell number and the number of scans (NS)

Different total cell numbers of neutrophils (2.5, 3.5 and 9.7 x 10^6 cells per sample), were analysed using an increasing number of scans (NS), i.e. 128, 256, 512, 1,024 and 2,048. The number of scans is the number of times that a series of pulse-detect-wait sequences is repeated in NMR analyses. The increased number of scans builds up the total signal intensity, and at the same time, decreases the noise (the random signals with no metabolomic interpretation). However, the increased number of scans also requires the longer duration of NMR analyses, for example 15 min for NS of 128 and 4 h for NS of 2,048. The PCA was then performed to determine the reproducibility of data spectra in each experiment.

2.5.9.2 Quenching neutrophil metabolism: Heating neutrophils prior to the snap freezing

10^7 healthy neutrophils were collected either with or without a heating step prior to the collection of cell pellet (in Section 2.5.3). The heating step was the brief exposure of cell pellet to 100 ^oC heat for 1 min, immediately before the snap-freezing step. The following steps of intracellular extraction and lyophilisation were similarly processed. The spectral data analyses were evaluated, in order to detect the similarity of data, including the number of detected metabolites, between two groups.

2.5.9.3 Minimising the centrifugation times and metabolite loss during the extraction

Normally, neutrophil suspensions (1 - 2 mL) are centrifuged at 4,000 g for 3 min. However, in the metabolomic studies, a minimal isolation and processing time was required to increase the chances of metabolite collection and decrease the chances for metabolite loss.

Two cell concentrations, 2.5 x 10^6 and 10^7 neutrophils per 1 mL media (RPMI-1640), were collected and centrifuged at 4,000 g for either 2 or 3 min. The size of the pellets was visually compared.

2.5.10 Experiments to determine any loss of NADP+ during sample preparation for NMR

Purified NADP+ (Sigma Aldrich, USA) was added into the samples under three different conditions. First, 10 μg NADP+ were added into the cell pellets of 9.7 x 10^6 neutrophils before the heating steps. The cell pellets then went through the intracellular extraction and lyophilisation procedures. Second, 10 μg NADP+ was added into the PBS (no cell pellets). The mixture, NADP+ and PBS, was then heat shocked, and extracted and lyophilised. Third, 20 μg NADP+, without any processing, was analysed as a positive control.

CHAPTER 3 MSCs AND DIABETIC WOUND HEALING

Use of MSCs to accelerate wound healing in diabetic nude mice and role of exogenous vitamin C

3.1 Introduction

In diabetes mellitus, chronic hyperglycaemia alters the wound microenvironment (38), leading to delayed and impaired wound healing. The inflammatory response in the diabetic wound is prolonged, therefore, dysregulates the wound healing phases in diabetes mellitus. Patients with diabetic wound have increases the risk of infections, and sometimes amputations. However, current approaches to wound healing fail to recognise the underlying pathophysiology in diabetic wounds. New approaches are therefore needed to address the problem of non-healing of chronic wounds to prevent morbidity and mortality, particularly in diabetic patients.

In this study, we utilised both *in vitro* and *in vivo* wound healing models to investigate the effects of vitamin C on MSC function during wound healing under hyperglycaemic conditions. We identified vitamin C as a factor that enhances MSC functions under hyperglycemic conditions, and propose that this small molecule may be therapeutically administered simultaneously with MSC treatment, to accelerate diabetic wound healing. Our results therefore highlight the beneficial effects of administering oral vitamin C to diabetic patients to enhance wound healing.

3.2 Aims and objectives

The aims of the research in this Chapter were to determine the effects of hyperglycaemia on the ability of MSCs to generate angiogenic growth factors and to determine if the dietary antioxidant, vitamin C had any effect on this function. Another aim was to determine if externally applied MSCs would enhance wound healing in diabetic or control nude mice and whether orally-administered vitamin C had any effect on the properties of the MSCs, in particular in the diabetic mice. The objectives therefore were to:

1. Measure the effects of TGF-β1 on the expression of angiogenic and extracellular matrix-producing genes in MSCs incubated under normoglycaemia and hyperglycaemia.
2. To determine the effects of exogenously-added vitamin C on the expression of these genes.
3. To determine if orally-administered vitamin C could accelerate wound healing in control and diabetic mice who were also treated with MSCs

3.2.1 Conceptual framework

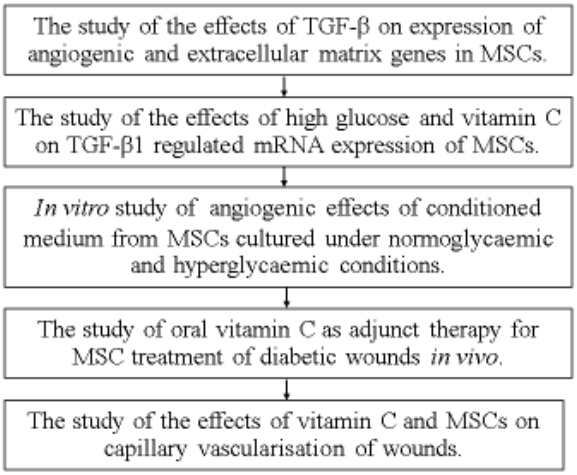

Figure 3.1: Conceptual framework for the study of MSCs and diabetic wound healing

3.3 Results

3.3.1 Upregulated expression of *mVEGF-α, mPDGF-BB, mFN-1* and *mTNC* in MSCs cultured in the presence of TGF-β1

The first experiments conducted aimed to study the potential function of BM-MSCs incubated under experimental conditions that may be present during the wound healing process. Transforming growth factor-β1 (TGF-β1) is recognised as a key cytokine orchestrating tissue-healing processes (132), including angiogenesis and extracellular matrix production (133). Therefore, mRNA expression of BM-MSCs was measured after culture for 24 h in the absence and presence of TGF-β1.

Eight genes that are key regulators during wound healing were investigated using quantitative *real time* RT-PCR. These genes are associated with either **angiogenesis**: (*vascular endothelial growth factor-α (mVEGF-α), angiopoietin-1 (mANGPT-1), platelet-derived growth factor-BB (mPDGF-BB), hepatocyte growth factor-1 (mHGF-1)*); or **extracellular matrix production** (*insulin-like growth factor-1 (mIGF-1), fibronectin-1 (mFN-1), stromal cell-derived factor-1 (mSDF-1), tenascin C (mTNC)*). It was found that mRNA expression levels of four genes (*mVEGF-α, mPDGF-BB*, *mTNC* and *mFN-1*) were upregulated in BM-MSCs in the presence of TGF-β1 (Figure 3.2). Increased expression of these genes could potentially play a role in wound healing.

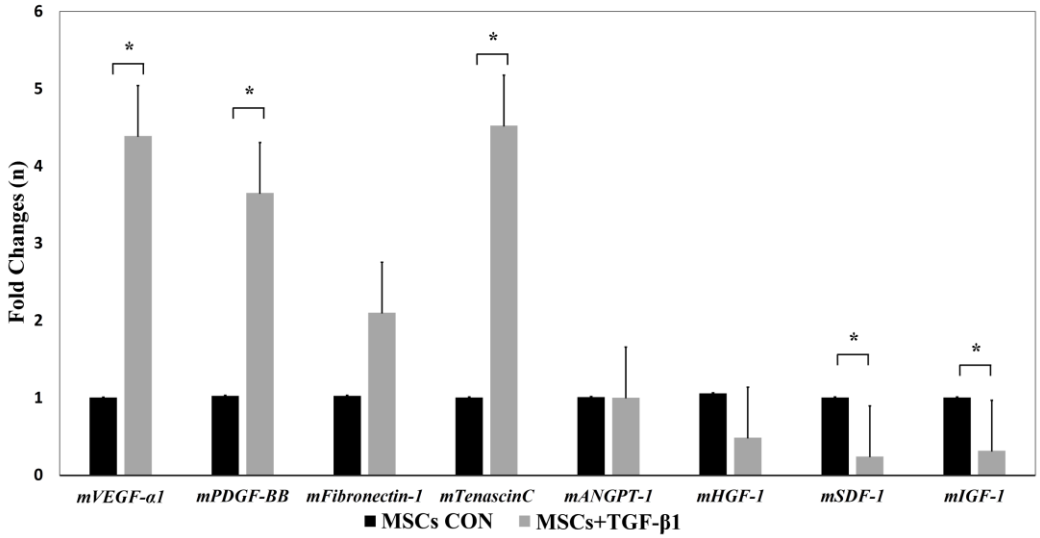

Figure 3.2: Effects of TGF-β on expression of angiogenic and extracellular matrix genes in MSCs. MSCs (seeded at 10^4 cells/well) were incubated in the absence (MSCs CON) or presence of TGF-β1 (MSCs+TGF-β1) at 20 ng/mL for 24 h. RNA was then isolated and quantitative *real time* RT-PCR was used to quantify expression of eight genes associated with either **angiogenesis**: *vascular endothelial growth factor-α (mVEGF-α)*; *angiopoietin-1 (mANGPT-1)*; *platelet-derived growth factor-BB (mPDGF-BB)*; *hepatocyte growth factor-1 (mHGF-1)*; or **extracellular matrix production**: *insulin-like growth factor-1 (mIGF-1)*; *fibronectin-1 (mFN-1)*; *stromal cell-derived factor-1 (mSDF-1)*; *tenascin C (mTNC)*. Expression levels were normalised to those of the house-keeping gene, *glyceraldehyde-3-phosphate dehydrogenase (mGADPH)*. Values presented are means (± SD, n = 3) and * indicates a p value ≤ 0.05. **BLACK** bars = MSCs CON; **GREY** bars = MSCs+TGF-β1.

3.3.2 Decreased *mVEGF-α* mRNA expression in TGF-β1-treated MSCs cultured under high glucose conditions

As high glucose concentrations can adversely affect MSC proliferation (54,134,135), their differentiation capacity and secretion of paracrine factors (135), it was investigated whether exposure of cultured MSCs to high glucose concentrations could affect expression of these TGF-β1-upregulated genes. MSCs were cultured in either normal or high glucose levels to observe any effects of prolonged high glucose exposure on expression of these genes. To ensure that the cells had sufficient time to become conditioned to the effects of prolonged hyperglycaemia, MSCs were cultured in high glucose media (α-MEM, 20% FBS, and 55.56 mmol/L (1,000 mg/dL) D-glucose) for at least 1 month prior to these experiments. Cell count at day 1, 3 and 5, was decreased by ~30% compared to when cells were cultured under normal glucose concentrations (data not shown). The decreased cell count could result from either increase in apoptosis or decrease in proliferation. Figure 3.3 shows that mRNA expression of a key angiogenic cytokine, *mVEGF-α*, which was upregulated under normal glucose conditions by TGF-β1 (Figure 3.3), was significantly decreased in MSCs cultured in hyperglycaemic media (Figure 3.3 i, p value $\leq$ 0.05). Hyperglycaemia also partially blocked TGF-β1 upregulation of *mPDGF-BB* (p value = 0.06), but had little effect on TGF-β1 upregulation of *mFN-1* or *mTNC* (Figure 3.3 ii-iv).

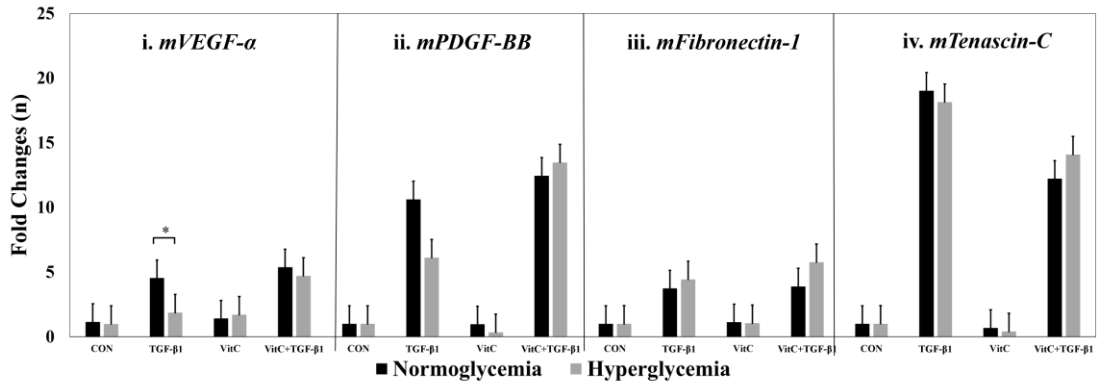

Figure 3.3: Effects of high glucose and vitamin C on TGF-β1-regulated mRNA expression of MSCs. MSCs CON and MSCs+TGF-β1 were incubated as described in the legend to Figure 3.2. All TGF-β1 cultures contained 20 ng/mL of TGF-β1. In the vitamin C treatment groups (VitC and VitC+TGF-β1), vitamin C 50 µg/mL was added into the culture media. MSCs were incubated in either normoglycaemic or hyperglycaemic conditions. After 24 h incubation, mRNA expression of the 4 genes regulated by TGF-β1 (*mVEGF-α*, *mPDGF-BB*, *mFN-1* and *mTNC*) was analysed qPCR. Expression levels were normalised to those of the house-keeping gene, *mGADPH*. Values presented are means (± SD, n = 3) and * indicates a p value ≤ 0.05. **Abbreviations**; CON = control group (no treatment), TGF-β1 = MSCs cultured in the presence of 20 ng/mL of TGF-β1, plus 50 µg/mL of vitamin C (VitC+ TGF-β1), and VitC = MSCs cultured in the presence of 50 µg/mL of vitamin C. **BLACK** bars = Normoglycaemia; **GREY** bars = Hyperglycaemia

3.3.3 Vitamin C reverses the hyperglycaemic suppression of TGF-β1 regulation of *mVEGF-α* and *mPDGF-BB* expression

To investigate whether vitamin C could reverse the suppressive effects of hyperglycaemia on TGF-β1 induced *mVEGF-α* or *mPDGF-BB* expression, MSCs were incubated in the absence and presence of vitamin C (50 μg/mL), which was added to the culture media for at least two weeks before quantifying gene expression levels. In human small intestine, oral ascorbic acid is absorbed *via* active transport (using Sodium-Ascorbate Co-Transporters (SVCTs) and Hexose transporters (GLUTs)) and simple diffusion, and enter the circulation in form of ascorbic acid (136). The addition of vitamin C had little effect on expression levels of *mVEGF-α*, *mPDGF-BB*, *mFN-1* and *mTNC* mRNA of control MSCs incubated under either normoglycaemic or hyperglycaemic conditions (Figure 3.3 i-iv). However, vitamin C reversed the inhibitory effect of hyperglycaemia on TGF-β1-induced *mVEGF-α* and *mPDGF-BB* expression (Figure 3.3 i-iv, $p \leq 0.05$). In the presence of vitamin C under hyperglycaemia, levels of expression of these two genes were equivalent to those observed under normoglycaemia.

3.3.4 Effect of hyperglycaemia on the secretion of angiogenic cytokines into the culture medium of MSCs

In MSCs cultured under prolonged hyperglycaemic conditions, mRNA expression of two TGF-β1-regulated angiogenic cytokines (*mVEGF-α* and *mPDGF-BB*) was decreased (Figure 3.3). Therefore, a tubular formation assay by HUVECs was used to measure the presence of angiogenic factors secreted into conditoned medium. Figure 3.4 shows that HUVEC medium (Figure 3.4 i), but not basal medium (Figure 3.4 ii) induced tubular formation in HUVECs that may be attributable to the presence of angiogenic factors in the former, but not in the latter medium. While conditioned medium from MSCs incubated under normoglycaemic and hyperglycaemic conditions could both induce tubular formation (measured by area density and tubular length), this activity was significantly impaired in conditioned medium from MSCs incubated in hyperglycaemic conditions (Figure 3.4 iii, iv, Figure 3.5 A-D). Tubular length (Figure 3.5 A), tubular area (Figure 3.5 B), number of branch points (Figure 3.5 C), but not thickness (Figure 3.5 D) were all decreased after culture of HUVECs with conditioned medium from MSCs cultured under hyperglycaemic conditions. These

data strongly suggest that long term culture under hyperglycaemia greatly decreases the secretion of angiogenic factors by MSCs.

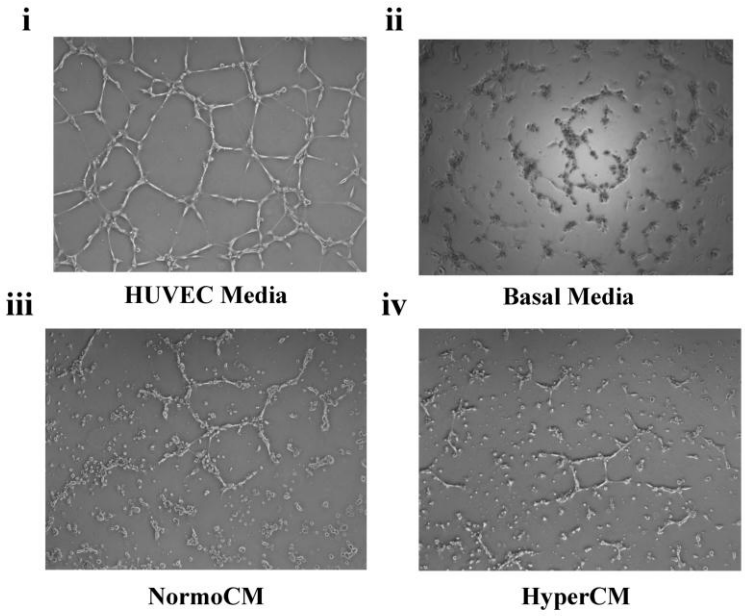

Figure 3.4: Angiogenic effects of conditioned medium from MSCs cultured under normoglycaemic and hyperglycaemic conditions. MSCs were cultured for 24 h in normoglycaemic (NormoCM) or hyperglycaemic (HyperCM) conditions, and conditioned medium was collected. A shows images of HUVECs incubated for 6 h in the presence of Endothelial Cell Growth medium (HUVEC medium, Lonza, USA) (i), basal (fresh) medium (used as a positive control), (ii) or conditioned medium from MSCs cultured for 24 h in normoglycaemic (iii) or hyperglycaemic (iv) media.

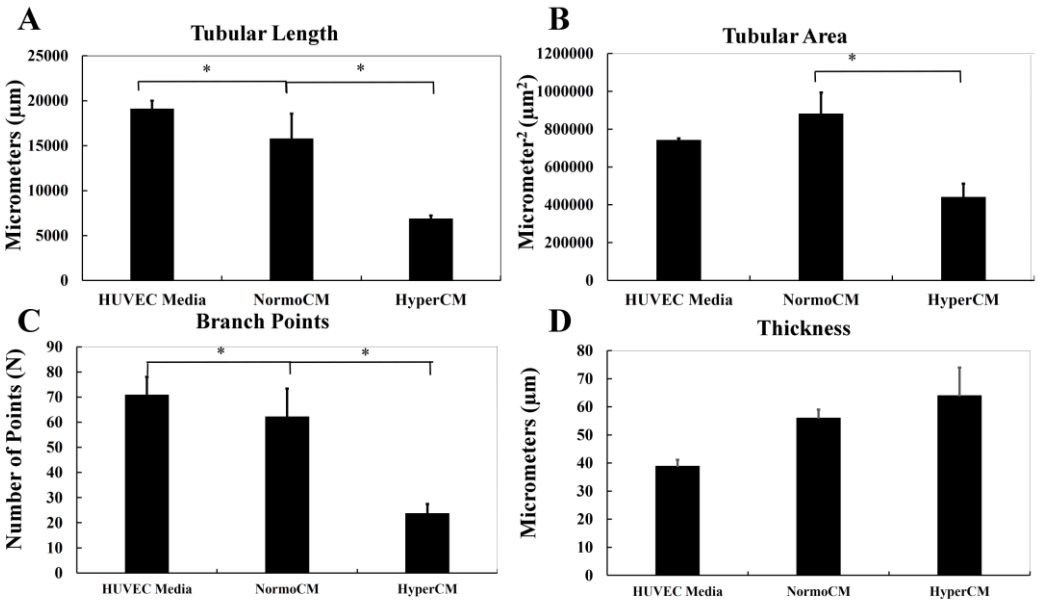

Figure 3.5: The effects of HUVEC medium on tubular formation. The measurements of tubular length (A), tubular area (B), number of branch points (C) and branch thickness (D) are shown. Values shown are means (n = 3) ± SD and * represents a p value of ≤ 0.05. (**Abbreviations**: HyperCM, Conditioned media derived from MSCs cultured under hyperglycaemia; NormoCM, Conditioned media derived from MSCs cultured under normoglycaemia).

3.3.5 Effects of vitamin C on wound closure

The effects of vitamin C and MSCs in a wound healing model of normal and induced-diabetes mellitus mice were then measured. In these experiments, vitamin C was orally administered to synergise the effects of topical MSC treatment in this diabetic wound model *in vivo*. STZ was used to induce diabetes mellitus in BALB/C nude mice which was confirmed by measuring tail-venous plasma glucose level (≥ 11.11 mmol/L (200 mg/dL)) at least twice prior to the wounding experiments. In these studies, the wound was stretched by tegaderm to cover 1 cm of normal skin around the wound to decrease the possibility of wound contraction, and thus to ensure that closure occurred by wound healing as a result of re-epithelialisation. In control (non-diabetic) mice (CON), wound healing was observed by 7 days (Figure 3.6; 3.7 A) and was approx. 87% complete by 14 days (Figure 3.6; 3.7 B). The rate of wound healing was significantly decreased in diabetic mice (DM) after both 7 and 14 days post-wounding and the topical administration of MSCs or supplementation of the diet with vitamin C, both significantly increased the rate of wound healing in the diabetic mice at both 7 and 14 days, to levels equivalent to those of healthy mice (CON). By 7 days post wounding, the combined effects of MSCs and vitamin C on diabetic mice did not enhance healing compared to the effects of MSCs or vitamin C used alone (Figure 3.6; 3.7 A), but by 14 days the rate of healing in the dual-treated diabetic mice (MSCs plus vitamin C) was greater than that observed with either agent alone (Figure 3.6; 3.7 B).

Histopathological studies confirmed that wound healing resulted from re-epithelialiasation rather than wound contraction, in every group of animals (example section shown in Figure 3.7 C).

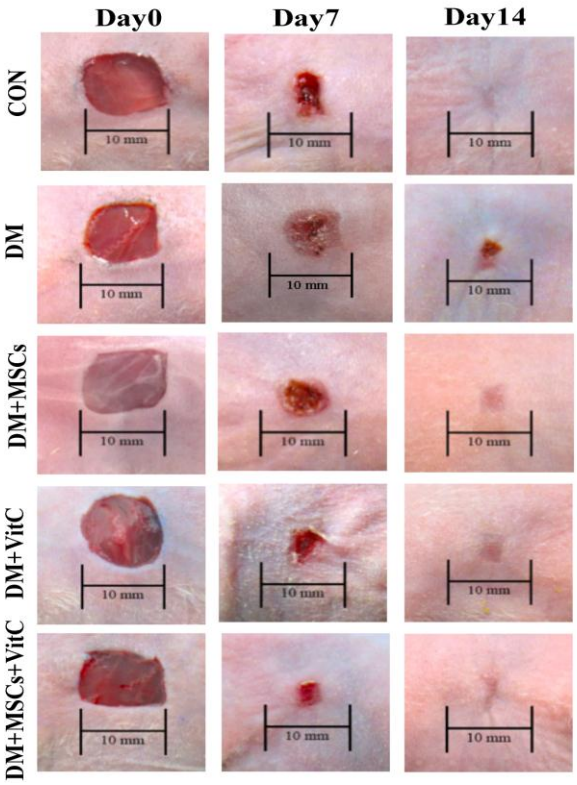

Figure 3.6: Vitamin C as adjunct therapy for MSC treatment of diabetic wounds *in vivo*. Wound healing was followed in five study groups of nude mice; wounded control (CON; n = 6); wounded diabetes mellitus (DM; n = 12); wounded diabetes mellitus treated with MSCs (DM+MSCs; n = 12); wounded diabetes mellitus treated with VitC (DM+VitC; n = 6); and wounded diabetes mellitus treated with MSCs and VitC (DM+MSCs+VitC; n = 12). Figure shows representative images of wounds from each of the five study groups at day 0, 7 and 14.

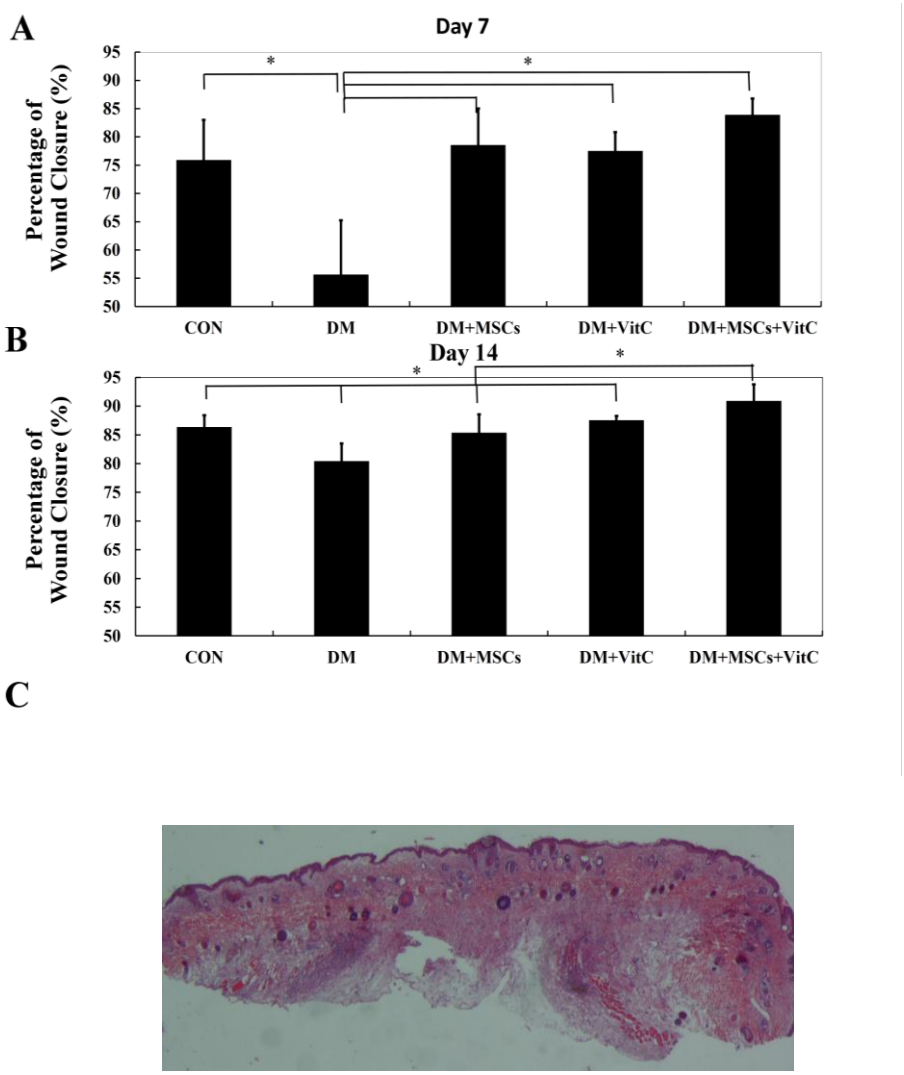

Figure 3.7: The percentage of wound closure. A and B show percentage wound closure (calculated as described in Methods) on day 7 and 14, respectively from experiments shown in Figure 3.6 above. * indicates a p value of ≤ 0.05. C shows a representative histochemical staining of a wound biopsy showing re-epithelialisation, confirming wound healing.

3.3.6 Measurement of capillary density during wound healing

The *in vitro* studies described above (Figure 3.2; 3.3) showed that vitamin C treatment enhanced the expression of two angiogenic cytokines (mVEGF-α and mPDGF-BB) after TGF-β1 treatment of MSCs cultured in high glucose. Furthermore, the experiments in Figure 3.4, 3.5, 3.6 and 3.7 show that vitamin C used as an adjunct therapy to MSCs could accelerate wound closure in diabetic nude mice. The effects of vitamin C and MSCs on wound microvasculature as the possible underlying mechanism of acceleration of wound healing were therefore determined. At day 7 post-wounding, vitamin C alone treatment that had significantly enhanced the percentage of capillary density in the diabetic mice (Figure 3.8; 3.9 A, B). However, by 14 days, the highest levels of capillary density were observed in the diabetic mice treated with the combination of MSCs plus vitamin C (Figure 3.8; 3.9 C). This high capillary density in these animals correlated with the highest rates of wound closure.

VEGF protein levels in wound tissues were then measured by ELISA. Tissue VEGF levels at day 7 in the control, the diabetic mice treated with MSCs and the diabetic mice treated with both MSCs and vitamin C were significantly increased when compared to the diabetic group alone (Figure 3.9 A, p value ≤ 0.05). This high tissue VEGF level at 7 days after wounding might help explain the mechanism regulating the high capillary density and rate of wound healing observed under these conditions.

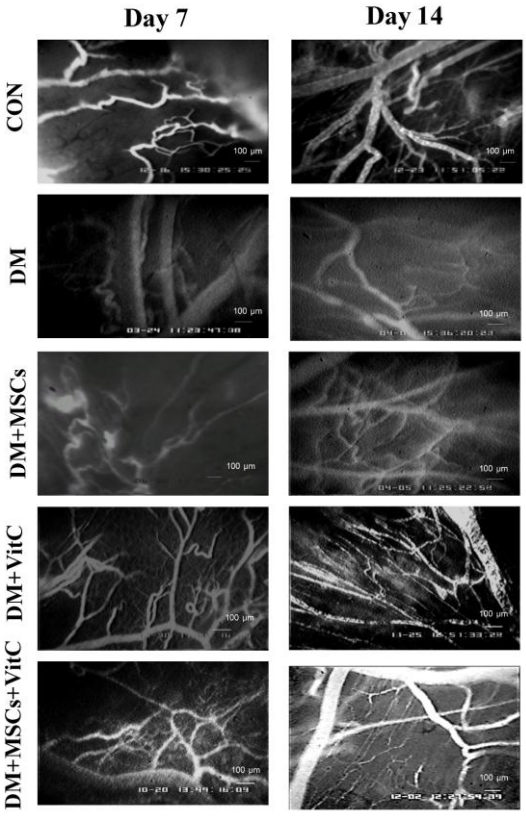

Figure 3.8: Effects of vitamin C and MSCs on vascularisation of wounds. Capillary vascularity was determined as described in Methods, 7 and 14 days after wound healing. Wound healing conditions were as follows: CON, control group; DM, diabetic mice; DM+MSCs, diabetic mice + MSCs; DM + VitC, diabetic mice + vitamin C supplementation; DM+MSC+VitC, diabetic mice + MSCs + vitamin C supplementation. Figure shows representative images day 7 and 14 after initiation of the wounds.

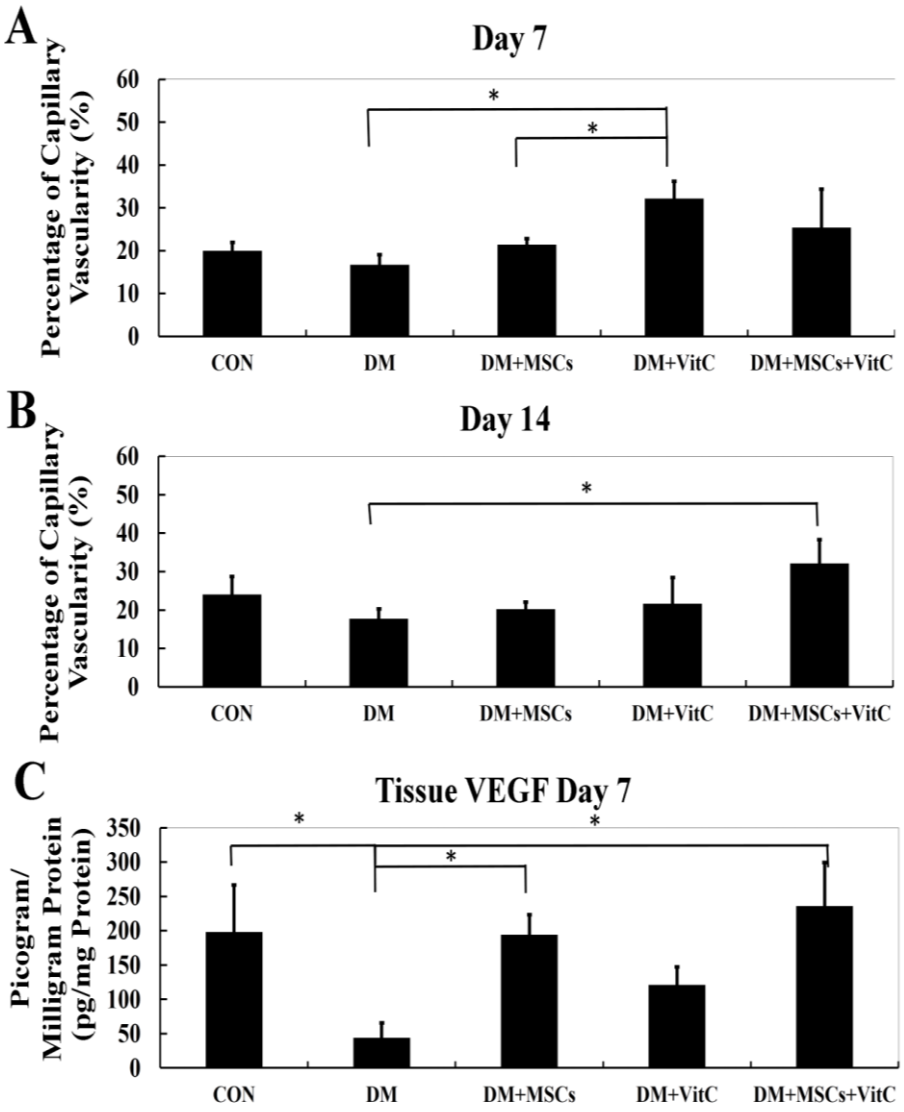

Figure 3.9: Effects of vitamin C and MSCs on vascularision of wounds. Figure shows % of capillary vascularity at day 7 and 14, respectively of the data shown in Figure 3.8. * Indicates a p value of ≤ 0.05.

3.4 Discussion

Current therapeutic procedures for the treatment of diabetic wounds largely focus upon preventing infections, rather than specifically aiming to promote wound healing. It is widely accepted that wound healing is problematic and delayed in diabetes mellitus as a result of elevated levels of glucose concentrations that can delay wound closure. Hence, new approaches that can accelerate healing of diabetic wounds offer the potential for new therapeutic procedures that both prevent infections and decrease the risk of amputations in these patients. In this Chapter, I have shown that oral vitamin C supplementation can enhance wound healing following topical MSC administration *in vivo* in animal models of diabetes mellitus. This accelerated wound healing was associated with enhanced capillary vascularity. These *in vitro* studies indicate that vitamin C can reverse the hyperglycaemia-induced suppression of TGF-β1 activated expression of angiogenic factors, which may, at least in part, explain the *in vivo* effects observed in diabetic nude mice.

In this study, we showed that administration of oral vitamin C and/or MSC therapy in diabetic wound model using nude mice, resulted in accelerated wound closure, that was detected as early as 7 days post-wounding that was associated with increased capillary density. In diabetes mellitus, prolonged exposure to hyperglycaemic conditions can impair several key cellular functions, including angiogenesis, wound healing and proliferation by mechanisms that include both oxidative and non-oxidative stresses (54,137). The excessive ROS production in diabetes mellitus, implicated by the formation of advanced glycation end-products e.g. HbA1c (glycated haemoglobin) can potentially contribute to those dysregulated cellular functions (138). For instance, impaired endothelial progenitor cell (EPC) proliferation from diabetic patients correlated with the level of HbA1c (higher HbA1c level, less EPC proliferation) (139).

Previous studies have demonstrated the promising potential benefits of MSC treatment in normal cutaneous wound healing that is likely to be associated with MSC paracrine signalling which could provide a mechanism that is responsible for new vessel formation and resulting wound repair (50,51,61). Similar to other progenitor cells, MSCs are regulated by and contribute to signals within their environment that can regulate processes involved in homeostasis and proliferation. In diabetes mellitus,

MSCs are affected by prolonged exposure to hyperglycaemic conditions, which can impair several key functions, including angiogenesis, wound healing and proliferation by mechanisms that include both oxidative and non-oxidative stresses (54,137). Vitamin C was previously shown to be deficient in diabetic patients (140) and an impaired vitamin C metabolism was observed in an animal experimental model e.g. STZ-induced diabetic rat (141,142). The oxidised form of vitamin C is transported into a variety of mammalian cells *via* a facilitative glucose transporter, mediated by members of the Glucose Transporter (GLUT) protein family (143). Consequently, high blood glucose levels can competitively inhibit vitamin C transport into mesenchymal cell types (such as fibroblasts) that would normally be participating in wound healing, thereby interfering with their cellular functions (144). In previous studies, the systemic administration of vitamin C has been shown to improve endothelial-dependent vasodilation in diabetic patients, but not in non-diabetic patients (145). Given the systemic and intracellular deficiencies of vitamin C that occur in diabetic patients, the effects of high glucose on mesenchymal cells may be responsible for impaired MSC function and therapeutic benefit in diabetic wounds.

In our wound model, the wound closure effects were validated as the consequences of each therapeutic agent, either single or combinations. Therefore, the wound closure in diabetes mellitus was measured in comparison with the control, non-diabetic wound, to demonstrate the delayed wound healing in diabetes mellitus. Moreover, the histopathological studies were perform to confirm the re-epithelialisation, not wound contraction, as the healing process.

In the studies shown in this Chapter, therefore, it was hypothesised that oral vitamin C supplementation would reverse the hyperglycaemia-induced changes in vitamin C metabolism and hence impairment of mesenchymal cell function. This hypothesis was based on the fact that that oral vitamin C supplementation may restore systemic vitamin C levels and consequently, improve the functions of both exogenous and endogenous MSCs. The results show that vitamin C, used as an adjunct to MSC therapy, can promote wound closure *in vivo* and promote vascularisation, and these *in vitro* experiments showed that it could restore the hyperglycaemia-induced suppression of expression of angiogenic cytokines by MSCs, which would enhance angiogenesis *in vivo*. It would be interesting to investigate whether vitamin C can

modulate the expression of other cytokines in addition to those involved in angiogenic pathways or which exert effects other than paracrine effects to facilitate wound healing e.g. in the regulation of inflammation.

Moreover, our diabetic wound model may facilitate the further experiments to confirm the hypothesis regarding the possible mechanism of stem cells and vitamin C on diabetic wound healing. If the effects of vitamin C are due to its antioxidant effects, then other antioxidants may be administered instead of oral vitamin C, and the wound closure effects compared. It would also be interesting to determine the effects of other antioxidants on gene expression of MSCs *in vitro* under normoglycaemia and hyperglycaemia. This would confirm whether the mechanism of action of vitamin C resulted from either its antioxidative activity or other unique properties of vitamin C.

Given the clinical importance of effective diabetic wound care in the face of an ever-increasing rise in the worldwide incidence of diabetes mellitus, these results open up new avenues to further explore the use of oral vitamin C in diabetic wound treatment. Oral vitamin C is a safe and simple supplement, and if these results are replicated in human diabetic patients, the accelerated wound closure time will minimise the risks of infection and amputations that are higher in these patients.

CHAPTER 4. WISKOTT-ALDRICH SYNDROME (WAS) AND PROPERTIES OF WAS NEUTROPHILS

4.1 WAS and neutrophil defects

The *Wiskott-Aldrich syndrome (WAS)* gene encodes the WAS protein (WASp) that regulates the actin cytoskeleton in haematopoietic cells. Therefore, the potential roles of WASp on neutrophil functions, including cell migration and others, have been widely studied, but not yet entirely understood. It would therefore be predicted that defective WASp expression would adversely affect neutrophil function and differentiation and two types of mutation in this gene have been observed: loss-of-function mutations in Wiskott-Aldrich syndrome (WAS) and gain-of-function mutations in X-linked neutropaenia (XLN), respectively. While WAS patients suffer from eczema, microthrombocytopaenia and are prone to infection and bloody diarrhoea, they have normal neutrophil counts. In contrast, the distinct pathological findings of XLN are low neutrophil counts, susceptibility to infection and predisposition to myelodysplasia in the absence of thrombocytopaenia and T-cell immunodeficiency. XLN results from an activating mutation in the *WAS* gene, giving rise to a constitutively-active protein (100,146). Neutropaenia is associated with haematopoietic maturation arrest at the promyelocyte/myelocyte stage in the bone marrow. In normal haematopoietic cells, WASp is ubiquitously expressed from early progenitors onwards. WASp function is regulated *via* an autoinhibitory mechanism. The activating mutation compromises normal auto-inhibition of WASp, leading to an unregulated activation of the actin-related protein 2/3 (Arp2/3) complex, and increased actin polymerising activity (147). Unregulated actin polymerisation by abnormal WASp causes defects of mitosis and cytokinesis, resulted in disrupted myelopoiesis (147). There are very few instances in which activating and inactivating mutations in genes encoding signal molecules cause such distinct hereditary disorders.

4.2 Modelling neutrophil defects in genetic disease

Currently, the two main types of models for used to study human neutrophil-associated diseases are the use of haematopoietic progenitor cells (or CD34+ cells), which can be differentiated *in vitro,* and peripheral blood neutrophils, which are terminally-differentiated. However, neutrophils derived from these sources are extremely limited in their usefulness for studies of development and understanding of disease mechanisms, due to their short half life *in vitro*, limited proliferation and low abundance. The percentage of CD34+ cells present in different sources is as follows: peripheral blood (0.15%), bone marrow (1.68%) and cord blood (0.83%) (148). The ability of CD34+ cells to expand and proliferate *in vitro* is problematic and very limited. For these reasons, genetic studies on human neutrophils are extremely restricted. Due to the distinct haematopoietic processes in animals, most of the clinical or cellular characteristics of human diseases cannot be reproduced exactly in animal models (149). In inherited diseases, the same genetic mutation can result in different clinical phenotypes and severity in different animal models. For example, the mutation of *ADAMTS13* (150) gene encoding von Willebrand factor-cleaving protease in humans results in congenital thrombotic thrombocytopaenic purpura in human, but normal platelet counts in mice. Therefore, the use of animal models for human haematopoietic diseases is of limited benefit. In addition, genetic manipulations to study the role of specific genes affecting clinical features are difficult, particularly with regard to the events regulating human haematopoiesis. The use and limitations of cultured cell lines that can be induced *in vitro* to differentiate into mature blood cells (e.g. neutrophils) is discussed in Chapter 5.

However, neutrophil precursors can proliferate from iPSCs and then be induced to differentiate into mature cells *in vitro* (129,151). The major advantages of iPSC technology result from the opportunity to generate disease- or patient-specific iPSCs through the reprogramming of somatic cells from patients with specific diseases. However, major considerations for the use of iPSCs as disease models of genetic neutrophil defects include the development of effective methods for differentiating iPSCs into mature neutrophils, and to ensure that the properties of iPSC-derived neutrophils (iPSC-Neu) match those of mature, peripheral blood neutrophils (106). Furthermore, while both genetic and environmental factors may

contribute to disease mechanisms, only genetic factors can be effectively manipulated when iPSCs are used as a disease model. Recently, iPSC-derived neutrophils have been used as a disease model in NADPH oxidase-deficient neutrophils in chronic granulomatous disease (128). This model was able to validate iPSC-derived neutrophils with oxidase deficiency, which mirrored the phenotype of the mature, circulating cells.

4.3 iPSC as a disease model for WAS neutrophils

One of the major roles of WASp is to regulate the actin cytoskeleton in haematologic cells. Therefore, in WAS, the absence of WASp may interfere either the movement or the functions of haematologic cells that require cytoskeletal re-arrangements, and thus contribute to the clinical characteristics of WAS patients, including bleeding and infection. In WAS patients with the loss-of-function mutation of the *WAS* gene, neutrophil counts are normal, but the major cause of death is from bacterial infections. Therefore, WAS neutrophils have been studied to determine their functions, in particular chemotaxis (movement of neutrophils in response to chemoattractants) as cellular migration is highly dependent on the WASp. However, the clinical data from WAS neutrophils remains controversial (89). For example, some studies demonstrated chemotactic defects of WAS neutrophils in response to C5a, a potent chemotactic agent derived from complement component C5 (95). In these studies, all patients had experienced major bacterial infections, and one of them died of overwhelming pneumococcal meningitis. In contrast, chemotaxis of WAS neutrophils was reported to be normal in response to the chemoattractant, fMLP. Interestingly, in peripheral blood neutrophils isolated from XLN patients, neutrophil functions, including NADPH-oxidase activation by Fcγ or fMLP receptor ligation, and phagocytosis of opsonised bacteria, were reported to be markedly impaired (98). Thus, the activating mutation of *WAS,* resulting in active WASp, also affects neutrophil functions.

In previous studies, the effects of WASp on neutrophil chemotaxis capability are variable from patient to patient. The generation of haematopoietic stem cells (HSC) from iPSCs of patients, offers a promising approach to model disease pathology (152). However, the differentiated cells must be characterised as morphologically mature neutrophils with the same functional properties as the mature cells from the original patients. The first steps of this research were to study the effects of WASp on mature neutrophil functions in patients attending Chulalongkorn Hospital. Once this was achieved, neutrophils derived from WAS-iPSCs could be characterised to demonstrate similar defects to neutrophils isolated from WAS patient's peripheral blood (WAS neutrophils).

Thus, this study aimed to determine if neutrophil chemotaxis was defective in WAS patients attending Chulalongkorn University Hospital, and further demonstrate if similar defects were observed in WAS-iPSC-derived neutrophils, in order to validate the usefulness of WAS-iPSCs as a model of human disease.

4.4 Aims and objectives

The aims of the research in this Chapter were to explore the chemotactic functions of WAS peripheral blood neutrophils, which might be responsible for the clinical manifestation of proneness to bacterial infection. Another aim was to demonstrate the capability of WAS-iPSC-derived neutrophils to differentiate towards mature neutrophils, as detected by morphological criteria. The objectives therefore were to:

1. To measure the chemotactic function of WAS peripheral blood neutrophils.

2. To determine if the morphology of corrected WAS-iPSC-derived neutrophils after differentiation *in vitro*. For these experiments, WAS-iPSCs were genetically modified *in vitro* to correct their genetic defect by re-introducing the *WAS* gene.

4.4.1 Conceptual framework

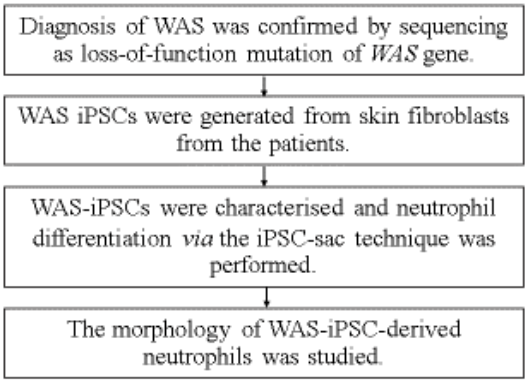

Figure 4.1: Conceptual framework for the study of Wiskott-Aldrich syndrome (WAS) and properties of WAS neutrophils

4.5 Experiments using WAS patient peripheral blood neutrophils

4.5.1 Functional studies

Chemotaxis of WAS neutrophils was studied and compared with that of healthy controls. Briefly, in this chemotaxis study, neutrophils migrated through the 3-μm-sized pores towards the chemoattractant, in this case fMLP, which is a formylated oligopeptide that is similar to the N-formyl oligopeptides released from bacteria. It is a chemoattractant for neutrophils and activates them by binding to specific G-protein coupled receptors on their cell surface (153). Using a 24 well-plate assay, 3-μm-pore-sized hanging inserts separated the well into upper and lower compartments, and the fMLP was added into the lower compartment. 10^6 cells/200 μL were added into the upper chamber, and were allowed to migrate for 120 min. In order for the cells to migrate towards the chemoattractant, the cells must first adhere to the membrane, undergo actin remodeling, and migrate through the pores that are of a smaller diameter than the cell. The chemotaxis study through the transwell migration is therefore suitable to evaluate the functions of the neutrophil actin cytoskeleton that is reported to be regulated by WASp.

Neutrophils were isolated from the patient's whole blood on three separated occasions (n = 3). The control neutrophils were isolated from 7 different healthy individuals (n = 7). In the chemotaxis assay, the percentage of migrating neutrophils were calculated (see Section 2.2.6). The results revealed defective chemotaxis activity, in response to fMLP, in WAS neutrophils (mean ± SD, 27.23% ± 7.53, n = 3) in comparison to the healthy controls (90.0% ± 7.52, n = 7, $p \leq 0.05$) (Figure 4.2).

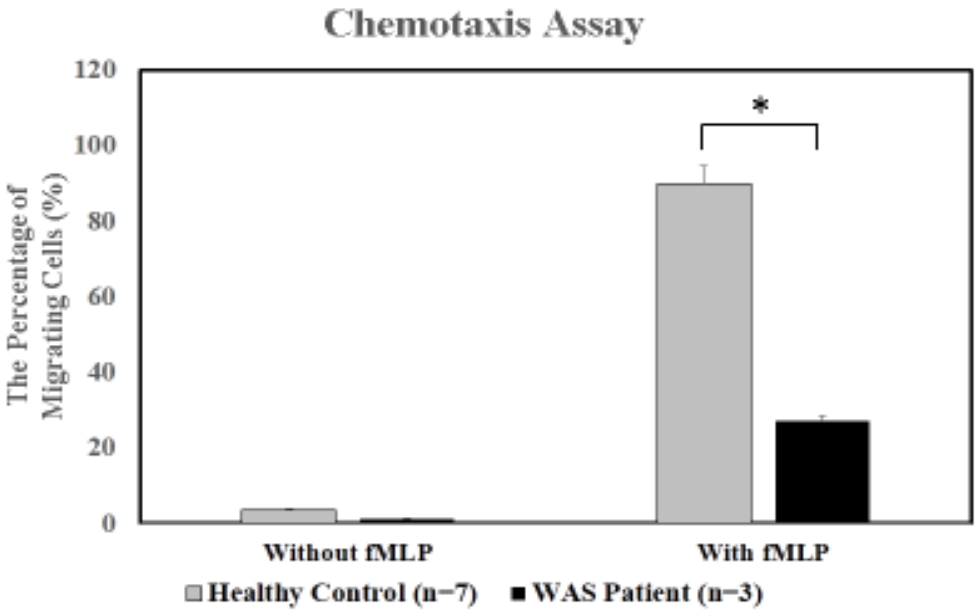

Figure 4.2: Impaired chemotaxis activity of WAS neutrophils. WAS neutrophils shown impaired chemotaxis activity in response to fMLP, a chemoattractant, when compared to the healthy controls. Without fMLP, the migration of both WAS and healthy neutrophils were minimal (2.0% and 0.8% respectively) and resulted from a random movement. In the presence of a chemoattractant, fMLP, the migration of WAS neutrophils (27.23% ± 7.53, n = 3) was significantly lower when compared to healthy neutrophils (90.0% ± 7.52, n = 7) (mean ± SD, * indicates $p \leq 0.05$).

4.6 Experiments with WAS-iPSC-derived neutrophils

4.6.1 Preliminary data with WAS-iPSCs

These preliminary results were obtained by Stem Cell and Cell Therapy Research Unit, and Medical Genetics and Metabolism Unit, Department of Paediatrics, Faculty of Medicine, Chulalongkorn University. They are presented here to show "proof of principle" of the experimental approach used in my studies.

This research was designed to study the role of WASp in haematopoiesis and thrombopoiesis. WAS-iPSCs were derived from a patient's dermal fibroblasts, by reprogramming using retrovirus transfection techniques. WAS-iPSCs demonstrated the ability to generate most types of haematopoietic colonies. In addition, further culture of iPSC-derived haematopoietic progenitors (CD34+, CD45+) revealed decreased number of macrophage colonies when compared with the wild-type iPSCs (WT- iPSCs), which produced smaller-sized colonies (Figure 4.3).

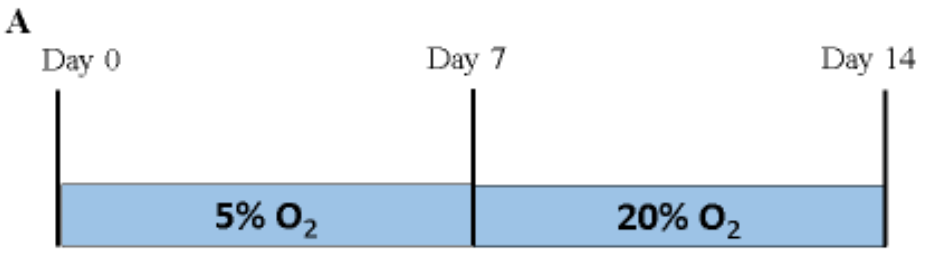

IMDM + 15% FBS + 20 ng/mL VEGF media and OP9 feeder cells.

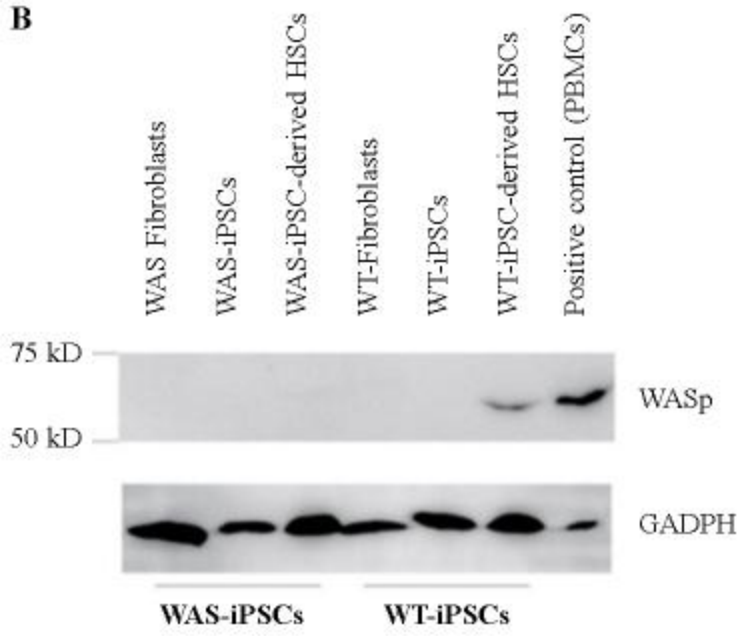

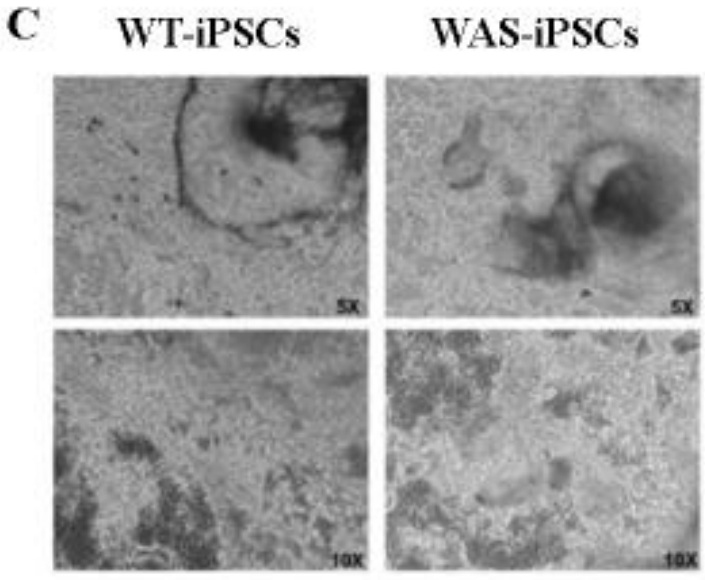

Figure 4.3: Haematopoietic stem cell (HSC) differentiation of WAS-iPSCs. (A) Schematic diagram of the *in vitro* haematopoietic stem cell differentiation protocol, or iPS-sac formation protocol. Cells were cultured for 7 days under hypoxia (5% O_2) followed by 7 days under normoxia (20% O_2) over the OP9 feeder cells. iPS-sac. (B) Western blot analysis showing WASp expression in haematopoietic stem cells (HSCs) derived from WT-iPSCs but not in fibroblasts, iPSCs, or HSCs from WAS-iPSCs. Peripheral blood mononuclear cells (PBMCs) expressing WASp were used as a positive control. (C) Phase contrast photomicrographs of iPS-sacs generated from WT-iPSCs and WAS-iPSCs on day 14; magnification 4X and 10X. iPS-sac was a VEGF-promoted structures that concentrate haematopoietic progenitors. The sac-like structures consisted of multiple cysts demarcated by cellular monolayers that retained some of the properties of endothelial cells. (**Abbreviations**: HSCs = Haematopoietic stem cells, iPSCs = induced pluripotent stem cells, WT = Wild type, WAS = Wiskott-Aldrich syndrome, IMDM = Iscove's Modified Dulbecco's Media, FBS = Fetal bovine serum, VEGF = Vascular endothelial growth factor).

4.6.2 Terminal differentiation of mature neutrophils from WAS-iPSCs

Following the protocols developed in published studies (129), iPSCs were differentiated into haematopoietic stem cells (HSCs) using the iPS-sac formation method (see Chapter 2). HSCs developed inside the sac-like structure, the so called iPS-sac. Using flow cytometry analyses, the progenitor cells derived from the iPS-sac at 14 days after differentiation stained positive for CD34 and CD45, the haematopoietic surface markers.

Once haematopoietic stem cells (HSCs) were derived from the iPS-sac, they were further cultured in neutrophil differentiation media. In this differentiation media, the key cytokine, e.g. G-CSF, was added into the media to direct the differentiation towards mature neutrophils.

At 14 days after incubation in terminal differentiation media, the cells were collected to evaluate the morphology of iPSC-derived neutrophils. Using a cytospin, the cells on the slide were stained with Giemsa and the morphology was assessed. iPSC-derived neutrophils were morphologically similar to mature neutrophils from peripheral blood (Figure 4.4).

For comparison, the morphology of CD34+-derived neutrophils and mature neutrophils isolated from the blood of healthy volunteers, is shown in Figure 4.4. Of note, the differentiated cells, both from CD34+ cells and from the iPSCs, have the distinctive multi-lobe nucleus that defines a mature neutrophil. The iPSC-derived neutrophil also has a very distinctive granular cytoplasm, which again is also seen in mature neutrophils. This granular cytoplasm represents the development of granules, small membrane-bound organelles containing a variety of proteins required for effective neutrophil function.

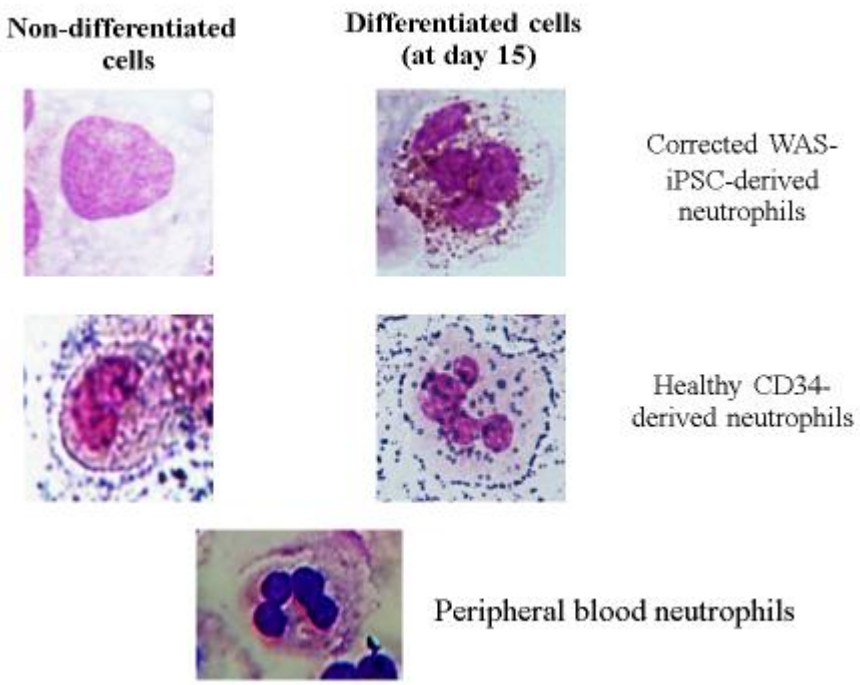

Figure 4.4: iPSC-derived neutrophils. WAS-iPSCs with genetic correction (Corrected WAS-iPSCs) were differentiated into neutrophils *via* iPS-sac formation method. At day 15 after differentiation, the morphology of cells was visualised using Giemsa stain. The positive control was neutrophils derived from human CD 34+ cells (CD 34 is a haematopoietic progenitor and stem cell marker.). The morphology was compared with peripheral blood mature neutrophils. (**Abbreviations**: Corrected WAS-iPSC-derived neutrophils = Neutrophils derived from WAS-iPSCs with genetic correction)

4.7 Discussion and limitations

The initial aim of the research described in this Chapter was to culture iPSCs from fibroblasts derived from a patient with Wiskott-Aldrich syndrome, characterise and then correct the genetic defect, and then to differentiate these iPSCs into mature neutrophils. The aim of this approach was to correct the functional defect in the mature neutrophils of these patients. This would provide the basis for considering the use of this approach to develop a new therapeutic approach for this genetic defect by the re-introduction of genetically corrected stem cells back into the patient. As (a) the stem cells were derived from somatic cells and (b) the stem cells would be re-introduced back into the same patient, there would not be the same ethical considerations and concerns as there are currently with the use of embryonic stem cells. Furthermore, as the patient's own cells would be corrected and then re-introduced, there would be no issues over tissue compatibility and the need for tissue matching or immune-suppression of the graft. Such an approach could, theoretically be applied to any human disease that results from a genetic defect that affects any type of leukocyte.

The initial parts of this approach have been achieved. First, these experiments confirmed that the WAS neutrophils had a defect in their rates of chemotaxis, which is reportedly due to the WASp playing a role in regulation of cytoskeletal re-arrangements (154,155). The actin cytoskeleton is composed of the network of polymerised actin filaments. The polymerisation actin is initiated by three classes of actin nucleator: the Arp2/3 complex; the formin family and the Spire, cordon-bleu, and leiomodin family. The unique activity of the Arp2/3 to form branched actin network is regulated by the WASp and other members of the WAS family (154). Therefore, defective WASp would prevent the actin branching and hence formation of the cytoskeleton and cytoskeletal re-arrangements during processes such as chemotaxis. It was also shown in this thesis that iPSCs could be isolated from fibroblasts from these patients and their genetic defect was identified and then corrected experimentally. Third, these iPSCs could be cultured *in vitro* and then differentiated into cells that acquired the features of mature, blood neutrophils, namely a multi-lobed nucleus and a granular cytoplasm.

The clinical manifestation of the *WAS* loss-of-function mutation, presents with normal neutrophil counts, while in the *WAS* gain-of-function mutation, the clinical

phenotype results in X-linked neutropaenia (94,96). Furthermore, in both forms of the disease, the patients suffer from increased susceptibility to bacterial infections that is often fatal (94,96). The patient studied in this thesis had the loss of function mutation, and in agreement with previous observations had normal neutrophil counts. However, it was shown here that this patient had a chemotatic defect in their neutrophils, which could at least in part explain the clinical manifestation of a proneness to infection. Neutrophils are cells of innate immunity, and the first barrier (after the penetration of endothelial or epithelial barriers), to protect our body from bacterial infections. However, their role in host defense requires them to move from the blood into the site of infection, usually transmigrating across membrane barriers. Chemotactic defects in WAS neutrophils as a result of impaired actin cytoskeleton re-arrangements as a result of *WAS* loss-of-function mutation would prevent their transmigration to the site of infection (156). As phagocytosis of bacteria also requires actin cytoskeletal re-arrangements, it would be predicted that this defect would also impair this important step in control of infections. Defective WASp expression therefore affects a number of neutrophil functions associated with control of infections. The first step of these studies was therefore to validate WAS-iPSC-derived cells as a neutrophil model, and carry out functional studies of iPSC-derived neutrophils which were expected to demonstrate the same defects as in neutrophils from WAS patients.

As the role of WASp is in the regulation of the specific actin nucleator, Arp2/3 protein, the absence of WASp, resulting from the *WAS* loss-of-function mutation, could interfere with the branch formation of actin cytoskeleton. It would be interesting to use the iPSC technology to observe the effects of loss-of-function mutation of *WAS* on the actin cytoskeleton either in resting state or during chemotaxis *via* the live imaging technology after specific staining on the actin. For example, phalloidin staining could be used to detect such changes in actin polymerisation during activation of WAS neutrophils or in neutrophils derived after differentiation of WAS-iPSCs.

However, it was not possible for me to continue these studies with iPSC-derived WAS neutrophils and to fully characterise their functions. This was partly due to technical reasons and partly due to changes in the organisation of my laboratory training. The next steps would be to determine the functional properties of both normal (healthy) and WAS neutrophils derived from differentiated iPSCs and determine if

they were both similar to those of mature neutrophils from healthy controls and WAS patients. In future functional studies, WAS iPSC-derived neutrophils should demonstrate chemotactic defects similar to the WAS neutrophils, which would confirm the use of WAS iPSCs as a model of disease. Furthermore, the chemotactic function is expected to be restored in the corrected WAS iPSC-derived neutrophils. Other neutrophil functions that require cytoskeletal re-arrangements such as phagocytosis could also be measured.

The numbers of cells derived from these iPSCs was relatively low (only a tens of cells) and so these assays would be based on microscopic techniques using specific stains or immuno-histochemistry or immuno-fluorescence. Some functional assays, such as phagocytosis and chemotaxis could also be performed by microscope-based assays. It would then be possible to determine if normal neutrophil function was restored in the WAS-defect corrected iPSCs that were differentiated into mature neutrophils.

In summary, the limited data in this Chapter show that it is feasible to isolate iPSCs from healthy control and patients with specific genetic defects and differentiate them *in vitro* into neutrophils. It is notable that the mature cells after differentiation show the characteristic granular cytoplasm and multi-lobed nucleus of mature, bloodstream cells. These characteristics are not always visible in other types of "neutrophil-like" myeloid cells that have been induced to differentiate *in vitro* (see Chapter 5). The preliminary data shown in this Chapter demonstrate clear "proof of principle" that this approach should be further developed as it offers great potential to both understand and then treat genetic diseases associated with impaired neutrophil function and increased morbidity and mortality form infections.

CHAPTER 5. PLB-985 CELLS

5.1 The myeloid cell line, PLB-985, as a model for neutrophil differentiation and understanding of human genetic conditions

Neutrophils are the major immune cells that are responsible for the clearance of bacterial and fungal infections (74), but neutrophil dysfunctions also contribute to several diseases including autoimmune diseases (157–159). However, the usefulness of peripheral blood mature neutrophils to model a particular disease is limited due to their short lifespan and inability to proliferate. Moreover, transfection of neutrophils is not possible, as the cells cannot survive long enough for clonal selection and the transfection protocols often perturb neutrophil function and induce apoptosis. Thus, it is impossible to study a particular gene of interest in human neutrophils by transfection methods and there have been few reports to reproducibly demonstrate this, in spite of many attempts (160).

Because of the difficulties in transfecting primary immune cells, alternative approaches have used animal models to characterise the functions of particular genes, particularly using gene "knock-outs" or "knock-ins" in mice. However, because of the distinct haematopoietic processes in animals, and different structural and functional properties of key genes and proteins in humans and mice, many of the clinical or cellular characteristics of human diseases cannot be reproduced exactly in these animal models (13). Therefore, the use of animal models for the study of human haematopoietic diseases is of limited usefulness. One alternative approach (other than the use of stem cells, described in Chapters 3 and 4 of this thesis), is the differentiation of human myeloid cell lines towards neutrophils. This approach uses myeloid cells isolated from human patients with malignant disease, and so the cells retain their proliferative potential, but can be induced to differentiate after suitable culture *in vitro*. However, there are a number of limitations to this approach, including the efficiency of differentiation methods and the properties of the differentiated cells. Many studies, have shown that such differentiated cells demonstrate only partial characteristics of mature neutrophils, including morphology of the nucleus, appearance of cytoplasmic granules, cell surface CD markers, and some functional capacities, in comparison to mature neutrophils (161). Therefore, the differentiated cells are generally considered

as “neutrophil-like” cells, but not fully-differentiated neutrophils. However, these cells do have many experimental advantages over other systems to study the effects of gene modifications. For example, the cultured cells are usually easy to maintain and proliferate *in vitro*, and do not require any specialised facilities other than standard tissue culture equipment. Second, they are relatively cheap to maintain in culture and do not require any expensive growth factors (other than those in serum) to be maintained. Third, they only adhere very weakly in tissue culture flasks, therefore not requiring trypsin treatment to isolate them, which can perturb the cell membrane and damage cell surface receptor expression. Fourth, they can be grown in large volumes. Fifth, there are few ethical issues to consider when manipulating the expression of particular genes and/or testing the effects of new inhibitors or potential drugs. Such cell lines are therefore widely used by many neutrophil biologists worldwide, and it is generally accepted that results obtained with differentiated “neutrophil-like” cell lines can give important insights into the functional and molecular properties of mature neutrophils.

5.2 Human myeloid cell lines as models of neutrophil function

There are several myeloid cell lines with potential to differentiate into neutrophil-like cells, with HL-60 and PLB-985 cells being the most commonly-used. Although studies of neutrophil-like cells using these cell lines have contributed many important insights into neutrophil biology, challenges remain in determining if the functional and molecular characteristics of such differentiated neutrophil-like cells completely match those of mature, peripheral blood neutrophils. In some cases, the differentiated cells do not possess all of these properties.

HL-60 cells were originally isolated from the peripheral blood of a patient with acute promyelocytic leukaemia, and the cells are at the promyelocyte stage of development with marked karyotypic abnormalities (45X, -5, -8, -16, -X, where 45X means an individual has 44 autosomes and a single X-chromosome (a normal individual has 44 autosomes with 2 sex chromosomes (either XX (female) or XY (male): -5, -8, -16, -X mean a deletion of chromosome 5, 8, 16 and one X chromosome.) (162). In previous studies, the cells can be induced into neutrophil-like cells (163) with some functional characteristics similar to mature neutrophils, for example, response to chemoattractants, including fMLP (3), and phagocytosis of certain microorganisms, including *Escherichia coli* Strain C1845 (164). However, despite their leukaemic origins, these cells have karyotypic abnormalities and limited capability to differentiate towards terminal mature neutrophils.

5.3 PLB-985 differentiated cells

The PLB-985 cell line was originally isolated from the peripheral blood of an acute nonlymphocytic leukaemia (ANLL) patient with no chromosomal translocations, and the cells have the potential to differentiate towards either neutrophils or monocytes. From DNA fingerprinting, *PLB-985* cells are considered a subclone of the *HL-60* line, despite being described as isolated years apart and from different patients (165). Previous studies revealed that PLB-985-differentiated cells could demonstrate the capability to degranulate cell compartments, which is a similar property to the terminal differentiated neutrophils in the peripheral blood (3). Therefore, PLB-985 cells can potentially be used as a model of neutrophil function, with the capacity to alter the expression of key genes ("knock-ins" or "knock-outs") and determine their effects on function. Currently our laboratory is optimising the protocols to induce the differentiation of the cells towards the mature neutrophils and to characterise their functional properties.

5.4 *Myeloid Cell Leukaemia 1(Mcl-1)* gene and neutrophils

One of the most characteristic properties of human neutrophils is their high rate of spontaneous apoptosis (166). This poses a particular problem when attempting to differentiate cells lines into mature neutrophils: as cell lines acquire the properties of mature neutrophils, they will also acquire the property of spontaneous apoptosis. Thus, very soon after differentiation they will die by apoptosis. Much research has focused on understanding the molecular mechanisms that control neutrophil survival and apoptosis, and it has been shown that *Mcl-1* is the major survival protein (166,167). *Mcl-1 (Myeloid Cell Leukaemia 1)* is an anti-apoptotic protein of the *B-cell lymphoma 2 (Bcl-2)* family, which are a group of proteins with roles in both the intrinsic and extrinsic apoptosis pathways, ultimately regulating mitochondrial integrity (1). The members of this protein family are identified by having one or more motifs of sequence homology to the eponymous Bcl-2 protein, or Bcl-2 homology (BH) domains, in their protein structure. *Mcl-1* contains 3 putative BH domains, but a unique characteristic of *Mcl-1* is the presence of regulatory residues and motifs, or PEST sequences (proline (P), glutamic acid (E), serine (S), and threonine (T)) in the N-terminal domain. This region of the protein, which is unique within the Bcl-2 family, includes sites for ubiquitination, cleavage and phosphorylation, which alter the protein's stability, localisation, dimerisation and function (168).

The altered expression of *Bcl-2* family members, usually over-expression of the protective anti-apoptotic proteins, is a common feature of ANLL and other leukaemias, in particular chemoresistant clones (169). Among the anti-apoptotic *Bcl-2* family members, *Mcl-1* is reported to be critical in the survival of ANLL cells, as deletion of the *Mcl-1* gene, but not *Bcl-*X_L, resulted in ANLL cell death (170). However, *Mcl-1* expression in mature neutrophils is more dynamic. Neutrophils constitutively undergo apoptosis such that their normal lifespan is between 8 - 20 h, but this can be extended in response to a variety of agents (171). Mcl-1 protein normally has a short half life in neutrophils, with a high rate of turnover due to its PEST motifs, which target the protein for rapid proteolysis *via* ubiquitination. In neutrophils, the role of Mcl-1 is to block the pro-apoptotic actions of Bak (and/or Bim) at the outer mitochondrial membrane and thus delay neutrophil apoptosis (167).

As mature neutrophils do not express *Bcl-2* or *Bcl-X* (171), differentiated PLB-985 cells should become less dependent on these two proteins and more dependent on *Mcl-1* for their survival. However, as stated above, because of the short half life of neutrophils, fully differentiated PLB-985 cells should also undergo spontaneous apoptosis. Therefore, one way to extend the lifespan of fully differentiated PLB-985 cells may be to over-express *Mcl-1*. The aim of this Chapter, therefore, was to generate PLB-985 clones stably transfected with an inducible *Mcl-1:EGFP* gene, to determine the sub-cellular localisation of this protein and assess if its inducible expression could prolong the lifespan of fully differentiated cells. If the survival of PLB-985 cells differentiated into mature neutrophils could be extended experimentally, then this would allow for a more useful experimental system to study the effects of genetic manipulations on the function of mature neutrophils.

5.5 pLVX-TetOne-Puro system, and the study of *Mcl-1* gene in neutrophil model

For these experiments, the pLVX-TetOne-Puro system (Clontech, USA) which is one of the Tet-One systems, was used. This vector allows for inducible gene expression within mammalian cells and contains all the necessary components for inducible expression in a single lentiviral vector. After transducing the cells with lentivirus, the cells will express the Tet-On 3G transactivator protein and contain the cloned gene of interest (GOI) under the tight control of a TRE3G promoter (P_{TRE3GS}). When doxycycline (Dox) is present in the cell culture, this antibiotic binds to the Tet-On 3G protein to induce a conformational change to allow the protein to bind to the *tet* operator sequences in the P_{TRE3GS} promoter, initiating the transcription of the GOI. Therefore, in order to maintain inducible GOI expression, the cell culture medium should be replenished with doxycycline every 48 h.

5.6 KCL-22 versus PLB-985 as cell lines suitable for differentiation into mature neutrophils

During a recent Ph.D. project (172), another myelogenous leukaemic cell line, namely KCL-22, was studied and characterised for its ability to resist apoptosis. The KCL-22 cell line is originally derived from the pleural effusion of a patient with chronic myelogenous leukaemia in blast crisis. Chromosome analysis revealed a female karyotype with double Philadelphia chromosomes (genetic abnormality in chromosome 22 due to reciprocal translocation of genetic material between chromosome 9 and 22, to result in a fusion gene called *BCR-ABL1*, a constitutively active tyrosine kinase) and additional chromosome abnormalities (173).

It was reported in this thesis (172) that KCL-22 cells (a CML cell line) do not express *Bcl-2* but they do express *Mcl-1*. This suggests that they may represent immature cells committed to the neutrophil lineage. Therefore, preliminary experiments were also performed to determine if KCL-22 cells could differentiate *in vitro* to acquire the properties of mature neutrophils. The ability of these cells to differentiate was compared to that of PLB-985 cells.

5.7 Aim and objectives

The aims of this Chapter are to determine the efficiency of differentiation of PLB-985 cells into mature neutrophils and to develop stably-transfected cell lines expressing *Mcl-1:EGFP*. The objectives therefore were to:

1. To compare the efficiency of differentiation of PLB-985 cells with that of CML cell line, KCL-22

2. To clone *Mcl-1:EGFP* into an inducible lentiviral expression vector to establish transfected PLB-985 cell line

3. To differentiate PLB-985 cells into neutrophil-like cells

5.7.1 Conceptual framework

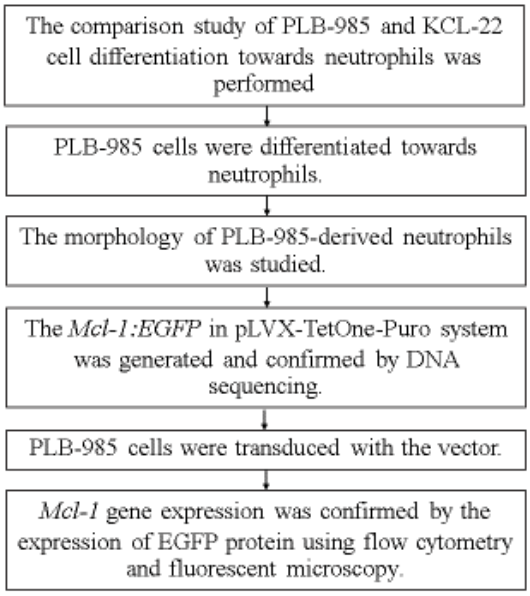

Figure 5.1: Conceptual framework for the study of myeloid cell line, PLB-985, as a model for neutrophil differentiation and understanding of human genetic conditions

5.8 Results

5.8.1 Differentiation of PLB-985 cells and KCL-22 cells into neutrophils

PLB-985 cells and KCL-22 cells are myelogenous leukaemic cell lines that have the potential differentiate into neutrophils. The differentiation capability of KCL-22 cells into neutrophils were studied in comparison with PLB-985 cells, as previous work in this laboratory showed that KCL-22 cells are more neutrophil-like in terms of the expression of Bcl-2 family protein (172). This suggests that KCL-22 cells are more mature along the neutrophil differentiation pathway than PLB-985 cells, as mature neutrophils do not express Bcl-2 or Bcl-X_L. At either day 5 or 7 of culture in differentiation media (see Methods), the cells were collected and cytospins were stained with Rapid Romanowsky stain (30 s in methanol for a fixation, 20 s in an anionic dye, Eosin Y, and 30 s in a cationic dye, Azure B). The cell morphology was evaluated using the criteria in Table 2.4 and Figure 2.4. One hundred cells were randomly counted, and the percentage of cell differentiation at different stages were evaluated. The cell viability was assessed using ViaCount® reagent and flow cytometry.

In PLB-985 cell experiments, the cells were collected every day at 08.30 (also time zero) and 18.30 to closely observe the time of differentiation. At timepoint 18.30 on day 3 of the differentiation, approx. 30% of cells were differentiated into the poly-segmented cells (Table 5.1). During day 4 and 5 of the differentiation, the number of the differentiated cells increased, with the more mature nuclear morphology of differentiated cells, including increased appearance of a hypersegmented (4 – 5 segments) nucleus similar to that found in mature neutrophils.

As a control, PLB-985 cells were also cultured in the maintenance culture medium in parallel. The morphological characteristics of non-differentiated PLB-985 cells, including mononuclear appearance with deep blue cytoplasm, were unchanged throughout the experiments. In the study of cell viability, the percentages of viable cells were > 90% until day 4 of the experiments. However, the cell viability in both differentiation and control (no differentiation) studies revealed similar trends during 5 days of the experiments (Figure 5.3). The percentages of differentiated cells at day 5 were as follows: differentiated cells (67.5%), band form/segmented/partially

differentiated cells (22.35%), and non-differentiated cells (10.15%). (Table 5.1; Figure 5.2)

Table 5.1: The percentages of PLB-985 cell differentiation. Cytospins were obtained at the time-points indicated and the percentages of fully-, partial- and non-differentiated cells was calculated. Fields of cells were selected at random and for each field, at least 100 cells were counted and compared. Three cytospins were prepared at each time-point.

Differentiation day (and time)	**Percentages of differentiated cells**	**Percentages of band form/ segmented/ partially differentiated cells**	**Percentages of non-differentiated cells**
1	The differentiated cells were rarely observed.		
2	The differentiated cells were rarely observed.		
3 (8.30)	The differentiated cells were rarely observed.		
3 (18.30)	30.1	25	44.9
4 (8.30)	31.7	42.0	26.3
4 (18.30)	54.7	29.9	15.4
5 (8.30)	61.5	27.6	10.9
5 (18.30)	67.5	22.4	10.1

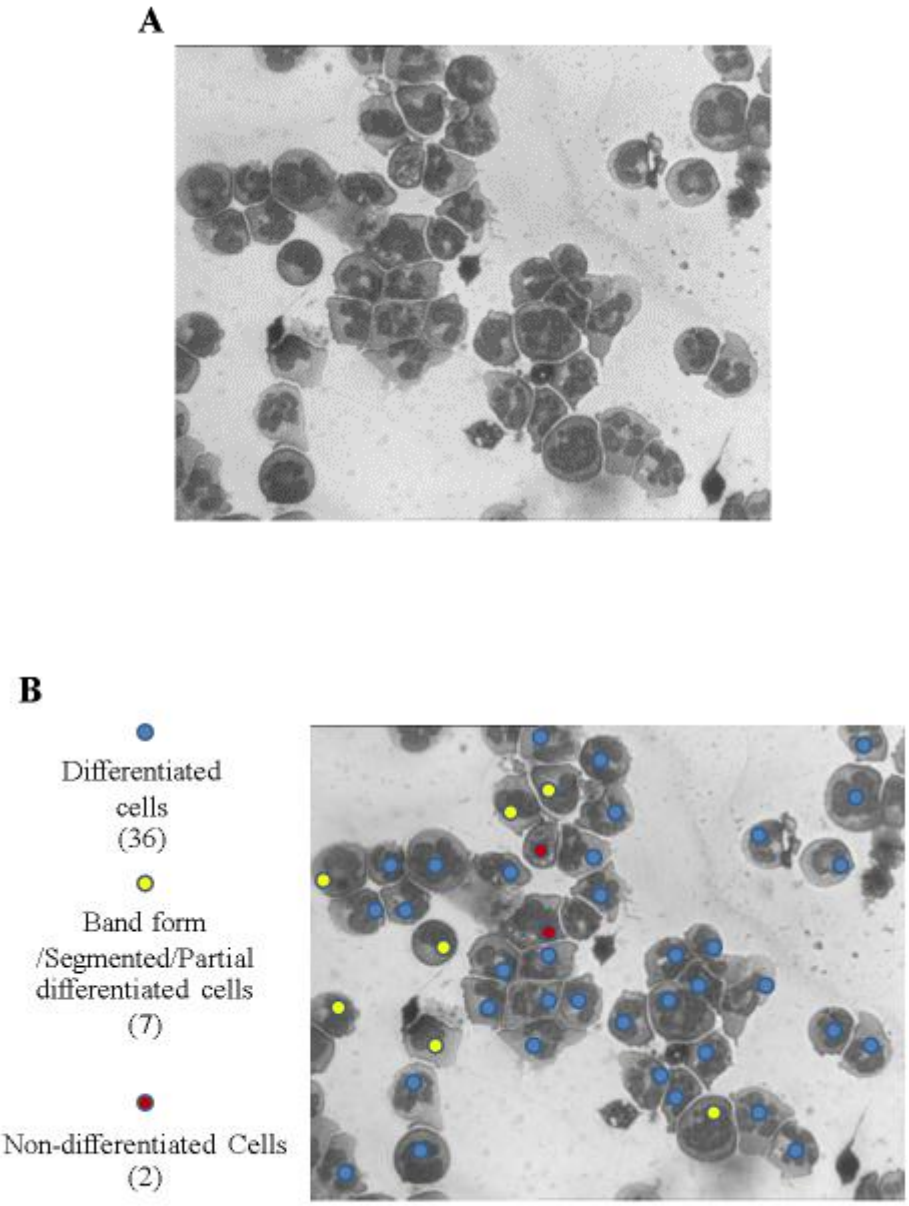

Figure 5.2: The catergorisation of PLB-985 cell differentiation. The images shown were obtained from the PLB-985 cells at day 5 (18.30) of culture in differentiation medium. Each circle was used to label the cells at the different stages of the differentiation (see Table 2.4; Figure 2.4). A **BLUE** circle was used to identify the differentiated cells. A **YELLOW** circle was used to label the band form/ segmented/partially differentiated cells. A **RED** circle was used to label the non-differentiated cells.

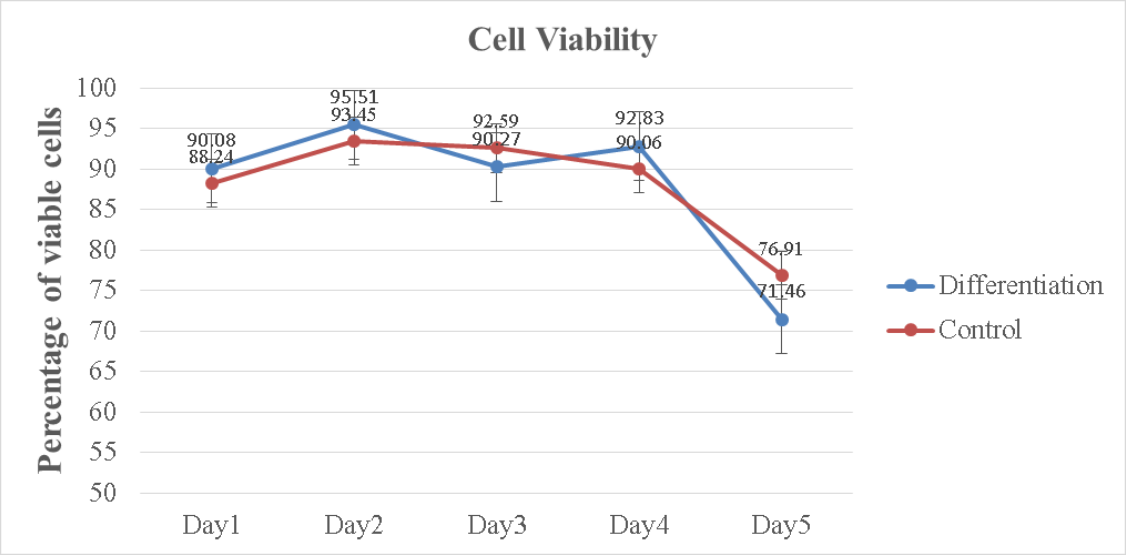

Figure 5.3: The percentage of viable cells during culture of PLB-985 cells in maintenance medium or differentiation medium. The **BLUE** line indicates the PLB-985 cells in the differentiation medium, the **RED** line indicates the PLB-985 cells in the maintenance medium as a negative control. During the first four days of the experiments, the percentages of viable cells were more than 90% in both groups, but, the % viable cells were significantly decreased to approx. 70% at the final day of the experiment.

For KCL-22 cells, the cells were poorly differentiated into neutrophil-like cells when the PLB-985 cell differentiation protocol was applied (see Section 2.3.1;2.3.2) (Figure 5.4). Therefore, the differentiation time was increased (from 5 to 7 days) and the potential differentiating and survival agents were added into the differentiating media including GM-CSF, dimethyl sulfoxide (DMSO) and human AB serum. However, these differentiating and survival agents did not seem to improve the differentiation efficiency of KCL-22 cells. However, interesting findings were found in the differentiation media 3 (with the addition of 5 ng/mL GM-CSF) and 4 (with human AB serum instead of FBS). The nuclear morphology observed after incubation in these two conditions changed into the partially-segmented forms at as early as day 2 differentiation (27% in differentiation media 3 and 45% in differentiation media 4). However, these morphological changes in the nucleus could not be maintained and these neutrophil-like cells could not be observed in the following days of culture (Figure 5.5).

In conclusion, using the current protocols that have been optimised for differentiation of PLB-985 cells were not efficient for differentiation of KCL-22 cells after day 5 incubation. Despite the previous study in our lab (172) suggesting the possible origin of KCL-22 cells as immature neutrophil lineage, the current available protocols could not differentiate the cells into the stage of the neutrophil-like cells. Therefore, the PLB-985 cells were selected for the further studies as a model for neutrophil study.

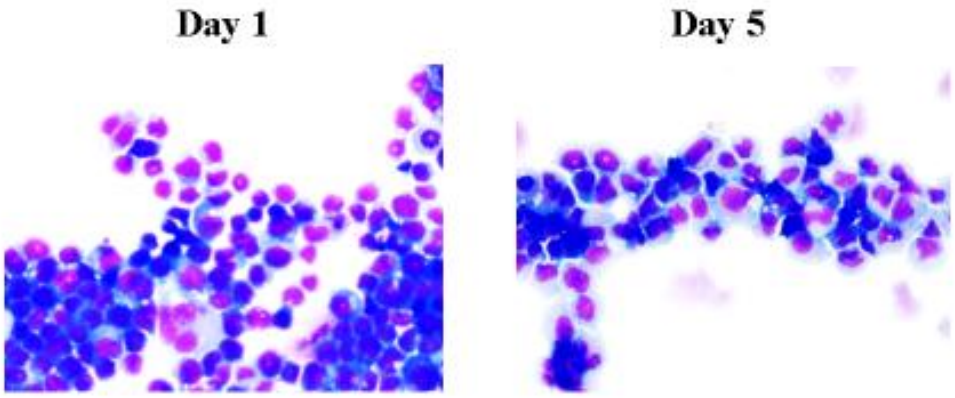

Figure 5.4: KCL-22 cells cultured in differentiation medium. The PLB-985 differentiation protocol was applied to KCL-22 cells, however, at day 5, no KCL-22 cells were differentiated into neutrophil-like cells.

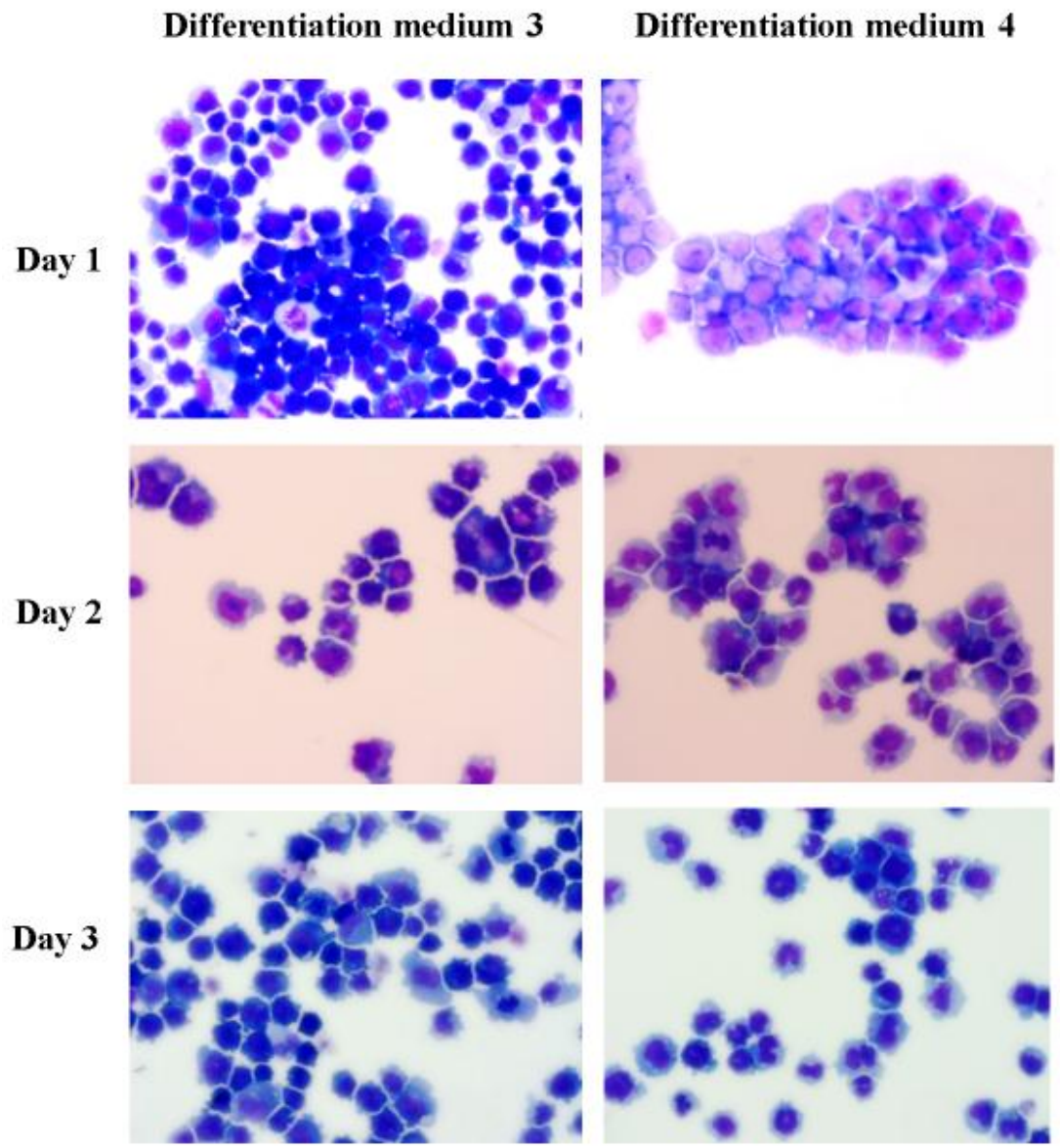

Figure 5.5: The KCL-22 cells in differentiation media 3 and 4 during the first 3 days of culture. The differentiation media were described in Table 2.3 (in Chapter 2). Briefly, in differentiation medium 3, 5 ng/mL GM-CSF was added to the differentiation medium 1 (similar to PLB-985 cell differentiation medium), and in differentiation medium 4, human AB serum replaced FBS. Unlike for the other differentiation media, the KCL-22 cells in these 2 media were partially differentiated at as early as day 2. However, no differentiation could be observed in the following days.

5.8.2 The generation of *Mcl-1:EGFP* in pLVX-TetOne-Puro vector

One of the main objectives of the work in this Chapter was to generate transfected clones of PLB-985 cells that could be induced to express a *Mcl-1:EGFP* chimeric protein. Such chimeric proteins (and mutants thereof) have been useful to probe structure/function relationships of key residues in this anti-apoptotic protein and to visualise the location of this protein by confocal microscopy (168,174,175). Cloning of this gene under the control of an inducible promoter will enable the role of this protein to be explored in differentiated cells that are normally subject to high rates of apoptosis.

The *Mcl-1* gene was originally cloned in pEGFP-C3 (Clontech, USA), in which *Mcl-1* gene is located next to *EGFP* gene (Figure 5.6). The *Mcl-1* gene was ligated into the pEGFP-C3 vector between the restriction sites, HindIII and BamHI. The first aim was to sub-clone this chimeric cDNA into the new inducible expression vector (pLVX-TetOne-Puro) to allow for the transfection of the PLB-985 cells.

A

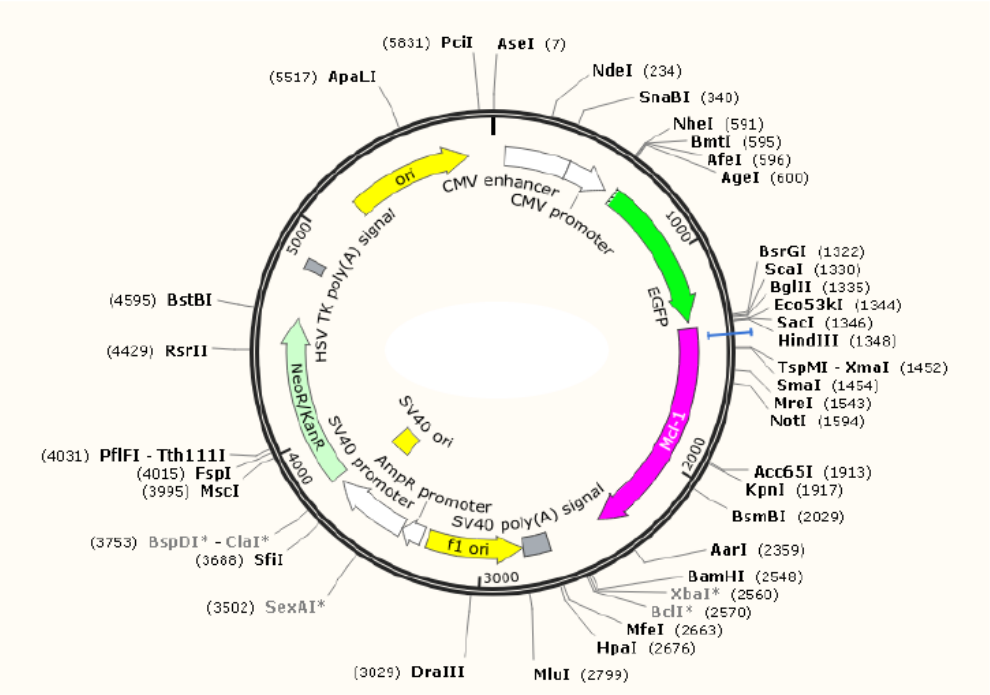

Mcl-1 in pEGFP-C3
5,889 bp

B

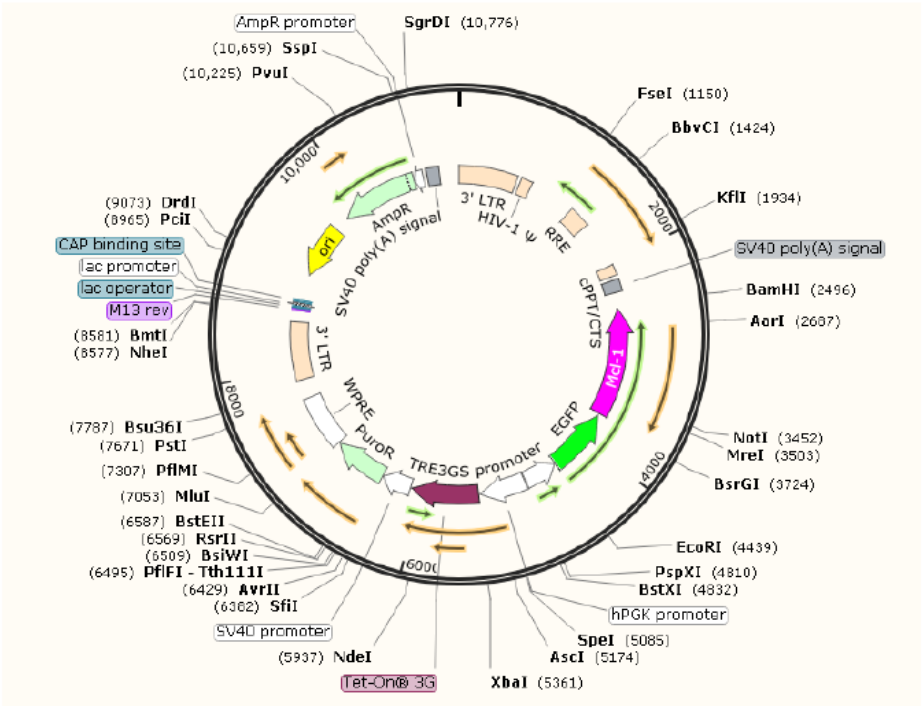

***Mcl-1:EGFP* cDNA into pLVX-TetOne-Puro vector**
11,144 bp

Figure 5.6: Restriction maps of *Mcl-1:EGFP* in the original pEGFPC3 (A) and after sub-cloning in pLVX-TetOne-Puro (B).

5.8.3 Sequence analyses of the *Mcl-1:EGFP* cDNA in the pLVX-TetOne-Puro vector

The sequence of the new expression vector containing the *Mcl-1:EGFP* cDNA was confirmed to determine whether the gene was correctly inserted into the vector, and whether the sequence of the insert gene, *Mcl-1:EGFP*, was correct. Sanger sequencing, the method of DNA sequencing based on the selective incorporation of chain-terminating dideoxynucleotides by DNA polymerase, was performed by Macrogen Korea to determine the nucleotide sequence in the insert cDNA. The Sanger sequencing results were provided as coloured chromatographic peaks. The first step in the analysis was to ensure the quality of the peaks, and then the sequences were studied in comparison with the original sequences of *Mcl-1* and *EGFP* from the database (Figure 5.7; 5.8). The Basic Local Alignment Search Tool (BLAST), National Center for Biotechnology Information (NCBI), USA, was used to compare the nucleotide sequences (the sequencing results) to those deposited in sequence databases.

The sequencing results obtained from using the primer covering the junctional area, between *Mcl-1* and *EGFP*, were first analysed. The results were matched with the original sequence from the database, however, towards the end, the nucleotide sequences were mismatched, from 7G in the database to 8G in the sequencing results (Figure 5.8). The Sanger sequencing results were re-evaluated and revealed the low-quality of sequencing data at that area. Therefore, the sequencing results from the primer to cover the *Mcl-1* gene were analysed, and these revealed perfectly matched sequences. As a consequence, the *Mcl-1:EGFP* in the pLVX-TetOne-Puro vector was successfully cloned and hence used in the subsequent experiments.

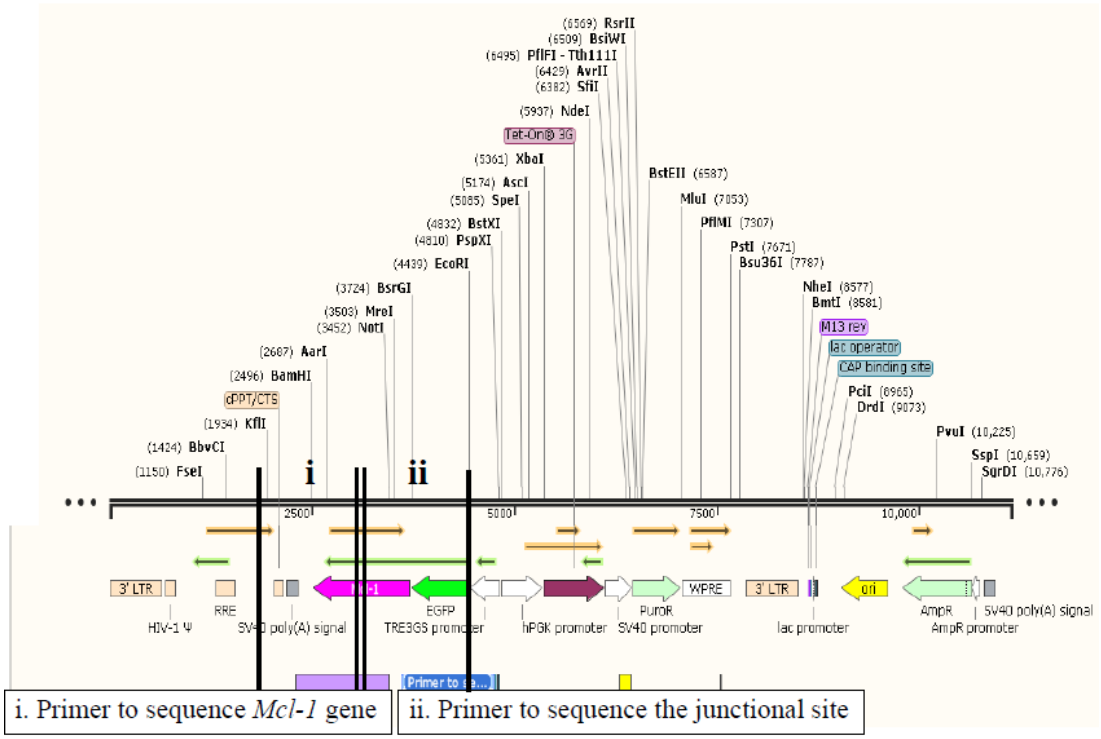

***Mcl-1:EGFP* cDNA into pLVX-TetOne-Puro vector**
11,144 bp

Figure 5.7: The mapping sequence of a *Mcl-1:EGFP* cDNA in the pLVX-TetOne-Puro vector. The **PINK** and **GREEN** arrows indicate the *Mcl-1* and *EGFP* insertions, respectively. (i) The DNA segment that was sequenced by the primer designed for covering the *Mcl-1* gene and the insertion site. (ii) The DNA segment that was sequenced by the primer designed for covering the junction between *Mcl-1* and *EGFP* genes.

A

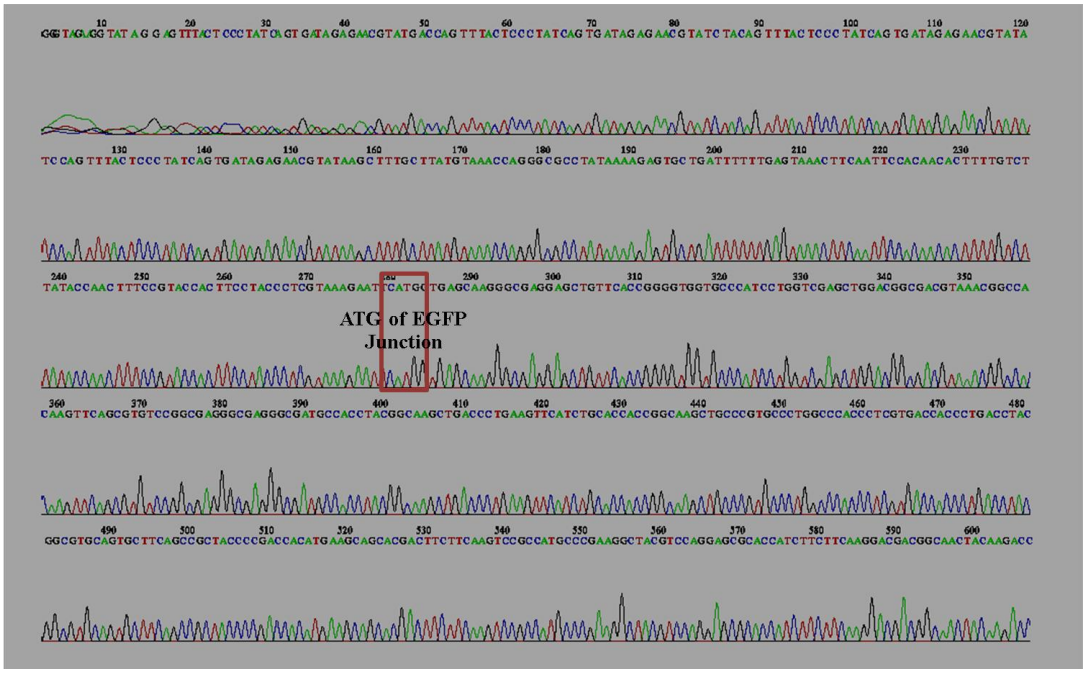

B

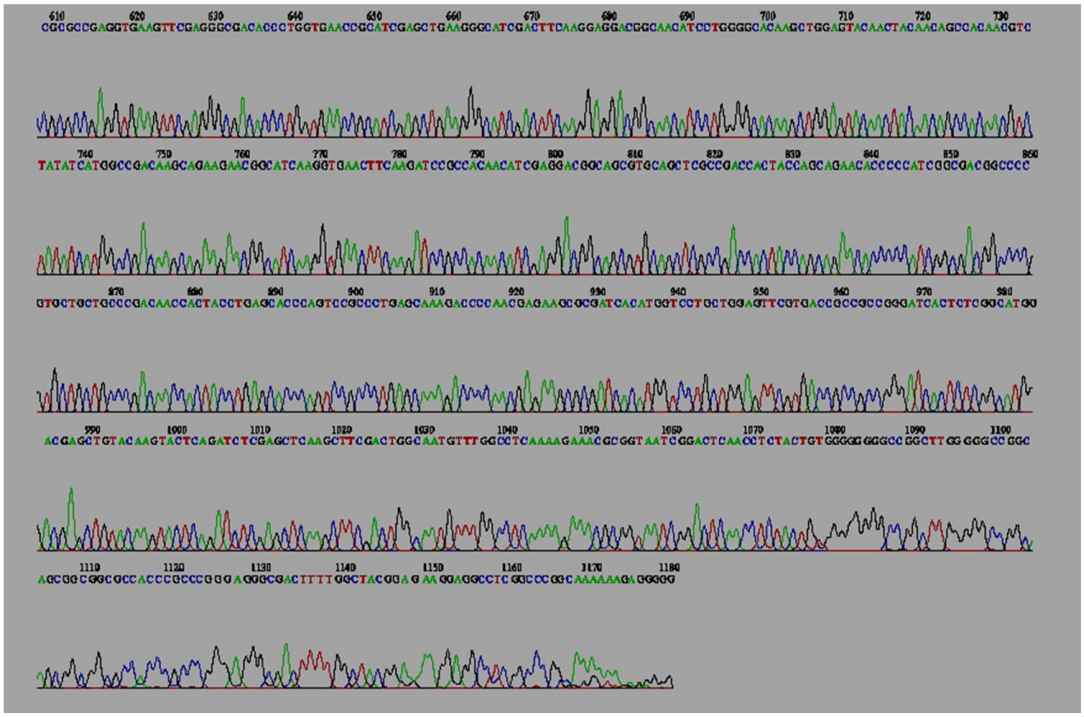

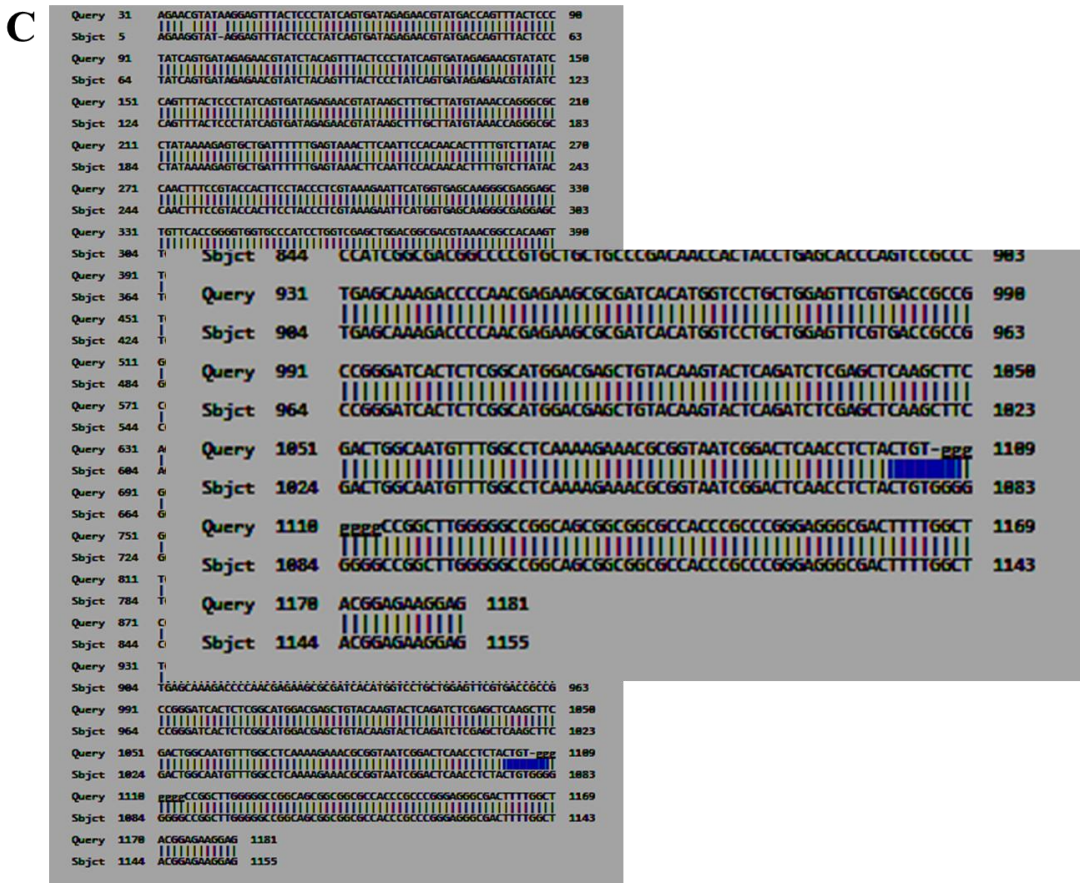

Figure 5.8: The sequencing results of *Mcl-1*:*EGFP* cDNA in the pLVX-TetOne-Puro vector. (A, B) The Sanger sequencing results of the primer designed to cover the junctional area between *Mcl-1* and *EGFP* in the vector. (C) The comparison of the nucleotide sequences and the database sequences using Basic Local Alignment Search Tool (BLAST) online programme.

5.8.4 The PLB-985 cell transduced with *Mcl-1:EGFP* in pLVX-TetOne-Puro vector

The PLB-985 cells were then transduced with *Mcl-1:EGFP* in pLVX-TetOne-Puro vector and transformants were selected by the addition of puromycin antibiotics. However, it was possible that some colonies arose from more than one transformed PLB-985 cell, and some transformed cells were transfected with more than one copy of the vector. Therefore, clonal selection was performed to ensure that only clones containing a single copy of the vector were used in subsequent studies. The serial dilution method was used, and 16 individual clones of the transduced PLB-985 cells were derived.

Experiments were then conducted to induce the expression of *Mcl-1:EGFP* chimeric gene by the addition of 100 ng/mL doxycycline, and to allow the protein expression (measured after 24 h in the presence of the antibiotic). As the *Mcl-1* gene was tagged by *EGFP*, the Mcl-1 protein expression should be observed by the fluorescence of the EGFP, using either flow cytometry or the fluorescence microscopy to visualise the green fluorescence. Initially, flow cytometry was performed. However, the data was inconsistent. In one experiments, green fluorescence was detected in all 16 clones, but in subsequent experiment to confirm the expression prior to the fluorescence microscopy, the flow cytometry failed to detect the green fluorescence in all 16 clones despite multiple attempts. Therefore, further experiments should be conducted to directly confirm the presence of the vector in the cells, rather than indirect confirmation based on the puromycin resistant properties on the PLB cells. Additionally, re-cloning the transformants using alternative methods, including the fluorescence activated cell sorting (FACs) could improve the confidence in obtaining single clones.

5.9 Discussion

Despite the recognised role of neutrophils as the major innate immune cells in eliminating bacteria and fungi during infections, and the importance of neutrophil dysfunctions in the underlying pathologies of many diseases (159), the use of the peripheral blood neutrophils to study and model the disease is limited partly due to their short life span. Moreover, the transduction of neutrophils to genetically modify their function, is rarely successful. Therefore, myeloid leukaemic cell lines are still the main resource to model human neutrophil function *in vitro*.

In this thesis, the two myeloid leukaemic cell lines, PLB-985 and KCL-22 cells, were compared, to determine their efficiency to differentiate into neutrophil-like cells, in these experiments determined by the appearance of a polymorphic nucleus. This was performed to select which line would be more suitable to establish the transfected *Mcl-1:EGFP* in an inducible lentiviral expression vector. However, the differentiation protocol used, containing all-trans retinoic acid and N,N-dimethyl formamide as differentiating agents, was first developed for PLB-985 cells. Using this protocol and medium, it was shown that the percentage of differentiated cells at day 5 was as high as 67.5% and the nuclear morphology of the differentiated cells was also similar to that of mature neutrophils (Table 5.1). Ongoing studies in our lab are explore other characteristics and functional properties of differentiated PLB-985 cells, in comparison with those of peripheral blood neutrophils.

A previous study in our lab reported (172) that KCL-22 cells (a CML cell line) did not express *Bcl-2* but they do express *Mcl-1*, suggesting that these immature cells are committed to the neutrophil lineage. It was postulated, therefore, that it would be relatively easy to fully differentiate these cells into neutrophils, as they already displayed some of the molecular properties of mature cells. While different medium supplements were tested, the percentages of differentiated cells were significantly lower compared to those obtained after differentiation of PLB-985 cells. However, in differentiation media 3 and 4, the cells began to develop into partially differentiated cells, but not fully differentiated to neutrophil-like cells, as seen by a change in the morphology of their nuclei. These nuclear changes, however, could be observed as early as day 2, compared to the day 3 in PLB-985 cells, but differentiated cells were not seen in later days of incubation. This could be because only a small population of

cells underwent differentiation, and these differentiated cells that were observed after the first few days in culture then underwent apoptosis. Further experiments, employing more systematic changes to the composition of the differentiating media should be conducted in future to determine if differentiation efficiency can be improved and there is any experimental advantages in using KCL-22 cells as models for neutrophil differentiation.

It was concluded that rather than attempting this systematic attempt to improve the differentiation conditions for KCL-22 cells, to instead use PLB-985 cells as a neutrophil-like cell line for the transfection experiments. PLB-985 cells were therefore transduced with the *Mcl-1:EGFP* cDNA cloned into an inducible lentiviral expression vector to establish transfected PLB-985 cell lines. The expression system has two particular advantages for studying the role of *Mcl-1* expression on the survival of differentiated PLB-985 cells. First, the system can allow for the controlled, inducible expression of *Mcl-1* by the addition of the doxycycline. Therefore, the *Mcl-1* expression could be "turned on" (in the presence of doxycycline) and "turned off" (in the absence of doxycycline) at any particular stages of PLB-985 cell differentiation, and the effects of these changes on differentiation, function and apoptosis determined. Second, the *Mcl-1* was tagged with *EGFP*, and so *EGFP* expression could be used as an easily-measured reporter for expression of *Mcl-1*.

In the first step of this approach, the PLB-985 cells were transduced with the *Mcl-1:EGFP* in the inducible lentiviral expression vector, and the sequence was confirmed. Also, initial analyses using flow cytometry confirmed EGFP expression in all clones. However, following isolation of single clones, expression of EGFP could not be re-induced in all clones obtained. The possible explanations to this failure to detect expression of the EGFP reporter could be as follows:

1. Failure of the doxycycline to induce expression. It was first assumed that the doxycycline stock had degraded and lost activity, and so a new batch was used. However, this new batch also failed to induce expression of the reporter.
2. The initial results on the mixed cell populations was in fact a false positive of the green fluorescent detection by flow cytometry. While care was taken to set up the flow cytometer correctly, it may be that the initial experiments actually detected endogenous fluorescence rather than EGFP fluorescence.

3. PLB-985 cells are myeloid leukaemic cells that multiply at a high rate. Therefore, it is possible that they were cultured for too long were limited in a particular nutrient, and because of this they either failed to express the exogenous gene or in the initial experiments, the stressed cells expressed a high level of endogenous fluorescence.
4. It is possible that either the lentivirus was excised from the genome or became dysfunctional during the cell cloning procedures, or that the cloning procedure only selected non-transformed cells.

However, the parallel experiments being conducted in this laboratory on PLB-985 differentiation into neutrophils is extremely promising and the differentiated cells display many of the properties of mature neutrophils including a multi-lobed nucleus. Therefore, although the experiments in this Chapter did not reach a conclusion, they should be followed up. In particular, more work should be done to isolate transfected PLB-985 cells with *Mcl-1:EGFP* and to confirm inducible expression of this protein. This would appear to be a useful avenue to fully exploit the usefulness of this neutrophil like cell model.

CHAPTER 6 METABOLOMICS

6.1 Post-genomic technologies

Recent developments in post-genomics technologies have provided unprecedented information on the fine details of the components of living cells and tissues. Advances in next-generation sequencing in the early 2000s and the development of new sequencing platforms greatly decreased both the times and costs of DNA sequencing and as a consequence there has been an unparalleled acquisition of knowledge and information about the genomes and transcriptomes of a wide variety of tissues and species. Advances in proteomics technologies have also developed greatly during this period, but high-throughput, non-biased methodologies based on chromatography and mass spectrometry have been more difficult to develop. However, advances in this field of post-genomics biology have been considerable, and both approaches generate vast amounts of data that has necessitated the parallel development of software and algorithms to capture, record and interpret the data that are generated.

A criticism of transcriptome studies sometimes raised is that the transcriptome only provides the potential templates for proteins that may, or may not be translated. Quite often, it is necessary to confirm that a change in expression of a protein in a cell type or tissue corresponds with a change in the level of a transcript (176). However, even such a dual measurement (of a gene and a protein) is insufficient to measure the *activity* of a gene product within a cell. The activity of a protein, say an enzyme, is dependent on the total amount of enzyme expressed and its activity, which may be reversibly regulated by post-translational modifications (for example reversible phosphorylation), but also by other control mechanisms such as allosteric control (binding of an activator or inhibitor) or by the concentrations of substrates or products. Changes in the concentrations of substrates or products can result in either positive or negative feedback control mechanisms. For these reasons, there is a need to measure the total *concentrations of metabolites* in a cell or tissue to gain a full understanding of the biological functions of that cell or tissue.

6.2 Metabolomics

Metabolomics is the quantitative study of the complement of metabolites produced or present within a biological system. Currently, there are the two major metabolomic analytical platforms: nuclear magnetic resonance (NMR) spectroscopy and mass spectrometry.

NMR spectroscopy is an analytical chemistry technique using the application of an external magnetic field and complex radio frequency 'pulses' to observe the resonance or chemical shift from each atom of a particular nucleus (typically ^{1}H). Once the external magnetic field is applied, the protons in a molecule align themselves either with or against the magnetic field, thus creating an energy difference between two states, of lower and higher energy transition states. The NMR spectrum is observed when the radiation applied matches with these energy differences. In this manner, a spectrum is produced with multiple signals arising from each molecule. The location of each signal is recorded as the chemical shift, which is a measure of how different in chemical environment (or how shielded) the ^{1}H is compared to the reference compound signal. The chemical environment of each ^{1}H is affected by electronegativity, chemical bonds, charged nuclei, hydrophobic interactions etc. The unit of chemical shift is parts per million (ppm). Apart from the external magnetic field, the molecules already contain their own magnetic environment due to the movement of electrons around the protons, thus shielding the effect of the external magnetic field (called diamagnetic shielding). Thus, the protons in electron dense environments are enormously shielded, and therefore will require a lower frequency to exhibit resonance because the energy difference is smaller. The ppm will be smaller and located farther towards the right side hand of the spectrum (towards null ppm), and *vice versa*.

Mass spectrometry metabolomics is an analytical technique that requires the chemical molecules to be ionised and sorted according to their mass-to-charge ratios (177). To enhance the information on the chemical properties of metabolites, other separation techniques, for example liquid or gas chromatography, are often applied prior to the samples becoming introduced into the spectrometer (178). This pre-step requires more time for sample preparation, which may increase the chance of metabolite losses, for example as a result of breakdown or instability. Therefore, the

complexity of mass spectral data is decreased due to this metabolite separation step and also processing times are increased. There also needs to be some selection of the type of separation step required in order that a particular set of metabolites are introduced into the spectrometer. Nevertheless, the technique provides abundant information of low-molecular mass metabolites (< 1,500 Da**).**

Table 6.1 Comparison of two major metabolomics analytical platforms (nuclear magnetic resonance (NMR) spectroscopy metabolomics and mass spectrometry (MS) metabolomics)

	NMR Spectroscopy Metabolomics	**Mass Spectrometry Metabolomics**
Preparation process and time	Less time, non-destructive	More time, derivitisation required
Detected metabolites	Untargeted, metabolic fingerprinting	Targeted, metabolic profiling
Analyses	Quantitative analyses, pattern comparison	Quantitative analyses, metabolite libraries
Sensitivity	Only medium to high abundance metabolites	High sensitivity
Considerations	True “omics” data	Not true “omics” data
Advantages	Metabolic pathway analyses	Identify specific metabolites

6.3 NMR spectroscopy for neutrophil metabolomics

It was decided to use the NMR methodology to study neutrophil metabolomics, as this technique allows quantitative analyses of untargeted metabolomic profiles, while MS metabolomics is more suitable when specific metabolites are being targeted. Briefly, NMR spectroscopy exploits the magnetic properties of certain atomic nuclei, to determine their chemical and physical properties. Any molecules containing the atomic nucleus of interest, ^{1}H in this case, will be detected. Therefore, as the ^{1}H nucleus is abundantly present in many metabolites, ^{1}H-NMR spectroscopy is highly suitable for use as a metabolic profiling technique in biological samples. However, there are no published reports of the use of this technique in the study of neutrophil function. Therefore, for this study, NMR protocols for the identification and quantitation of metabolomic profiles of human neutrophils have been developed for the first time.

In biofluid NMR, there are two preferential pulse sequences, where the observed peak intensities are edited, for metabolomic profiling (130). First, the 1D Nuclear Overhauser Effect Spectroscopy with pre-saturation (NOESYpresat) approach provides adequate suppression of the solvent (water) resonance. The NOESY spectrum is high sensitivity and therefore suitable for identifying specific metabolites present in low quantities. Second, the 1D Carr-Purcell-Meiboom-Gill (CPMG) sequence allows for magnetic filtering for metabolites of low molecular weight (less than 1,000 Da) and macromolecular species in the sample (e.g. proteins, lipoproteins) from the spectrum, without any physical manipulation of the sample required. With the higher discrimination power, the CPMG spectrum provides more distinct peaks which allows the comparison of spectral peaks in each samples (179).

NMR spectra of biofluids and pattern recognition methods in metabolomics have enabled the identification and quantitation of metabolites in different biological samples, thus providing highly informative data about the functional state of living organisms, including humans.

6.4 Neutrophil metabolomics

Neutrophils are innate immune cells that kill invading microbes mainly through the phagocytosis and production of reactive oxygen species (ROS). These reactions are activated in the matter of seconds, and so analysis of samples taken after suitable experimental time-points are an important consideration when planning metabolomic experiments to detect changes in neutrophil function. For example, one of the hallmarks of neutrophil function is the activation of the normally dormant NADPH oxidase during phagocytosis or other forms of activation, which can result in large but transient changes in the NADP+/NADPH ratio very rapidly after cell stimulation (Figure 6.1). This activation occurs rapidly, is sustained for several minutes and then declines. This is likely to be accompanied by transient and rapidly changing profiles of other metabolites.

Figure 6.1: The chemical equation of NADPH oxidase reaction in neutrophils

The first aim of this study was to establish the optimal methods to study changes in the neutrophil metabolomic profile during various forms of *in vivo* or *in vitro* activation. Therefore, it was necessary to establish protocols to optimise sample preparation, extractions and analysis methods that minimise the chemical and physical degradation of metabolites due to their natural diversity, instability and high turnover rate. This protocol development is necessary because this study represents the first time that metabolomic profiling of neutrophils has been attempted in this way. In NMR metabolomics, there is no excessive preparation time required, thus increasing the potential to detect any transient metabolites in neutrophils, provided that they can be extracted appropriately.

Therefore, the first experiments in this study were to optimise the extraction and analysis procedures and to compare the metabolomic profiles obtained with spectra of known standards. Once this was established, it could then be possible to determine how the metabolome of neutrophils changes over time during activation *in*

vitro (e.g. using fMLP, PMA) or following priming by cytokines (e.g. GM-CSF, TNF). Once this was established, it would then be possible to identify the metabolome of neutrophils activated *in vivo*, for example in patients with rheumatoid arthritis.

6.5 Conceptual framework

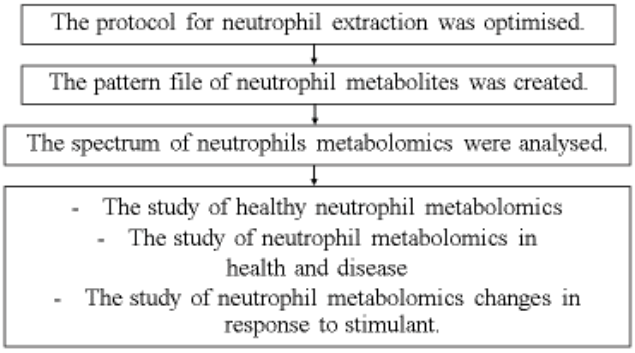

Figure 6.2: Conceptual framework for optimising protocols and analytical methods for neutrophil NMR metabolomics

Definition of terms used in this Chapter

- Spectrum/Spectra/Spectral, define the whole range of peaks in the NMR sample.

- Peak, defines the specific peak in the spectrum.

- Metabolic, is used to specify anything related to specific metabolites.

- Metabolomics, is used to specify anything related to the metabolomic study.

- NMR, is used when the technique of NMR analyses was being focused.

6.6 Preliminary spectral analyses and the generation of a pattern file for neutrophil NMR metabolomics

In metabolomics, the metabolites are recognised by their specific spectral patterns. Chenomx Profiler® software (version 8.2 standard) is used to detect the specific spectral pattern in the NMR data, interpret these patterns and then provide identification of the metabolites. Pattern files are therefore generated by the use of the Chenomx Profiler® software (version 8.2 standard) and the NMR spectra visualised by the Bruker TopSpin® software, to provide lists of molecules (pattern files).

To create the pattern files, the NMR spectral data of a sample that was assumed to contain the highest number of metabolites was analysed. As circulating blood neutrophils are in a resting state in healthy individuals, blood neutrophils from a healthy control were stimulated *in vitro* before extraction and analysis. As this approach had not been applied to human neutrophils previously, intracellular concentrations of metabolites detected by this technique were not known. Therefore, the initial experiments used a sample of 10^7 healthy control neutrophils stimulated for 10 min with phorbol-12-miristate-13-acetate (PMA), which induces a very large respiratory burst *via* activation of the NADPH oxidase and activates many intracellular kinase systems including protein kinase C. Samples were analysed using the NOESY pulse sequence technique (to detect low quantity metabolites) and the number of scans was set at 16,384, which required 12 h processing time. This first experiment was performed in this way to ensure capture of as many metabolites as possible in order to generate the pattern files. In general, the NMR spectra are analysed after 32 scans for NOESY pulse sequence analysis, which normally requires only 5 min processing time.

For the next step, the selected spectrum was opened simultaneously in two software packages, Chenomx Profiler® (version 8.2 standard) and TopSpin®. Chenomx Profiler® is an automated metabolite analyses appraisal software, in which the metabolite patterns were recognised. Bruker TopSpin® is an acquisition and processing of NMR spectra software package, where the peaks was selected and identified. Using reference standards of known metabolites, these approaches were used to create the pattern files for neutrophil metabolomics that included the details of

the peak location (ppm) with range, and the possible metabolites identified by the peaks (Figure 6.3) (see Supplementary data: The neutrophil pattern file).

1	PATTERN	= Human Neutrophils			
2	GROUP	= Healthy			
3	DESCRIPTION	= 10^7 plus PMA			
4	AUTHOR	= Susama Chokesuwattanaskul			
5	DIM	= 2			
6	ORIGIN	= 1			
7	ITEMS	= 1056			
8	0.0000	0.0000	9.3498	9.3402	0 NAD01
9	0.0000	0.0000	9.3066	9.2954	0 NADP01
10	0.0000	0.0000	9.1557	9.1517	0 NAD02
11	0.0000	0.0000	9.1474	9.1442	0 NAD03
12	0.0000	0.0000	9.1155	9.1075	0 NADP02
13	0.0000	0.0000	9.1054	9.1006	0 UNKNOWN01
14	0.0000	0.0000	8.8530	8.8330	0 NAD04
15	0.0000	0.0000	8.8288	8.8272	0 NADP03
16	0.0000	0.0000	8.8186	8.8146	0 NADP04
17	0.0000	0.0000	8.618	8.61	0 UNKNOWN02
18	0.0000	0.0000	8.591	8.583	0 UNKNOWN03
19	0.0000	0.0000	8.5526	8.543	0 ATP01
20	0.0000	0.0000	8.5457	8.5377	0 ADP01
21	0.0000	0.0000	8.4637	8.4565	0 FORMATE01
22	0.0000	0.0000	8.4343	8.4296	0 UNKNOWN04
23	0.0000	0.0000	8.4304	8.4257	0 NADP05,NAD05
24	0.0000	0.0000	8.4255	8.4183	0 UNKNOWN05
25	0.0000	0.0000	8.385	8.381	0 UNKNOWN06
26	0.0000	0.0000	8.3546	8.3466	0 INOSINE01,ADENOSINE01

Figure 6.3: An example of the pattern file of human neutrophils. The descriptions in lines 1 to 4 described the details of spectral samples, which were from the experiments of 10^7 healthy human neutrophils, and the author. The number of items (line 7) was the number of spectral peaks identified in the pattern file, which was 1056 for this sample from human neutrophils in this study. From lines 8 to 26, examples of the spectral peak information, in terms of the ppm range and the possible metabolites identified (from a peak identification) by Chenomx Profiler® software (version 8.2 standard). The spectral peaks that are unable to be identified by the software were labelled as UNKNOWN.

6.7 Spectral and statistical analyses using Chenomx Profiler® software (version 8.2 standard) and Metaboanalyst programme

For further and more detailed analyses, the spectral data were interpreted into a "bucket table" *via* Amix® software (Figure 6.4). The bucket table describes the spectral data in terms of the peak intensity with identification (possible metabolites), defined by the pattern file.

Statistical analyses were then performed using an online programme, Metaboanalyst® (From: http://www.metaboanalyst.ca/), which uses the R package of statistical computing software. The experimental data in the bucket table, or a peak intensity table format, was first normalised by median centering. This normalisation of data is to make the samples comparable (Figure 6.5). In addition, Pareto scaling was applied to make the variables in the data more similar in scale, so that the statistical differences were not influenced by the larger variables, or the larger spectral peaks. This allows for the application of some linear analysis methods, including principal component analysis (PCA). Pareto scaling is obtained from mean-centered data and is divided by the square root of the standard deviation of each variable.

1	Sample	Healthy1_1_21	Healthy1_2_21	Healthy1_3_21	Healthy2_1_41	Healthy2_2_41	Healthy2_3_41	Healthy3_
2	Class	Healthy1	Healthy1	Healthy1	Healthy2	Healthy2	Healthy2	Healthy3
3	NAD01	0.43450258	0.43450258	0.43450258	0.05216855	0.05216855	0.05216855	0.0949
4	NADP01	0.30253904	0.30253904	0.30253904	0.09345948	0.09345948	0.09345948	0.0593
5	NAD02	0.29274293	0.29274293	0.29274293	0.26381048	0.26381048	0.26381048	0.1412
6	NAD03	0.29716718	0.29716718	0.29716718	0.20318748	0.20318748	0.20318748	-0.0376
7	NADP02	0.08789374	0.08789374	0.08789374	0.18877176	0.18877176	0.18877176	0.0940
8	UNKNOWN01	0.18531561	0.18531561	0.18531561	0.05804204	0.05804204	0.05804204	0.1392
9	NAD04	0.1642984	0.1642984	0.1642984	0.24981654	0.24981654	0.24981654	0.0500
10	NADP03	0.60832397	0.60832397	0.60832397	-0.0528801	-0.0528801	-0.0528801	0.1457
11	NADP04	0.12645634	0.12645634	0.12645634	0.17252606	0.17252606	0.17252606	0.0537
12	UNKNOWN02	1.79603427	1.79603427	1.79603427	0.27916098	0.27916098	0.27916098	0.7073
13	UNKNOWN03	0.9201089	0.9201089	0.9201089	0.08431035	0.08431035	0.08431035	0.1058
14	ATP01	6.12932004	6.12932004	6.12932004	0.75580355	0.75580355	0.75580355	1.2143
15	ADP01	4.5634452	4.5634452	4.5634452	0.79460283	0.79460283	0.79460283	1.5094
16	FORMATE01	3.01433773	3.01433773	3.01433773	2.48815183	2.48815183	2.48815183	1.3009
17	UNKNOWN04	0.76711819	0.76711819	0.76711819	0.19498301	0.19498301	0.19498301	0.132
18	NADP05,NAD05	0.10441833	0.10441833	0.10441833	0.22050309	0.22050309	0.22050309	0.0109
19	UNKNOWN05	0.36522786	0.36522786	0.36522786	0.18000196	0.18000196	0.18000196	0.1668
20	UNKNOWN06	0.14103055	0.14103055	0.14103055	-0.00827632	-0.00827632	-0.00827632	0.0779
21	INOSINE01,ADENOSINE01	0.28337862	0.28337862	0.28337862	0.16301154	0.16301154	0.16301154	0.0825
22	UNKNOWN07,	0.33681176	0.33681176	0.33681176	0.15575637	0.15575637	0.15575637	0.1917
23	OXYPURINOL01,ADP02,ATP02	4.85573816	4.85573816	4.85573816	0.78744563	0.78744563	0.78744563	1.5435
24	ADENOSINE02,GLUTATHIONE01	0.37730409	0.37730409	0.37730409	0.21351192	0.21351192	0.21351192	0.1735
25	INOSINE02,GLUTATHIONE02	0.243209	0.243209	0.243209	0.05672659	0.05672659	0.05672659	0.1024
26	UNKNOWN08	0.77115481	0.77115481	0.77115481	0.01569509	0.01569509	0.01569509	0.0851

Figure 6.4: The bucket table of metabolites from healthy neutrophils. The figure demonstrates the bucket table, which describes the spectral peaks in terms of the peak intensity (from the spectral data) and identification (from the pattern file, see Figure 6.3; Supplementary data: The neutrophil pattern file).

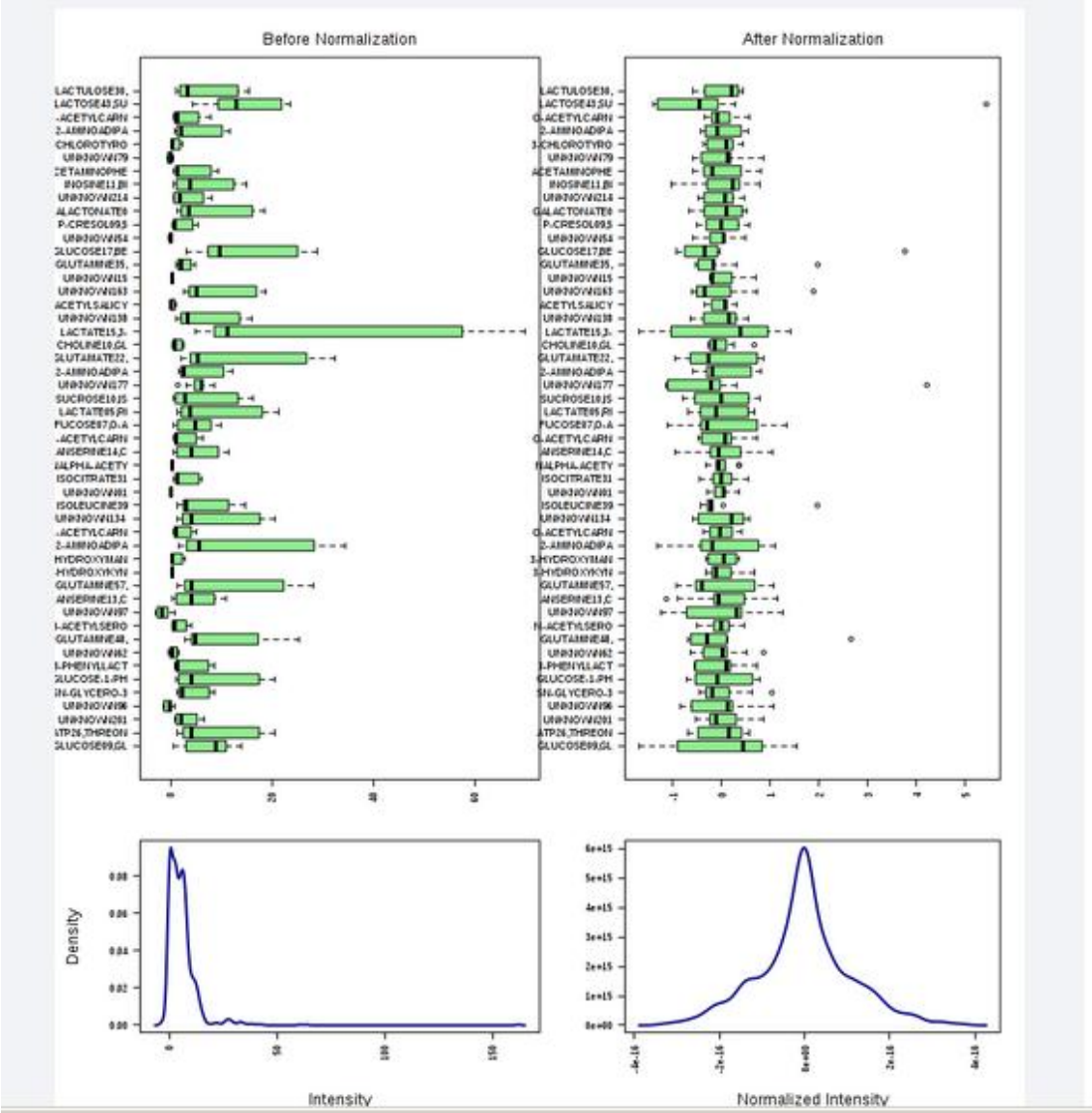

Figure 6.5: Normalisation of the data and the data scaling. The original spectral data (**left**) was normalised by median and the application of Pareto scaling to the normalised and scaled spectral data (**right**), which allowed the comparison between samples. The box and whisker plots represented the normalisation of each metabolomic spectrum.

After the statistical analyses, the spectral peaks that showed significant differences were listed. The statistical analyses methods were selected for each experimental design. Briefly, fold change analysis was selected in the time-point experiments, e.g. PMA treatment. For the spectral data of neutrophils from healthy controls and patients with disease, e.g. rheumatoid arthritis, either ANOVA or T-test with *post-hoc* analyses were applied with regards to the number of different groups. The p value for the spectral analyses was set at 0.01 because the NMR metabolomics has the sensitivity to measure very small metabolomic changes. Once the list of significant peaks identified as possible metabolites was obtained, the retrospective check with the original spectrum *via* Bruker TopSpin® and Chenomx Profiler® (version 8.2 standard) software was performed to confirm the possible metabolites.

6.7.1 Principal Component Analysis (180)

As the high-dimensional characteristics of NMR metabolomic data limit simple exploration of the data, principal component analysis (PCA), a complex mathematical algorithm including linear algebra, can decrease the dimensionality of the data but still retain all of the variations. The decrease is accomplished by identifying directions as new variables, called principal components, which are the linear combinations of the original variables: the variation in the data is still maximal. By using few components, values for thousands of variables can be represented by relatively few numbers. The visual assessment of similarities and differences between samples then becomes possible. However, in two- or three-dimensional visualisation, much information will be missing, and so different combinations of components are required for visualisation in a data set.

6.7.2 Pathway analyses

Metabolic pathway analysis was carried out on those metabolites that showed a significant increase/decrease between samples (e.g. +/- PMA, disease versus healthy) using Metaboanalyst® Pathway Analyses software. The metabolite data were input either as a list of compound names or other compound labels (including Human Metabolome Database (HMDB) or Kyoto Encyclopaedia of Genes and Genomes (KEGG)). HMDB is the online database for small molecule metabolites found in human samples (181–183). KEGG is the database resource for understanding high-

level functions and utilities of the biological system. The KEGG compound contains the small molecules database. The first step was to standardise the metabolite data into matched compounds with identified HMDB or KEGG reference numbers. However, the programme allows for the manual selection of the metabolites from the approximate matched compounds. Metabolites for which no match could be found were not included into the pathway analysis. In the next step, a pathway library, categorised by sample species, was selected. In *homo sapiens* (human), there were 80 pathways available in the programme. The algorithms for pathway enrichment analysis, or the over-representation analysis, test if metabolites involved in a particular pathway are enriched compared to random hits (or represented more than expected by chance). The hypergeometric test was selected.

The pathway topology analysis was used to estimate the node importance. It is well-known that changes in more important positions of a network would impact more severely on the pathway than changes in marginal or relatively isolated positions. There are two well-established node centrality measures to estimate node importance: degree centrality and betweenness centrality. The degree centrality measure focuses more on local connectivities, while the betweenness centrality measure focuses more on global network topology. The relative betweenness centrality was selected in the study. The impacted metabolic pathways were then analysed in correlation with the biomedical background of patient samples and experimental design.

6.8 Optimising protocols for NMR metabolomic analyses of human neutrophils: challenges and advantages

Sample collection, preparation, storage and analysis can all affect the metabolomic profiles obtained, and therefore, highly consistent preparation and analysis procedures are required. No established protocols have yet been developed for the measurement of the metabolomic profiles of human neutrophils. The first objective was to optimise these procedures in view of the challenges and potential advantages of different protocols.

6.8.1 Optimising sample preparation protocols

6.8.1.1 Optimal neutrophil cell number and the number of scans (NS)

Aim: To determine the minimum cell number that could provide full NMR spectrum coverage.

Objectives:

1. Intracellular metabolite extraction of neutrophils with different total number of cells

2. NMR spectrum coverage to be identified by Chenomx Profiler® software (version 8.2 standard)

This cell number optimisation was necessary because the total numbers of neutrophils that can obtained from the blood or inflammatory fluid of a patient or donor can be low. For clinical samples, particularly from paediatric patients, the total number of neutrophils that can be obtained from a single blood sample may be as low as 2 x 10^6 cells. Therefore, the first step was to determine the minimum number of neutrophils required to detect the highest possible number of distinct NMR spectra of metabolites and to generate reproducible spectral patterns.

In the first experiments, data obtained from three different cell numbers (i.e. 2.5, 3.5 and 9.7 x 10^6 cells) were analysed using five different number of scans (NS) (i.e. 128, 256, 512, 1,024 and 2,048). Samples were prepared as described in Chapter 2.5. In a 3D-scores plot, each colour indicates each NS and one point indicates one

sample. In Figure 6.6 A, B, the **DEEP BLUE**, **LIGHT BLUE** and **PINK** points represent the analyses after the number of scans of 512, 1,024 and 2,048, respectively. In the plot, the clustering of the points in these three colours, aka NS, was observed in two different locations. For each location, the cell numbers of 3.5 and 9.7 x 10^6 were represented in the points in each locations (Figure 6.6 A, B). Therefore, the number of scans and the number of cells affected the analyses of the spectral data. A cell number of 3.5 x 10^6 demonstrated similarity of the data at the NS of 512 (Figure 6.7 C). When the lower number of cells (2.5 x 10^6) were analysed, a higher NS, at least 1,024, was required to produce the similar results (Figure 6.7 D). Moreover, at the highest cell number (9.7 x 10^6), the points from the NS of 128 and 256 also produced a less compacted grouping of points (**GREEN**) (Figure 6.7 A, B). On the contrary, the data obtained at a cell number of 2.5 x 10^6 were scattered, even at the high NS of 2,048 (Figure 6.7 E).

In conclusion, the higher total number of neutrophils is recommended for all future experiments, as the results revealed good technical replication even at the low number of scans, which means a shorter short processing time. From this study, a number of total neutrophils at least 3.5 x 10^6 cells are required, with the optimal number of scans at 512.

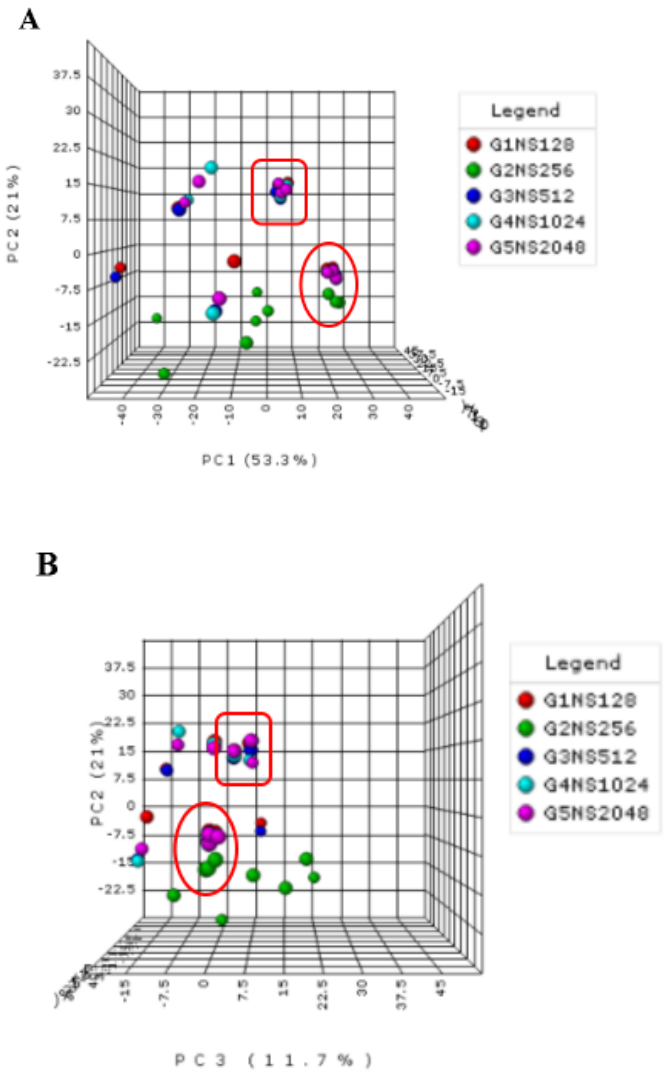

Figure 6.6: The principal component analysis of the data from three different neutrophil cell numbers (2.5, 3.5 and 9.7 x 10^6 cells) after five different numbers of scans (NS) (128, 256, 512, 1,024 and 2,048). (A) Comparison of principal component 1 (PC1) (53.3%) and principal component 2 (PC2) (21%), two clusters of points were observed, marked in a **RED** circle and **RED** square. In the **RED** circle, the clustering contained the points represented the data of 9.7 x 10^6 cells at every NS. The looser sub-clustering of points (**GREEN** points) represented the NS of 256. In (B) the **RED** square depicts another clustering of points that contained the points representing the data of 3.5 x 10^6 cells at the highest number of scans, but excluding NS of 128 and 256. (**Abbreviations**: NS = Number of scans, G1, G2, G3, G4 and G5 = The number of scans at 128, 256, 512, 1,024 and 2,048, respectively. The samples were technical triplicates).

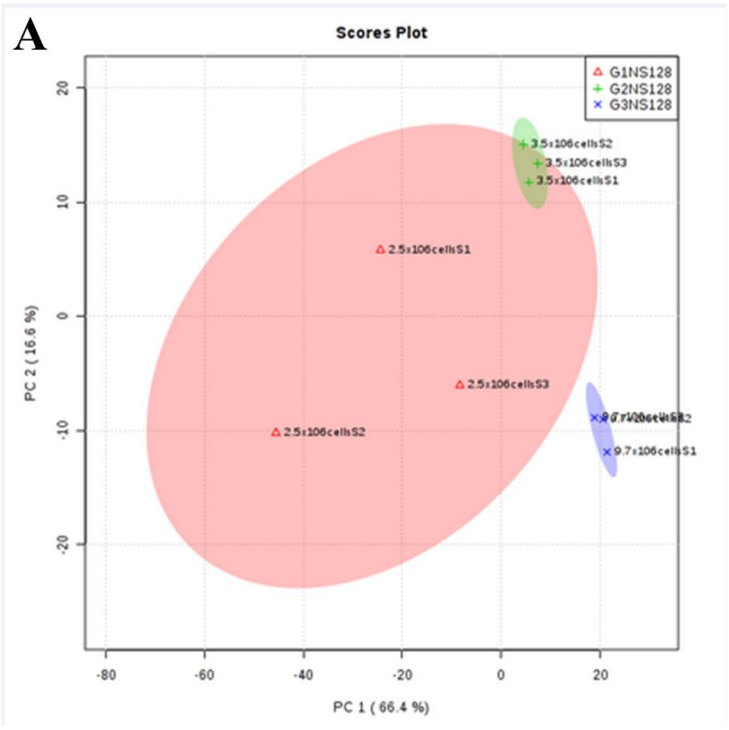
A
Scores Plot
G1NS128
G2NS128
G3NS128
3.5x106cellsS2
3.5x106cellsS3
3.5x106cellsS1
2.5x106cellsS1
2.5x106cellsS3
2.5x106cellsS2
9.7x106cellsS1
PC 2 (16.6 %)
PC 1 (66.4 %)
20
10
0
-10
-20
-80
-60
-40
-20
0
20

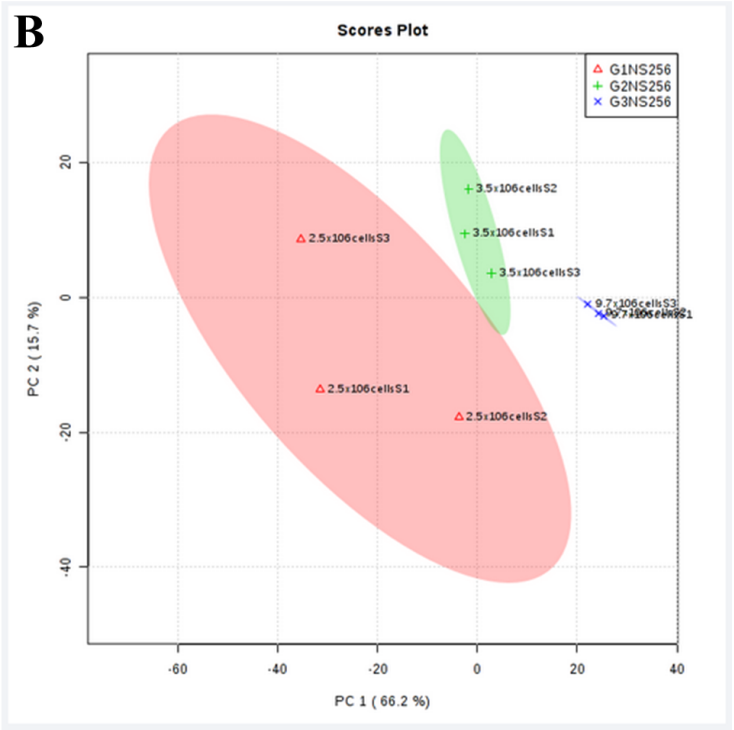
B
Scores Plot
G1NS256
G2NS256
G3NS256
3.5x106cellsS2
3.5x106cellsS1
3.5x106cellsS3
2.5x106cellsS3
2.5x106cellsS1
2.5x106cellsS2
9.7x106cellsS3
PC 2 (15.7 %)
PC 1 (66.2 %)
20
0
-20
-40
-60
-40
-20
0
20
40

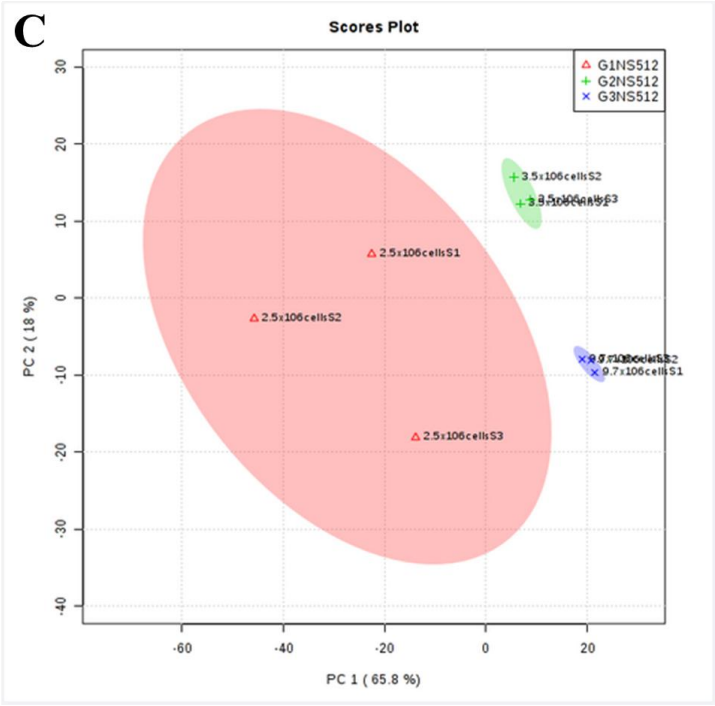
C
Scores Plot
G1NS512
G2NS512
G3NS512
3.5x106cellsS2
2.5x106cellsS1
2.5x106cellsS2
2.5x106cellsS3
9.7x106cellsS1
PC 2 (18 %)
PC 1 (65.8 %)

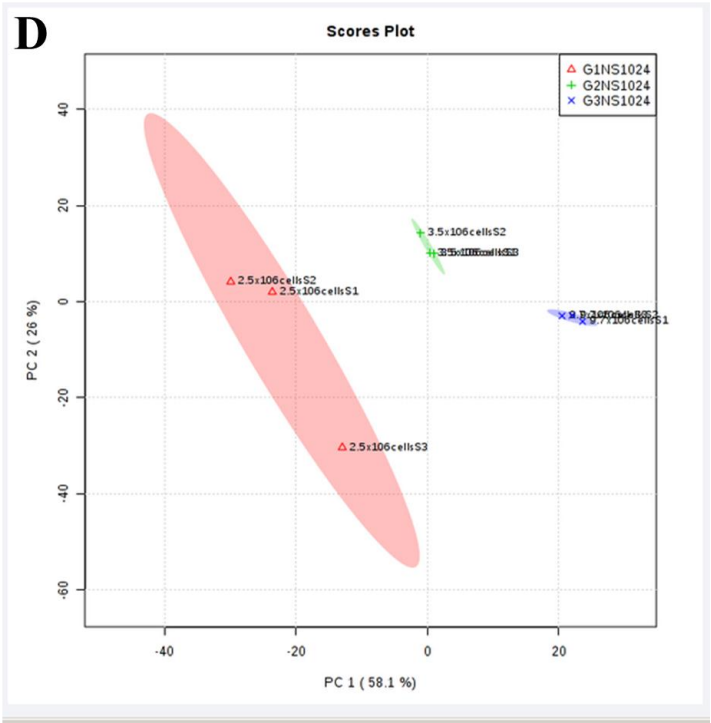
D
Scores Plot
G1NS1024
G2NS1024
G3NS1024
3.5x106cellsS2
2.5x106cellsS2
2.5x106cellsS1
2.5x106cellsS3
PC 2 (26 %)
PC 1 (58.1 %)

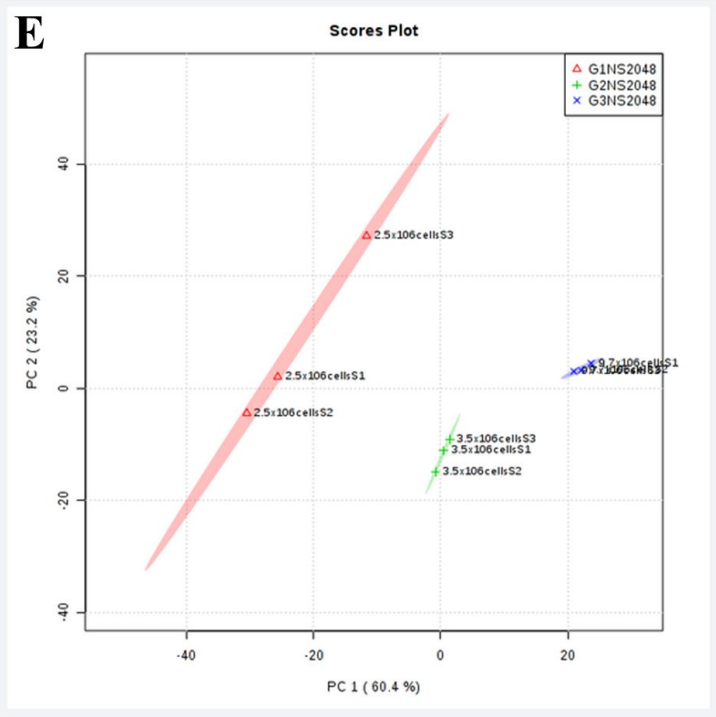

Figure 6.7: Principal component analysis of the data of three different cell numbers (2.5, 3.5 and 9.7 x 10^6 cells) at each number of scans (NS). The number of scans ranged from 128 (A), 256 (B), 512 (C), 1,024 (D) and 2,048 (E). (**Abbreviations**: S = Sample, G1, G2 and G3 = Total cell number of 2.5, 3.5 and 9.7 x 10^6 cells, respectively. The samples were technical triplicates.)

6.8.1.2 Quenching neutrophil metabolism: Heating neutrophils prior to the snap freezing

Aim: To detect the metabolites present in resting and stimulated neutrophils from healthy controls.

Objectives:

1. To stabilise all metabolites and metabolic enzymes in neutrophils

2. To prevent unwanted cellular reactions that could alter the concentrations of these metabolites

Neutrophils are normally in a resting state in the circulation, but can be activated either intentionally (e.g. through a PMA treatment, that activates the signal transduction enzyme protein kinase C (PKC)) or unintentionally (through the process of neutrophil isolation or rough handling/sample processing). Samples were heated to 100 ^{o}C for 1 min in order to denature metabolic enzymes (which could be released during extraction) and hence stabilise all metabolites and protect them from further cellular reactions.

In these experiments, the total cell number of cells (10^6) was incubated with PMA (0.1 µg/mL). 10 min after treatment, heat shock was applied to one sample while another sample was extracted without the heat shock treatment. The objectives of the study were to assess whether the heat shock could stabilise all the metabolites either at their resting state or in the activated state. After extraction, the number of metabolites and the similarity of the data within the two groups, with and without heat shock, were evaluated. In Figure 6.8, the spectrum representing PMA-treated neutrophils (**BLUE**) that were subject to the heat shock demonstrated an overall higher level of metabolites than the **RED** spectrum that represented the samples extracted without the heat shock. In conclusion, the heat shock could enhance the detection of metabolites in the neutrophil extracts, and should be applied in all further experiments.

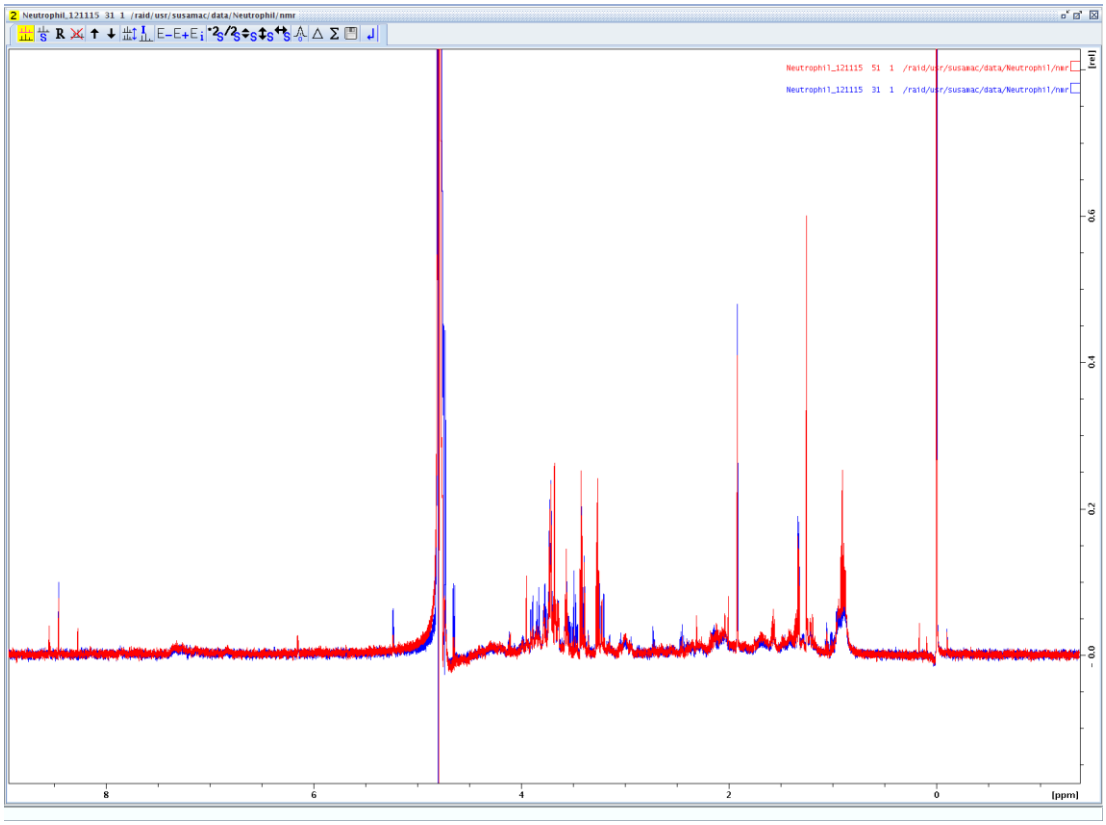

Figure 6.8: Effect of heat shock on extraction of neutrophil metabolites. 10^6 neutrophils were activated with PMA (0.1 µg/mL) prior to metabolomic extraction. The **RED** spectrum represented the PMA-treated neutrophils without the heat shock, while the **BLUE** spectrum represented the PMA-treated neutrophils without this heat shock treatment.

6.8.1.3 Minimising the processing times and metabolite loss during extraction

Aim: To decrease the processing time and procedures in order to minimise metabolic changes following extraction

Objectives:

1. To decrease the number of washing steps in neutrophil isolation in order to prevent cell loss and minimise perturbations to cellular metabolism

2. To minimise the centrifugation time but still recover all of the cells

As the total number of cells and number of scans were crucial factors in neutrophil metabolomics (Section 6.8.1.1), the optimal process to minimise cell loss or perturbation during the neutrophil isolation and metabolite extraction procedures were investigated. During the isolation process, all of the washing steps were decreased as appropriate without comprising the numbers of cells collected. Therefore, the washing step after centrifugation in Ficoll-Paque reagent was eliminated. In a normal preparation, the cell pellets would be washed with RPMI-1640 medium to remove all the Ficoll-Paque residue. For these and subsequent experiments, the polymorphonuclear (PMN) pellets were resuspended in RPMI-1640 media with phosphate buffer, and the ammonium chloride was added to lyse the RBCs as described in Chapter 2.5. After centrifugation, the cell pellets were collected and re-suspended in RPMI-1640/phosphate buffer. The cell suspension was counted and immediately aliquoted into triplicate samples.

In order to investigate the effect of washing steps, the neutrophil suspensions were equally distributed into two tubes, at the concentration of 3.5×10^6 cells/mL for 3 mL. Both tubes were centrifuged at 500 g for 3 min. In one tube (washed sample), the media was discarded and 3 mL RPMI-1640 media with phosphate buffer was added. After the red blood cell lysis step, the cell pellet was resuspended and recounted. The cell concentration was decreased to 3×10^6 cells/mL. In another tube (non-washed sample), the only difference is that, after the Ficoll-Paque centrifugation, the media was not discarded and used to resuspend the cell pellet again. The cell suspensions were then aliqouted into three tubes for the technical replicates. The

aliquoted cell suspensions were centrifuged, and the cell pellets were collected. The NMR spectra were visibly different, and more metabolites could be detected in the non-washed sample (Figure 6.9). Moreover, the possible contamination of the spectra by of Ficoll-Paque was not observed in the spectra. Therefore, in subsequent experiments in this thesis, the washing step after centrifugation in Ficoll-Paque was not performed.

For some experiments, including after PMA treatment, the cells had to be collected at defined time-points, and so optimising the minimal processing time, in terms of washing and centrifugation without cell loss, was necessary. Therefore, in these experiments, the numbers of cells recovered in cell pellets after different centrifugation times were compared. In these experiments, the neutrophil suspensions were centrifuged at 1,000 g for 2 and 3 min, and cell recovery was equivalent. Therefore, in the further metabolomic experiments, a centrifugation time at 1,000 g for 2 min was applied.

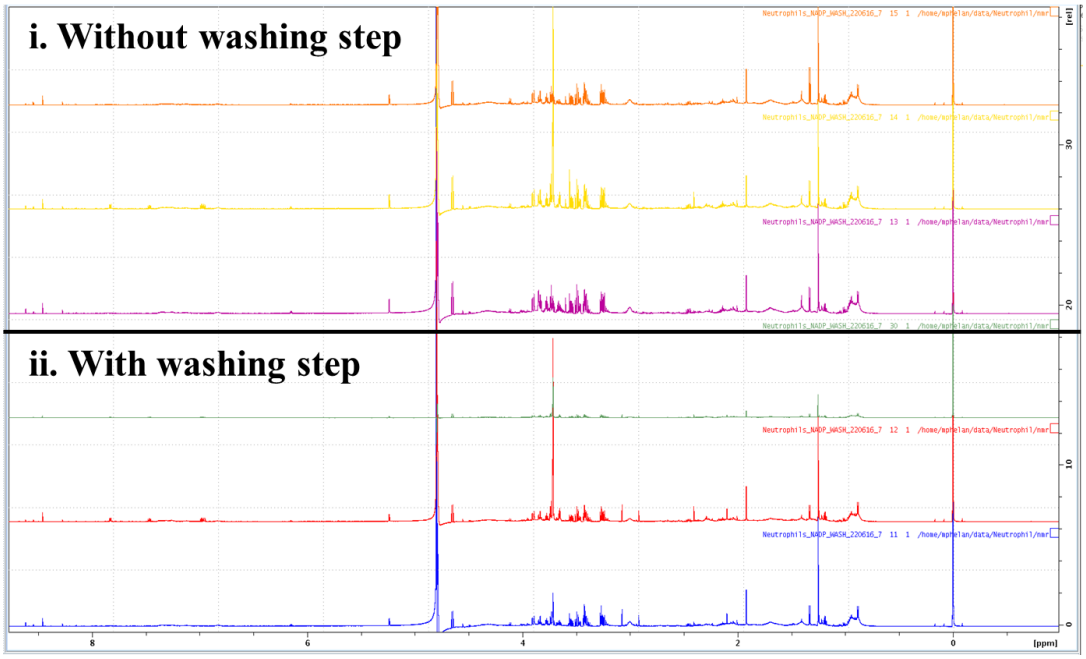

Figure 6.9: Experiment to determine the effects of decreasing the number of washing steps on neutrophil metabolites. i) Three technical-replicate spectra derived from the neutrophils undergoing the isolation process **without the washing step** after the centrifugation in Ficoll-Paque. ii) Three technical-replicate spectra derived from the neutrophils undergoing the isolation process **with the washing step**.

6.8.1.4 Minimising contaminants that may be introduced into neutrophil extracts

Aim: To detect the NMR metabolomics and their changes in response to different stimulants, without interference from contaminating molecules introduced during the extraction/isolation process

Objectives:

1. The avoidance of all contaminating external metabolites, for example, alcohol and buffers (HEPES)

2. The avoidance of HEPES in RPMI-1640 media

3. The use of 25 mM phosphate buffer pH 7.4 in RPMI-1640 media

NMR metabolomics has the potential to detect intracellular metabolites at very low levels, for example as low as 500 ng of pure compound (184). However, these low quantity metabolites are detected as low intensity peaks, which can be easily obscured by the presence of high concentration metabolites, which can commonly be contaminants or introduced by external interference, e.g. specific foods or drinks taken by the patients prior to blood withdrawal.

As the NMR technique is a very sensitive tool, all possible contaminants, including chemicals and disinfectants used in cell preparation/isolation, were considered and then eliminated as far as possible. In a preliminary study in healthy volunteers, those with a 48 h history of no alcohol consumption or medications were included in the study. The possible contaminants from the isolation/extraction procedures were reviewed thoroughly. In the isolation of neutrophils, RPMI-1640 media with HEPES buffer was initially used, in order to maintain the pH of the media around 7.2 - 7.5, which is a normal requirement of cell culture to maintain viable human neutrophils. Moreover, altered pH of the samples could influence the chemical shifts of the NMR spectrum (185). However, it was found that residual HEPES in the neutrophil extracts (from the RPMI-1640 medium) provided undesirable, multiple high peaks, in the NMR spectra (Figure 6.10). Therefore, in all subsequent experiments, 25 mM phosphate buffer was added into the media in place of HEPES,

to maintain the pH at 7.4. The colour of the phenol red, a pH indicator in the media, was observed and visually compared to when HEPES was used, and no differences were observed (data not shown). The colour of the media with HEPES buffer and pH 7.4 phosphate buffer appeared to have the similar pink/red colour, which indicated a similar pH of both media. As the phosphate buffer provide only a clear distinct peak in NMR metabolomics with much less interfere to the overall NMR spectrum, phosphate buffer was used in all subsequent neutrophil NMR metabolomic experiments.

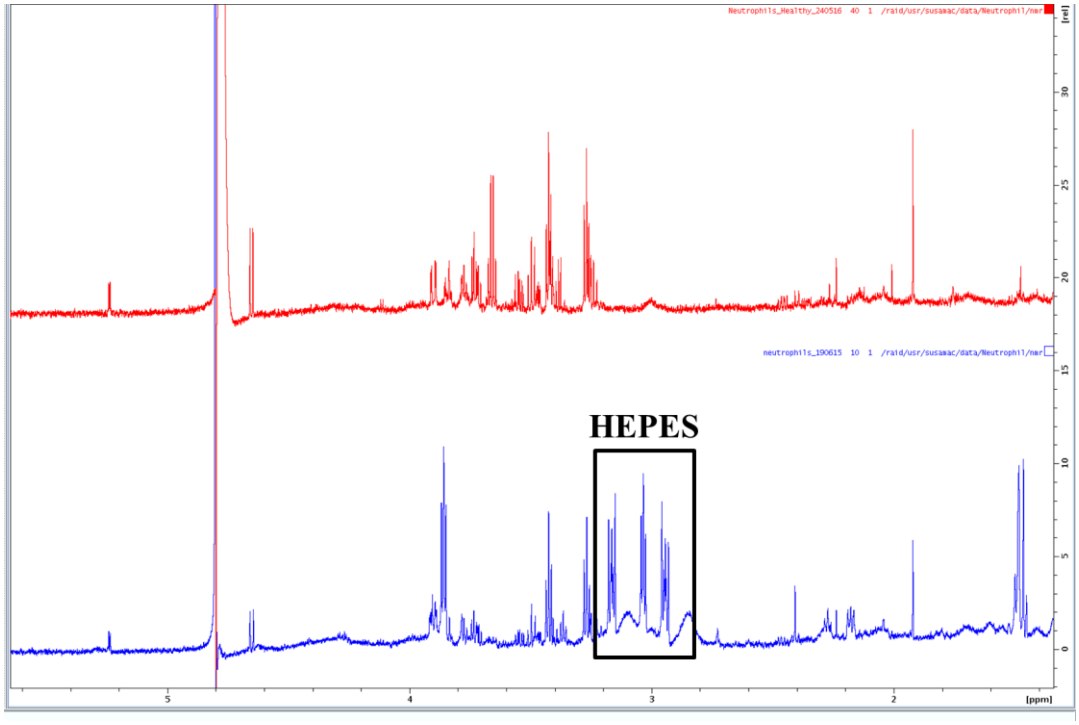

Figure 6.10: The interference peaks of HEPES. The **BLUE** spectrum represented the neutrophil metabolomics when the HEPES-containing media was used during the isolation of neutrophils. In the **BLACK** circle, the multiple peaks of HEPES were present. The **RED** spectrum represented the neutrophil metabolomics when the HEPES was removed.

6.8.2 Optimising the NMR analyses to detect low level metabolites

Aim: To optimise protocol for the detection of low quantity metabolite

Objectives:

1. To determine if metabolites such as NADP+ are lost during the extraction protocols

2. Refine the sensitivity of the parameter sets for NMR spectral analyses to detect NADP+

Neutrophils are aggressive, bacteria-killing immune cells, and possess sophisticated mechanisms for the phagocytosis and killing of bacteria. These include

the generation of reactive oxygen metabolites *via* the NADPH oxidase which is rapidly activated during cell stimulation (186). Therefore, there are dynamic changes in the concentrations and ratios of NADPH and NADP+ during neutrophil activation. However, in the preliminary studies above using 10^7 neutrophils after PMA treatment, the spectral peaks representing NADP+ and NADPH were barely detectable (Figure 6.11). Therefore, experiments were performed in order to determine whether the detection of the spectral peaks could be enhanced by increasing sensitivity of the NMR spectral analyses. For this, more sensitive parameter sets for NMR spectral analyses, NOESY, were applied for samples collected and processed after different incubation times. The study revealed the presence of more prominent NADP+ and NADPH spectral peaks at the number of scans of 4,096, using NOESY parameter sets (Figure 6.11C). Usually, 32 scans is the default setting for NOESY parameter sets (Figure 6.11B). Using this approach, the metabolites of interest were present in the sample, however, at low levels.

In conclusion, the current protocol of intracellular neutrophil extraction was able to stabilise some highly active metabolites, including NADP+, in neutrophils. However, it may be that the low intensity of the spectral peaks are the result of high turnover rate of this molecule. Therefore, in subsequent experiments, higher sensitivity NMR analyses was applied in order to study specific metabolic pathways. Also, further experiments were performed to determine whether or not NADP+ was lost during the intracellular extraction of neutrophils (see Section 6.9.2)

A

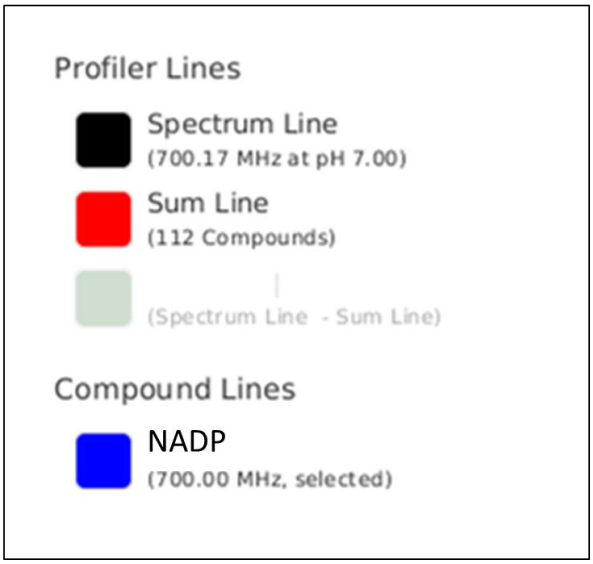
Profiler Lines
Spectrum Line
(700.17 MHz at pH 7.00)
Sum Line
(112 Compounds)
(Spectrum Line - Sum Line)
Compound Lines
NADP
(700.00 MHz, selected)

B

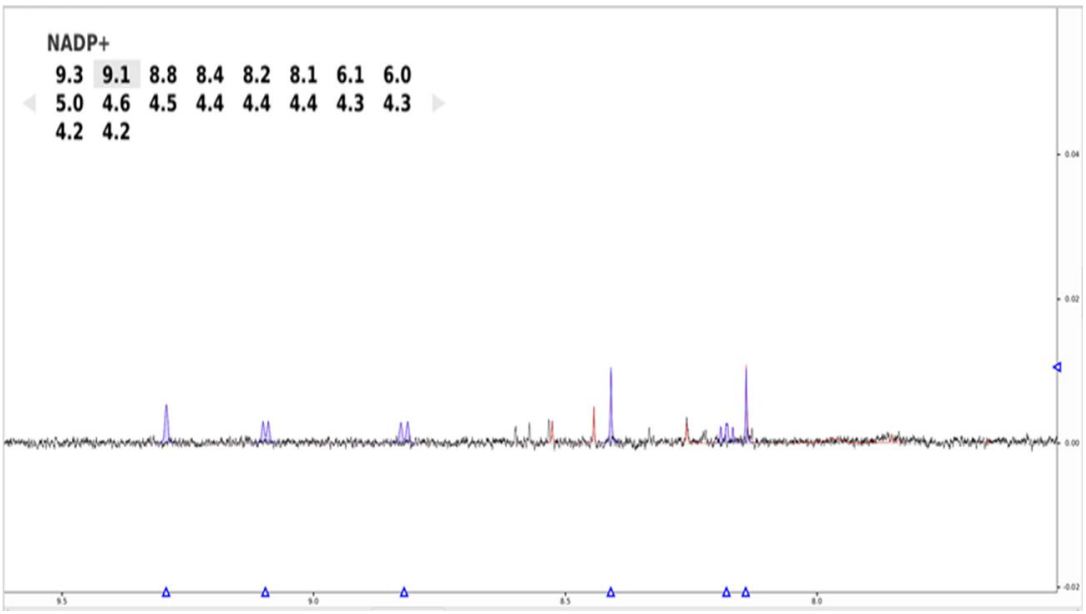
NADP+
9.3 9.1 8.8 8.4 8.2 8.1 6.1 6.0
5.0 4.6 4.5 4.4 4.4 4.4 4.3 4.3
4.2 4.2

C

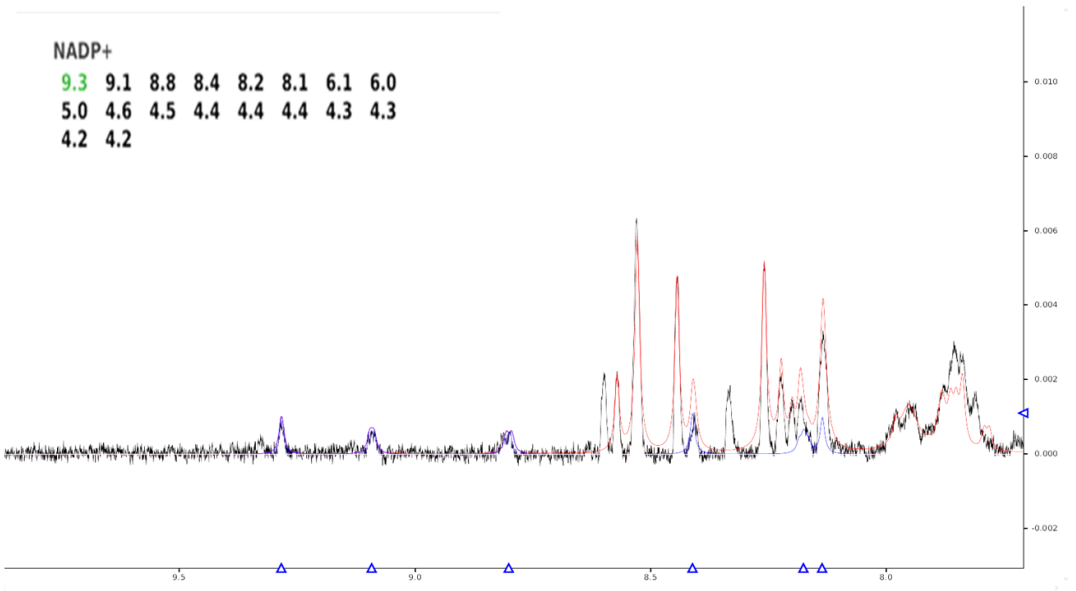

Figure 6.11: NADP+ peak identification using Chenomx Profiler® software (version 8.2 standard). The NMR spectral data of the sample of 10^7 neutrophils after PMA treatment were analysed by the same parameter sets, NOESY, at different numbers of scans: 32 in (B) and 4,096 in (C). (B, C) The NADP metabolite was identified in two different NMR spectrum. (A) In Chenomx Profiler® software, there are three different coloured spectral lines; two profiler spectra (**RED** and **BLACK**) and one compound spectrum (**BLUE**). The **BLACK** line indicates the NMR spectrum of neutrophil sample. The **BLUE** line indicates the predicted compound (NADP+) spectrum by Chenomx Profiler® software (version 8.2 standard). The **RED** line indicates the sum line of metabolic compounds at that location (ppm). At the left upper corners, all peak locations of NADP+ metabolite were informed in ppm, the **GREEN** digits indicated in the spectral peaks (**BLACK** line) at that location (ppm) were matched with the predicted spectral peaks (**BLUE** line). (B) The neutrophil samples were analysed by NOESY parameter sets at NS of 32 (5 min processing time). The NADP+ spectral peaks were barely evident. (C) The same sample was re-analysed by NOESY parameter sets at NS of 4,096 (6 h processing time) and then prominent NADP+ spectral peaks were observed.

6.9 Special considerations in neutrophil NMR analyses

6.9.1 Contaminants or unidentified metabolites in neutrophil extracts

As the NMR technique is very sensitive, it is possible that contaminants, including chemicals in buffers and disinfectants, appear in extracts and are included in the NMR spectra. It is clearly necessary to identify and then eliminate such contaminants. In the neutrophil experiments for metabolomics, HEPES was avoided, as it produces an NMR spectrum that interferes with the neutrophil signals (Figure 6.9). However, as the pH of samples can influence the chemical shifts of the NMR spectrum, phosphate buffer was added to maintain the pH to around 7.2 and 7.5.

6.9.2 High turnover rate metabolites

Neutrophils are dynamic cells whose activity is highly regulated in order to eliminate infection, and at the same time, to control inflammation. Therefore, neutrophil metabolites are expected to turnover at a high rate. However, as NMR metabolomic analysis provides a snapshot at a single point in time, it is necessary to distinguish metabolites that are present either at a steady low level and those which are transiently generated at high levels, but have a high turnover rate. During the initial analysis of neutrophils metabolomic spectral data, some specific metabolites, including NAD+, NADH, NADP+ and NADPH, were detected at low levels, which was counter-intuitive considering the reported importance of these molecules in neutrophil metabolism (187). There are a number of potential reasons for this observation: these metabolites may be highly unstable; they might be degraded by neutrophil intracellular enzymes or chemicals during the extraction process; the metabolites might have a high turnover rate or finally, they may genuinely be present in neutrophils at lower levels than those that were anticipated.

To exclude the possibility of metabolite loss during the extraction procedure, the specific spectra for NAD+, NADH, NADP+ and NADPH were analysed in different cell types using similar extraction techniques to those used for the neutrophil metabolite. Extracts were made from the cell line, PLB-985 (myeloid leukaemic cell line). The peaks of NAD+ and NADP+ were readily clearly observed these samples (data not shown). Therefore, additional experiments were designed to determine if

NADP+ was lost during the extraction protocol. For these experiments, purified NADP+ (Sigma Aldrich, USA) was added into the samples under three different conditions: with cell pellets (9.7 x 10^6 neutrophils) which then went through the extraction (to detect any loss from the intracellular enzymes and the extraction process); in PBS without cell pellets and undergoing the extraction process (to detect any loss during the extraction process); NADP+ alone without any extraction process (a positive control) (Table 6.2). The data in Figure 6.12 shows that NADP+ was not significantly lost during the extraction process, as the amounts of NADP+, determined by the height of the peak (in the **RED** circle), were similar in the control groups and the other two groups (processed with and without cells). The final amount of NADP+ after the extraction process, either in the presence or the absence of neutrophils, was similar. The NADP+ was unlikely to be degraded by the released intracellular enzymes and metabolites during the extraction process.

In conclusion, the very low levels of NADP+ detected in neutrophil extracts might be explained by the presence of only low levels of this metabolite in the cells, rather than technical/extraction errors. This suggests that the steady-state levels of NADP+, which is involved in neutrophils in producing toxic oxygen radicals, are low and likely to be as a result of its high-turnover rate. The analyses also reflect one limitation of NMR metabolomics as it only measures steady state levels of molecules at a single time-point i.e. a snapshot of the metabolites at the time of sampling. Therefore, to overcome this limitation, neutrophils were stimulated (by PMA) and samples were collected as a time-point series following activation.

Table 6.2: Experiments to determine loss of NADP+ during sample preparation for NMR.

Conditions	Amount of NADP+ (µg)	The step of NADP+ addition	Objectives
NADP+ control	20	No processing	A positive control
NADP+ with no cells	10	Before the heating step and prior to intracellular extraction	To detect any loss from the extraction process
NADP+ added to the cell pellets	10	Before the heating step and prior to intracellular extraction	To detect any loss from the intracellular enzymes and the extraction process

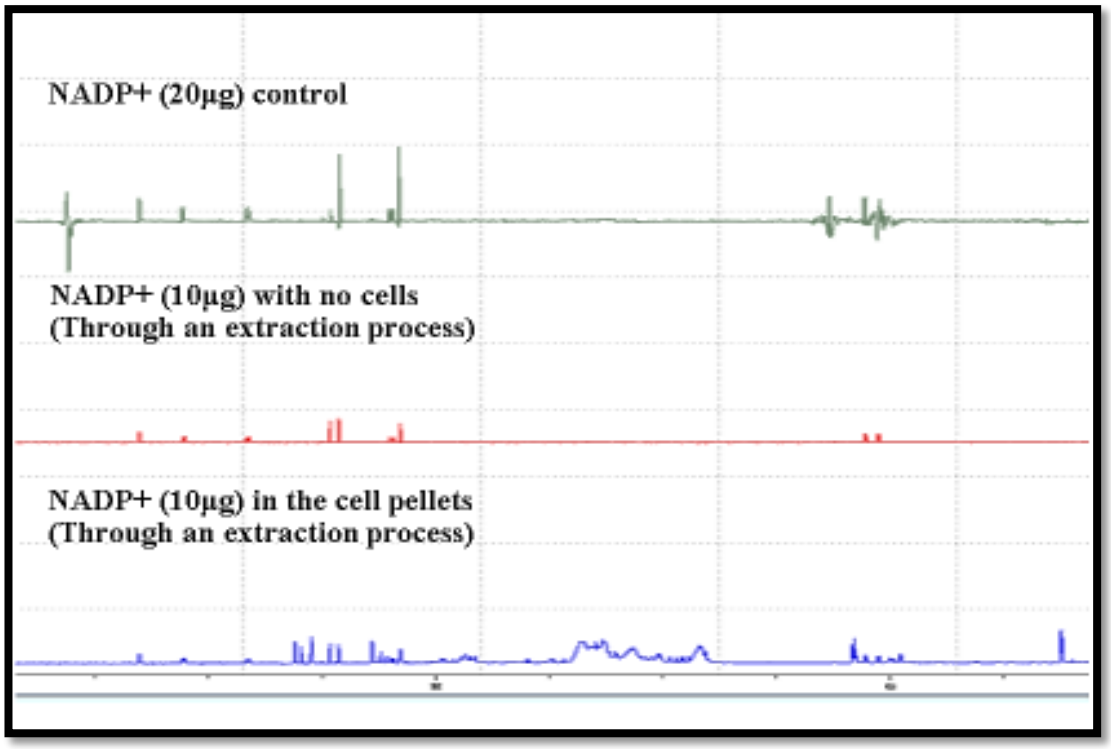

Figure 6.12 No significant loss of NADP+ signals during the extraction process. The peaks of NADP+ was observed in all three experimental conditions: NADP+ control (20 µg) **(GREEN)**, NADP+ (10 µg) was added into the PBS which then went through the extraction process **(RED)**, and NADP+ (10 µg) which was added into the cell pellets and which then went through the extraction process **(BLUE)**.

6.10 The current optimised protocol for NMR analyses of human neutrophils

All of these preliminary experiments were performed to optimise the extraction/analysis of neutrophil metabolites, and the optimised protocol is fully described in Chapter 2.5 (Methods: Metabolomics).

6.11 NMR Metabolomics of healthy human neutrophils

Neutrophils were isolated from the whole blood of healthy volunteers (see protocol in Chapter 2.5). After RBC lysis, the neutrophils in media (RPMI-1640 media with 25 mM phosphate buffer) were equally aliquoted into three tubes for technical replicates. From this step onwards, all technical triplicates were separately extracted and analysed by NMR.

The NMR spectra of 11 healthy controls were analysed to identify the similarities in the healthy group (Figure 6.14). The baseline neutrophil metabolites were found to be highly variable (n = 11) (Figure 6.14) with abnormally distinct peaks present in some samples (**RED** circle, Figure 6.14). In this study, Chenomx Profiler® software (version 8.2 standard) was used to identify the metabolites from NMR spectra, and 338 metabolites were positively identified by the software. Notably, Figure 6.13 demonstrates the peaks of two distinct compounds: H_2O (**left** label), the major spectral interference which is dramatically suppressed but still prominent (as H_2O is the major source of intracellular ^1H.), and TSP (**right** label), the internal reference. These peaks were present in all neutrophil metabolomic samples. Approximately 30% of the overall peaks could not be attributed to specific metabolites, including the contaminants/unidentified metabolites. To distinguish between the contaminants and the unidentified metabolites, the analytical criteria (see Table 6.3) were created based on the fact that all metabolites in the cells should not be substantially different from other intracellular metabolites and the technically triplicated samples could produce similar spectra. Therefore, the peaks were visualised one by one, and in all three replicates. The possible characteristics of the contaminant peaks included the high intensity peaks that were observed in some, but not all, triplicates or samples (Figure 6.13; 6.14) or the peaks that were extremely high in comparison to other metabolites.

Table 6.3: The criteria to distinguish between an unidentified metabolite and a contaminant.

Criteria	Likely to be an unidentified metabolite	Likely to be a contaminant
Reproducibility in all triplicates	Yes	No
Reproducibility in all samples	Yes	No
The distinct peak e.g. singlet or doublet peaks	Yes	No
Abnormally high peak intensity (comparable to H_2O)	No	Yes

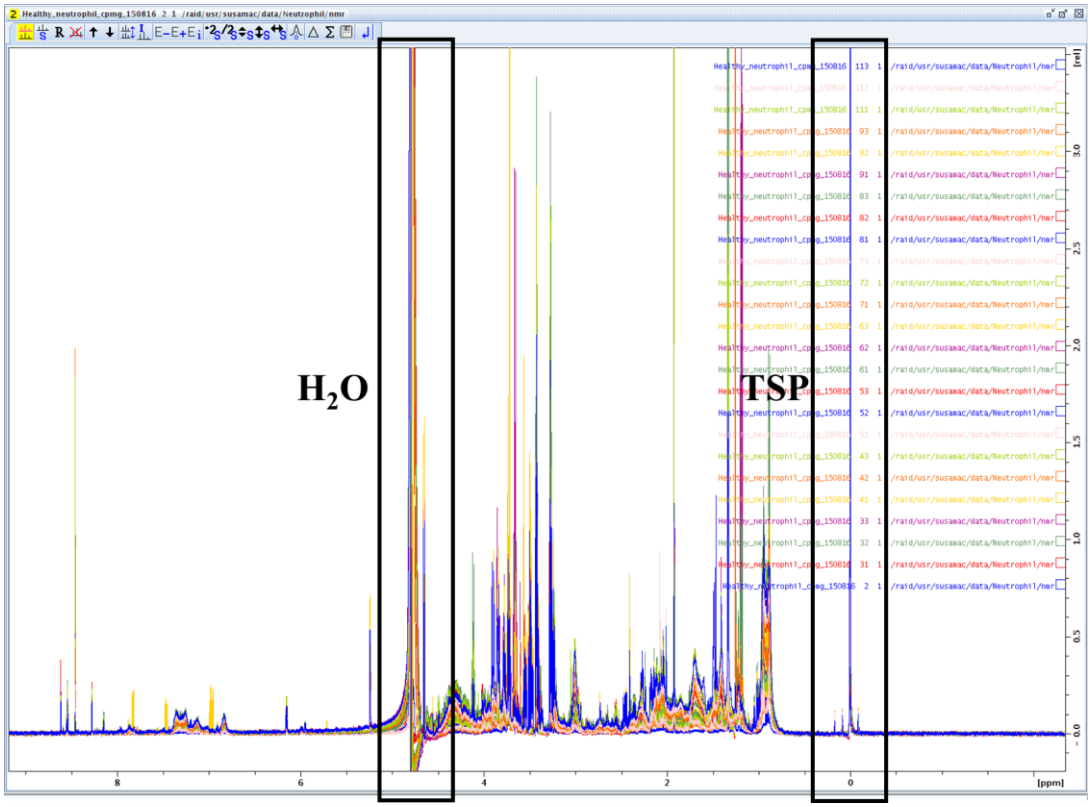

Figure 6.13: The spectral data of healthy neutrophils. The spectral data of healthy neutrophils (n = 11) were visualised by Bruker TopSpin® software. The **BLACK** square marked the peaks of two distinct compounds: H_2O (**left** label), the major spectral interference which was dramatically suppressed but still prominent, and TSP (**right** label), the internal reference.

A

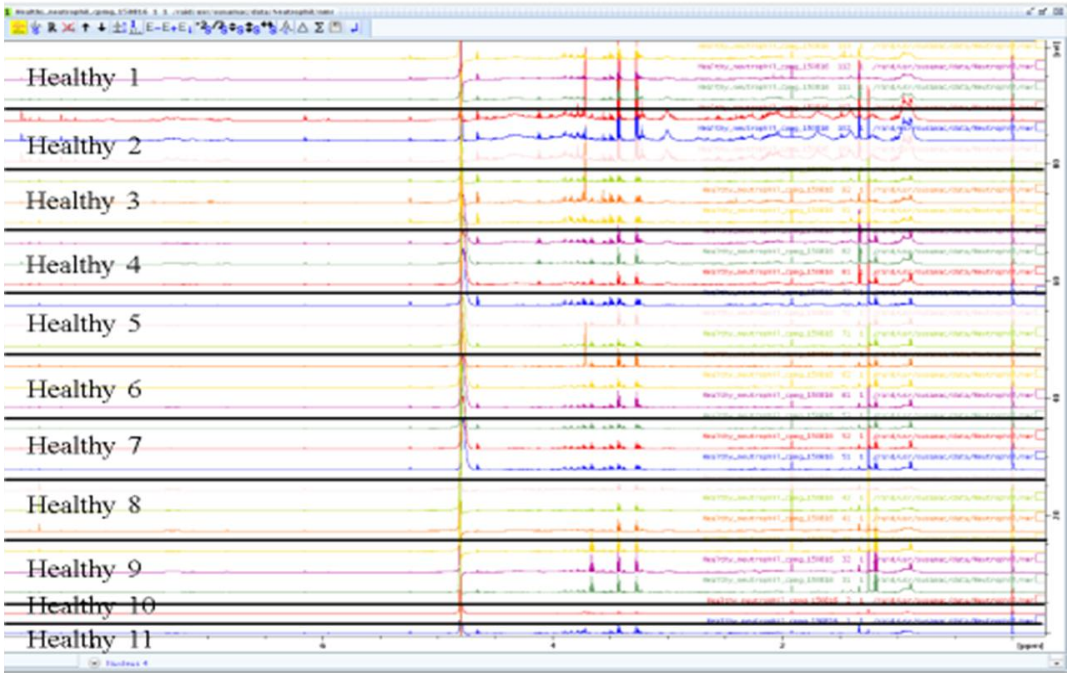

B

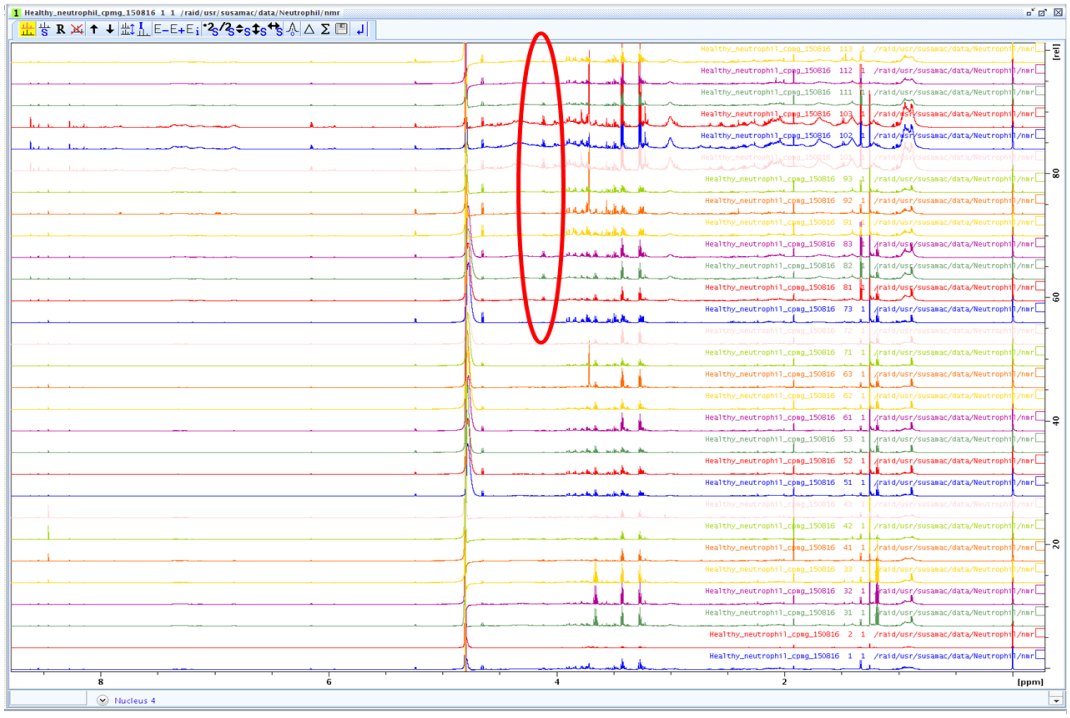

Figure 6.14: Neutrophil metabolomics of healthy individuals (n=11, measured in triplicate). (A) The shape and height of peaks vary between samples and (B) the abnormally high peaks were observed in some samples, which may represent contaminants or unidentified metabolites (in **RED** circle).

Table 6.4: Common metabolites in healthy neutrophils. The total number of metabolites detected by Chenomx Profiler® software (version 8.2 standard) was 338 (the total metabolite pattern available in Chenomx Profiler® software), and of these 89 were reproducibly detected in human healthy neutrophils. (n=11, each with 3 technical replicates)

Common Metabolites in Healthy Neutrophils				
1,3-Dihydroxyacetone	Acetate	Glucose	N6-Acetyllysine	Ribose
2-Hydroxyphenylacetate	Acetoin	Glutaric acid monomethyl ester	N-Acetylaspartate	Saccharopine
2-Oxoisocaproate	Acetone	Glycine	N-Acetylornithine	sn-Glycero-3-phosphocholine
3,4-Dihydroxybenzeneacetate	Alanine	Glycylproline	N-Acetylserotonin	Succinate
3-Aminoisobutyrate	Anserine	Guanidoacetate	N-Acetyltyrosine	Succinylacetone
3-Hydroxy-3-methylglutarate	Betaine	Homovanillate	NAD+	Sucrose
3-Hydroxyisovalerate	Biotin	Indole-3-acetate	NADH	Taurine
3-Hydroxyphenylacetate	Choline	Isocitrate	NADP+	Threonine
3-Methylglutarate	Creatine	Isoeugenol	NADPH	Thymol
3-Methylxanthine	Creatine phosphate	Isoleucine	N-Methylhydantoin	Trimethylamine N-oxide
3-Phenylpropionate	Creatinine	Kynurenine	N-Phenylacetylglycine	UDP-N-Acetylglucosamine
4-Hydroxy-3-methoxymandelate	Ethylene glycol	Lactate	O-Acetylcholine	Valine
4-Pyridoxate	Ferulate	Lactose	O-Phosphocholine	Vanillate
5-Aminolevulinate	Formate	Lactulose	Oxypurinol	Xylitol
5-Hydroxyindole-3-acetate	Fructose	Levulinate	Pantothenate	γ-Glutamylphenylalanine
5-Hydroxylysine	Galactitol	Mannose	p-Cresol	π-Methylhistidine
5-Methoxysalicylate	Galactonate	Melatonin	Phenylacetate	τ-Methylhistidine
Acetamide	Gluconate	Methanol	Propionate	

6.12 NMR metabolomics of human neutrophils in response to PMA

Phorbol-12-myristate-13-acetate (PMA), a phorbol ester, directly stimulates protein kinase C (PKC) in neutrophils, which then activates the NADPH oxidase through redistribution and activation of PKC and subsequent phosphorylation of several proteins, including $p47^{phox}$, the cytosolic NADPH-oxidase component (188). Following PMA treatment, neutrophils become highly activated and many metabolic pathways are stimulated, including the production of superoxide anions. The PMA-induced neutrophil NADPH-oxidase activation is very rapid but transient. For example, the maximal superoxide production is observed at 5 - 8 min after treatment, is sustained for around 15 min and then gradual declines to baseline levels (188).

Because of its ability to rapidly and extensively (but transiently) activate neutrophils, PMA was chosen as the agonist to initially characterise the metabolomic changes following activation, and to establish the kinetics of these responses. In these experiments, the metabolomic changes in neutrophils were evaluated at 5 and 15 min after PMA treatment.

The experiments were performed on three different preparations of neutrophils, with total cell numbers of: 4×10^6 (experiment G1); 4×10^6 (experiment G2); 3.6×10^6 (experiment G3), and using the NS of 256. Each sample was analysed in triplicate (3 technical repeats). The data at baseline were quite scattered (Figure 6.15), presumably that in the un-activated cells, levels of metabolites were quite low and this low signal:noise ratio led to apparent scattering of data. However, when all three experiments were analysed using PCA, a consistent pattern of neutrophil metabolomics in response to PMA was observed.

At 5 min after the PMA treatment, two distinct metabolomic responses were observed (Figure 6.15A). The points of the triplicated samples at each time-point became more clustered, meaning that the triplicated data became more similar, compared to the wider scatter of the pre-treatment samples that were more disperse and therefore not very similar to each other. Second, the triplicated points representing the neutrophil spectral data at 5 min after the PMA treatment (GxPMA5) of each of the three preparations of neutrophils (**BLUE** points in **RED** circle, **YELLOW** points

in **YELLOW** circle and **RED** points in **BLUE** circle) tended to move towards the same area. There are two possible explanations for these two observations of neutrophil metabolomics in response to PMA.

The first explanation is the technical limitation of the NMR metabolomics to detect the low level metabolites present in resting neutrophils (see Section 6.8.2). Therefore, the triplicated data did not generate very similar spectral data and the signal to noise ratio was low. Based on the experimental study to optimise the number of cells required for neutrophil NMR metabolomics, the number of cells significantly impacted the interpretation of the spectral data, and also the confidence level in the comparison study (see Section 6.12; 6.13). This study suggested that when the number of neutrophils was 3.5×10^6 cells, the number of scans should be at least 512 to allow the comparison study between groups. However, in the current experiments of neutrophil metabolomics in response to PMA treatment, the NS of 256 was applied. However, 5 min after treatment with PMA resulted in the generation of higher levels of metabolites, therefore providing the higher peak intensity, and a greater signal to noise ratio. The high peak intensity, could possibly compensate for or overcome the limitation of the NMR approach when low numbers of cells were used.

A second explanation may be the similarity of neutrophil metabolomics in response to the PMA treatment, despite the significantly different baseline spectra (or at resting state) (see Section 6.11). Due to the fact that PMA is a strong protein kinase C activator, high levels of similar metabolites are likely to be produced in neutrophils in response to this treatment. These cellular responses should be similar in neutrophils from healthy controls, and provide the similar patterns of metabolomic profiles in response 5 min after activation with this agent.

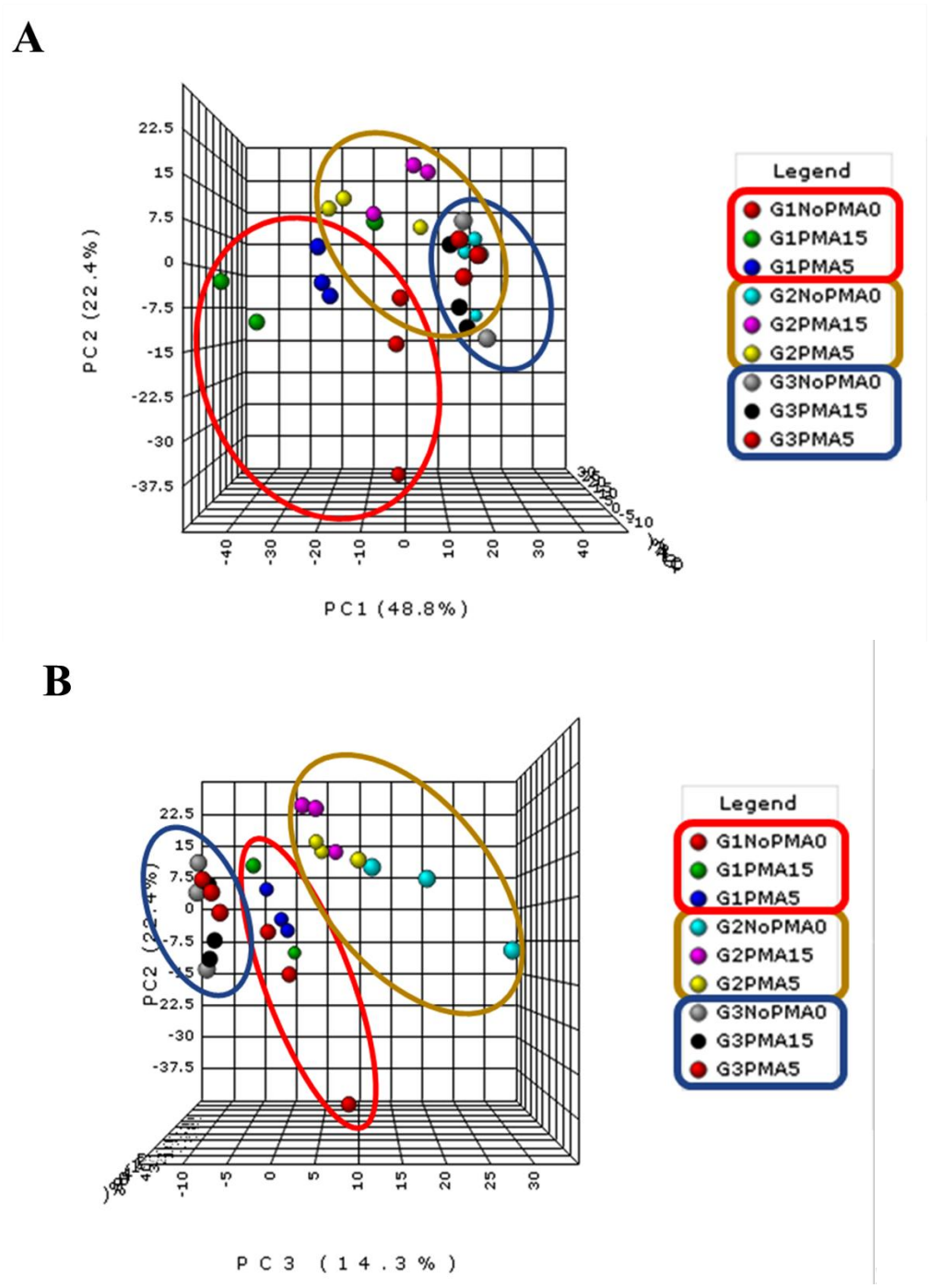

Figure 6.15: Neutrophil metabolomic changes in response to PMA treatment. In PCA, the 3D scores plots of PC 1 (48.8%) and PC 2 (22.4%) in (A), and PC 2 (22.4%) and PC 3 (14.3%) in (B) are presented. (**Abbreviations** are: G1NoPMA0 = preparation 1, no PMA added at time zero; G3PMA5 = preparation 3 PMA added for 5 min etc.)

In the subsequent analyses (Figure 6.16), neutrophil metabolomics at baseline (NoPMA0 group), 5 min after the PMA treatment (PMA5 group) and 15 min after the PMA treatment (PMA15 group) were compared. In PCA, the principal components that represented the variables of neutrophil metabolomics in three different states of response (NoPMA0, PMA5 and PMA15 groups) were clearly different from each other (Figure 6.16). The neutrophil metabolomic profiles at 5 and 15 min were different from the profiles at resting state (or baseline). Therefore, in the next steps, the metabolites that were significantly changed in response to the PMA treatment were investigated.

The principal component analysis allowed for the preliminary visualisation of the spectral data of neutrophil metabolomics in response to the PMA treatment. This allowed for visual distinctions of the similarities and differences of the spectral data at each time-point, (NoPMA0, PMA5 and PMA15). The neutrophil metabolomics at the baseline were highly variable from one healthy individual to another, and within the technical replicates. However, the PMA treatment was likely to activate similar sets of metabolites in neutrophils (see Section 6.12). However, as the objectives of the study were to detect changes in metabolites in response to the PMA treatment, the fold change analysis of the spectra at either 5 or 10 min after PMA treatment were compared to the spectra at baseline. The fold change threshold was 2.

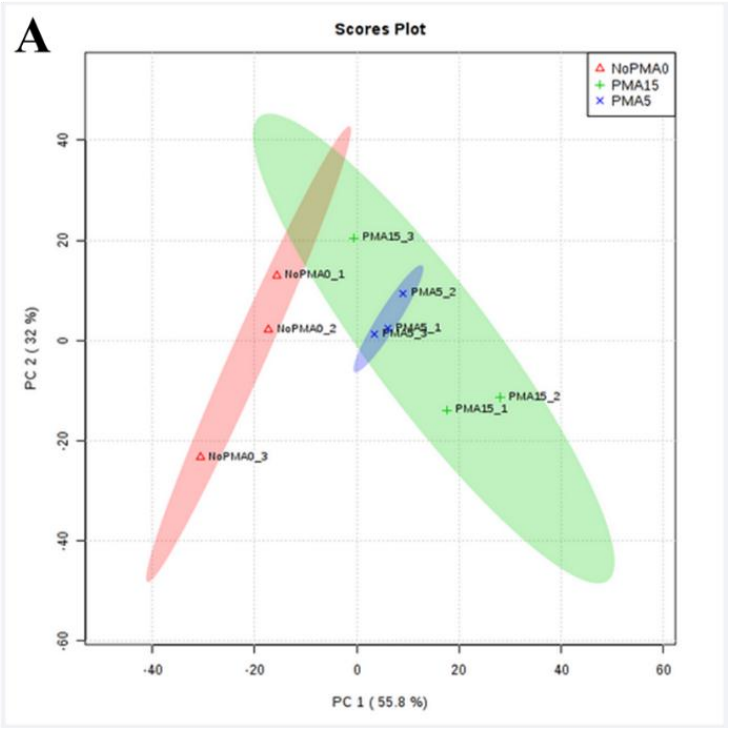
A
Scores Plot
NoPMA0
PMA15
PMA5
PMA15_3
NoPMA0_1
PMA5_2
NoPMA0_2
PMA15_2
PMA15_1
NoPMA0_3
PC 2 (32 %)
PC 1 (55.8 %)

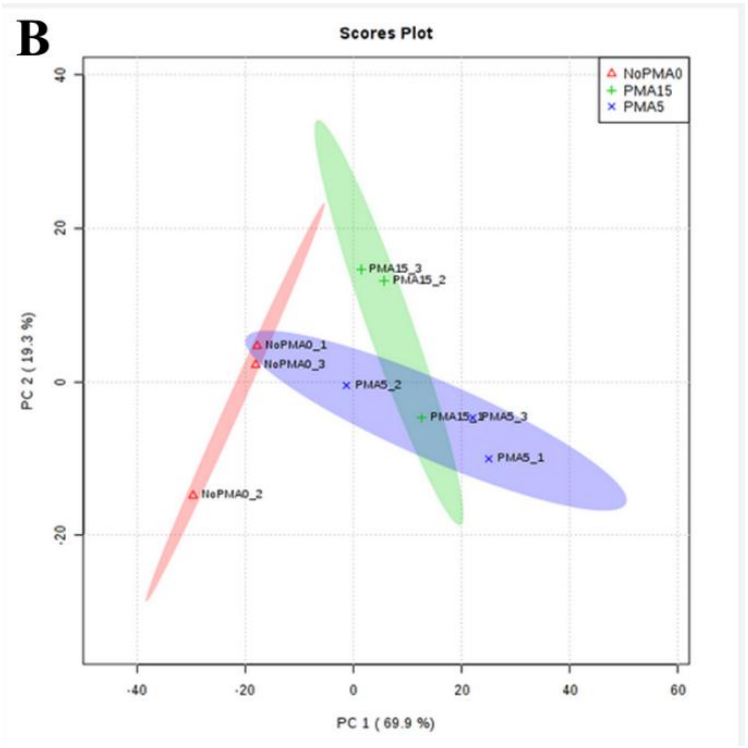
B
Scores Plot
NoPMA0
PMA15
PMA5
PMA15_3
PMA15_2
NoPMA0_1
NoPMA0_3
PMA5_2
PMA15
PMA5_3
PMA5_1
NoPMA0_2
PC 2 (19.3 %)
PC 1 (69.9 %)

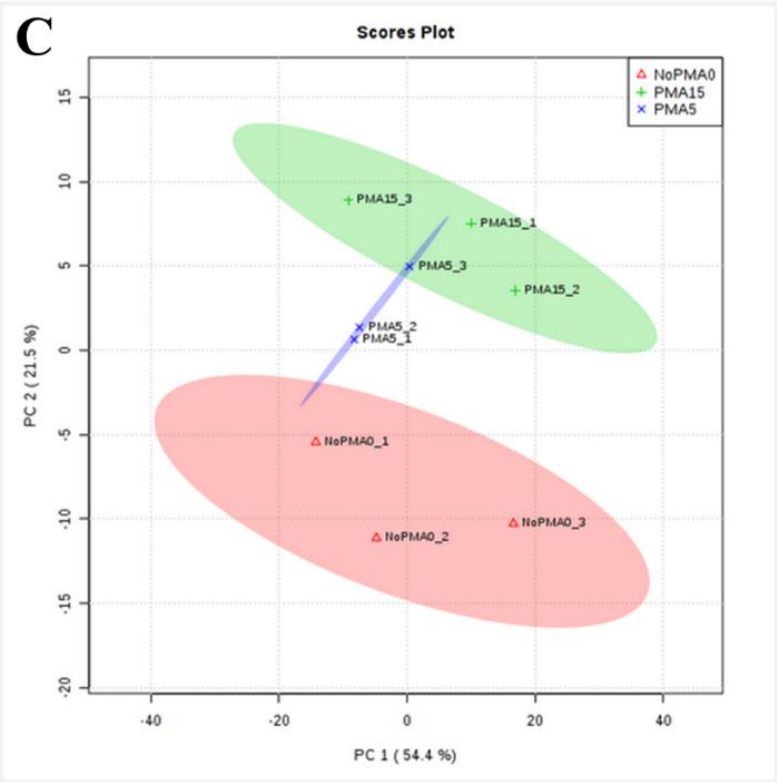

Figure 6.16: The PCA of the neutrophil metabolites in response to PMA treatment. In each experiment, the three groups of neutrophils, NoPMA0 (in **RED** circle), PMA5 (in **GREEN** circle) and PMA10 (in **BLUE** circle), were grouped and compared. **(Abbreviations**: NoPMA0 = neutrophil metabolomics at baseline, PMA5 = neutrophil metabolomics at 5 min after PMA treatment, PMA10 = neutrophil metabolomics at 10 min after PMA treatment. A, B and C represent three different preparations of neutrophils, with three technical replicates at each time-point.)

Using the online programme Metaboanalyst®, the fold change analysis in each study group (PMA5 and NoPMA0: PMA15 and NoPMA0) was performed. Three lists of spectral peaks were obtained for each study group (n=3 for: PMA5 and NoPMA0; PMA15 and NoPMA0). In the PMA5 and NoPMA0 comparison, the number of spectral peaks that were changed ≥ two fold in the PMA5 group compared to NoPMA0 group, were 29, 129 and 24 for experiments 1, 2 and 3 respectively. In the PMA15 and NoPMA0 comparison, the number of spectral peaks that were changed ≥ two fold compared to NoPMA0 group, were 60, 219 and 39 for experiments 1, 2 and 3, respectively. The spectral peaks were then selected for further analyses if they were detected in at least 2 out of 3 experiments. In the comparison study between the PMA5 and NoPMA0, 43 metabolites were identified as changed spectral peaks (Table 6.5), however, only 7 metabolites were confirmed to change ≥ two fold in the PMA5 group compared to NoPMA0 (Table 6.6). For the comparison study between PMA15 and NoPMA0, 40 metabolites were identified as changed spectral peaks (Table 6.7), and 7 metabolites were confirmed to change ≥ two fold in the PMA15 group compared to NoPMA0 (Table 6.8). To confirm identity of the metabolites represented by the spectral peaks, manual appraisal of possible metabolites was performed.

The spectral peaks were manually appraised using Chenomx Profiler® and Bruker TopSpin® software by applying the following criteria. First, the peaks representing the specific metabolites were defined as either the distinct or the non-distinct peaks. The distinct peak means either a spectral peak represented only one dominant metabolite or a spectral peak absolutely matched with the metabolite peak (from Chenomx Profiler® software). In general, the distinct peaks usually locate in the area represented by the specific chemical structure, for example, aromatic rings and methyl groups. If the spectral peak was the distinct peak of the metabolites, then that identified metabolite was likely to change. Second, if the spectral peak was slightly matched with the metabolite peak, then the other peaks that represented that metabolite would be reviewed and if other distinct peaks representing that metabolite was not changed, then that metabolite was less likely to have changed.

Table 6.5: The manual appraisal of possible metabolites. All 43 identified metabolites that were different by ≥ 2 fold in the PMA5 group compared to the NoPMA0 group, were appraised one by one. Only 7 metabolites were subsequently confirmed to be significantly different (Table 6.6).

	Metabolites	Significant Peaks (Location)	Conclusion
2	2-AMINOADIPATE	13	Not likely
3	2-FUROATE	5	Not likely
4	3-HYDROXYKYNURENINE	1	Not likely
5	ADENOSINE	1	Not likely
6	ADP	7, 8, 9, 11	Not likely
7	ANSERINE	10	Not likely
8	ATP	8, 9, 10, 12,13,14	Not likely
9	BETAINE	12	Likely
10	BIOTIN	2, 3, 4	Not likely
11	CARNITINE	1, 2, 4, 5, 6, 9	Not likely
12	CARNOSINE	5	Not likely
13	CYTIDINE	10, 11	Not likely
14	DIMETHYLAMINE	2	Likely
15	FORMATE	1	Likely
16	FUCOSE	4, 5, 9	Not likely
17	GALACTOSE	5, 6, 7, 9, 57	Not likely
18	GAMMA-METHYLHISTIDINE	3	Likely
19	GLUCOSE	5, 9, 11, 12, 52, 64	Likely
20	GLUCOSE-1-PHOSPHATE	44	Not likely
21	GLUCOSE-6-PHOSPHATE	10, 36, 44, 49	Not likely
22	GLUTAMINE	5	Not likely
23	GLUTATHIONE	3, 4, 5, 7, 8, 13, 14	Not likely
24	GLYCYLPROLINE	19	Not likely
25	GTP	2, 6, 7	Not likely
26	GUANOSINE	4	Not likely
27	INDOLE-3-ACETATE	3	Not likely
28	INOSINE	1	Not likely
29	LACTOSE	4, 88, 99	Not likely
30	LACTULOSE	1, 2, 4, 5, 6	Not likely
31	METHYLGUANIDINE	2	Likely
32	NAD	5, 20, 21	Not likely
33	NADP	5, 20, 21, 23	Not likely
34	O-ACETYLCHOLINE	2, 3, 7	Not likely
35	P-CRESOL	12	Not likely
36	PHENYLALANINE	22	Not likely
37	SUCCINYLACETONE	4, 12	Likely
38	SUCROSE	25	Not likely
39	TAURINE	29	Not likely
40	THYMOL	13	Not likely
41	TRIMETHYLAMINE-N-OXIDE	3	Not likely
42	TRYPTOPHAN	4	Not likely
43	VALINE	8	Not likely
44	XYLOSE	3, 4, 8, 9	Not likely

Table 6.6: The list of changed identified metabolites between PMA5 and NoPMA0 groups. Seven identified metabolites were confirmed visually to be different. The threshold of the fold change analysis was 2.

Compound Names	HMDB	PubChem	KEGG
Betaine	HMDB00043	247	C00719
Dimethylamine	HMDB00087	674	C00543
Formic acid	HMDB00142	284	C00058
3-Methylhistidine	HMDB12897	64961	C20157
D-Glucose	HMDB00122	5793	C00031
Methylguanidine	HMDB01522	10111	C02294

(**Abbreviations**: HMDB = Human Metabolome Database, KEGG = Kyoto Encyclopedia of Genes and Genomes, PubChem = PubChem project of National Center for Biotechnology Information (NCBI))

Table 6.7: The manual appraisal of possible metabolites. All 39 identified metabolites that were different by ≥ 2 fold in the PMA15 group compared to the NoPMA0 group, were appraised one by one. Only 7 metabolites were subsequently confirmed to be significantly different (Table 6.8).

	Metabolites	Significant Peaks (Location)	Conclusion
2	2-FUROATE	5, 7	Not likely
3	2-AMINOADIPATE	14	Not likely
4	3-METHYLGLUTARATE	1	Not likely
5	ADENINE	3	Not likely
6	ADENOSINE	1, 5	Not likely
7	ADP	1, 2, 7, 8, 9, 11	Not likely
8	ANSERINE	10, 11, 12, 13	Not likely
9	ATP	1, 2, 9, 13, 14	Not likely
10	BIOTIN	2, 3, 4, 6, 8	Not likely
11	CARNITINE	1, 2, 4, 5, 6, 8, 9	Not likely
12	CARNOSINE	5, 6, 7, 8, 13	Not likely
13	CHOLINE	9	Not likely
14	CYTIDINE	7	Not likely
15	DIMETHYLAMINE	10	Likely
16	FUCOSE	1, 4, 5, 8, 9, 20	Not likely
17	GALACTOSE	1, 5, 6, 7, 9, 57	Not likely
18	GAMMA-METHYLHISTIDINE	2	Likely
19	GLUCOSE	1, 5, 9, 11, 12, 60, 64, 75	Likely
20	GLUCOSE-1-PHOSPHATE	1, 24, 44	Not likely
21	GLUCOSE-6-PHOSPHATE	10, 40, 44	Likely
22	GLUTATHIONE	3, 4, 5, 7, 8, 9, 12, 13, 14	Not likely
23	GLYCYLPROLINE	23, 31	Not likely
24	GTP	2, 6, 7, 10	Not likely
25	INOSINE	1	Not likely
26	LACTOSE	4, 9	Not likely
27	LACTULOSE	1, 2, 4, 12	Not likely
28	N-ACETYLSEROTONIN	25	Not likely
29	NAD	10, 15, 19, 20, 21, 22, 23	Not likely
30	NADP	13, 16, 20, 21, 23, 24, 25	Not likely
31	O-ACETYLCARNITINE	4	Not likely
32	O-ACETYLCHOLINE	2, 3, 4, 6, 7	Not likely
33	OXYPURINOL	1	Likely
34	P-CRESOL	13	Not likely
35	RIBOSE	57	Not likely
36	SUCCINYLACETONE	13	Likely
37	TAURINE	4	Likely
38	UDP-GALACTOSE	8, 9	Not likely
39	VALINE	9	Not likely
40	XYLOSE	3, 4, 6, 8, 9	Not likely

Table 6.8: The list of changed identified metabolites between PMA15 and NoPMA0 groups. Seven identified metabolites were confirmed visually to be different. The threshold of the fold change analysis was 2.

Compound Names	HMDB	PubChem	KEGG
Dimethylamine	HMDB00087	674	C00543
3-Methylhistidine	HMDB00479	64969	C01152
D-Glucose	HMDB00122	5793	C00031
Glucose 6-phosphate	HMDB01401	5958	C00092
Oxypurinol	HMDB00786	4644	C07599
Succinylacetone	HMDB00635	5312	NA
Taurine	HMDB00251	1123	C00245

(**Abbreviations**: HMDB = Human Metabolome Database, KEGG = Kyoto Encyclopedia of Genes and Genomes, PubChem = PubChem project of National Center for Biotechnology Information (NCBI), USA, NA = not available)

6.13 The study of neutrophil NMR metabolomics in health and rheumatoid arthritis

Rheumatoid arthritis (RA) is a systemic inflammatory autoimmune disease that primarily affects the synovium of joints (see Section 6.14). Evidence suggests that neutrophils (158) contribute to the pathophysiology of RA through the release of cytotoxic and immunoregulatory molecules (75). In the affected joints, neutrophils are the majority of immune cells deposited in the synovium (189) and constitute up to ~90% of immune cells in synovial fluid. Moreover, the peripheral blood neutrophils from RA patients have an activated phenotype including delayed apoptosis, increased capacity to produce reactive oxygen species, active gene expression and membrane expression of high-affinity Fcγ receptors (FcγR) (190,191). This study, therefore, aimed to use NMR metabolomics to characterise the distinct phenotype of RA neutrophils.

RA neutrophils were freshly isolated from whole blood as described in section 2.5. The demographic data of the patients and the healthy controls were described in Table 6.9. The number of cells in each sample varied due to the total number derived from the whole blood, and were technically triplicated. All the healthy controls and the rheumatoid arthritis patients were Caucasian. The mean age was 34.75 ± 14.38 years old for healthy controls, and 63.25 ± 11.02 years old for rheumatoid arthritis patients.

Table 6.9: The clinical data of the healthy and the RA neutrophils

Samples	Sex	Age	Total cell number	Duration from the diagnosis	Remarks (e.g. time from diagnosis, special medications)
Healthy1	Male	55	3.6×10^6	-	-
Healthy2	Male	35	4×10^6	-	-
Healthy3	Male	24	4×10^6	-	-
Healthy4	Female	25	8.5×10^6	-	-
RA1	Male	47	7×10^6	6 months	Methotrexate
RA2	Female	69	4.5×10^6	3 months	Methotrexate, Sulfasalazine and Hydroxychloriquine
RA3	Male	66	10×10^6	6 months	Methotrexate and Hydroxychloriquine
RA4	Male	71	8.5×10^6	15 years	Rituximab. Active disease.

(**Note**: Rituximab is a biological therapy for severe rheumatoid arthritis. It is a monoclonal antibody against the protein CD20, which is primarily found on the surface of B cells. RA4 patient was later excluded from the study analysis to the fact that this drug was used and that the patient had a long and difficult clinical history.)

In the first experiments, the principal component analyses were performed to visualise the spectral data of the two groups. In the 3D scores plot, the principal components of the two groups, RA and healthy neutrophils, were likely to be distinguished from each other. However, the RA4 sample represented by three **GREEN** points in the **BLUE** circle was clustered at the same area as the healthy samples (Figure 6.17). Therefore, the clinical data of the RA4 sample was reviewed and revealed the significantly different clinical history of this patient from the others. RA4 patient's disease was active and the biological medication, Rituximab, was prescribed at the time of the neutrophil collection. Rituximab is a monoclonal antibody against the protein CD20, which is primarily found on the surface of immune system B cells, and therefore destroys B cells. Moreover, in a previous study of NMR-based serum metabolomics of the RA patients (192), the serum metabolomics in the patients receiving biological treatment revealed the distinct metabolomics spectrum from either the healthy control or the pre-treatment RA patients. Due to the significant difference in clinical background, which highly modulates the neutrophil phenotype, sample RA4 was excluded from further analyses.

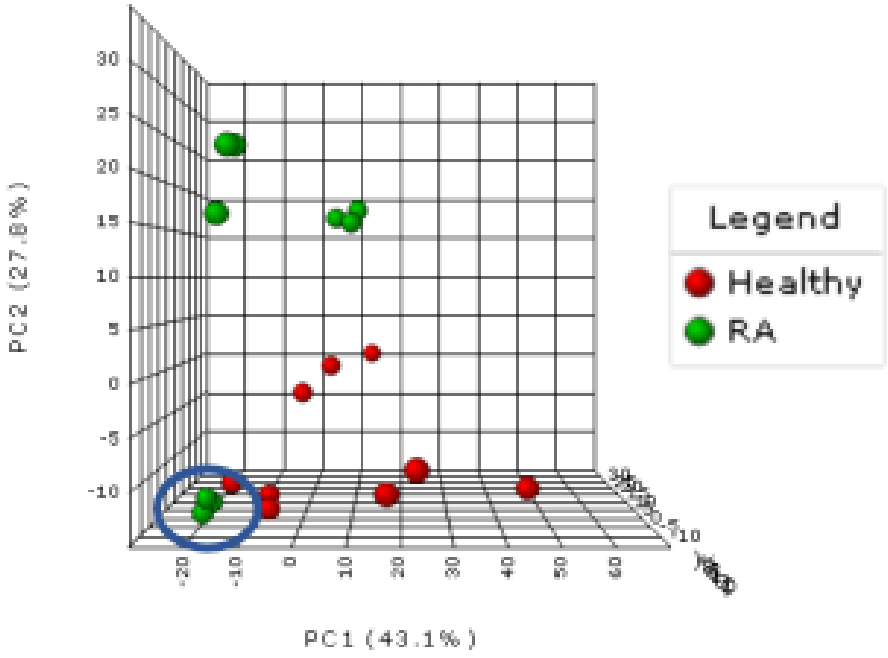

Figure 6.17: PCA of neutrophil NMR metabolomics in healthy controls and RA patients. The healthy neutrophil group (n = 4) was represented by the **RED** points, while the RA neutrophil group (n = 4) was represented by the **GREEN** points. However, one RA sample (the **GREEN** points in the **BLUE** circle) was excluded from the further study due to the significant difference in clinical background.

For the further analyses, the number of RA samples was 3, while the healthy controls were 4. The principal component analyses revealed the two distinct groups of samples, RA and healthy neutrophils (Figure 6.17; 6.18). Therefore, at a first step, the common metabolites in RA neutrophils were listed and then compared with those in healthy controls. To define the common metabolites, the same criteria of metabolites present in ≥ 50% of samples (in this case, 2 out of 3) was applied. As a result, 97 metabolites were found in common between all 3 RA samples (see Table 6.10), while 89 common metabolites were identified in the 4 healthy controls (see Table 6.11). The comparison of the metabolites revealed 17 metabolites were present in RA neutrophils but absent in healthy neutrophils, and 12 metabolites were present *vice versa* (Table 6.12).

Table 6.10: Common metabolites in RA neutrophils. The total number of metabolites detected by Chenomx Profiler® software (version 8.2 standard) was 338 (the total metabolite pattern available in Chenomx Profiler® software), and of these 97 were reproducibly detected in human RA neutrophils. (n = 3, each with 3 technical replicates)

Common Metabolites in RA Neutrophils				
1,3-Dihydroxyacetone	Acetamide	Glutamate	N-Acetylaspartate	Pyruvate
1,7-Dimethylxanthine	Acetate	Glutathione	N-Acetylcysteine	Ribose
2-Hydroxy-3-methylvalerate	Acetoin	Glycine	N-Acetylglucosamine	Saccharopine
2-Hydroxyisovalerate	Acetone	Glycylproline	N-Acetylglycine	sn-Glycero-3-phosphocholine
2-Hydroxyvalerate	Acetylsalicylate	Guanidoacetate	N-Acetylserotonin	Succinate
2-Oxoisocaproate	Alanine	Homovanillate	N-Acetyltyrosine	Succinylacetone
3,4-Dihydroxybenzeneacetate	Anserine	Isocitrate	NAD+	Sucrose
3-Aminoisobutyrate	Betaine	Isoeugenol	NADH	Taurine
3-Hydroxy-3-methylglutarate	Choline	Isoleucine	NADP+	Thymol
3-Hydroxyisovalerate	Creatine	Kynurenine	NADPH	Trimethylamine N-oxide
3-Hydroxyphenylacetate	Creatine phosphate	Lactate	N-Carbamoylaspartate	UDP-N-Acetylglucosamine
3-Methyladipate	Creatinine	Lactose	N-Phenylacetylglycine	Valerate
3-Methylglutarate	Ethylene glycol	Lactulose	O-Acetylcarnitine	Valine
3-Methylxanthine	Ferulate	Levulinate	O-Phosphocholine	Vanillate
3-Phenylpropionate	Formate	Malonate	Ornithine	Xylitol
4-Hydroxy-3-methoxymandelate	Fructose	Mannose	Oxypurinol	π-Methylhistidine
4-Pyridoxate	Galactitol	Melatonin	p-Cresol	τ-Methylhistidine
5-Aminolevulinate	Galactonate	Methanol	Phenylacetate	
5-Hydroxyindole-3-acetate	Glucitol	Methylamine	Propionate	
5-Methoxysalicylate	Glucose	N6-Acetyllysine	Pyridoxine	

Table 6.11: Common metabolites (n = 17) present in RA neutrophils, but not present in healthy neutrophils. The total number of metabolites identified by Chenomx Profiler® software (version 8.2 standard) was 338 (the total metabolite pattern available in Chenomx Profiler® software).

Common metabolites in RA neutrophils, but not present in healthy neutrophils (n=17)		
1,7-Dimethylxanthine	Malonate	O-Acetylcarnitine
2-Hydroxyisovalerate	Methylamine	Ornithine
3-Methyladipate	N-Acetylcysteine	Pyridoxine
Glucitol	N-Acetylglucosamine	Pyruvate
Glutamate	N-Acetylglycine	Valerate
Glutathione	N-Carbamoylaspartate	

Table 6.12: Common metabolites (n = 12) present in healthy neutrophils, but not present in RA neutrophils. The total number of metabolites identified by Chenomx Profiler® software (version 8.2 standard) was 338 (the total metabolite pattern available in Chenomx Profiler® software).

Common metabolites in healthy neutrophils, but not present in RA neutrophils (n=12)		
2-Hydroxyphenylacetate	Glutaric acid monomethyl ester	O-Acetylcholine
5-Hydroxylysine	Indole-3-acetate	Pantothenate
Biotin	N-Acetylornithine	Threonine
Gluconate	N-Methylhydantoin	γ-Glutamylphenylalanine

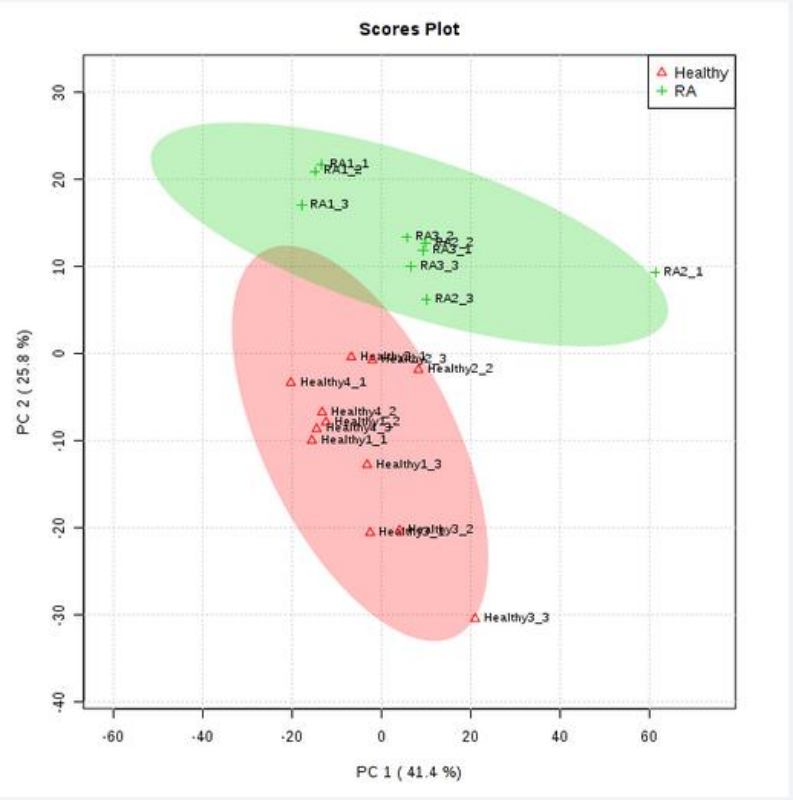

Figure 6.18: The PCA of the healthy and rheumatoid arthritis (RA) neutrophils. The principal components of the healthy neutrophil NMR spectra (n = 4) were displayed in **PINK** circle, while the principal components of the RA neutrophil samples (n = 3) were displayed in **GREEN** circle. All samples were technically triplicated.

Using the online programme Metaboanalyst®, the statistical analyses of the metabolomic spectra between two groups, RA and healthy neutrophils, were performed. The fold change analysis, at the threshold of 2, revealed that 68 spectral peaks were ≥ 2 fold different in healthy compared to the RA group. Among 68 spectral peaks, 57 metabolites were identified. However, to confirm identity of the metabolites represented by the spectral peaks, manual appraisal of possible metabolites was performed (Table 6.13). Only 14 metabolites were changed at least 2 folds in the healthy group when compared to the RA group (Table 6.14).

The pathway analyses were performed using those 14 metabolites (Figure 6.19; Table 6.15). Using the pathway analyses in the Metaboanalyst® programme, the metabolites were analysed through pathway analysis algorithms (Hypergeometric test for an over representation analysis and Pathway topology analysis for a pathway impact value). The pathways involved in the metabolomic changes were listed in Table 6.15. The most impacted pathway is phenylalanine metabolism.

Table 6.13: The manual appraisal of possible metabolites. All 57 identified metabolites that were different by ≥ 2 fold in the healthy group compared to the RA group, were appraised one by one. Only 14 metabolites were subsequently confirmed to be significantly different (Table 6.14).

	Metabolites	Significant Peaks (Location)	Conclusion
2	1,3-DIMETHYLURATE	1, 4	Not likely
3	1,7-DIMETHYLXANTHINE	6	Not likely
4	2-FUROATE	5, 6	Not likely
5	3-HYDROXY-3-METHYLGLUTARATE	8	Likely
6	3-HYDROXYISOVALERATE	3	Likely
7	3-HYDROXYKYNURENINE	3	Not likely
8	4-HYDROXYPHENYLACETATE	14	Not likely
9	5-AMINOLEVULINATE	5, 9	Likely
10	ADP	4	Not likely
11	ANSERINE	2	Not likely
12	ATP	1, 4	Not likely
13	BETAINE	8, 13, 14, 15	Not likely
14	BIOTIN	16	Not likely
15	CARNITINE	8, 11, 12, 18	Not likely
16	DIMETHYLAMINE	4	Not likely
17	EPICATHECHIN	9	Not likely
18	ETHANOL	1, 2,3, 7, 10, 11, 12	Not likely
19	FORMATE	1	Likely
20	FUCOSE	8, 19, 20, 22, 23, 24, 28	Not likely
21	GALACTONATE	17, 18	Not likely
22	GALACTOSE	51, 53	Not likely
23	GAMMA-METHYLHISTIDINE	3	Not likely
24	GLUCOSE	5, 8, 9, 10, 74, 75, 77, 78, 79, 80, 81, 89, 91, 92	Likely
25	GLUCOSE-1-PHOSPHATE	47, 48	Likely
26	GLUCOSE-6-PHOSPHATE	10	Likely
27	GLUTAMATE	8	Not likely
28	GLUTAMINE	2, 41	Likely
29	GLUTATHIONE	12, 48	Likely
30	GTP	1, 10	Not likely
31	HISTAMINE	3, 5	Not likely
32	INDOLE-3-ACETATE	5	Not likely
33	INOSINE	7	Not likely
34	ISOCITRATE	33	Likely
35	ISOLEUCINE	21, 22, 23, 24, 28	Not likely
36	LACTOSE	4, 5, 72, 73, 94, 96	Not likely
37	MALATE	30	Not likely
38	MANNOSE	40, 47	Not likely
39	METHANOL	1	Likely
40	N6-ACETYLLYSINE	2	Not likely
41	N-ACETYLASPARTATE	1, 14	Not likely
42	N-ACETYLORNITHINE	3	Not likely
43	N-ACETYLSEROTONIN	24, 25	Not likely
44	NAD	1, 3, 13, 16, 19	Not likely
45	NADP	2, 9, 15, 17	Not likely
46	NALPHA-ACETYLLYSINE	1	Not likely
47	O-ACETYLCARNITINE	5, 6, 27	Likely
48	O-ACETYLCHOLINE	6	Not likely
49	PHENYLALANINE	18	Not likely
50	PI-METHYLHISTIDINE	11, 12	Not likely
51	PYROGLUTAMATE	14, 24	Not likely
52	SEBACATE	17	Not likely
53	SUCCINYLACETONE	6, 8	Not likely
54	TAURINE	3, 4, 6, 7, 8, 9, 10, 23, 25, 30, 31, 32, 33	Likely
55	THYMOL	16, 17	Not likely
56	TRIMETHYLAMINE_N-OXIDE	4, 5, 6, 7	Likely
57	UDP-GALACTOSE	10, 11	Not likely
58	XYLOSE	9	Not likely

Table 6.14: The list of changed identified metabolites between RA and healthy neutrophils. Fourteen identified metabolites were confirmed visually to be different. The threshold of the fold change analysis was 2.

Compound Names	HMDB	PubChem	KEGG
3-Hydroxymethylglutaric acid	HMDB00355	1662	C03761
3-Hydroxyisovaleric acid	HMDB00754	69362	NA
5-Aminolevulinic acid	HMDB01149	137	C00430
Formic acid	HMDB00142	284	C00058
D-Glucose	HMDB00122	5793	C00031
Glucose 1-phosphate	HMDB01586	439165	C00103
Glucose 6-phosphate	HMDB01401	5958	C00092
L-Glutamine	HMDB00641	5961	C00064
Glutathione	HMDB00125	124886	C00051
Isocitric acid	HMDB00193	1198	C00311
Methanol	HMDB01875	887	C00132
L-Acetylcarnitine	HMDB00201	1	C02571

Compound Names	HMDB	PubChem	KEGG
Taurine	HMDB00251	1123	C00245
Trimethylamine N-oxide	HMDB00925	1145	C01104

(**Abbreviations**: HMDB = Human Metabolome Database, KEGG = Kyoto Encyclopedia of Genes and Genomes, PubChem = PubChem project of National Center for Biotechnology Information (NCBI), USA)

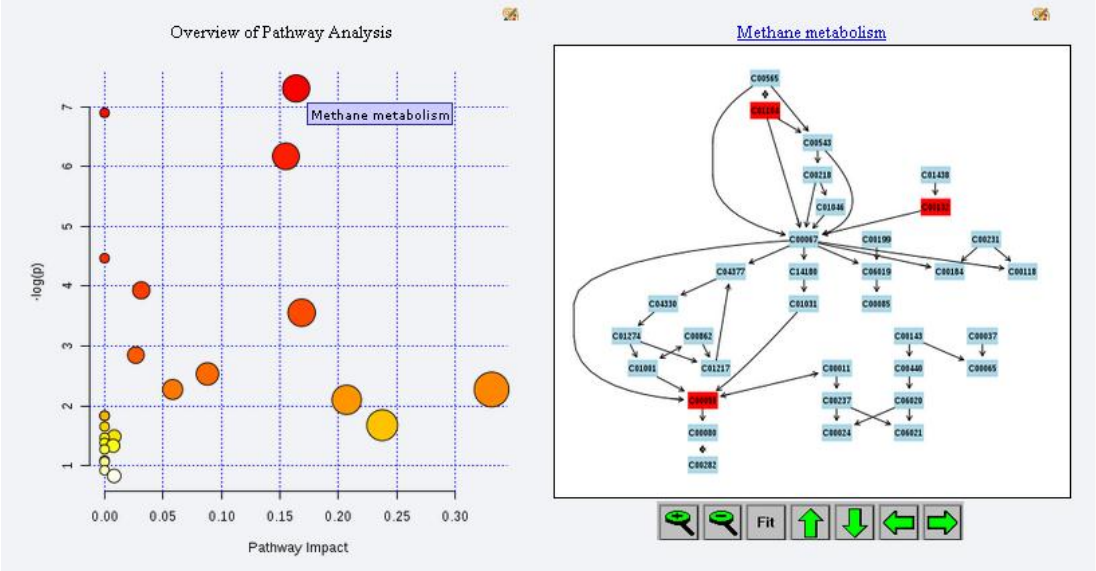

Figure 6.19: Pathway analysis. In the overview of pathway analysis (**left**), each point represented the impacted pathway, for example phenylalanine metabolism (the labelled red point at the right upper of the graph). The x axis represents the pathway impact (implies the contribution of the changed metabolites to that pathway, for example the node (more impacted) or the end product (less impacted)), and the y axis is the p value (implies the number of changed metabolites in that pathway). The methane metabolism pathway was demonstrated (**right**), where the **RED** boxes represented the changed metabolites and the **BLUE** boxes represented the other unchanged metabolites. The methane metabolism pathway that was highly impacted by metabolomic changes in synovial fluid from RA and IA (non-RA inflammatory arthritis).

Table 6.15: List of the pathway names that impacted by the changed metabolites. (The threshold of the fold change analysis was 2.)

Pathway Name	Total	Hits	P	Impact
Methane metabolism	34	3	0.000669	0.16384
Nitrogen metabolism	39	3	0.001006	0
Starch and sucrose metabolism	50	3	0.002084	0.15505
Glycolysis or Gluconeogenesis	31	2	0.011465	0
Galactose metabolism	41	2	0.019612	0.03137
Glyoxylate and dicarboxylate metabolism	50	2	0.028507	0.16853
D-Glutamine and D-glutamate metabolism	11	1	0.057949	0.02674
Amino sugar and nucleotide sugar metabolism	88	2	0.079377	0.08797

Pathway Name	Total	Hits	P	Impact
Citrate cycle (TCA cycle)	20	1	0.10304	0.05826
Taurine and hypotaurine metabolism	20	1	0.10304	0.33094
Alanine, aspartate and glutamate metabolism	24	1	0.12243	0.20703
Pentose phosphate pathway	32	1	0.16006	0
Pyruvate metabolism	32	1	0.16006	0
Glutathione metabolism	38	1	0.1873	0.23743
Inositol phosphate metabolism	39	1	0.19176	0
Primary bile acid biosynthesis	47	1	0.22663	0.00822

Pathway Name	Total	Hits	P	Impact
Glycine, serine and threonine metabolism	48	1	0.23089	0

(**Abbreviations**: **Total** is the total number of compounds in the pathway. **Hits** is the number of the actually matched metabolites. "**p**" is the p value calculated from the enrichment analysis. **Impact** is the pathway impact value calculated from pathway topology analysis.)

6.14 NMR metabolomics of synovial fluid

Synovial fluid is the viscous fluid secreted from the cells lining the synovium of joints, which include fibroblasts and fibroblast-like synoviocytes (193). The role of synovial fluid is to protect the joints by decreasing the friction between two articular cartilage surfaces during movement or joint loading. Synovial fluid also provides the nutrients and lubrication for the joints (194). As synovial fluid is normally an ultrafiltrate of plasma plus hyaluronic acid (the carbohydrate lubricant), its biochemical properties are similar in physiologic conditions. However, in joint diseases, the physiologic conditions of synovial fluid are disturbed and the volume and composition of synovial fluid changes. Identifying the metabolites in such fluids could help identify the biological functions that are perturbed in these joints and identify biomarkers to identify efficacy of drug treatments.

The synovial fluid samples used in this study were obtained from patients with inflammatory joint diseases and have increased amounts of proteins, cells (including inflammatory cells), cytokines and metabolic enzymes. These components will potentially interfere with the synovial fluid NMR metabolomic study, as they could obscure the peaks of low-quantity metabolites. Therefore, the preparation steps for synovial fluid were different from those used for extraction of intracellular neutrophil metabolites. In particular, it was necessary to remove the proteins and some large molecules in the diseased synovial fluids. Moreover, the internal reference, for example TSP, could not added into the synovial fluid, as TSP-protein complexes will be formed.

Despite the fact that the extraction procedures were altered, the analytical processes for synovial fluid NMR metabolomics were similar those used for neutrophils: the preliminary spectral analyses, the creation of a pattern file (see Supplementary data: The synovial fluid pattern file), and the spectral and statistical analyses were all similar.

6.15 The study of synovial fluid NMR metabolomics in rheumatoid arthritis

In rheumatoid arthritis (RA), the underlying pathology is immune-mediated inflammatory joint disease (193). The RA joints are marked by inflammation of the synovium and destruction of articular cartilage and bones. The RA synovium becomes hyperplastic with infiltration by a variety of immunocompetent cells (activated neutrophils in particular). Therefore, RA synovial fluid components are enriched with cytokines, inflammatory mediators and proteolytic enzymes that degrade the extracellular matrix (195).

According to the European League Against Rheumatism (*EULAR*) RA classification criteria (196), there are no definite diagnosis criteria for RA. However, the classification criteria (Table 6.16) is recommended to facilitate clinical diagnosis, where the definite diagnosis is likely if the score is ≥ 6. Interestingly, although the synovial fluid analyses and profiles are essential in the diagnosis of joint disease, they are not included in the classification criteria. RA has a distinct pathophysiology leading to joint inflammation and destruction, but the current simple synovial analyses cannot distinguish between RA and other inflammatory joint diseases.

Table 6.16: The 2010 classification criteria of rheumatoid arthritis of European League Against Rheumatism (*EULAR*)

Criteria	Score
JOINTS DISTRIBUTION (0 - 5)	
1 large joint	0
2 - 10 large joints	1
1 - 3 small joints (large joints not counted)	2
4 - 10 small joints (large joints not counted)	3
> 10 joints (at least one small joint)	5
SEROLOGY (0 - 3)	
Negative RF AND negative ACPA	0
Low positive RF OR low positive ACPA	2
High positive RF OR high positive ACPA	3
SYMPTOM DURATION (0 - 1)	
< 6 weeks	0
≥ 6 weeks	1

ACUTE PHASE REACTANTS (0-1)	
Normal CRP AND normal ESR	0
Abnormal CRP OR abnormal ESR	1

(**Abbreviations**: RF = rheumatoid factor, ACPA = Anti-Citrullinated protein antibody, CRP = C-reactive protein, ESR = Erythrocyte sedimentation rate)

NMR metabolomics was therefore used to characterise the metabolomic patterns of synovial fluid in rheumatoid arthritis, which may have diagnostic/prognostic values. Moreover, the study of metabolomic changes and pathway analyses could possibly shed new insights into the understanding in RA pathology within joints.

The synovial fluid samples were as follows: 14 synovial fluid samples from RA and 14 from other inflammatory joint diseases (non-RA inflammatory arthritis, IA) (gout/crystal arthropathy (n = 4), reactive arthritis (n = 3) and n = 1 each of SLE, JIA, Behçets disease, ulcerative colitis, ankylosing spondylitis, palindromic arthritis and inflammatory monoarthritis). Spectral data of synovial fluids from RA and IA were visualised using Bruker Topspin® software. The spectral alignments were observed, because for these for synovial fluid NMR data, there was no internal reference (TSP could not be added into the samples.). The spectra had to be aligned in order to compare them with the bucket table data of both groups, RA and IA. Two statistical analyses, unpaired T-Test and ANOVA, were performed and the results were compared.

A) Unpaired T-Test

Using Amix® software, the spectral data of RA and IA synovial fluids were interpreted into the bucket table with peak intensity value. The statistical analyses were performed *via* the online programme, Metaboanalyst®. The unpaired T-test analysis was selected for the comparison of two groups, RA and IA. The p value was at 0.01.

As a consequence, 36 spectral peaks were identified that were significantly different between RA and IA (non-RA inflammatory arthritis) groups. However, only 22 identified metabolites were related to the significantly changed spectral peaks (Table 6.17). In the next step, the peaks at the locations were visualised individually to confirm that they represented the specific metabolites. When analysing spectral patterns, one spectral peak may represent either the specific metabolites (the so called "distinct peaks"), or the summation of several metabolites (the so called "non-distinct peaks"). The changes in the distinct peaks were more likely to be interpreted as the changes in concentrations of the identified metabolites, rather than from other unspecified metabolites. For example, the spectral peaks of phenylalanine comprises 17 peaks in total, of which 5 are distinct peaks and 12 are non-distinct peaks. The spectral peaks were significantly different in 8 out of the 17 peaks, including 2 distinct peaks and 6 non-distinct peaks. Therefore, phenylalanine was likely to be confirmed as a significantly changed metabolite when compared between RA and IA groups. All 22 possible metabolites were appraised one by one, and only 15 metabolites were subsequently confirmed to be significantly different (Table 6.18).

Table 6.17: The manual appraisal of possible metabolites. All 22 identified metabolites that were significantly different between two groups, RA and IA synovial fluids, were appraised one by one. Only 15 metabolites were subsequently confirmed to be significantly different.

Metabolites	Distinct Peaks (location)	Total No. Distinct Peaks	Non-Distinct Peaks (location)	Total No. Non-Distinct Peaks	Conclusion
2-HYDROXYVALERATE		0	825	9	Not likely
2-PHENYLPROPIONATE		1	73, 74, 75	7	Not likely
3-HYDROXY-3-METHYLGLUTARATE		0	675, 676	3	Likely
3-HYDROXYBUTYRATE		2	840	10	Likely
3-HYDROXYGLUTARATE		3	677	3	Likely
3-PHENYLLACTATE	69, 70	12		0	Likely
3-PHENYLPROPIONATE		3	73, 74, 75	14	Likely
3,5-DIBROMOTYROSINE		0	75	1	Not likely
5-AMINOLEVULINATE	595	3		10	Not likely
ACETATE		0	761, 762	2	Likely
BIOTIN	799, 800	3		7	Not likely
FUCOSE		3	434, 840	6	Likely
GLUTAMINE	723, 724	26		23	Likely
KYNURENINE		8	61, 62, 63	7	Likely
LACTATE	331, 327, 328, 330, 831, 832	6	825	13	Likely
LYSINE		21	761, 762	10	Likely
MALATE		0	674, 675, 676, 677	8	Not likely
MYO-INOSITOL		2	434	6	Likely
P-CRESOL	110, 111, 112, 114, 115	5		1	Not likely
PHENYLALANINE	76, 80	5	61, 62, 63, 73, 74, 75	12	Likely
SUCCINATE		0	674	2	Likely
VALINE	438	11		8	Likely

Table 6.18: List of significantly changed, identified metabolites between RA and IA (non-RA inflammatory arthritis) (n=15). The identified metabolites that the spectra were confirmed visually to be significantly different. The statistical analysis was an unpaired T-Test with p value of 0.01.

Compound Names	HMDB	PubChem	KEGG
3-hydroxy-3-methylglutarate	HMDB00355	1662	C03761
3-hydroxybutyrate	HMDB00357	441	C01089
3-hydroxyglutarate	HMDB00428	181976	NA
3-phenyllactate	HMDB00779	3848	C01479
3-phenylpropionate	HMDB00764	107	C05629
Acetate	HMDB00042	176	C00033
Fucose	HMDB00174	17106	C01019
Glutamine	HMDB00641	5961	C00064
Kynurenine	HMDB00684	161166	C00328
Lactate	HMDB00190	107689	C00186
Lysine	HMDB00182	5962	C00047

Compound Names	HMDB	PubChem	KEGG
Myo-inositol	HMDB00211	NA	C00137
Phenylalanine	HMDB00159	6140	C00079
Succinate	HMDB00254	1110	C00042
Valine	HMDB00883	6287	C00183

(**Abbreviations**: HMDB = Human Metabolome Database, KEGG = Kyoto Encyclopedia of Genes and Genomes, PubChem = PubChem project of National Center for Biotechnology Information (NCBI), USA, NA = not available)

B) ANOVA

Using Amix® software, the spectral data of RA and IA synovial fluids were interpreted into the bucket table with peak intensity value. The statistical analyses were performed *via* the online programme, Metaboanalyst®. ANOVA with Fisher's LSD *post hoc* analysis was selected for the comparison of more than two groups (e.g. for further comparison with fluids from different degenerative joint diseases such as osteoarthritis), with unpaired data. The p value was at 0.01.

As a consequence, 18 spectral peaks were that were significantly different between RA and IA (non-RA inflammatory arthritis) groups. However, only 8 identified metabolites, (3-phenyllactate, 2-phenylpropionate, 3-phenylpropionate, 5-aminolevulinate, biotin, glutamine, kynurenine and phenylalanine), were related to the significantly changed spectral peaks. In the next step, the peaks at the locations were visualised individually to confirm that they represented the specific metabolites. When analysing spectral patterns, one spectral peak may represent either the specific metabolites (the so called "distinct peaks"), or the summation of several metabolites (the so called "non-distinct peaks"). The changes in the distinct peaks were more likely to be interpreted as the changes in concentrations of the identified metabolites, rather

than from other unspecified metabolites. For example, the spectral peaks of phenylalanine comprises 17 peaks in total, which are 5 distinct peaks and 12 non-distinct peaks. The spectral peaks were significantly different in 8 out of the 17 peaks, including 2 distinct peaks and 6 non-distinct peaks. Therefore, phenylalanine was likely to be confirmed as a significantly changed metabolite when compared between RA and IA groups. All 8 possible metabolites were appraised one by one, and only 4 metabolites, 3-phenyllactate, 3-phenylpropionate, kynurenine and phenylalanine, were subsequently confirmed to be significantly different (Table 6.19).

Table 6.19: List of metabolites in synovial fluid that were significantly different between RA and other inflammatory joint disease (non-RA inflammatory arthritis (IA)) (n = 4). Statistical analyses method is ANOVA with Fisher's LSD *post hoc*, p value = 0.01.

Compound Names	HMDB	PubChem	KEGG
3-Phenyllactate	HMDB00779	3848	C01479
3-Phenylpropionate	HMDB00764	107	C05629
Kynurenine	HMDB00684	161166	C00328
Phenylalanine	HMDB00159	6140	C00079

(**Abbreviations**: HMDB = Human Metabolome Database, KEGG = Kyoto Encyclopedia of Genes and Genomes, PubChem = PubChem project of National Center for Biotechnology Information (NCBI), USA)

When the spectral peaks were analysed using two statistical analyses methods, T-Test and ANOVA, the number of the changed metabolites was different. However, the identified metabolites (n = 5) by ANOVA with Fisher's LSD *post hoc* were the subset of the results of the T-Test (n = 14). In order to study the metabolomic changes

in rheumatoid arthritis, each metabolites were appraised in correlation with the biology (See Discussion).

6.16 Discussion

The aim of this chapter was to develop protocols for the study of human neutrophils using ^{1}H NMR metabolomics and then apply the protocols to study changes of neutrophil metabolism in disease. Protocols were developed to take into account the low levels of metabolites in human neutrophils, and to develop optimal conditions for the detection of metabolites such as NADP+ which have high rates of turn-over during activation of neutrophils.

In order to optimise protocols for neutrophil metabolomics, it was necessary to study both unactivated (freshly isolated healthy control) and activated neutrophils. It was decided to use PMA as the activating factor for *in vitro* optimisation experiments. PMA is an analogue of diacylglycerol, which rapidly activates protein kinase C, generating a respiratory burst through activation of the NADPH oxidase (197). It is used experimentally to activate ROS production (*via* the respiratory burst) from primed and unprimed neutrophils, and is a potent activator of neutrophil extracellular trap formation (NETosis) (158). The experiments demonstrated a dynamic regulation of glucose levels in response to PMA; after 5 min incubation, glucose levels were significantly higher, and after 15 min glucose levels were significantly lower. This could represent a rapid import of glucose at 5 min (to support the rapid increase in metabolic activity in response to PMA) followed by exhaustion of glucose by 15 min. Alternatively, these intracellular increases in glucose could result from the mobilisation of glycogen stores of neutrophils. A significant change was also observed in the levels of glucose-6-phosphate. This metabolite, in conjunction with NADP+, is a substrate for glucose-6-phosphate dehydrogenase to produce NADPH *via* the hexose monophosphate shunt (197). A number of inhibitors of ROS levels were also increased by PMA-stimulation, including methyl-guanidine and taurine. These metabolites are scavengers of H_2O_2 and HOCl, both of which are produced during the neutrophil respiratory burst (198,199), and the in increased levels of these anti-oxidants by PMA-treatment may represent a form of feedback inhibition of ROS production.

Table 6.20: Key metabolites changed in response to PMA treatment

Metabolites	At 5 min	At 15 min	Pathways	Implications
Glucose	↑	↓	Glucose metabolism	The rapid increase of metabolic activity in response to PMA.
Glucose-6-phosphate	↓	↑	Hexose monophosphate shunt	The metabolite, in conjunction with NADP+, is a substrate for glucose-6-phosphate dehydrogenase to produce NADPH.
Methylguanidine, Taurine	↔	↓	Neutrophil respiratory burst	Inhibitors of reactive oxygen species (ROS).

Once protocols for NMR neutrophil metabolomics had been optimised, the next step was to study neutrophils activated *in vivo* by inflammation, in this case neutrophils from patients with rheumatoid arthritis. Rheumatoid arthritis (RA) neutrophils have previously been shown to circulate in the blood stream in an activated form, and have dynamic changes in gene expression compared to healthy control neutrophils (191). Indeed, transcriptomic analysis of RA neutrophils can be used to stratify patients into responders and non-responders to anti-TNF therapy (200). My hypothesis therefore was that the metabolome of RA neutrophils would be significantly different to that of healthy control neutrophils. PCA analysis was able to discriminate between RA and healthy control neutrophil samples, and it was determined that 43 metabolites were present in significantly different levels between RA and healthy (present in one but not the other group, or present at significantly different levels). A number of the metabolites that were identified in RA neutrophils

may be attributed to known mechanisms of disease. Methylamine (present in RA and not healthy neutrophils) is a by-product of the activation of protein arginine deiminase 4 (PAD4). PAD4, an enzyme which plays a key role in the chemical modification of arginine to citrulline, has been identified in a genome-wide association study (GWAS) as a susceptibility gene for the development of RA (201). Citrullination of histones by PAD4 is a key regulator of gene expression; the replacement of positively charged arginines with negatively charged citrullines leads to chromatin decondensation within the nucleus, which is important for the initiation of gene expression (202). RA neutrophils exhibit higher levels of citrullinated histones, especially histone H2A, H3 and H4. Citrullination of histones is a key component of NETosis (202), allowing decondensation of chromatin prior to DNA release, and in RA, a number of hypercitrullinated proteins can be found within synovial joints, including vimentin and aggrecan (203). A hallmark of severe RA is the presence of serum anti-citrullinated peptide antibodies (ACPA), and the hypothesis is that citrullination of peptides *via* PAD4 by neutrophils, followed by exposure of citrullinated peptides in NETs to cells of the adaptive immune system, is a key step in the development of ACPA in early RA pathology (204). Also elevated in RA neutrophils was ornithine. This metabolite has previously been identified in serum from RA patients and from patients with periodontal disease (205). Interestingly, it has been shown that patients with periodontal disease have increased PAD4 activity due to the presence of pathogens such as *Porphyromonas gingivalis*, leading to increased protein citrullination (206). Incidence of periodontal disease is higher in RA compared to the healthy population (205).

Another key metabolite elevated in RA was myo-inositol. Synthesis of inositol metabolites is a key pathway regulating the activation of neutrophils, which occurs downstream of G-protein activation of phospholipase C (PLC). PLC hydrolyses phosphatidylinositol 4,5-bisphosphate (PIP_2) to produce inositol 1,4,5-triphosphate (Ins 1,4,5-P3), which induces the release of calcium from intracellular stores, and the release of diacylglycerol (DAG) from the plasma membrane, both of which activate protein kinase C (PKC) (197,207) leading to rapid activation of cell signalling, NADPH oxidase assembly and the respiratory burst. Neutrophils from patients with RA show evidence of activation *in vivo* and do not require priming to generate a respiratory burst (159). In addition, reports of increased levels of spontaneous NETosis

(204) in RA neutrophils would support the evidence that the NADPH oxidase is already assembled and active in RA neutrophils.

A number of metabolites implicated in the production of inflammatory mediators were found to be elevated in RA neutrophils. Kynurenine is a metabolite of tryptophan metabolism, and is a vasodilator implicated in systemic inflammation (208). Tryptophan metabolism has previously been reported to be elevated in both RA serum and synovial fluid (209–212), and was identified in my analysis of RA and IA synovial fluid as being elevated in RA. N-acetylcystine (a precursor of L-cystine) and glutamate were also elevated in RA neutrophils. These metabolites are part of the glutathione synthesis pathway (glutathione was also elevated in RA). Activation of this pathway leads to the activation of leukotriene synthesis (197). Leukotrienes are eicosanoid inflammatory mediators, produced by neutrophils *via* the oxidation of arachidonic acid. Leukotriene B4 is a potent neutrophil chemoattractant and can promote neutrophil adherence *via* upregulation of CD11b (MAC-1) (213).

This study identified a number of metabolites, elevated in RA neutrophils and RA synovial fluid, that are implicated in ketosis, including 2-hydroxyisovalerate, pyruvate, 3-hydroxy-3-methyl glutarate, 3-hydroxybutarate and 3-hydroxyglutarate. Ketosis has previously been reported as a metabolic pathway elevated in RA serum and synovial fluid, and been attributed to the limited energy source caused by low oxygen conditions in pathogenically challenged tissues. Whilst this may indeed be the case, another possibility to consider is the fasting state of donors (RA and healthy) at the time of sample collection. Ketosis can occur *via* a shift in metabolism during glucose limitation: in the absence of glucose e.g. *via* dietary limitation or decreased mobilisation of glycogen stores, (or during oxygen limitation) metabolism of stored lipids is stimulated to increase the supply of acetyl CoA. If this molecule cannot be further metabolised in the citric acid cycle (e.g. because of decreased levels of intermediates or oxygen limitation), then excess acetyl CoA is converted to ketone bodies such as acetoacetate, acetate and hydroxybutyrate. Therefore, if a donor had not eaten breakfast on the day of sample donation this could significantly alter the metabolite profile of biofluids and cells including neutrophils. Information on fasting state were not recorded as part of this study, and should be a consideration for the design of follow-on studies.

Table 6.21: Key metabolites changed in RA neutrophils

Metabolites	Relative level in RA compare to healthy control	Pathways	Implications
Methylamine	↑	The activation of protein arginine deiminase 4 (PAD4).	PAD4, an enzyme which plays a key role in the chemical modification of arginine to citrulline, and has been identified in GWAS studies as a susceptibility gene for the development of RA.
Ornithine	↑	Unknown	Previously identified in serum from RA patients and from patients with periodontal disease, which the incidence is higher in RA patients.
Myo-inositol	↑	Synthesis of inositol metabolites	A key pathway regulating the activation of neutrophils, which occurs downstream

Metabolites	Relative level in RA compare to healthy control	Pathways	Implications
			of G-protein activation of phospholipase C (PLC).
Kynurenine	↑	Tryptophan metabolism	A vasodilator implicated in systemic inflammation.
N-acetylcystine, Glutamate	↑	The glutathione synthesis pathway	Activation of this pathway leads to the activation of leukotriene synthesis, an eicosanoid inflammatory mediator, produced by neutrophils.
2-Hydroxyisovalerate, pyruvate, 3-Hydroxy-3-methyl glutarate, 3-Hydroxybutarate, 3-Hydroxyglutarate	↑	Ketosis	The limited energy source caused by low oxygen conditions in pathogenically challenged tissues.

To date, metabolomic studies in RA have focused on biofluids, including urine, serum and synovial fluid (210), and the potential of metabolomics to identify biomarkers to predict response to therapy. 3-hydroxybutyrate, a key metabolite in ketosis, was identified by a number of studies as being elevated in RA serum (214). Levels of this metabolite were significantly decreased following successful treatment with the anti-TNF drug etanercept (214). These studies have also reported increased activation of the tricarboxylic (TCA) cycle and amino acid metabolism in RA biofluids (210). A number of lipid metabolites have been previously reported to be lower in RA biofluids, with a possible explanation being lipids as a source of energy within the hypoxic joint (215). These previous studies were confirmed by my analysis of RA synovial fluid. Alteration of lipid metabolism is associated with changes in membrane composition/permeability, gene expression and protein distribution and function, as well as in cellular functions such as cell growth, proliferation, differentiation, survival, apoptosis and chemotaxis, implicated in the RA disease process (216). Metabolomic analysis of urine from RA patients prior to commencement of anti-TNF therapy identified the upregulation of histamine, glutamine, phenylacetic acid, xanthine, xanthurenic acid and creatinine, and downregulation of ethanolamine, p-hydroxyphenylpyruvic acid and phosphocreatine as biomarkers of a good response to therapy (217). Serum biomarkers can also distinguish responders and non-responders to methotrexate (211). A number of metabolites and metabolic pathways have been shown to correlate with markers of inflammation such as C-reactive protein (CRP), including arginine metabolism (arginine and ornithine), tryptophan metabolism (serotonin and tryptophan) and branched-chain amino acids (isoleucine, leucine and valine) (209).

The results in this Chapter show that this approach of NMR metabolomics has great potential to identify functional changes in neutrophils activated *in vitro* or *in vivo* during inflammatory activation of these cells. The metabolomic changes identified map well with the known and predicted changes in function of these cells and further work is now needed to perform these analyses on neutrophils stimulated *in vitro* with a wider range of agonists. It will also be necessary to study the metabolomic profiles of RA neutrophils, including a larger patient cohort to identify disease heterogeneity and also during the course of their treatment to determine if changes in these metabolomic profiles correlate with disease improvement of resistance to therapy.

This new approach has great potential to further study neutrophil function, both *in vivo* in inflammatory/metabolic disorders and after *in vitro* activation. For example, transcriptomic analyses (176) have shown great differences in mRNA profiles of neutrophils from patients with rheumatoid arthritis, compared to healthy controls. These transcriptomic changes would be predicted to result in changes in the function and hence metabolic activity of RA neutrophils. Indeed, the pilot experiments described in this Chapter show that RA neutrophils have quite a distinct metabolomic profile to those of control neutrophils. These metabolomic changes are likely to reflect altered cell signalling processes and/or altered cellular composition of neutrophils as a result of disease. The above-mentioned transcriptomic studies have also revealed considerable neutrophil heterogeneity in different RA patents (200,218) and this may be reflected in their different responsiveness to anti-inflammatory drugs. It would be interesting, therefore, to undertake a larger scale study of the neutrophil metabolome in different RA patients, both before and post therapy, and to determine if changes in the metabolome can be used to identify different disease sub-types and/or differential responses to therapy. If so, then neutrophil metabolomics may serve as a useful prognostic indicator of likely response to therapy.

Another potential use of this approach would be to compare the metabolomic profiles of WAS patients (Chapter 4) with those of healthy controls. An altered actin cytoskeleton in these patients may also be reflected by an altered metabolome, particularly in cells activated to undergo cytoskeletal re-arrangements. If so, then a metabolomic profile of WAS-corrected neutrophils could be a useful indicator of the success of genetic correction of stem cells in these patients.

Furthermore, this technique could also be applied to confirm the efficiency of differentiation of iPSCs into different types of mature blood cells. It is predicted that different types of mature blood cells (neutrophils, eosinophils, mononuclear phagocytes, lymphocytes) would have different resting and activated metabolomic profiles. Therefore, determining the metabolomic profiles of iPSCs that have been induced to differentiate into different types of blood cells could be a useful molecular "fingerprint" to evaluate the efficiency and specificity of differentiation of these cells.

CHAPTER 7 GENERAL DISCUSSION AND FUTURE WORK

This thesis describes a number of technologies that can be applied to study the molecular basis of human disease and to determine the how particular cellular processes are regulated in a number of human conditions. Stem cell technologies have great potential for either the study of human biological processes or the development of new therapeutic approaches. In this thesis, two stem cell technologies, mesenchymal stem cells (MSCs) and induced pluripotent stem cells (iPSCs) have been explored to understand the molecular basis of human disease. First, the potential role of MSCs, in combination with oral vitamin C, as a new diabetic wound therapy have been studied both *in vivo*, using a diabetic nude mouse model, and *in vitro*, using proliferation and tubular formation assays and by measuring the expression of angiogenic growth factors after *in vitro* culture of MSCs. Second, the iPSC technology was used to model neutrophil functions due to impaired signalling *via* Wiskott-Aldrich syndrome protein (WASp). The morphology of mature blood neutrophils were compared with those of iPSC-derived neutrophils and differentiated myeloid cell lines. Additionally, the new technique, NMR metabolomics, was used to study the function of neutrophils activated *in vitro* or *in vivo* and identify altered neutrophil metabolism in human diseases, e.g. rheumatoid arthritis.

In the MSC experiments, the potential of mesenchymal stem cells (MSCs) and vitamin C supplementation in the treatment of diabetic wounds using the diabetic nude mouse model was investigated. The main findings of my study in this part of the thesis were as follows:

1. Upregulated expression of *mVEGF-α*, *mPDGF-BB*, *mFN-1* and *mTNC* in MSCs cultured in the presence of TGF-β1
2. Decreased *mVEGF-α* and *mPDGF-BB* mRNA expression in TGF-β1-treated MSCs cultured under high glucose conditions and vitamin C reversal of the hyperglycaemic suppression of TGF-β1 regulation of *mVEGF-α* and *mPDGF-BB* expression.
3. Effect of hyperglycaemia on the secretion of angiogenic cytokines into the culture medium of MSCs, which resulted in the impaired tubular formation

4. Vitamin C as adjunct therapy for MSC treatment of diabetic wounds *in vivo* accelerated the wound closure, which was likely due to effects of increasing capillary vascularisation.

This study showed that vitamin C supplementation could reverse the effects of hyperglycemia on MSC function, and opens the possibility that oral vitamin C could be used as an adjunct therapy. The current therapeutic approaches for diabetic wound treatment is not specific to the underlying pathology of the disease. In this thesis, the vitamin C supplement could potentiate the angiogenic effects of both intrinsic (natural) factors and extrinsic (topical application) mesenchymal stem cells (MSCs). Moreover, the serum vitamin C level in diabetic patients is generally low due to the high renal excretion rate. Oral vitamin C supplement is safe and therefore should be considered as an adjunct therapy in patients with diabetic wound. However, in my study, the only *in vivo* experiment was in diabetic nude mice, and so clinical trials should be conducted in future to determine the effects of topical MSCs with vitamin C supplement in the treatment of diabetic wounds. Vitamin C is considered a safe and cheap option to enhance wound healing.

In the study on Wiskott-Aldrich syndrome (WAS) and properties of WAS neutrophils, the potential role of genetically-corrected, induced pluripotent stem cells (iPSCs) for the treatment of Wiskott-Aldrich syndrome was the original aim of the study. The study originally aimed to isolate iPSCs from a WAS patient, identify and experimentally correct the genetic defect and determine if neutrophils-derived *in vitro* from these genetically-corrected iPSCs had restored, normal neutrophil function. However, because of changes in my training programme, only preliminary experiments were obtained and only neutrophil function from WAS patients was measured. It was also demonstrated that iPSCs from WAS fibroblasts could be successfully cultures and then differentiated into neutrophil-like cells. Nevertheless, interesting results were obtained a "proof of principle" experiments showed that this approach should be further explored in future studies. The main findings of my study in this part were as follows:

1. WAS neutrophils demonstrated impaired chemotaxis activity in response to fMLP, when compared to the healthy neutrophils

2. The differentiation of corrected-WAS-iPSCs into neutrophils *via* iPS-sac formation could generate the morphologically mature neutrophils.

Clearly, these preliminary data justify further work on this system. In the present study blood neutrophils isolated from the WAS patient revealed marked chemotactic defects, in response to fMLP. This would appear to confirm a functional defect in these neutrophils as a consequence of the genetic defect. Further work should include determination if this is a generic chemotactic defect or just restricted to responses to fMLP. For example, chemotaxis in response to agents such as IL-8, C5a could be performed. Also, further functional assays such as phagocytosis and respiratory burst activation should be conducted as these, particularly the former function, are dependent on the function of the cytoskeleton, which is reported to be the major defect in these patients. Other approaches that should be taken include functional characterisation of the *in vitro* differentiated neutrophils derived from the WAS iPSCs and whether these cells have impaired chemotaxis. It would also be necessary to assess if the neutrophils derived from the genetically-corrected iPSCs have restored chemotaxis activity. In the preliminary study, the differentiation of iPSCs to neutrophils provided the morphologically mature neutrophils, however, as the number of iPSC-derived neutrophils were limited. Future studies aimed at increasing the number of iPSC-derived neutrophils are required so that these functions can be fully evaluated.

In the PLB-985 study, the aims were to develop a cell-line model of neutrophil differentiation and to produce a set of transfected clones expressing *EGFP*-tagged Myeloid Cell Leukaemia-1 (Mcl-1), an anti-apoptotic protein that plays a key role in regulating neutrophil survival. The efficiency of the differentiation was compared in two myeloid leukaemic cell lines, PLB-985 and KCL-22 cells. The latter was chosen because a previous Ph.D. project in this laboratory indicated that this chronic myeloid leukaemia cell line had a number of molecular properties, such as an absence of *Bcl-2* expression, that were characteristic of mature neutrophils. This suggested that they were committed to the neutrophil lineage, and hence perhaps easier to differentiate *in vitro* into neutrophil-like cells. However, these experiments revealed that the KCL-22 cells did not differentiate into neutrophil-like cells as well as the PLB-985 cells, although time did not permit a thorough study to optimise the differentiation media for

the KCL-22 cells. In these experiments both cell lines were cultured in similar media. As a consequence, the PLB-985 cell line was selected to transfect and produce transfected clones expressing a *Mcl-1:EGFP* in pLVX-TetOne-Puro system (an inducible expression system with antibiotic). The main findings of this part of the study were as follows:

1. The efficiency of differentiation of PLB-985 cells was higher, in terms of the percentage of the differentiated cells at day 5, when compared to KCL-22 cells.
2. The establishment of the transduced PLB-985 cells with a *Mcl-1:EGFP* in pLVX-TetOne-Puro system

While the KCL-22 cells could be induced into neutrophil-like cells, there were quite wide fluctuations in the percentages of differentiated cells obtained. The reasons for this are unknown at present. Also, as mentioned above, a thorough and systematic investigation of the culture conditions was not performed, partly because of time limitations and partly because another project in this laboratory had spent considerable time optimising the differentiation protocols for PLB-985 cells. A major problem in these experiments is that terminally-differentiated neutrophils have a very short half life because they undergo constitutive apoptosis. Therefore, once differentiated in culture, they will die within a day or so unless precautions are taken (e.g. addition of apoptosis-delaying agents such as pro-inflammatory cytokines). Therefore, this part of the thesis was to produce a set of a transfected clones expressing a *Mcl-1:EGFP* in pLVX-TetOne-Puro system. This should then allow for the extended survival in culture of differentiated PLB-985 cells in culture, making them a more useful experimental system to study the effects of manipulation of particular genes on neutrophil function. However, the process of the clonal selection is still ongoing. When single clones are derived, the inducible induction of expression (using antibiotics) will enable the role of the *Mcl-1* gene in control of cell survival to be studied. Moreover, as the *Mcl-1* gene was tagged with *EGFP*, this allows for the intracellular tracking and location of Mcl-1 protein by confocal microscopy.

In the metabolomic study, the optimised protocols to profile of metabolome of human neutrophils using ^{1}H NMR spectroscopy have been developed. This was the first time, the human neutrophils have described in terms of metabolomic profiles, and the first time that this technique has been applied to these cells. Therefore, the

extraction and the analysis protocols needed to be optimised in order to ensure that all intracellular metabolites were extracted and captured in order to accurately define the neutrophil metabolomic profiles. Additionally, comparison studies of neutrophil metabolomic profiles in resting neutrophils and neutrophils activated both *in vivo* (rheumatoid arthritis, RA), and *in vitro* (PMA, the protein kinase C activator) were conducted. The protocols to optimise the identification of the metabolomic profiles of synovial fluid from RA and non-RA patients were also developed and profiles compared. The main findings of this part of the study were as follows:

1. The optimised extraction protocols and analysis methodologies of neutrophil NMR metabolomics have been established.
2. The neutrophil NMR metabolomic study of neutrophils from healthy individuals and rheumatoid arthritis patients revealed distinct metabolomic pattern between two groups.

The protocols for the NMR metabolomic study in neutrophils have been established for the first time. However, in the preliminary studies in this thesis, some experiments require further repeats or additional experimental variables to be tested. The baseline profiles of healthy neutrophil metabolomics were highly variable, but studies using different neutrophil numbers and varying number of scans could improve the signal:noise ratio of the metabolomic spectra analysed by the principal component analysis. The comparison of neutrophil metabolomic profiles of healthy and diseased (e.g. rheumatoid arthritis) neutrophils revealed distinct metabolomic profiles between the two groups. However, the number of the RA patients was only 3, and so the increasing number of samples would improve the reliability of the results. Moreover, the number of scans in this experiments was at 256, but in other experiments on the number of scans in this thesis, 512 or higher are recommended for the future study. Therefore, re-analyses of the RA samples at the higher number of scans has been planned.

However, these NMR experiments revealed that this is a highly useful approach to study the function of neutrophils both *in vivo* and *in vitro*. Further experiments should also measure the metabolomic profiles of healthy neutrophils activated *in vitro* (e.g. after chemotaxis, phagocytosis, ROS production, adherence) and after priming *in vitro* with a range of cytokines or other agents (e.g.

lipopolysaccharide (LPS)) that could activate them during inflammation or in inflammatory disease. Comparison of the metabolomic profiles of neutrophils isolated from the blood or inflammatory lesions (e.g. synovial fluid, bronchoalveolar lavage (BAL)) could then be compared with those profiles of neutrophils activated *in vivo* with these different agonists. Such comparative analyses could help predict the functions of neutrophils activated *in vivo* and also the agonist/signalling pathways responsible for their activation. This could not only help understand the function and role of these cells in disease, but could help in the design of targeted therapeutic interventions.

REFERENCES

1. Akgul C, Moulding DA, Edwards SW. Molecular control of neutrophil apoptosis. FEBS Lett. 2001;487(3):318–322.

2. Pivot-Pajot C, Chouinard FC, El Azreq MA, Harbour D, Bourgoin SG. Characterisation of degranulation and phagocytic capacity of a human neutrophilic cellular model, PLB-985 cells. Immunobiology. 2010;215(1):38–52.

3. Pedruzzi E, Fay M, Elbim C, Gougerot-Pocidalo M-A. Differentiation of PLB-985 myeloid cells into mature neutrophils, shown by degranulation of terminally differentiated compartments in response to N-formyl peptide and priming of superoxide anion production by granulocyte–macrophage colony-stimulating factor. Br J Haematol. 2002;117(3):719–726.

4. Volk APD, Barber BM, Goss KL, Ruff JG, Heise CK, Hook JS, et al. Priming of neutrophils and differentiated PLB-985 cells by pathophysiological concentrations of TNF-α is partially oxygen dependent. J Innate Immun. 2010;3(3):298–314.

5. Conradt B, Horvitz HR. The C. elegans protein EGL-1 is required for programmed cell death and interacts with the Bcl-2–like protein CED-9. Cell. 1998;93(4):519–529.

6. McGinnis N, Kuziora MA, McGinnis W. Human Hox-4.2 and Drosophila deformed encode similar regulatory specificities in Drosophila embryos and larvae. Cell. 1990;63(5):969–976.

7. Lewis EB. A gene complex controlling segmentation in Drosophila. In: Genes, Development and Cancer [Internet]. Springer; 1978 [cited 2016 Sep 27]. p. 205–217. Available from: http://link.springer.com/chapter/10.1007/978-1-4419-8981-9_13

8. Hereford LM, Osley MA, Ludwig JR, McLaughlin CS. Cell-cycle regulation of yeast histone mRNA. Cell. 1981;24(2):367–375.

9. Mali P, Yang L, Esvelt KM, Aach J, Guell M, DiCarlo JE, et al. RNA-guided human genome engineering via Cas9. Science. 2013;339(6121):823–826.

10. Andrews BS, Eisenberg RA, Theofilopoulos AN, Izui S, Wilson CB, McConahey PJ, et al. Spontaneous murine lupus-like syndromes. Clinical and immunopathological manifestations in several strains. J Exp Med. 1978;148(5):1198–1215.

11. Stuart JM, Cremer MA, Townes AS, Kang AH. Type II collagen-induced arthritis in rats. Passive transfer with serum and evidence that IgG anticollagen antibodies can cause arthritis. J Exp Med. 1982;155(1):1–16.

12. Like AA, Rossini AA. Streptozotocin-induced pancreatic insulitis: new model of diabetes mellitus. Science. 1976;193(4251):415–417.

13. Mestas J, Hughes CC. Of mice and not men: differences between mouse and human immunology. J Immunol. 2004;172(5):2731–2738.

14. Ran FA, Hsu PD, Lin C-Y, Gootenberg JS, Konermann S, Trevino AE, et al. Double nicking by RNA-guided CRISPR Cas9 for enhanced genome editing specificity. Cell. 2013;154(6):1380–1389.

15. Friedenstein AJ, Piatetzky-Shapiro II, Petrakova KV. Osteogenesis in transplants of bone marrow cells. Development. 1966;16(3):381–390.

16. Snykers S, De Kock J, Rogiers V, Vanhaecke T. In vitro differentiation of embryonic and adult stem cells into hepatocytes: state of the art. Stem Cells. 2009;27(3):577–605.

17. Oswald J, Boxberger S, Jørgensen B, Feldmann S, Ehninger G, Bornhäuser M, et al. Mesenchymal stem cells can be differentiated into endothelial cells in vitro. Stem Cells. 2004;22(3):377–384.

18. Arthur A, Rychkov G, Shi S, Koblar SA, Gronthos S. Adult human dental pulp stem cells differentiate toward functionally active neurons under appropriate environmental cues. Stem Cells. 2008;26(7):1787–1795.

19. Dominici M, Le Blanc K, Mueller I, Slaper-Cortenbach I, Marini FC, Krause DS, et al. Minimal criteria for defining multipotent mesenchymal stromal cells. The International Society for Cellular Therapy position statement. Cytotherapy. 2006;8(4):315–317.

20. Muraglia A, Cancedda R, Quarto R. Clonal mesenchymal progenitors from human bone marrow differentiate in vitro according to a hierarchical model. J Cell Sci. 2000;113(7):1161–1166.

21. DiGirolamo CM, Stokes D, Colter D, Phinney DG, Class R, Prockop DJ. Propagation and senescence of human marrow stromal cells in culture: a simple colony-forming assay identifies samples with the greatest potential to propagate and differentiate. Br J Haematol. 1999;107(2):275–281.

22. Takahashi K, Yamanaka S. Induction of pluripotent stem cells from mouse embryonic and adult fibroblast cultures by defined factors. cell. 2006;126(4):663–676.

23. Avior Y, Sagi I, Benvenisty N. Pluripotent stem cells in disease modelling and drug discovery. Nat Rev Mol Cell Biol [Internet]. 2016 [cited 2016 Sep 27]; Available from: http://www.nature.com/nrm/journal/vaop/ncurrent/full/nrm.2015.27.html

24. Soldner F, Jaenisch R. iPSC disease modeling. Science. 2012;338(6111):1155–1156.

25. Polo JM, Liu S, Figueroa ME, Kulalert W, Eminli S, Tan KY, et al. Cell type of origin influences the molecular and functional properties of mouse induced pluripotent stem cells. Nat Biotechnol. 2010;28(8):848–855.

26. Kim K, Doi A, Wen B, Ng K, Zhao R, Cahan P, et al. Epigenetic memory in induced pluripotent stem cells. Nature. 2010;467(7313):285–290.

27. Association AD, others. Diagnosis and classification of diabetes mellitus. Diabetes Care. 2006;29(1):S43.

28. Aguiree F, Brown A, Cho NH, Dahlquist G, Dodd S, Dunning T, et al. IDF diabetes atlas. 2013 [cited 2016 Sep 27]; Available from: http://dro.deakin.edu.au/view/DU:30060687

29. Middle-aged men twice as likely to have diabetes as women - Diabetes UK [Internet]. [cited 2016 Sep 27]. Available from: https://www.diabetes.org.uk/About_us/News_Landing_Page/Middle-aged-men-twice-as-likely-to-have-diabetes-as-women/

30. WHO | Definition and diagnosis of diabetes mellitus and intermediate hyperglycaemia [Internet]. WHO. [cited 2016 Sep 27]. Available from: http://www.who.int/diabetes/publications/diagnosis_diabetes2006/en/

31. Type 1 Diabetes Mellitus: Practice Essentials, Background, Pathophysiology. 2016 Aug 18 [cited 2016 Sep 27]; Available from: http://emedicine.medscape.com/article/117739-overview#a3

32. Type 2 Diabetes Mellitus: Practice Essentials, Background, Pathophysiology. 2016 Aug 18 [cited 2016 Sep 27]; Available from: http://emedicine.medscape.com/article/117853-overview

33. Fowler MJ. Microvascular and Macrovascular Complications of Diabetes. Clin Diabetes. 2008 Apr 1;26(2):77–82.

34. Morrish NJ, Wang S-L, Stevens LK, Fuller JH, Keen H, Group WMS, et al. Mortality and causes of death in the WHO Multinational Study of Vascular Disease in Diabetes. Diabetologia. 2001;44(2):S14–S21.

35. Cade WT. Diabetes-related microvascular and macrovascular diseases in the physical therapy setting. Phys Ther. 2008;88(11):1322–1335.

36. Galkowska H, Wojewodzka U, Olszewski WL. Chemokines, cytokines, and growth factors in keratinocytes and dermal endothelial cells in the margin of chronic diabetic foot ulcers. Wound Repair Regen. 2006;14(5):558–565.

37. Goren I, Müller E, Pfeilschifter J, Frank S. Severely impaired insulin signaling in chronic wounds of diabetic ob/ob mice: a potential role of tumor necrosis factor-α. Am J Pathol. 2006;168(3):765–777.

38. Falanga V. Wound healing and its impairment in the diabetic foot. The Lancet. 2005;366(9498):1736–1743.

39. Galiano RD, Tepper OM, Pelo CR, Bhatt KA, Callaghan M, Bastidas N, et al. Topical vascular endothelial growth factor accelerates diabetic wound healing through increased angiogenesis and by mobilizing and recruiting bone marrow-derived cells. Am J Pathol. 2004;164(6):1935–1947.

40. Lobmann R, Ambrosch A, Schultz G, Waldmann K, Schiweck S, Lehnert H. Expression of matrix-metalloproteinases and their inhibitors in the wounds of diabetic and non-diabetic patients. Diabetologia. 2002;45(7):1011–1016.

41. Maruyama K, Asai J, Ii M, Thorne T, Losordo DW, D'Amore PA. Decreased macrophage number and activation lead to reduced lymphatic vessel formation and contribute to impaired diabetic wound healing. Am J Pathol. 2007;170(4):1178–1191.

42. Ayello EA. What Does the Wound Say?: Why Determining Etiology Is Essential for Appropriate Wound Care. Adv Skin Wound Care. 2005;18(2):98–109.

43. Robson MC, Barbul A. Guidelines for the best care of chronic wounds. Wound Repair Regen. 2006;14(6):647–648.

44. Heldin C-H, Westermark B. Mechanism of action and in vivo role of platelet-derived growth factor. Physiol Rev. 1999;79(4):1283–1316.

45. Veves A, Falanga V, Armstrong DG, Sabolinski ML. Graftskin, a human skin equivalent, is effective in the management of noninfected neuropathic diabetic foot ulcers a prospective randomized multicenter clinical trial. Diabetes Care. 2001;24(2):290–295.

46. Bennett SP, Griffiths GD, Schor AM, Leese GP, Schor SL. Growth factors in the treatment of diabetic foot ulcers. Br J Surg. 2003;90(2):133–146.

47. Margolis DJ, Bartus C, Hoffstad O, Malay S, Berlin JA. Effectiveness of recombinant human platelet-derived growth factor for the treatment of diabetic neuropathic foot ulcers. Wound Repair Regen. 2005;13(6):531–536.

48. Eming SA, Martin P, Tomic-Canic M. Wound repair and regeneration: mechanisms, signaling, and translation. Sci Transl Med. 2014;6(265):265sr6–265sr6.

49. Liang X, Ding Y, Zhang Y, Tse H-F, Lian Q. Paracrine mechanisms of mesenchymal stem cell-based therapy: current status and perspectives. Cell Transplant. 2014;23(9):1045–1059.

50. Gnecchi M, Zhang Z, Ni A, Dzau VJ. Paracrine mechanisms in adult stem cell signaling and therapy. Circ Res. 2008;103(11):1204–1219.

51. Chen L, Tredget EE, Wu PY, Wu Y. Paracrine factors of mesenchymal stem cells recruit macrophages and endothelial lineage cells and enhance wound healing. PloS One. 2008;3(4):e1886.

52. Lu D, Chen B, Liang Z, Deng W, Jiang Y, Li S, et al. Comparison of bone marrow mesenchymal stem cells with bone marrow-derived mononuclear cells for treatment of diabetic critical limb ischemia and foot ulcer: a double-blind, randomized, controlled trial. Diabetes Res Clin Pract. 2011;92(1):26–36.

53. Wu Y, Chen L, Scott PG, Tredget EE. Mesenchymal stem cells enhance wound healing through differentiation and angiogenesis. Stem Cells. 2007;25(10):2648–2659.

54. Khan M, Akhtar S, Mohsin S, N. Khan S, Riazuddin S. Growth factor preconditioning increases the function of diabetes-impaired mesenchymal stem cells. Stem Cells Dev. 2010;20(1):67–75.

55. Cramer C, Freisinger E, Jones RK, Slakey DP, Dupin CL, Newsome ER, et al. Persistent high glucose concentrations alter the regenerative potential of mesenchymal stem cells. Stem Cells Dev. 2010;19(12):1875–1884.

56. Prockop DJ. 'Stemness' does not explain the repair of many tissues by mesenchymal stem/multipotent stromal cells (MSCs). Clin Pharmacol Ther [Internet]. 2007 [cited 2016 Sep 27];82(3). Available from: http://search.ebscohost.com/login.aspx?direct=true&profile=ehost&scope=site&authtype=crawler&jrnl=00099236&AN=32723375&h=uqXRVJnGfp8Rlz0FLeaU3r3Gb%2BDc0C%2FR%2FkGWrBEXlIsiIYJi1DyqsB1kN%2FEBwAXDAbzpSXYHKBXVGWl%2FfNkiTA%3D%3D&crl=c

57. Nakagawa H, Akita S, Fukui M, Fujii T, Akino K. Human mesenchymal stem cells successfully improve skin-substitute wound healing. Br J Dermatol. 2005;153(1):29–36.

58. Ren G, Zhang L, Zhao X, Xu G, Zhang Y, Roberts AI, et al. Mesenchymal stem cell-mediated immunosuppression occurs via concerted action of chemokines and nitric oxide. Cell Stem Cell. 2008;2(2):141–150.

59. McFarlin K, Gao X, Liu YB, Dulchavsky DS, Kwon D, Arbab AS, et al. Bone marrow-derived mesenchymal stromal cells accelerate wound healing in the rat. Wound Repair Regen. 2006;14(4):471–478.

60. Ries C, Egea V, Karow M, Kolb H, Jochum M, Neth P. MMP-2, MT1-MMP, and TIMP-2 are essential for the invasive capacity of human mesenchymal stem cells: differential regulation by inflammatory cytokines. Blood. 2007;109(9):4055–4063.

61. Hocking AM, Gibran NS. Mesenchymal stem cells: paracrine signaling and differentiation during cutaneous wound repair. Exp Cell Res. 2010;316(14):2213–2219.

62. Dash NR, Dash SN, Routray P, Mohapatra S, Mohapatra PC. Targeting nonhealing ulcers of lower extremity in human through autologous bone marrow-derived mesenchymal stem cells. Rejuvenation Res. 2009;12(5):359–366.

63. Stolzing A, Coleman N, Scutt A. Glucose-induced replicative senescence in mesenchymal stem cells. Rejuvenation Res. 2006;9(1):31–35.

64. Khan M, Ali F, Mohsin S, Akhtar S, Mehmood A, Choudhery MS, et al. Preconditioning diabetic mesenchymal stem cells with myogenic medium

increases their ability to repair diabetic heart. Stem Cell Res Ther. 2013;4(3):1.

65. Choi K-M, Seo Y-K, Yoon H-H, Song K-Y, Kwon S-Y, Lee H-S, et al. Effect of ascorbic acid on bone marrow-derived mesenchymal stem cell proliferation and differentiation. J Biosci Bioeng. 2008;105(6):586–594.

66. Esteban MA, Wang T, Qin B, Yang J, Qin D, Cai J, et al. Vitamin C enhances the generation of mouse and human induced pluripotent stem cells. Cell Stem Cell. 2010;6(1):71–79.

67. Takahashi T, Lord B, Schulze PC, Fryer RM, Sarang SS, Gullans SR, et al. Ascorbic acid enhances differentiation of embryonic stem cells into cardiac myocytes. Circulation. 2003;107(14):1912–1916.

68. Vater C, Kasten P, Stiehler M. Culture media for the differentiation of mesenchymal stromal cells. Acta Biomater. 2011;7(2):463–477.

69. Moores J. Vitamin C: a wound healing perspective. Br J Community Nurs [Internet]. 2013 [cited 2016 Sep 28];18. Available from: http://search.ebscohost.com/login.aspx?direct=true&profile=ehost&scope=site&authtype=crawler&jrnl=14624753&AN=93251401&h=x8NnYx1SF%2FtkksIcKuS8zkh30ytmvnUzX5LD8KxGfcAyUht0UmJhpG%2B1hvVzNmijZalAkW0uVbvKaVQzysE2eg%3D%3D&crl=c

70. Lanman TH, Ingalls TH. Vitamin C deficiency and wound healing: An experimental and clinical study. Ann Surg. 1937;105(4):616.

71. Chen MS, Hutchinson ML, Pecoraro RE, Lee WY, Labbé RF. Hyperglycemia-induced intracellular depletion of ascorbic acid in human mononuclear leukocytes. Diabetes. 1983;32(11):1078–1081.

72. Iino K, Fukui T, Anzai K, Iwase M, Kogawa K, Ogimoto M, et al. Serum vitamin C levels in type 2 diabetic nephropathy. Diabetes Care. 2005;28(11):2808–2809.

73. Nourshargh S, Alon R. Leukocyte migration into inflamed tissues. Immunity. 2014;41(5):694–707.

74. Amulic B, Cazalet C, Hayes GL, Metzler KD, Zychlinsky A. Neutrophil function: from mechanisms to disease. Annu Rev Immunol. 2012;30:459–489.

75. Mantovani A, Cassatella MA, Costantini C, Jaillon S. Neutrophils in the activation and regulation of innate and adaptive immunity. Nat Rev Immunol. 2011;11(8):519–531.

76. Heyworth PG, Cross AR, Curnutte JT. Chronic granulomatous disease. Curr Opin Immunol. 2003;15(5):578–584.

77. Leiding JW, Holland SM. Chronic granulomatous disease. 2016 [cited 2016 Sep 28]; Available from: http://www.ncbi.nlm.nih.gov/books/NBK99496/?report=reader

78. Mclean-Tooke AP, Aldridge C, Gilmour K, Higgins B, Hudson M, Spickett GP. An unusual cause of granulomatous disease. BMC Clin Pathol. 2007;7(1):1.

79. Noack D, Rae J, Cross AR, Ellis BA, Newburger PE, Curnutte JT, et al. Autosomal recessive chronic granulomatous disease caused by defects in NCF-1, the gene encoding the phagocyte p47-phox: mutations not arising in theNCF-1 pseudogenes. Blood. 2001;97(1):305–311.

80. Noack D, Rae J, Cross AR, Muñoz J, Salmen S, Mendoza JA, et al. Autosomal recessive chronic granulomatous disease caused by novel mutations in NCF-2, the gene encoding the p67-phox component of phagocyte NADPH oxidase. Hum Genet. 1999;105(5):460–467.

81. Rae J, Newburger PE, Dinauer MC, Noack D, Hopkins PJ, Kuruto R, et al. X-Linked chronic granulomatous disease: mutations in the CYBB gene encoding the gp91-phox component of respiratory-burst oxidase. Am J Hum Genet. 1998;62(6):1320–1331.

82. Ott MG, Schmidt M, Schwarzwaelder K, Stein S, Siler U, Koehl U, et al. Correction of X-linked chronic granulomatous disease by gene therapy, augmented by insertional activation of MDS1-EVI1, PRDM16 or SETBP1. Nat Med. 2006;12(4):401–409.

83. Crowley CA, Curnutte JT, Rosin RE, André-Schwartz J, Gallin JI, Klempner M, et al. An inherited abnormality of neutrophil adhesion: its genetic transmission and its association with a missing protein. N Engl J Med. 1980;302(21):1163–1168.

84. Kitahara M, Eyre HJ, Simonian Y, Atkin CL, Hasstedt SJ. Hereditary myeloperoxidase deficiency. Blood. 1981;57(5):888–893.

85. Alon R, Aker M, Feigelson S, Sokolovsky-Eisenberg M, Staunton DE, Cinamon G, et al. A novel genetic leukocyte adhesion deficiency in subsecond triggering of integrin avidity by endothelial chemokines results in impaired leukocyte arrest on vascular endothelium under shear flow. Blood. 2003;101(11):4437–4445.

86. Diamond MS, Staunton DE, De Fougerolles AR, Stacker SA, Garcia-Aguilar J, Hibbs ML, et al. ICAM-1 (CD54): a counter-receptor for Mac-1 (CD11b/CD18). J Cell Biol. 1990;111(6):3129–3139.

87. PARRY MF, ROOT RK, METCALF JA, DELANEY KK, KAPLOW LS, RICHAR WJ. Myeloperoxidase deficiency: prevalence and clinical significance. Ann Intern Med. 1981;95(3):293–301.

88. Lanza F. Clinical manifestation of myeloperoxidase deficiency. J Mol Med. 1998;76(10):676–681.

89. Bouma G, Burns SO, Thrasher AJ. Wiskott–Aldrich Syndrome: Immunodeficiency resulting from defective cell migration and impaired immunostimulatory activation. Immunobiology. 2009;214(9):778–790.

90. Aiuti A, Slavin S, Aker M, Ficara F, Deola S, Mortellaro A, et al. Correction of ADA-SCID by stem cell gene therapy combined with nonmyeloablative conditioning. Science. 2002;296(5577):2410–2413.

91. Derry JM, Ochs HD, Francke U. Isolation of a novel gene mutated in Wiskott-Aldrich syndrome. Cell. 1994;78(4):635–644.

92. Jin Y, Mazza C, Christie JR, Giliani S, Fiorini M, Mella P, et al. Mutations of the Wiskott-Aldrich Syndrome Protein (WASP): hotspots, effect on transcription, and translation and phenotype/genotype correlation. Blood. 2004;104(13):4010–4019.

93. Ochs HD, Thrasher AJ. The wiskott-aldrich syndrome. J Allergy Clin Immunol. 2006;117(4):725–738.

94. Perry GS, Spector BD, Schuman LM, Mandel JS, Anderson VE, McHugh RB, et al. The Wiskott-Aldrich syndrome in the United States and Canada (1892–1979). J Pediatr. 1980;97(1):72–78.

95. Ochs HD, Slichter SJ, Harker LA, Von Behrens WE, Clark RA, Wedgwood RJ. The Wiskott-Aldrich syndrome. Blood. 1980;55(2):243–252.

96. Thrasher AJ, Burns SO. WASP: a key immunological multitasker. Nat Rev Immunol. 2010;10(3):182–192.

97. Beel K, Cotter MM, Blatny J, Bond J, Lucas G, Green F, et al. A large kindred with X-linked neutropenia with an I294T mutation of the Wiskott-Aldrich syndrome gene. Br J Haematol. 2009;144(1):120–126.

98. Ancliff PJ, Blundell MP, Cory GO, Calle Y, Worth A, Kempski H, et al. Two novel activating mutations in the Wiskott-Aldrich syndrome protein result in congenital neutropenia. Blood. 2006;108(7):2182–2189.

99. Kolluri R, Tolias KF, Carpenter CL, Rosen FS, Kirchhausen T. Direct interaction of the Wiskott-Aldrich syndrome protein with the GTPase Cdc42. Proc Natl Acad Sci. 1996;93(11):5615–5618.

100. Devriendt K, Kim AS, Mathijs G, Frints SG, Schwartz M, Van den Oord JJ, et al. Constitutively activating mutation in WASP causes X-linked severe congenital neutropenia. Nat Genet. 2001;27(3):313–317.

101. Derry JM, Wiedemann P, Blair P, Wang Y, Kerns JA, Lemahieu V, et al. The mouse homolog of the Wiskott–Aldrich syndrome protein (WASP) gene is highly conserved and maps near the scurfy (sf) mutation on the X chromosome. Genomics. 1995;29(2):471–477.

102. Lyon MF, Peters J, Glenister PH, Ball S, Wright E. The scurfy mouse mutant has previously unrecognized hematological abnormalities and resembles Wiskott-Aldrich syndrome. Proc Natl Acad Sci. 1990;87(7):2433–2437.

103. Rouet P, Smih F, Jasin M. Expression of a site-specific endonuclease stimulates homologous recombination in mammalian cells. Proc Natl Acad Sci. 1994;91(13):6064–6068.

104. Hockemeyer D, Soldner F, Beard C, Gao Q, Mitalipova M, DeKelver RC, et al. Efficient targeting of expressed and silent genes in human ESCs and iPSCs using zinc-finger nucleases. Nat Biotechnol. 2009;27(9):851–857.

105. Raya Á, Rodríguez-Pizà I, Guenechea G, Vassena R, Navarro S, Barrero MJ, et al. Disease-corrected haematopoietic progenitors from Fanconi anaemia induced pluripotent stem cells. Nature. 2009;460(7251):53–59.

106. Morishima T, Watanabe K, Niwa A, Fujino H, Matsubara H, Adachi S, et al. Neutrophil differentiation from human-induced pluripotent stem cells. J Cell Physiol. 2011;226(5):1283–1291.

107. Sasaki M, Abe R, Fujita Y, Ando S, Inokuma D, Shimizu H. Mesenchymal stem cells are recruited into wounded skin and contribute to wound repair by transdifferentiation into multiple skin cell type. J Immunol. 2008;180(4):2581–2587.

108. Kelly BD, Hackett SF, Hirota K, Oshima Y, Cai Z, Berg-Dixon S, et al. Cell type–specific regulation of angiogenic growth factor gene expression and induction of angiogenesis in nonischemic tissue by a constitutively active form of hypoxia-inducible factor 1. Circ Res. 2003;93(11):1074–1081.

109. Cao R, Björndahl MA, Religa P, Clasper S, Garvin S, Galter D, et al. PDGF-BB induces intratumoral lymphangiogenesis and promotes lymphatic metastasis. Cancer Cell. 2004;6(4):333–345.

110. Vong QP, Chan KM, Cheng CH. Quantification of common carp (Cyprinus carpio) IGF-I and IGF-II mRNA by real-time PCR: differential regulation of expression by GH. J Endocrinol. 2003;178(3):513–521.

111. Thijssen VL, Brandwijk RJ, Dings RP, Griffioen AW. Angiogenesis gene expression profiling in xenograft models to study cellular interactions. Exp Cell Res. 2004;299(2):286–293.

112. Sakai T, Larsen M, Yamada KM. Fibronectin requirement in branching morphogenesis. Nature. 2003;423(6942):876–881.

113. El-Karef A, Yoshida T, Gabazza EC, Nishioka T, Inada H, Sakakura T, et al. Deficiency of tenascin-C attenuates liver fibrosis in immune-mediated chronic hepatitis in mice. J Pathol. 2007;211(1):86–94.

114. Ip JE, Wu Y, Huang J, Zhang L, Pratt RE, Dzau VJ. Mesenchymal stem cells use integrin β1 not CXC chemokine receptor 4 for myocardial migration and engraftment. Mol Biol Cell. 2007;18(8):2873–2882.

115. Sasaki T, Giltay R, Talts U, Timpl R, Talts JF. Expression and distribution of laminin α1 and α2 chains in embryonic and adult mouse tissues: an immunochemical approach. Exp Cell Res. 2002;275(2):185–199.

116. Nakatsu MN, Sainson RC, Aoto JN, Taylor KL, Aitkenhead M, Pérez-del-Pulgar S, et al. Angiogenic sprouting and capillary lumen formation modeled by human umbilical vein endothelial cells (HUVEC) in fibrin gels: the role of fibroblasts and Angiopoietin-1☆. Microvasc Res. 2003;66(2):102–112.

117. Wei F, Qu C, Song T, Ding G, Fan Z, Liu D, et al. Vitamin C treatment promotes mesenchymal stem cell sheet formation and tissue regeneration by elevating telomerase activity. J Cell Physiol. 2012;227(9):3216–3224.

118. Sukpat S, Isarasena N, Wongphoom J, Patumraj S. Vasculoprotective effects of combined endothelial progenitor cells and mesenchymal stem cells in diabetic wound care: their potential role in decreasing wound-oxidative stress. BioMed Res Int [Internet]. 2013 [cited 2016 Sep 28];2013. Available from: http://www.hindawi.com/journals/bmri/2013/459196/abs/

119. Vangipuram M, Ting D, Kim S, Diaz R, Schüle B. Skin punch biopsy explant culture for derivation of primary human fibroblasts. J Vis Exp JoVE [Internet]. 2013 [cited 2016 Sep 28];(77). Available from: http://www.ncbi.nlm.nih.gov/pmc/articles/PMC3731437/

120. Boulting GL, Kiskinis E, Croft GF, Amoroso MW, Oakley DH, Wainger BJ, et al. A functionally characterized test set of human induced pluripotent stem cells. Nat Biotechnol. 2011;29(3):279–286.

121. Park I-H, Arora N, Huo H, Maherali N, Ahfeldt T, Shimamura A, et al. Disease-specific induced pluripotent stem cells. cell. 2008;134(5):877–886.

122. Mali P, Ye Z, Chou B-K, Yen J, Cheng L. An improved method for generating and identifying human induced pluripotent stem cells. Cell Program Reprogramming Methods Protoc. 2010;191–205.

123. Tanaka A, Woltjen K, Miyake K, Hotta A, Ikeya M, Yamamoto T, et al. Efficient and reproducible myogenic differentiation from human iPS cells: prospects for modeling Miyoshi Myopathy in vitro. PLoS One. 2013;8(4):e61540.

124. Qing LI, Yong FAN, Xiaofang SUN, Yanhong YU. Generation of induced pluripotent stem cells from human amniotic fluid cells by reprogramming with two factors in feeder-free conditions. J Reprod Dev. 2013;59(1):72–77.

125. Mesquita FCP, Kasai-Brunswick TH, Borgonovo T, Silva-dos-Santos D, de Araújo DS, Campos-de-Carvalho AC, et al. Generation of human iPS cell line ihFib3. 2 from dermal fibroblasts. Stem Cell Res. 2015;15(3):445–448.

126. Takayama N, Eto K. In vitro generation of megakaryocytes and platelets from human embryonic stem cells and induced pluripotent stem cells. Platelets Megakaryocytes Vol 3 Addit Protoc Perspect. 2012;205–217.

127. Takayama N, Nishikii H, Usui J, Tsukui H, Sawaguchi A, Hiroyama T, et al. Generation of functional platelets from human embryonic stem cells in vitro

via ES-sacs, VEGF-promoted structures that concentrate hematopoietic progenitors. Blood. 2008;111(11):5298–5306.

128. Zou J, Sweeney CL, Chou B-K, Choi U, Pan J, Wang H, et al. Oxidase-deficient neutrophils from X-linked chronic granulomatous disease iPS cells: functional correction by zinc finger nuclease–mediated safe harbor targeting. Blood. 2011;117(21):5561–5572.

129. Yokoyama Y, Suzuki T, Sakata-Yanagimoto M, Kumano K, Higashi K, Takato T, et al. Derivation of functional mature neutrophils from human embryonic stem cells. Blood. 2009;113(26):6584–6592.

130. Beckonert O, Keun HC, Ebbels TM, Bundy J, Holmes E, Lindon JC, et al. Metabolic profiling, metabolomic and metabonomic procedures for NMR spectroscopy of urine, plasma, serum and tissue extracts. Nat Protoc. 2007;2(11):2692–2703.

131. Arnett FC, Edworthy SM, Bloch DA, McShane DJ, Fries JF, Cooper NS, et al. The American Rheumatism Association 1987 revised criteria for the classification of rheumatoid arthritis. Arthritis Rheum. 1988 Mar;31(3):315–24.

132. Pakyari M, Farrokhi A, Maharlooei MK, Ghahary A. Critical role of transforming growth factor beta in different phases of wound healing. Adv Wound Care. 2013;2(5):215–224.

133. Verrecchia F, Mauviel A. Transforming Growth Factor-&bgr; Signaling Through the Smad Pathway: Role in Extracellular Matrix Gene Expression and Regulation. J Invest Dermatol. 2002;118(2):211–215.

134. Stolzing A, Bauer E, Scutt A. Suspension cultures of bone-marrow-derived mesenchymal stem cells: effects of donor age and glucose level. Stem Cells Dev. 2012;21(14):2718–2723.

135. Jin P, Zhang X, Wu Y, Li L, Yin Q, Zheng L, et al. Streptozotocin-induced diabetic rat–derived bone marrow mesenchymal stem cells have impaired abilities in proliferation, paracrine, antiapoptosis, and myogenic differentiation. In: Transplantation proceedings [Internet]. Elsevier; 2010 [cited 2016 Sep 28]. p. 2745–2752. Available from: http://www.sciencedirect.com/science/article/pii/S004113451000895X

136. Said HM. Intestinal absorption of water-soluble vitamins in health and disease. Biochem J. 2011;437(3):357–372.

137. Shin L, Peterson DA. Impaired therapeutic capacity of autologous stem cells in a model of type 2 diabetes. Stem Cells Transl Med. 2012;1(2):125–135.

138. Huijberts MS, Schaper NC, Schalkwijk CG. Advanced glycation end products and diabetic foot disease. Diabetes Metab Res Rev. 2008;24(S1):S19–S24.

139. Tepper OM, Galiano RD, Capla JM, Kalka C, Gagne PJ, Jacobowitz GR, et al. Human endothelial progenitor cells from type II diabetics exhibit impaired

proliferation, adhesion, and incorporation into vascular structures. Circulation. 2002;106(22):2781–2786.

140. Hirsch IB, Atchley DH, Tsai E, Labbé RF, Chait A. Ascorbic acid clearance in diabetic nephropathy. J Diabetes Complications. 1998;12(5):259–263.

141. Yue DK, McLennan S, McGill M, Fisher E, Heffernan S, Capogreco C, et al. Abnormalities of ascorbic acid metabolism and diabetic control: differences between diabetic patients and diabetic rats. Diabetes Res Clin Pract. 1990;9(3):239–244.

142. Kashiba M, Oka J, Ichikawa R, Kasahara E, Inayama T, Kageyama A, et al. Impaired ascorbic acid metabolism in streptozotocin-induced diabetic rats. Free Radic Biol Med. 2002;33(9):1221–1230.

143. Price KD, Price CS, Reynolds RD. Hyperglycemia-induced ascorbic acid deficiency promotes endothelial dysfunction and the development of atherosclerosis. Atherosclerosis. 2001;158(1):1–12.

144. Padh H, Subramoniam A, Aleo JJ. Glucose inhibits cellular ascorbic acid uptake by fibroblasts in vitro. Cell Biol Int Rep. 1985;9(6):531–538.

145. Ting HH, Timimi FK, Haley EA, Roddy M-A, Ganz P, Creager MA. Vitamin C improves endothelium-dependent vasodilation in forearm resistance vessels of humans with hypercholesterolemia. Circulation. 1997;95(12):2617–2622.

146. Westerberg LS, Meelu P, Baptista M, Eston MA, Adamovich DA, Cotta-de-Almeida V, et al. Activating WASP mutations associated with X-linked neutropenia result in enhanced actin polymerization, altered cytoskeletal responses, and genomic instability in lymphocytes. J Exp Med. 2010;207(6):1145–1152.

147. Moulding DA, Blundell MP, Spiller DG, White MR, Cory GO, Calle Y, et al. Unregulated actin polymerization by WASp causes defects of mitosis and cytokinesis in X-linked neutropenia. J Exp Med. 2007;204(9):2213–2224.

148. Van Epps DE, Bender J, Lee W, Schilling M, Smith A, Smith S, et al. Harvesting, characterization, and culture of CD34+ cells from human bone marrow, peripheral blood, and cord blood. Blood Cells. 1993;20(2–3):411–423.

149. Liao B-Y, Zhang J. Null mutations in human and mouse orthologs frequently result in different phenotypes. Proc Natl Acad Sci. 2008;105(19):6987–6992.

150. Kokame K, Matsumoto M, Soejima K, Yagi H, Ishizashi H, Funato M, et al. Mutations and common polymorphisms in ADAMTS13 gene responsible for von Willebrand factor-cleaving protease activity. Proc Natl Acad Sci. 2002;99(18):11902–11907.

151. Kaufman DS, Hanson ET, Lewis RL, Auerbach R, Thomson JA. Hematopoietic colony-forming cells derived from human embryonic stem cells. Proc Natl Acad Sci. 2001;98(19):10716–10721.

152. Vo LT, Daley GQ. De novo generation of HSCs from somatic and pluripotent stem cell sources. Blood. 2015;125(17):2641–2648.

153. Torres M, Hall FL, O'neill K. Stimulation of human neutrophils with formyl-methionyl-leucyl-phenylalanine induces tyrosine phosphorylation and activation of two distinct mitogen-activated protein-kinases. J Immunol. 1993;150(4):1563–1577.

154. Millard TH, Sharp SJ, Machesky LM. Signalling to actin assembly via the WASP (Wiskott-Aldrich syndrome protein)-family proteins and the Arp2/3 complex. Biochem J. 2004;380(1):1–17.

155. Miki H, Miura K, Takenawa T. N-WASP, a novel actin-depolymerizing protein, regulates the cortical cytoskeletal rearrangement in a PIP2-dependent manner downstream of tyrosine kinases. EMBO J. 1996;15(19):5326.

156. Moulding DA, Record J, Malinova D, Thrasher AJ. Actin cytoskeletal defects in immunodeficiency. Immunol Rev. 2013;256(1):282–299.

157. Thieblemont N, Wright HL, Edwards SW, Witko-Sarsat V. Human neutrophils in auto-immunity. In: Seminars in immunology [Internet]. Elsevier; 2016 [cited 2016 Sep 28]. p. 159–173. Available from: http://www.sciencedirect.com/science/article/pii/S1044532316000117

158. Wright HL, Moots RJ, Edwards SW. The multifactorial role of neutrophils in rheumatoid arthritis. Nat Rev Rheumatol. 2014;10(10):593–601.

159. Wright HL, Moots RJ, Bucknall RC, Edwards SW. Neutrophil function in inflammation and inflammatory diseases. Rheumatology. 2010;49(9):1618–1631.

160. Johnson JL, Ellis BA, Munafo DB, Brzezinska AA, Catz SD. Gene transfer and expression in human neutrophils. The phox homology domain of p47 phox translocates to the plasma membrane but not to the membrane of mature phagosomes. BMC Immunol. 2006;7(1):1.

161. Hauert AB. Comparison of Human Neutrophils and Differentiated HL-60 Cells: The Role of Signalling Enzymes in Motile Responses to Chemotactic Peptide. 2001.

162. Koeffler HP, Golde DW. Human myeloid leukemia cell lines: a review. Blood. 1980;56(3):344–350.

163. Collins SJ, Gallo RC, Gallagher RE. Continuous growth and differentiation of human myeloid leukaemic cells in suspension culture. 1977 [cited 2016 Sep 28]; Available from: http://www.nature.com/nature/journal/v270/n5635/abs/270347a0.html

164. Marin-Esteban V, Turbica I, Dufour G, Semiramoth N, Gleizes A, Gorges R, et al. Afa/Dr diffusely adhering Escherichia coli strain C1845 induces neutrophil extracellular traps that kill bacteria and damage human enterocyte-like cells. Infect Immun. 2012;80(5):1891–1899.

165. Tucker KA, Lilly MB, Heck LJ, Rado TA. Characterization of a new human diploid myeloid leukemia cell line (PLB-985) with granulocytic and monocytic differentiating capacity. Blood. 1987;70(2):372–378.

166. Edwards SW, Derouet M, Howse M, Moots RJ. Regulation of neutrophil apoptosis by Mcl-1. Biochem Soc Trans. 2004;32(3):489–492.

167. Milot E, Filep JG. Regulation of neutrophil survival/apoptosis by Mcl-1. Sci World J. 2011;11:1948–1962.

168. Thomas LW, Lam C, Edwards SW. Mcl-1; the molecular regulation of protein function. FEBS Lett. 2010;584(14):2981–2989.

169. Del Poeta G, Venditti A, Del Principe MI, Maurillo L, Buccisano F, Tamburini A, et al. Amount of spontaneous apoptosis detected by Bax/Bcl-2 ratio predicts outcome in acute myeloid leukemia (AML). Blood. 2003;101(6):2125–2131.

170. Glaser SP, Lee EF, Trounson E, Bouillet P, Wei A, Fairlie WD, et al. Anti-apoptotic Mcl-1 is essential for the development and sustained growth of acute myeloid leukemia. Genes Dev. 2012;26(2):120–125.

171. Moulding DA, Quayle JA, Hart CA, Edwards SW. Mcl-1 expression in human neutrophils: regulation by cytokines and correlation with cell survival. Blood. 1998;92(7):2495–2502.

172. Phoomvuthisarn P. Effects of purvalanol A on imatinib-sensitive and-insensitive chronic myeloid leukaemia cell lines [Internet]. University of Liverpool; 2015 [cited 2016 Sep 29]. Available from: http://ethos.bl.uk/OrderDetails.do?uin=uk.bl.ethos.677582

173. Kubonishi I, Miyoshi I. Establishment of a Ph1 chromosome-positive cell line from chronic myelogenous leukemia in blast crisis. Int J Cell Cloning. 1983;1(2):105–117.

174. Feilmeier BJ, Iseminger G, Schroeder D, Webber H, Phillips GJ. Green fluorescent protein functions as a reporter for protein localization in Escherichia coli. J Bacteriol. 2000;182(14):4068–4076.

175. Michaelson D, Philips M. The use of GFP to localize Rho GTPases in living cells. Methods Enzymol. 2006;406:296–315.

176. Wright HL, Thomas HB, Moots RJ, Edwards SW. RNA-seq reveals activation of both common and cytokine-specific pathways following neutrophil priming. PloS One. 2013;8(3):e58598.

177. Dettmer K, Aronov PA, Hammock BD. Mass spectrometry-based metabolomics. Mass Spectrom Rev. 2007;26(1):51–78.

178. Milne SB, Mathews TP, Myers DS, Ivanova PT, Brown HA. Sum of the parts: mass spectrometry-based metabolomics. Biochemistry (Mosc). 2013;52(22):3829–3840.

179. Segal AW, Dorling J, Coade S. Kinetics of fusion of the cytoplasmic granules with phagocytic vacuoles in human polymorphonuclear leukocytes. Biochemical and morphological studies. J Cell Biol. 1980;85(1):42–59.

180. Ringnér M. What is principal component analysis? Nat Biotechnol. 2008;26(3):303–304.

181. Wishart DS, Tzur D, Knox C, others. HMDB: the Human Metabolome Database. Nucleic Acids Res. Database. 2007;(D521-6).

182. Wishart DS, Knox C, Guo AC, Eisner R, Young N, Gautam B, et al. HMDB: a knowledgebase for the human metabolome. Nucleic Acids Res. 2009;37(suppl 1):D603–D610.

183. Wishart DS, Jewison T, Guo AC, Wilson M, Knox C, Liu Y, et al. HMDB 3.0—the human metabolome database in 2013. Nucleic Acids Res. 2012;gks1065.

184. Zhang D, Zhu M, Humphreys WG. Drug metabolism in drug design and development [Internet]. John Wiley & Sons; 2007 [cited 2016 Sep 29]. Available from: https://books.google.co.uk/books?hl=en&lr=&id=7JrFamzQSUMC&oi=fnd&pg=PR5&dq=Introduction+to+NMR+and+its+application.+Drug+Metabolism+in+Drug+Design+and+Development+edited+by+Donglu+Zhang,+Mingshe+Zhu,+William+G.+Humphreys+Wiley+publisher&ots=6hCuy6m_NX&sig=HXrycQWFXy4InN1hSYulz_QE_7M

185. Smolinska A, Attali A, Blanchet L, Ampt K, Tuinstra T, van Aken H, et al. NMR and pattern recognition can distinguish neuroinflammation and peripheral inflammation. J Proteome Res. 2011;10(10):4428–4438.

186. Rossi F. The O2–forming NADPH oxidase of the phagocytes: nature, mechanisms of activation and function. Biochim Biophys Acta BBA-Rev Bioenerg. 1986;853(1):65–89.

187. Ying W. NAD+/NADH and NADP+/NADPH in cellular functions and cell death: regulation and biological consequences. Antioxid Redox Signal. 2008;10(2):179–206.

188. Karlsson A, Nixon JB, McPhail LC. Phorbol myristate acetate induces neutrophil NADPH-oxidase activity by two separate signal transduction pathways: dependent or independent of phosphatidylinositol 3-kinase. J Leukoc Biol. 2000;67(3):396–404.

189. Weissmann G, Korchak H. Rheumatoid arthritis. Inflammation. 1984;8(1):S3–S14.

190. Wright HL, Chikura B, Bucknall RC, Moots RJ, Edwards SW. Changes in expression of membrane TNF, NF-κB activation and neutrophil apoptosis during active and resolved inflammation. Ann Rheum Dis. 2011;70(3):537–543.

191. Wright HL, Thomas HB, Moots RJ, Edwards SW. Interferon gene expression signature in rheumatoid arthritis neutrophils correlates with a good response to TNFi therapy. Rheumatology. 2015;54(1):188–193.

192. Zabek A, Swierkot J, Malak A, Zawadzka I, Deja S, Bogunia-Kubik K, et al. Application of 1 H NMR-based serum metabolomic studies for monitoring female patients with rheumatoid arthritis. J Pharm Biomed Anal. 2016;117:544–550.

193. Bartok B, Firestein GS. Fibroblast-like synoviocytes: key effector cells in rheumatoid arthritis. Immunol Rev. 2010;233(1):233–255.

194. Strasinger SK, Di Lorenzo MS. Urinalysis & Body Fluids [Internet]. FA Davis; 2008 [cited 2016 Sep 29]. Available from: https://books.google.co.uk/books?hl=en&lr=&id=ZWP2AAAAQBAJ&oi=fnd&pg=PA1&dq=Urinalysis+and+Body+Fluids&ots=uhIkeD3xUv&sig=zwkrkCRQ4IR3v--I0wXSG_IDaB4

195. Wright HL, Bucknall RC, Moots RJ, Edwards SW. Analysis of SF and plasma cytokines provides insights into the mechanisms of inflammatory arthritis and may predict response to therapy. Rheumatology. 2012;51(3):451–459.

196. Aletaha D, Neogi T, Silman AJ, Funovits J, Felson DT, Bingham CO, et al. 2010 rheumatoid arthritis classification criteria: an American College of Rheumatology/European League Against Rheumatism collaborative initiative. Arthritis Rheum. 2010;62(9):2569–2581.

197. Edwards SW. Biochemistry and Physiology of the Neutrophil [Internet]. Cambridge University Press; 2005 [cited 2016 Sep 29]. Available from: https://books.google.co.uk/books?hl=en&lr=&id=fywG1DrnbgYC&oi=fnd&pg=PP1&dq=SW+Edwards,+Biochemistry+and+Physiology+of+the+neutrophil.&ots=w2GpMPgm3L&sig=aSQGcd94nQbKwVFyrjWhkBCOl_A

198. Yildiz G, Demiryürek AT, Sahin-Erdemli I, Kanzik I. Comparison of antioxidant activities of aminoguanidine, methylguanidine and guanidine by luminol-enhanced chemiluminescence. Br J Pharmacol. 1998;124(5):905–910.

199. Ekremoğlu M, Türközkan N, Erdamar H, Kurt Y, Yaman H. Protective effect of taurine on respiratory burst activity of polymorphonuclear leukocytes in endotoxemia. Amino Acids. 2007;32(3):413–417.

200. Wright HL, Cox T, Moots RJ, Edwards SW. A novel set of biomarkers predicts response to therapy with tumour necrosis factor inhibitors in patients with rheumatoid arthritis. J Leukoc Biol. 2016;In Press.

201. Viatte S, Plant D, Raychaudhuri S. Genetics and epigenetics of rheumatoid arthritis. Nat Rev Rheumatol. 2013;9(3):141–153.

202. Wang Y, Li M, Stadler S, Correll S, Li P, Wang D, et al. Histone hypercitrullination mediates chromatin decondensation and neutrophil extracellular trap formation. J Cell Biol. 2009;184(2):205–213.

203. Scally SW, Petersen J, Law SC, Dudek NL, Nel HJ, Loh KL, et al. A molecular basis for the association of the HLA-DRB1 locus, citrullination, and rheumatoid arthritis. J Exp Med. 2013;210(12):2569–2582.

204. Khandpur R, Carmona-Rivera C, Vivekanandan-Giri A, Gizinski A, Yalavarthi S, Knight JS, et al. NETs are a source of citrullinated autoantigens and stimulate inflammatory responses in rheumatoid arthritis. Sci Transl Med. 2013;5(178):178ra40–178ra40.

205. Kobayashi T, Okada M, Ito S, Kobayashi D, Shinhara A, Muramatsu T, et al. Amino acid profiles in relation to chronic periodontitis and rheumatoid arthritis. Open J Stomatol. 2014;4(2):49.

206. Maresz KJ, Hellvard A, Sroka A, Adamowicz K, Bielecka E, Koziel J, et al. Porphyromonas gingivalis facilitates the development and progression of destructive arthritis through its unique bacterial peptidylarginine deiminase (PAD). PLoS Pathog. 2013;9(9):e1003627.

207. Wu D, Huang C-K, Jiang H. Roles of phospholipid signaling in chemoattractant-induced responses. J Cell Sci. 2000;113(17):2935–2940.

208. Wang Y, Liu H, McKenzie G, Witting PK, Stasch J-P, Hahn M, et al. Kynurenine is a novel endothelium-derived vascular relaxing factor produced during inflammation. BMC Pharmacol. 2009;9(Suppl 1):S39.

209. Cuppen BV, Fu J, van Wietmarschen HA, Harms AC, Koval S, Marijnissen AC, et al. Exploring the Inflammatory Metabolomic Profile to Predict Response to TNF-α Inhibitors in Rheumatoid Arthritis. PloS One. 2016;11(9):e0163087.

210. Kim S, Hwang J, Xuan J, Jung YH, Cha H-S, Kim KH. Global metabolite profiling of synovial fluid for the specific diagnosis of rheumatoid arthritis from other inflammatory arthritis. PLoS One. 2014;9(6):e97501.

211. Wang Z, Chen ZHE, Yang S, Wang YU, Yu L, Zhang B, et al. 1H NMR-based metabolomic analysis for identifying serum biomarkers to evaluate methotrexate treatment in patients with early rheumatoid arthritis. Exp Ther Med. 2012;4(1):165–171.

212. Smolenska Z, Smolenski RT, Zdrojewski Z. Plasma concentrations of amino acid and nicotinamide metabolites in rheumatoid arthritis – potential biomarkers of disease activity and drug treatment. Biomarkers. 2016 Apr 2;21(3):218–24.

213. Tonnesen MG, Anderson DC, Springer TA, Knedler A, Avdi N, Henson PM. Adherence of neutrophils to cultured human microvascular endothelial cells. Stimulation by chemotactic peptides and lipid mediators and dependence upon the Mac-1, LFA-1, p150, 95 glycoprotein family. J Clin Invest. 1989;83(2):637.

214. Priori R, Casadei L, Valerio M, Scrivo R, Valesini G, Manetti C. 1 H-NMR-Based Metabolomic Study for Identifying Serum Profiles Associated with the

Response to Etanercept in Patients with Rheumatoid Arthritis. PloS One. 2015;10(11):e0138537.

215. Young SP, Kapoor SR, Viant MR, Byrne JJ, Filer A, Buckley CD, et al. The impact of inflammation on metabolomic profiles in patients with arthritis. Arthritis Rheum. 2013;65(8):2015–2023.

216. Guma M, Tiziani S, Firestein GS. Metabolomics in rheumatic diseases: desperately seeking biomarkers. Nat Rev Rheumatol [Internet]. 2016 [cited 2016 Sep 29]; Available from: http://www.nature.com/nrrheum/journal/vaop/ncurrent/full/nrrheum.2016.1.html

217. Kapoor SR, Filer A, Fitzpatrick MA, Fisher BA, Taylor PC, Buckley CD, et al. Metabolic profiling predicts response to anti–tumor necrosis factor α therapy in patients with rheumatoid arthritis. Arthritis Rheum. 2013;65(6):1448–1456.

218. Wright HL, Makki FA, Moots RJ, Edwards SW. Low-density granulocytes: functionally distinct, immature neutrophils in rheumatoid arthritis with altered properties and defective TNF signalling. J Leukoc Biol. 2016;jlb–5A0116.

SUPPLEMENTARY DATA

Supplementary data 1: The neutrophil pattern file

```
$##180216

PATTERN      = Human Neutrophils
GROUP        =
DESCRIPTION  = 10^7 plus PMA
AUTHOR       = Susama Chokesuwattanaskul
DIM          = 2
ORIGIN       = 1
ITEMS        = 1024
0.0000   0.0000  9.3498    9.3402        0 NAD01
0.0000   0.0000  9.3066    9.2954        0 NADP01
0.0000   0.0000  9.1557    9.1517        0 NAD02
0.0000   0.0000  9.1474    9.1442        0 NAD03
0.0000   0.0000  9.1155    9.1075        0 NADP02
0.0000   0.0000  9.1054    9.1006        0 UNKNOWN01
0.0000   0.0000  8.8530    8.8330        0 NAD04
0.0000   0.0000  8.8288    8.8272        0 NADP03
0.0000   0.0000  8.8186    8.8146        0 NADP04
0.0000   0.0000  8.618     8.61          0 UNKNOWN02
0.0000   0.0000  8.591     8.583         0 UNKNOWN03
0.0000   0.0000  8.5526    8.543         0 ATP01
0.0000   0.0000  8.5457    8.5377        0 ADP01
0.0000   0.0000  8.4637    8.4565        0 FORMATE01
0.0000   0.0000  8.4343    8.4296        0 UNKNOWN04
0.0000   0.0000  8.4304    8.4257        0 NADP05,NAD05
0.0000   0.0000  8.4255    8.4183        0 UNKNOWN05
0.0000   0.0000  8.385     8.381         0 UNKNOWN06
0.0000   0.0000  8.3546    8.3466        0 INOSINE01,ADENOSINE01
0.0000   0.0000  8.3436    8.338         0 UNKNOWN07,
0.0000   0.0000  8.2819    8.2707        0 OXYPURINOL01,ADP02,ATP02
0.0000   0.0000  8.2647    8.2620        0 ADENOSINE02,GLUTATHIONE01
0.0000   0.0000  8.2465    8.2401        0 INOSINE02,GLUTATHIONE02
0.0000   0.0000  8.2424    8.2352        0 UNKNOWN08
0.0000   0.0000  8.2369    8.2297        0 UNKNOWN09
0.0000   0.0000  8.2224    8.212         0 HYPOXANTHINE01,ADENINE01,NAD06
0.0000   0.0000  8.2035    8.1955        0 HYPOXANTHINE02,NADP06,NAD07
0.0000   0.0000  8.1917    8.1861        0 NAD08,HYPOXANTHINE03,IMIDAZOLE01,NADP07
0.0000   0.0000  8.1839    8.1759        0 ADENINE02,NADP08,NAD09
0.0000   0.0000  8.1768    8.1739        0 NAD10,ADENINE03
0.0000   0.0000  8.1595    8.1507        0 UNKNOWN10
0.0000   0.0000  8.1568    8.1452        0 NADP09,GTP01
0.0000   0.0000  8.1503    8.1415        0 UNKNWON11
0.0000   0.0000  8.1306    8.1274        0 UNKNOWN12
0.0000   0.0000  8.1244    8.1172        0 UNKNOWN13
0.0000   0.0000  8.1021    8.0772        0 CARNOSINE01
0.0000   0.0000  8.1006    8.095         0 UNKNOWN14
0.0000   0.0000  8.0732    8.0708        0 UNKNOWN15
0.0000   0.0000  8.0398    8.0117        0 N-ACETYLORNITHINE01,N6-ACETYLLYSINE01
0.0000   0.0000  8.0124    8.0044        0 ANSERINE01,N-ACETYLORNITHINE02,3-METHYLXANTHINE01,GUANOSINE01
0.0000   0.0000  8.001     7.993         0 UNKNOWN16
0.0000   0.0000  7.9953    7.9837        0 UNKNOWN17
0.0000   0.0000  7.9845    7.9705        0 ANSERINE02,NALPHA-ACETYLLYSINE01,N6-ACETYLLYSINE02,N-ACETYLORNITHINE03,N-ACETYLASPARTATE01,
0.0000   0.0000  7.9713    7.9649        0 N-ACETYLORNITHINE04,PI-METHYLHISTIDINE01,NALPHA-ACETYLLYSINE02,ANSERINE03,N-ACETYLASPARTATE02
0.0000   0.0000  7.9601    7.9529        0 HISTAMINE01,UDP-GALACTOSE01,NALPHA-ACETYLLYSINE03,N-ACETYLASPARTATE03,ANSERINE04,PI-METHYLHISTIDINE02
0.0000   0.0000  7.94712   7.94198       0 NALPHA-ACETYLLYSINE04,UDP-GALACTOSE02,N-ACETYLASPARTATE04,NALPHA-ACETYLLYSINE04
0.0000   0.0000  7.9365    7.9293        0 N,N-DIMETHYLFORMAMIDE01,XANTHINE01,N-ACETYLSEROTONIN01,N-ACETYLASPARTATE05
0.0000   0.0000  7.9291    7.9227        0 UNKNOWN18
0.0000   0.0000  7.9228    7.9172        0 UNKNOWN19
0.0000   0.0000  7.900435  7.91147       0 CAFFEINE01,N-ACETYLSEROTONIN02
0.0000   0.0000  7.8704    7.8564        0 HISTIDINE01,4-PYRIDOXATE01
0.0000   0.0000  7.8573    7.8541        0 CYTIDINE01,4-PYRIDOXATE02,HISTIDINE02,1,7-DIMETHYLXANTHINE01
0.0000   0.0000  7.85301   7.85190       0 CYTIDINE02,1,7-DIMETHYLXANTHINE02,HISTIDINE03,4-PYRIDOXATE03
0.0000   0.0000  7.8545    7.8441        0 1,7-DIMETHYLXANTHINE03,CYTIDINE03,HISTIDINE04,4-PYRIDOXATE04
0.0000   0.0000  7.8442    7.841         0 1,7-DIMETHYLXANTHINE04,CYTIDINE04
0.0000   0.0000  7.8397    7.8341        0 UNKNOWN20
0.0000   0.0000  7.74548   7.74344       0 TRYPTOPHAN01,PYROGLUTAMATE01
0.0000   0.0000  7.7513    7.7441        0 UNKNOWN21
0.0000   0.0000  7.7494    7.7394        0 UNKNOWN22
0.0000   0.0000  7.73428   7.73177       0 TRYPTOPHAN02,PYROGLUTAMATE02
0.0000   0.0000  7.7397    7.7333        0 UNKNWON23
0.0000   0.0000  7.7336    7.7264        0 UNKNOWN24
0.0000   0.0000  7.70172   7.69536       0 GAMMA-METHYLHISTIDINE01
0.0000   0.0000  7.69454   7.69279       0 GAMMA-METHYLHISTIDINE02,ACETYLSALICYLATE01
0.0000   0.0000  7.69233   7.69151       0 GAMMA-METHYLHISTIDINE03,ACETYLSALICYLATE02
0.0000   0.0000  7.68352   7.68136       0 GAMMA-METHYLHISTIDINE04,ACETYLSALICYLATE03,GLUTAMINE01
0.0000   0.0000  7.68147   7.68031       0 ACETYLSALICYLATE04,GLUTAMINE02
0.0000   0.0000  7.6822    7.6742        0 UNKNOWN25
0.0000   0.0000  7.6594    7.6498        0 UNKNOWN26
0.0000   0.0000  7.63048   7.62348       0 INDOLE-3-ACETATE01,GLUTAMINE03
0.0000   0.0000  7.61969   7.61222       0 INDOLE-3-ACETATE02,GLUTAMINE04,2-FUROATE01
0.0000   0.0000  7.6079    7.6031        0 UNKNOWN27
0.0000   0.0000  7.5999    7.5875        0 UNKNOWN28
0.0000   0.0000  7.5568    7.5496        0 TRYPTOPHAN02
0.0000   0.0000  7.5484    7.5352        0 TRYPTOPHAN03
```

0.0000	0.0000	7.5484	7.5352	0	TRYPTOPHAN03
0.0000	0.0000	7.53561	7.53392	0	ACETYLSALICYLATE05,TRYPTOPHAN04,3-HYDROXYKYNURENINE01,INDOLE-3-ACETATE03,GLUTAMINE05
0.0000	0.0000	7.5354	7.5314	0	UNKNOWN29
0.0000	0.0000	7.52392	7.53182	0	ACETYLSALICYLATE06,TRYPTOPHAN05,3-HYDROXYKYNURENINE02,GLUTAMINE06
0.0000	0.0000	7.52599	7.51823	0	INDOLE-3-ACETATE04,ACETYLSALICYLATE07
0.0000	0.0000	7.5189	7.5057	0	ACETYLSALICYLATE07,3-HYDROXYKYNURENINE03,INDOLE-3-ACETATE05
0.0000	0.0000	7.5038	7.4974	0	UNKNOWN30
0.0000	0.0000	7.46508	7.45417	0	3-HYDROXYKYNURENINE04
0.0000	0.0000	7.45417	7.44718	0	3-HYDROXYKYNURENINE05,PHENYLALANINE01
0.0000	0.0000	7.4599	7.4591	0	3-HYDROXYKYNURENINE06,PHENYLALANINE02
0.0000	0.0000	7.4468	7.4396	0	3-HYDROXYKYNURENINE07,PHENYLALANINE03
0.0000	0.0000	7.4396	7.4264	0	3-HYDROXYKYNURENINE08,PHENYLALANINE04
0.0000	0.0000	7.4286	7.4154	0	3-HYDROXYKYNURENINE09,PHENYLALANINE05
0.0000	0.0000	7.4122	7.4074	0	3-PHENYLLACTATE01,IMIDAZOLE02,3-HYDROXYKYNURENINE10,PHENYLALANINE06
0.0000	0.0000	7.4046	7.3982	0	N-ACETYLSEROTONIN02,PHENYLACETATE01,PHENYLALANINE07,3-PHENYLLACTATE02
0.0000	0.0000	7.3999	7.3911	0	N-ACETYLSEROTONIN03,PHENYLACETATE02,PHENYLALANINE08,3-PHENYLLACTATE03,3-PHENYLPROPIONATE01
0.0000	0.0000	7.4001	7.3829	0	N-ACETYLSEROTONIN04,PHENYLACETATE03,PHENYLALANINE09,3-PHENYLLACTATE04,3-PHENYLPROPIONATE02,5-HYDROXYINDOLE-3-ACETATE01
0.0000	0.0000	7.3905	7.3717	0	UNKNOWN31
0.0000	0.0000	7.38529	7.38339	0	UNKNOWN32
0.0000	0.0000	7.381	7.3714	0	5-HYDROXYINDOLE-3-ACETATE02,3-PHENYLLACTATE05,3-PHENYLPROPIONATE03,PHENYLACETATE04,PHENYLALANINE10
0.0000	0.0000	7.3744	7.3711	0	3-PHENYLLACTATE06,3-PHENYLPROPIONATE04,PHENYLACETATE05,PHENYLALANINE11,ACETYLSALICYLATE08
0.0000	0.0000	7.3645	7.3561	0	UNKNOWN33
0.0000	0.0000	7.3677	7.3521	0	3-PHENYLLACTATE07,3-PHENYLPROPIONATE05
0.0000	0.0000	7.3551	7.3471	0	UNKNOWN34
0.0000	0.0000	7.3523	7.3271	0	PHENYLACETATE06,3-PHENYLLACTATE08,3-PHENYLPROPIONATE06
0.0000	0.0000	7.3478	7.3118	0	3-PHENYLLACTATE09,3-PHENYLPROPIONATE07,PHENYLALANINE11,TRYPTOPHAN06
0.0000	0.0000	7.3256	7.3184	0	3-PHENYLLACTATE10,PHENYLACETATE07,3-PHENYLPROPIONATE08,3-CHLOROTYROSINE01
0.0000	0.0000	7.3179	7.3139	0	3-PHENYLLACTATE11,PHENYLACETATE08,3-HYDROXYMANDELATE01,3-CHLOROTYROSINE02
0.0000	0.0000	7.318	7.3032	0	3-PHENYLLACTATE12,PHENYLACETATE09
0.0000	0.0000	7.3034	7.2978	0	3-PHENYLLACTATE13,PHENYLACETATE10,TRYPTOPHAN07
0.0000	0.0000	7.2969	7.2944	0	3-PHENYLLACTATE14,PHENYLACETATE11,3-HYDROXYMANDELATE02
0.0000	0.0000	7.3021	7.2825	0	3-PHENYLPROPIONATE08,PHENYLACETATE12,TRYPTOPHAN08
0.0000	0.0000	7.2873	7.2825	0	3-PHENYLPROPIONATE09,3-PHENYLLACTATE15,PHENYLACETATE13,ACETAMINOPHEN01
0.0000	0.0000	7.2856	7.2716	0	3-PHENYLPROPIONATE10,ACETAMINOPHEN02
0.0000	0.0000	7.2741	7.2677	0	3-PHENYLPROPIONATE11,ACETAMINOPHEN03,INDOLE-3-ACETATE06
0.0000	0.0000	7.2677	7.2545	0	ACETAMINOPHEN04,INDOLE-3-ACETATE07
0.0000	0.0000	7.267	7.2474	0	UNKNOWN35
0.0000	0.0000	7.2544	7.2512	0	ACETAMINOPHEN05,INDOLE-3-ACETATE08
0.0000	0.0000	7.2495	7.2463	0	ACETAMINOPHEN06,INDOLE-3-ACETATE09,TYRAMINE01
0.0000	0.0000	7.2467	7.2287	0	UNKNOWN36
0.0000	0.0000	7.2388	7.2304	0	TYRAMINE02,THYMOL01
0.0000	0.0000	7.2222	7.2182	0	TYRAMINE03,THYMOL02,N-ACETYLSEROTONIN05,5-HYDROXYINDOLE-3-ACETATE03
0.0000	0.0000	7.2207	7.2111	0	TYRAMINE04,TRYPTOPHAN09,TYROSINE01,N-ACETYLSEROTONIN06,5-HYDROXYINDOLE-3-ACETATE04,THYMOL03
0.0000	0.0000	7.2145	7.2127	0	TYRAMINE05,TRYPTOPHAN10,TYROSINE02,N-ACETYLSEROTONIN07,5-HYDROXYINDOLE-3-ACETATE04
0.0000	0.0000	7.2091	7.2011	0	TYRAMINE06,TRYPTOPHAN11,TYROSINE03,N-ACETYLSEROTONIN08,5-HYDROXYINDOLE-3-ACETATE05
0.0000	0.0000	7.2009	7.1853	0	TRYPTOPHAN12,TYROSINE04,N-ACETYLSEROTONIN09,PI-METHYLHISTIDINE02
0.0000	0.0000	7.1905	7.1875	0	TYROSINE05,N-ACETYLSEROTONIN10,PI-METHYLHISTIDINE03,HISTAMINE02
0.0000	0.0000	7.1836	7.1794	0	4-HYDROXYPHENYLACETATE01,INDOLE-3-ACETATE10,TYROSINE06
0.0000	0.0000	7.1798	7.175	0	4-HYDROXYPHENYLACETATE02,INDOLE-3-ACETATE11
0.0000	0.0000	7.1684	7.1652	0	4-HYDROXYPHENYLACETATE03,INDOLE-3-ACETATE12,P-CRESOL01
0.0000	0.0000	7.156	7.152	0	4-HYDROXYPHENYLACETATE04,INDOLE-3-ACETATE13,P-CRESOL02,ACETYLSALICYLATE09
0.0000	0.0000	7.147	7.1422	0	P-CRESOL03,ACETYLSALICYLATE10
0.0000	0.0000	7.1368	7.1328	0	UNKNOWN37
0.0000	0.0000	7.1244	7.1188	0	UNKNOWN38
0.0000	0.0000	7.1195	7.1163	0	3-CHLOROTYROSINE03,CARNOSINE02,ANSERINE05
0.0000	0.0000	7.1144	7.1112	0	3-CHLOROTYROSINE04,CARNOSINE03,ANSERINE06,HISTIDINE05
0.0000	0.0000	7.1109	7.1005	0	3-CHLOROTYROSINE05,CARNOSINE04,ANSERINE07,HISTIDINE06
0.0000	0.0000	7.0982	7.0834	0	N-ACETYLSEROTONIN11,CARNOSINE04,ANSERINE07
0.0000	0.0000	7.0704	7.068	0	EPICATECHIN01,3-HYDROXYKYNURENINE11,4-HYDROXY-3-METHOXYMANDELATE01,ANSERINE08
0.0000	0.0000	7.067	7.063	0	3-HYDROXYKYNURENINE12,4-HYDROXY-3-METHOXYMANDELATE02,ANSERINE09
0.0000	0.0000	7.0627	7.0563	0	3-HYDROXYKYNURENINE13,4-HYDROXY-3-METHOXYMANDELATE03
0.0000	0.0000	7.0569	7.0479	0	3-HYDROXYKYNURENINE14
0.0000	0.0000	7.0487	7.0455	0	UNKNOWN39
0.0000	0.0000	7.0465	7.0384	0	3-HYDROXYKYNURENINE15,5-HYDROXYINDOLE-3-ACETATE06
0.0000	0.0000	7.0391	7.0351	0	3-HYDROXYKYNURENINE16,GAMMA-METHYLHISTIDINE05
0.0000	0.0000	7.0347	7.0231	0	UNKNOWN40
0.0000	0.0000	7.0251	7.0139	0	3-CHLOROTYROSINE06,3-HYDROXYKYNURENINE17,GAMMA-METHYLHISTIDINE06
0.0000	0.0000	7.0165	7.0117	0	2-FURORATE02,3-CHLOROTYROSINE07,GAMMA-METHYLHISTIDINE07,3-HYDROXYKYNURENINE18
0.0000	0.0000	7.0102	7.0086	0	2-FURORATE03,3-CHLOROTYROSINE078,3-HYDROXYMANDELATE03
0.0000	0.0000	6.9943	6.9919	0	3-HYDROXYMANDELATE04,3-HYDROXYKYNURENINE19,GLUTAMINE07
0.0000	0.0000	6.9843	6.9819	0	EPICATECHIN02,GLUTAMINE08,3-HYDROXYMANDELATE05,3-HYDROXYKYNURENINE20
0.0000	0.0000	6.9722	6.9658	0	EPICATECHIN03,GLUTAMINE09,3-HYDROXYKYNURENINE21
0.0000	0.0000	6.9619	6.9537	0	EPICATECHIN04,GLUTAMINE10,3-HYDROXYMANDELATE06
0.0000	0.0000	6.9466	6.9402	0	UNKNOWN41
0.0000	0.0000	6.9334	6.931	0	3-HYDROXYMANDELATE07,GLUTAMINE11,4-HYDROXY-3-METHOXYMANDELATE04,TYRAMINE07
0.0000	0.0000	6.9283	6.9235	0	UNKNOWN42
0.0000	0.0000	6.9187	6.9163	0	GLUTAMINE12,4-HYDROXY-3-METHOXYMANDELATE05,TYRAMINE08
0.0000	0.0000	6.9178	6.9082	0	TYRAMINE09,TYROSINE07,ACETAMINOPHEN07,GLUTAMINE13
0.0000	0.0000	6.9056	6.896	0	TYRAMINE10,TYROSINE08,ACETAMINOPHEN08,GLUTAMINE14
0.0000	0.0000	6.9061	6.9029	0	TYRAMINE11,TYROSINE09,ACETAMINOPHEN09,GLUTAMINE15
0.0000	0.0000	6.9032	6.8988	0	TYRAMINE12,TYROSINE10,ACETAMINOPHEN10,GLUTAMINE16,4-HYDROXY-3-METHOXYMANDELATE06
0.0000	0.0000	6.8990	6.8943	0	TYRAMINE13,TYROSINE11,ACETAMINOPHEN11,GLUTAMINE17,4-HYDROXY-3-METHOXYMANDELATE07
0.0000	0.0000	6.8927	6.8880	0	TYRAMINE14,ACETAMINOPHEN12,GLUTAMINE18,4-HYDROXY-3-METHOXYMANDELATE08
0.0000	0.0000	6.8871	6.8823	0	UNKNOWN43

0.0000	0.0000	6.8871	6.8823	0	UNKNOWN43
0.0000	0.0000	6.8834	6.8786	0	3-HYDROXYMANDELATE08,GLUTAMINE19,4-HYDROXYPHENYLACETATE05,TYRAMINE15
0.0000	0.0000	6.8783	6.8731	0	3-HYDROXYMANDELATE09,GLUTAMINE20,4-HYDROXYPHENYLACETATE06
0.0000	0.0000	6.8737	6.8664	0	3-HYDROXYMANDELATE10,GLUTAMINE21,4-HYDROXYPHENYLACETATE07
0.0000	0.0000	6.8660	6.8598	0	GLUTAMINE22,4-HYDROXYPHENYLACETATE08
0.0000	0.0000	6.8608	6.8568	0	GLUTAMINE23,4-HYDROXYPHENYLACETATE09,N-ACETYLSEROTONIN12,P-CRESOL04
0.0000	0.0000	6.8577	6.8413	0	4-HYDROXYPHENYLACETATE10,N-ACETYLSEROTONIN13,THYMOL04,P-CRESOL05,GLUTAMINE24
0.0000	0.0000	6.8464	6.844	0	UNKNOWN44
0.0000	0.0000	6.8441	6.8353	0	N-ACETYLSEROTONIN14,THYMOL05,P-CRESOL06,5-HYDROXYINDOLE-3-ACETATE07
0.0000	0.0000	6.8344	6.828	0	N-ACETYLSEROTONIN15,THYMOL06,P-CRESOL07,5-HYDROXYINDOLE-3-ACETATE08
0.0000	0.0000	6.8297	6.824	0	N-ACETYLSEROTONIN16,P-CRESOL08,5-HYDROXYINDOLE-3-ACETATE09
0.0000	0.0000	6.824	6.82	0	P-CRESOL09,5-HYDROXYINDOLE-3-ACETATE10
0.0000	0.0000	6.8227	6.8163	0	UNKNOWN45
0.0000	0.0000	6.8185	6.8121	0	P-CRESOL10,5-HYDROXYINDOLE-3-ACETATE11
0.0000	0.0000	6.7753	6.7665	0	THYMOL07
0.0000	0.0000	6.7445	6.7389	0	UNKNOWN46
0.0000	0.0000	6.725	6.7218	0	3-HYDROXYKYNURENINE22
0.0000	0.0000	6.7134	6.707	0	3-HYDROXYKYNURENINE23
0.0000	0.0000	6.6991	6.6943	0	3-HYDROXYKYNURENINE24
0.0000	0.0000	6.5734	6.5678	0	2-FURORATE04
0.0000	0.0000	6.567	6.5662	0	2-FURORATE05
0.0000	0.0000	6.5653	6.5637	0	2-FURORATE06
0.0000	0.0000	6.5633	6.5617	0	2-FURORATE07
0.0000	0.0000	6.5612	6.5588	0	UNKNOWN47
0.0000	0.0000	6.52869	6.50356	0	BIOTIN01
0.0000	0.0000	6.4961	6.4945	0	UNKNOWN48
0.0000	0.0000	6.39467	6.39109	0	BIOTIN02,GTP02
0.0000	0.0000	6.39337	6.373	0	GTP03
0.0000	0.0000	6.1643	6.1531	0	UNKNOWN49
0.0000	0.0000	6.15484	6.15083	0	ADP03,ATP03
0.0000	0.0000	6.15114	6.14762	0	ADP04,ATP04
0.0000	0.0000	6.1586	6.1438	0	UNKNOWN50
0.0000	0.0000	6.1489	6.1385	0	ADP05,ATP05,EPICATECHIN05
0.0000	0.0000	6.1419	6.1371	0	ADP06,ATP06,EPICATECHIN06
0.0000	0.0000	6.1315	6.1275	0	UNKNOWN51
0.0000	0.0000	6.1203	6.1179	0	NADP10,INOSINE03,ATP07
0.0000	0.0000	6.1159	6.1055	0	NADP11,INOSINE04
0.0000	0.0000	6.1127	6.1011	0	UNKNOWN52
0.0000	0.0000	6.108	6.0976	0	NADP12,INOSINE05,NAD11,EPICATHECHIN07
0.0000	0.0000	6.1047	6.0943	0	INOSINE06,NAD12,EPICATHECHIN08
0.0000	0.0000	6.09691	6.09348	0	INOSINE07,NAD13,EPICATHECHIN09
0.0000	0.0000	6.0987	6.0971	0	UNKNOWN53
0.0000	0.0000	6.0958	6.0886	0	UNKNOWN54
0.0000	0.0000	6.08253	6.07933	0	ADENOSINE03,CYTIDINE05
0.0000	0.0000	6.0836	6.082	0	UNKNOWN55
0.0000	0.0000	6.0814	6.0758	0	ADENOSINE04,CYTIDINE06
0.0000	0.0000	6.0728	6.0696	0	ADENOSINE05,CYTIDINE07,NADP13
0.0000	0.0000	6.0704	6.0648	0	ADENOSINE06,CYTIDINE08,NADP14
0.0000	0.0000	6.0653	6.0589	0	NADP15
0.0000	0.0000	6.0547	6.0531	0	NADP16,NAD15
0.0000	0.0000	6.05	6.0444	0	NADP17,NAD16
0.0000	0.0000	6.0444	6.0332	0	NADP18,NAD17
0.0000	0.0000	6.0361	6.0257	0	UNKNOWN56
0.0000	0.0000	6.0078	5.9962	0	UNKNOWN57
0.0000	0.0000	6.0039	5.9951	0	UNKNOWN58
0.0000	0.0000	5.999	5.9894	0	UNKNOWN59
0.0000	0.0000	5.9913	5.9865	0	UNKNOWN60
0.0000	0.0000	5.9903	5.9855	0	UDP-GALACTOSE03
0.0000	0.0000	5.9874	5.9778	0	UNKNOWN61
0.0000	0.0000	5.9824	5.9776	0	UNKNOWN62
0.0000	0.0000	5.9785	5.9761	0	UDP-GALACTOSE04
0.0000	0.0000	5.9748	5.966	0	UNKNOWN63
0.0000	0.0000	5.9608	5.9584	0	UNKNOWN64
0.0000	0.0000	5.9571	5.9459	0	GTP04
0.0000	0.0000	5.9511	5.9363	0	GTP05
0.0000	0.0000	5.9272	5.9248	0	UNKNOWN65
0.0000	0.0000	5.9233	5.9169	0	UNKNOWN66
0.0000	0.0000	5.91943	5.91601	0	GUANOSINE02,CYTIDINE09
0.0000	0.0000	5.9162	5.9138	0	CYTIDINE10,GUANOSINE03
0.0000	0.0000	5.91334	5.90841	0	GUANOSINE04,CYTIDINE11
0.0000	0.0000	5.9083	5.9067	0	UNKNOWN67
0.0000	0.0000	5.9027	5.8987	0	UNKNOWN68
0.0000	0.0000	5.8977	5.8937	0	UNKNOWN69
0.0000	0.0000	5.8923	5.8851	0	UNKNOWN70
0.0000	0.0000	5.8805	5.8749	0	UNKNOWN71
0.0000	0.0000	5.8716	5.8668	0	UNKNOWN72
0.0000	0.0000	5.8639	5.8615	0	UNKNOWN73
0.0000	0.0000	5.8591	5.8535	0	UNKNOWN74
0.0000	0.0000	5.8425	5.8401	0	UNKNOWN75
0.0000	0.0000	5.8323	5.8283	0	UNKNOWN76
0.0000	0.0000	5.7394	5.72381	0	CIS-ACONITATE01
0.0000	0.0000	5.7292	5.7292	0	CIS-ACONITATE02
0.0000	0.0000	5.65845	5.65116	0	UDP-GALACTOSE05.O-ACETYLCARNITINE01
0.0000	0.0000	5.65232	5.64679	0	UDP-GALACTOSE06.O-ACETYLCARNITINE02

0.0000	0.0000	5.65232	5.64679	0	UDP-GALACTOSE06.O-ACETYLCARNITINE02
0.0000	0.0000	5.64626	5.64177	0	UDP-GALACTOSE07.O-ACETYLCARNITINE03
0.0000	0.0000	5.64157	5.63517	0	UDP-GALACTOSE08.O-ACETYLCARNITINE04
0.0000	0.0000	5.6258	5.6258	0	UNKNOWN77
0.0000	0.0000	5.62555	5.61795	0	O-ACETYLCARNITINE04,UDP-GALACTOSE09
0.0000	0.0000	5.6176	5.616	0	UNKNOWN78
0.0000	0.0000	5.6135	5.6111	0	O-ACETYLCARNITINE05,UDP-GALACTOSE10
0.0000	0.0000	5.609	5.605	0	UNKNOWN79
0.0000	0.0000	5.6027	5.6019	0	O-ACETYLCARNITINE06,UDP-GALACTOSE11
0.0000	0.0000	5.59365	5.58376	0	O-ACETYLCARNITINE07,UDP-GALACTOSE12
0.0000	0.0000	5.5301	5.5301	0	UNKNOWN80
0.0000	0.0000	5.5248	5.5248	0	UNKNOWN81
0.0000	0.0000	5.519	5.519	0	UNKNOWN82
0.0000	0.0000	5.5143	5.5143	0	UNKNOWN83
0.0000	0.0000	5.4779	5.4779	0	UNKNOWN84
0.0000	0.0000	5.475	5.4742	0	GLUCOSE-1-PHOSPHATE01
0.0000	0.0000	5.4702	5.4702	0	GLUCOSE-1-PHOSPHATE02
0.0000	0.0000	5.4638	5.4638	0	GLUCOSE-1-PHOSPHATE03
0.0000	0.0000	5.457	5.457	0	GLUCOSE-1-PHOSPHATE04
0.0000	0.0000	5.42135	5.41672	0	SUCROSE01
0.0000	0.0000	5.4168	5.416	0	UNKNOWN85
0.0000	0.0000	5.41611	5.40824	0	SUCROSE02
0.0000	0.0000	5.4075	5.4075	0	UNKNOWN86
0.0000	0.0000	5.395	5.395	0	RIBOSE01,SUCROSE03
0.0000	0.0000	5.3897	5.3897	0	RIBOSE02,SUCROSE04
0.0000	0.0000	5.3718	5.371	0	UNKNOWN87
0.0000	0.0000	5.3719	5.3663	0	UNKNOWN88
0.0000	0.0000	5.3617	5.3617	0	UNKNOWN89
0.0000	0.0000	5.3566	5.3566	0	UNKNOWN90
0.0000	0.0000	5.3529	5.3529	0	UNKNOWN91
0.0000	0.0000	5.3223	5.3223	0	UNKNOWN92
0.0000	0.0000	5.3143	5.3135	0	UNKNOWN93
0.0000	0.0000	5.2994	5.2994	0	UNKNOWN94
0.0000	0.0000	5.2901	5.28597	0	GALACTOSE01,FUCOSE01,GLUCOSE01
0.0000	0.0000	5.28451	5.2786	0	GALACTOSE02
0.0000	0.0000	5.2751	5.2751	0	GALACTOSE03
0.0000	0.0000	5.26467	5.25263	0	RIBOSE03,GLUCOSE02,GALACTOSE04,LACTOSE01,GLUCOSE-6-PHOSPHATE05
0.0000	0.0000	5.2466	5.2378	0	GLUCOSE03,LACTOSE02,GLUCOSE-6-PHOSPHATE06
0.0000	0.0000	5.2412	5.2324	0	GLUCOSE04,LACTOSE03,GLUCOSE-6-PHOSPHATE07
0.0000	0.0000	5.23381	5.2279	0	UNKNOWN95
0.0000	0.0000	5.2213	5.2205	0	UNKNOWN96
0.0000	0.0000	5.21299	5.20433	0	XYLOSE01,FUCOSE02
0.0000	0.0000	5.20433	5.19574	0	XYLOSE02,FUCOSE03
0.0000	0.0000	5.191	5.1902	0	MANNOSE01,XYLOSE03
0.0000	0.0000	5.0508	5.05	0	UNKNOWN97
0.0000	0.0000	5.03683	5.02635	0	EPICATECHIN10
0.0000	0.0000	5.01728	4.98629	0	NADP19
0.0000	0.0000	4.9672	4.9672	0	UNKNOWN98
0.0000	0.0000	4.9507	4.9507	0	UNKNOWN99
0.0000	0.0000	4.946	4.946	0	UNKNOWN100
0.0000	0.0000	4.94709	4.93755	0	RIBOSE04,3-HYDROXYMANDELATE11
0.0000	0.0000	4.93755	4.93147	0	RIBOSE05,4-HYDROXY-3-METHOXYMANDELATE09
0.0000	0.0000	4.9295	4.9295	0	UNKNOWN101
0.0000	0.0000	4.93147	4.92415	0	4-HYDROXY-3-METHOXYMANDELATE10,RIBOSE06
0.0000	0.0000	4.91862	4.90587	0	MANNOSE02
0.0000	0.0000	4.6893	4.6893	0	UNKNOWN102
0.0000	0.0000	4.68831	4.68127	0	LACTOSE04,GLUCOSE05
0.0000	0.0000	4.6717	4.6717	0	LACTOSE05,GLUCOSE06,GLUCOSE-6-PHOSPHATE08
0.0000	0.0000	4.6653	4.6653	0	GLUCOSE07,GLUCOSE-6-PHOSPHATE09
0.0000	0.0000	4.6614	4.6542	0	GLUCOSE08
0.0000	0.0000	4.6547	4.64959	0	GLUCOSE09,GLUCOSE-6-PHOSPHATE10
0.0000	0.0000	4.6514	4.649	0	UNKNOWN103
0.0000	0.0000	4.65	4.6428	0	GLUCOSE10
0.0000	0.0000	4.637	4.637	0	UNKNOWN104
0.0000	0.0000	4.63609	4.62851	0	BIOTIN03,GLUCOSE11,NADP20,XYLOSE03
0.0000	0.0000	4.6258	4.6234	0	BIOTIN04,GLUCOSE12,NADP21,XYLOSE04
0.0000	0.0000	4.6221	4.61853	0	BIOTIN05,GLUCOSE13,NADP22,XYLOSE05
0.0000	0.0000	4.6194	4.617	0	UNKNOWN105
0.0000	0.0000	4.61723	4.60889	0	XYLOSE06,BIOTIN06
0.0000	0.0000	4.6097	4.6065	0	XYLOSE07,GALACTOSE04
0.0000	0.0000	4.6022	4.5998	0	UNKNOWN106
0.0000	0.0000	4.5953	4.5945	0	UNKNOWN107
0.0000	0.0000	4.59408	4.58854	0	ADP07,GALACTOSE05,ATP08,GLUTATHIONE03,XYLOSE08,CARNITINE01
0.0000	0.0000	4.59206	4.58535	0	GALACTOSE06,GLUTATHIONE04,LACTULOSE01,ADP08,XYLOSE09,ATP09
0.0000	0.0000	4.58748	4.58169	0	GALACTOSE07,GLUTATHIONE05,LACTULOSE02,ADP09,ATP10,CARNITINE02
0.0000	0.0000	4.5814	4.5814	0	GALACTOSE08,GLUTATHIONE06,LACTULOSE03,ADP10,ATP11,CARNITINE03,O-ACETYLCHOLINE01
0.0000	0.0000	4.58068	4.57677	0	GALACTOSE09,GLUTATHIONE07,LACTULOSE04,ADP11,ATP12,CARNITINE04
0.0000	0.0000	4.567	4.5662	0	LACTULOSE05,GLUTATHIONE08,FUCOSE04,O-ACETYLCHOLINE02,CARNITINE05,ATP13,GTP06
0.0000	0.0000	4.56569	4.56045	0	LACTULOSE06,GLUTATHIONE09,FUCOSE05,O-ACETYLCHOLINE03,CARNITINE06,ATP14,GTP07
0.0000	0.0000	4.56045	4.54667	0	LACTULOSE07,GLUTATHIONE10,FUCOSE06,O-ACETYLCHOLINE04,CARNITINE07,ATP15,GTP08
0.0000	0.0000	4.5577	4.5553	0	FUCOSE07,O-ACETYLCHOLINE05,GTP09,GLUTATHIONE11,NAD18,LACTULOSE08
0.0000	0.0000	4.5551	4.5502	0	FUCOSE08,O-ACETYLCHOLINE06,GTP10,GLUTATHIONE12,NAD19,CARNITINE08
0.0000	0.0000	4.5502	4.54622	0	FUCOSE09,O-ACETYLCHOLINE07,GLUTATHIONE13,NAD20,CARNITINE09
0.0000	0.0000	4.5466	4.5442	0	UNKNOWN108

```
0.0000   0.0000  4.5466    4.5442        0 UNKNOWN108
0.0000   0.0000  4.5276    4.5228        0 UNKNOWN109
0.0000   0.0000  4.52344   4.52109       0 NAD21,NADP23,ANSERINE10,GLUTATHIONE14,CARNOSINE05
0.0000   0.0000  4.5229    4.5181        0 UNKNOWN110
0.0000   0.0000  4.5163    4.5099        0 NAD22,NADP24,ANSERINE11,CARNOSINE06
0.0000   0.0000  4.5107    4.5059        0 NAD23,NADP25,ANSERINE12,CARNOSINE07
0.0000   0.0000  4.50291   4.49904       0 ANSERINE13,CARNOSINE08,NAD21
0.0000   0.0000  4.5019    4.4923        0 UNKNOWN111
0.0000   0.0000  4.49414   4.49137       0 ANSERINE14,CARNOSINE09,NAD22
0.0000   0.0000  4.4927    4.4823        0 UNKNOWN112
0.0000   0.0000  4.48712   4.48014       0 CARNOSINE10,LACTULOSE09,ANSERINE15,NAD24,LACTOSE06
0.0000   0.0000  4.48014   4.47251       0 CARNOSINE11,LACTULOSE10,ANSERINE16,LACTOSE07
0.0000   0.0000  4.47016   4.46925       0 CARNOSINE12,LACTULOSE11,ANSERINE17,LACTOSE08,NADP26,BIOTIN07
0.0000   0.0000  4.46883   4.46591       0 LACTOSE09,CARNOSINE13,LACTULOSE12,BIOTIN08
0.0000   0.0000  4.4657    4.4641        0 LACTOSE10,CARNOSINE14,LACTULOSE13,BIOTIN09,NADP27
0.0000   0.0000  4.4626    4.461         0 UNKNOWN113
0.0000   0.0000  4.45953   4.45581       0 LACTOSE11,CARNOSINE15,LACTULOSE14,BIOTIN10,NADP28
0.0000   0.0000  4.45581   4.4521        0 LACTOSE12,BIOTIN11,LACTULOSE15,INOSINE08
0.0000   0.0000  4.4573    4.4469        0 UNKNOWN114
0.0000   0.0000  4.44947   4.44291       0 INOSINE09,BIOTIN12,LACTOSE13,ADENOSINE07,CARNOSINE16
0.0000   0.0000  4.4448    4.4432        0 UNKNOWN115
0.0000   0.0000  4.44291   4.43991       0 INOSINE10,BIOTIN13,LACTOSE14,ADENOSINE08,CARNOSINE17,NAD25
0.0000   0.0000  4.43391   4.43729       0 INOSINE11,BIOTIN14,LACTOSE15,ADENOSINE09,CARNOSINE18,NAD26,1,3-DIHYDROXYACETONE01
0.0000   0.0000  4.43574   4.43156       0 NAD27,ADENOSINE10,1,3-DIHYDROXYACETONE02,LACTOSE16,ATP16
0.0000   0.0000  4.43156   4.42159       0 1,3-DIHYDROXYACETONE03,ATP17,NAD28
0.0000   0.0000  4.4381    4.4357        0 UNKNOWN116
0.0000   0.0000  4.4325    4.4261        0 UNKNOWN117
0.0000   0.0000  4.42549   4.40792       0 ATP18,NADP29,GUANOSINE01,1,3-DIHYDROXYACETONE04,MALATE01,N-ACETYLASPARTATE06
0.0000   0.0000  4.4241    4.4217        0 UNKNOWN118
0.0000   0.0000  4.4169    4.4145        0 UNKNOWN119
0.0000   0.0000  4.4135    4.4031        0 ATP19,NADP30,N-ACETYLASPARTATE07,ADP12,MALATE02
0.0000   0.0000  4.4054    4.403         0 UNKNOWN120
0.0000   0.0000  4.40256   4.39941       0 ADP13,N-ACETYLASPARTATE08,ATP20
0.0000   0.0000  4.399     4.3966        0 ADP14,N-ACETYLASPARTATE09,HYDROXYACETONE01,MALATE04,NAD29
0.0000   0.0000  4.3874    4.385         0 ADP15,HYDROXYACETONE02,NAD29,UDP-GALACTOSE13
0.0000   0.0000  4.3836    4.3764        0 UNKNOWN121
0.0000   0.0000  4.37924   4.37615       0 UDP-GALACTOSE14,NADP31,NAD30,ADP16,MALATE03
0.0000   0.0000  4.3794    4.367         0 UNKNOWN122
0.0000   0.0000  4.37669   4.37408       0 UDP-GALACTOSE15,GTP09,MALATE04,ADP17,NAD31
0.0000   0.0000  4.3764    4.3592        0 UNKNOWN123
0.0000   0.0000  4.3633    4.3609        0 UNKNOWN124
0.0000   0.0000  4.357     4.3546        0 UNKNOWN125
0.0000   0.0000  4.3533    4.3509        0 UNKNOWN126
0.0000   0.0000  4.3481    4.3457        0 UNKNOWN127
0.0000   0.0000  4.3481    4.3333        0 MALATE05,SN-GLYCERO-3-PHOSPHOCHOLINE01,NADP32
0.0000   0.0000  4.33894   4.33489       0 MALATE06,SN-GLYCERO-3-PHOSPHOCHOLINE02,NADP33,LACTULOSE15
0.0000   0.0000  4.33537   4.33143       0 MALATE07,SN-GLYCERO-3-PHOSPHOCHOLINE03,NADP34,LACTULOSE16
0.0000   0.0000  4.3292    4.3268        0 MALATE08,SN-GLYCERO-3-PHOSPHOCHOLINE04,NADP35
0.0000   0.0000  4.3213    4.3189        0 UNKNOWN128
0.0000   0.0000  4.31876   4.31498       0 MALATE09,SN-GLYCERO-3-PHOSPHOCHOLINE05,NADP36,GLYCYLPROLINE01,CYTIDINE12
0.0000   0.0000  4.3141    4.3093        0 N-GLYCERO-3-PHOSPHOCHOLINE06,GLYCYLPROLINE02,CYTIDINE13,MALATE10,ATP21
0.0000   0.0000  4.31088   4.30545       0 LACTULOSE17,ATP22,GLYCYLPROLINE03,MALATE11,CYTIDINE14,ADENOSINE11
0.0000   0.0000  4.30279   4.29991       0 LACTULOSE18,ATP23,GLYCYLPROLINE04,MALATE12,UDP-GALACTOSE16,NADP37
0.0000   0.0000  4.2988    4.2964        0 LACTULOSE19,NADP38,UDP-GALACTOSE17,MALATE13,ATP24
0.0000   0.0000  4.2961    4.2937        0 UNKNOWN129
0.0000   0.0000  4.2925    4.2901        0 ATP21,3-PHENYLLACTATE16,UDP-GALACTOSE18,INOSINE08,MALATE14,LACTULOSE20,THREONINE01
0.0000   0.0000  4.2935    4.2787        0 3-PHENYLLACTATE17,ATP22,THREONINE02,GALACTONATE01,GALACTARATE01,UDP-GALACTOSE19,MALATE15
0.0000   0.0000  4.2875    4.2751        0 UNKNOWN130
0.0000   0.0000  4.28384   4.27404       0 GALACTARATE02,GALACTONATE02,3-PHENYLLACTATE18,ATP23,THREONINE03,LACTULOSE21
0.0000   0.0000  4.2786    4.2738        0 UNKNOWN131
0.0000   0.0000  4.274     4.2716        0 UNKNOWN132
0.0000   0.0000  4.27223   4.26605       0 THREONINE04,3-PHENYLLACTATE19,LACTULOSE22,ADP18,ATP24,GLYCYLPROLINE05,UDP-GALACTOSE22
0.0000   0.0000  4.2702    4.2578        0 ATP25,ADP19,THREONINE05,GLYCYLPROLINE06,GTP10,LACTULOSE23
0.0000   0.0000  4.26195   4.2603        0 ATP26,THREONINE06,ADP25,GTP11,3-PHENYLLACTATE20
0.0000   0.0000  4.2635    4.2571        0 UNKNOWN133
0.0000   0.0000  4.26104   4.25738       0 ATP27,ADP20,LACTULOSE24,THREONINE07,UDP-GALACTOSE20,NAD32,GTP12
0.0000   0.0000  4.2613    4.2509        0 UNKNOWN134
0.0000   0.0000  4.25493   4.25237       0 ATP28,ADP21,GTP13,UDP-GALACTOSE21,NAD33
0.0000   0.0000  4.2561    4.2457        0 ADP22,ATP29,GTP14,NAD34,UDP-GALACTOSE22,THREONINE08
0.0000   0.0000  4.24529   4.2413        0 ADP23,ATP30,GTP15,LACTULOSE25,NAD35,UDP-GALACTOSE23
0.0000   0.0000  4.23885   4.23661       0 ADP24,ATP31,GTP16,LACTULOSE26,GUANOSINE02
0.0000   0.0000  4.2606    4.233         0 ADP25,ATP32,GUANOSINE03,LACTULOSE27,GTP17,NADP39
0.0000   0.0000  4.2384    4.232         0 UNKNOWN135
0.0000   0.0000  4.23374   4.23134       0 ADP26,SUCROSE05,LACTULOSE28,NAD32,GTP18
0.0000   0.0000  4.2327    4.2271        0 UNKNOWN136
0.0000   0.0000  4.2307    4.2259        0 SUCROSE06,ADP27.LACTULOSE29,RIBOSE06,NAD33,GTP19,ATP33
0.0000   0.0000  4.2243    4.2219        0 LACTULOSE30,ADP28,RIBOSE07,UDP-GALACTOSE24
0.0000   0.0000  4.22208   4.22005       0 LACTULOSE31,ADP29,RIBOSE08,CYTIDINE15
0.0000   0.0000  4.2196    4.218         0 LACTULOSE32,ADP30,RIBOSE09,UDP-GALACTOSE25
0.0000   0.0000  4.21718   4.21446       0 SUCROSE07,LACTULOSE33,ADP31,NADP40,UDP-GALACTOSE26
0.0000   0.0000  4.218     4.2092        0 UNKNOWN137
0.0000   0.0000  4.2195    4.2031        0 NADP41,RIBOSE10,CYTIDINE16,UDP-GALACTOSE27,LACTULOSE34,NAD34,FUCOSE10
0.0000   0.0000  4.20887   4.19929       0 NADP42,FUCOSE11,UDP-GALACTOSE28,NAD35,CYTIDINE17,LACTULOSE35
0.0000   0.0000  4.215     4.1986        0 UNKNOWN138
```

0.0000	0.0000	4.215	4.1986	0	UNKNOWN138
0.0000	0.0000	4.1989	4.1949	0	FUCOSE12,UDP-GALACTOSE29,PYROGLUTAMATE03,N-ACETYLORNITHINE05,NADP43.GLUCARATE01
0.0000	0.0000	4.1993	4.1837	0	PYROGLUTAMATE04,N-ACETYLORNITHINE06,O-PHOSPHOCHOLINE01,GLUCARATE02,3-HYDROXYKYNURENINE25
0.0000	0.0000	4.1928	4.174	0	GLUCARATE03,PYROGLUTAMATE05,N-ACETYLORNITHINE07,O-PHOSPHOCHOLINE02,3-HYDROXYKYNURENINE26
0.0000	0.0000	4.1912	4.166	0	GLUCARATE04,PYROGLUTAMATE06,N-ACETYLORNITHINE08,O-PHOSPHOCHOLINE03,3-HYDROXYKYNURENINE27
0.0000	0.0000	4.17521	4.17183	0	3-HYDROXYKYNURENINE28,PYROGLUTAMATE07,N-ACETYLORNITHINE09,O-PHOSPHOCHOLINE04,UDP-GALACTOSE29
0.0000	0.0000	4.19	4.15	0	3-HYDROXYKYNURENINE29,PYROGLUTAMATE08,N-ACETYLORNITHINE10,O-PHOSPHOCHOLINE05,UDP-GALACTOSE30
0.0000	0.0000	4.16812	4.1647	0	3-HYDROXYKYNURENINE30,N-ACETYLORNITHINE11,UDP-GALACTOSE31,GLUCARATE05
0.0000	0.0000	4.1654	4.159	0	3-HYDROXYKYNURENINE31,N-ACETYLORNITHINE12,NALPHA-ACETYLLYSINE05,O-PHOSPHOCHOLINE06,UDP-GALACTOSE32
0.0000	0.0000	4.15992	4.15649	0	3-HYDROXYKYNURENINE32,N-ACETYLORNITHINE13,O-PHOSPHOCHOLINE07,LACTULOSE36
0.0000	0.0000	4.1575	4.1551	0	UNKNOWN139
0.0000	0.0000	4.15601	4.15185	0	LACTULOSE37,NALPHA-ACETYLLYSINE06,3-HYDROXYKYNURENINE33,GLUCARATE06,N-ACETYLORNITHINE14
0.0000	0.0000	4.1564	4.1416	0	LACTULOSE38,NALPHA-ACETYLLYSINE07,3-HYDROXYKYNURENINE34,N-ACETYLORNITHINE15,LACTATE01
0.0000	0.0000	4.14736	4.142	0	LACTULOSE39,NALPHA-ACETYLLYSINE08,3-HYDROXYKYNURENINE35,GLUCARATE07
0.0000	0.0000	4.142	4.13776	0	GLUCARATE08,LACTULOSE40,NALPHA-ACETYLLYSINE09,LACTATE02,RIBOSE11
0.0000	0.0000	4.1426	4.1302	0	UNKNOWN140
0.0000	0.0000	4.13619	4.13924	0	LACTULOSE41,GLUCARATE09,LACTATE03,NALPHA-ACETYLLYSINE10,RIBOSE12,CYTIDINE18
0.0000	0.0000	4.1354	4.1238	0	LACTATE04,NALPHA-ACETYLLYSINE11,RIBOSE13
0.0000	0.0000	4.1237	4.1157	0	LACTATE05,RIBOSE14
0.0000	0.0000	4.1138	4.1058	0	LACTATE06,RIBOSE15
0.0000	0.0000	4.1047	4.0951	0	5-AMINOLEVULINATE01,LACTATE07,N-METHYLHYDANTOIN01,GLUCARATE10,RIBOSE16
0.0000	0.0000	4.09636	4.09275	0	5-AMINOLEVULINATE02,GLUCARATE11,LACTATE08,ISOCITRATE01,RIBOSE17
0.0000	0.0000	4.0968	4.088	0	5-AMINOLEVULINATE03,GLUCARATE12,ISOCITRATE02,RIBOSE18
0.0000	0.0000	4.0939	4.0815	0	5-AMINOLEVULINATE04,GLUCARATE13,ISOCITRATE03,LACTATE09,GALACTOSE10
0.0000	0.0000	4.0872	4.0724	0	UNKNOWN141
0.0000	0.0000	4.08545	4.08358	0	CHOLINE01,ISOCITRATE04,GALACTOSE11,GLUCARATE14,LACTATE10
0.0000	0.0000	4.08288	4.08032	0	ISOCITRATE05,GALACTOSE12,CHOLINE02,GLUTARATE15,LACTATE11
0.0000	0.0000	4.0803	4.0639	0	UNKNOWN142
0.0000	0.0000	4.0781	4.07407	0	ISOCITRATE06,CHOLINE03,GALACTOSE13,TRYPTOPHAN12
0.0000	0.0000	4.0753	4.0613	0	ISOCITRATE07,GALACTOSE14,CHOLINE04,SUCROSE08
0.0000	0.0000	4.07407	4.06709	0	ISOCITRATE08,GALACTOSE15,CHOLINE05,CREATININE01,SUCROSE09
0.0000	0.0000	4.0726	4.057	0	UNKNOWN143
0.0000	0.0000	4.0695	4.0539	0	CREATININE02,ISOCITRATE09,GALACTOSE16,CHOLINE06,2-HYDROXYVALERATE01,GLUCOSE-6-PHOSPHATE11
0.0000	0.0000	4.0601	4.0553	0	SUCROSE10,ISOCITRATE10,2-HYDROXYVALERATE02,GLUCOSE-6-PHOSPHATE12,GALACTOSE17,CREATININE03
0.0000	0.0000	4.05651	4.0512	0	ISOCITRATE11,2-HYDROXYVALERATE03,GLUCOSE-6-PHOSPHATE13,LACTULOSE42
0.0000	0.0000	4.0561	4.0437	0	UNKNOWN144
0.0000	0.0000	4.04857	4.04455	0	ISOCITRATE12,2-HYDROXYVALERATE04,GLUCOSE-6-PHOSPHATE14,LACTULOSE42,UDP-GALACTOSE32
0.0000	0.0000	4.0535	4.0307	0	ISOCITRATE13,2-HYDROXYVALERATE05,GLUCOSE-6-PHOSPHATE15,LACTULOSE43,UDP-GALACTOSE33,SUCROSE11
0.0000	0.0000	4.0422	4.0334	0	LACTULOSE44,UDP-GALACTOSE34,ISOCITRATE14,2-HYDROXYVALERATE06
0.0000	0.0000	4.0415	4.0251	0	LACTULOSE45,UDP-GALACTOSE35,ISOCITRATE15,2-HYDROXYVALERATE07,GLUCOSE-6-PHOSPHATE16
0.0000	0.0000	4.0401	4.0125	0	UNKNOWN145
0.0000	0.0000	4.03241	4.02885	0	2-HYDROXYVALERATE08,GLUCOSE-6-PHOSPHATE17,LACTULOSE46
0.0000	0.0000	4.0306	4.0126	0	UNKNOWN146
0.0000	0.0000	4.0247	4.0099	0	LACTULOSE47,GLUCOSE-6-PHOSPHATE18
0.0000	0.0000	4.0226	4.0054	0	PHENYLALANINE12,GLUCOSE-6-PHOSPHATE19,LACTULOSE48
0.0000	0.0000	4.0147	4.0035	0	PHENYLALANINE13,GLUCOSE-6-PHOSPHATE20,GALACTONATE03
0.0000	0.0000	4.0125	4.0021	0	PHENYLALANINE14,GLUCOSE-6-PHOSPHATE21,GALACTONATE04
0.0000	0.0000	4.0115	3.9919	0	PHENYLALANINE15,GLUCOSE-6-PHOSPHATE22,HISTIDINE07,RIBOSE19,GALACTOSE18
0.0000	0.0000	4.0081	3.9869	0	UNKNOWN147
0.0000	0.0000	4.0065	4.00352	0	GLUCOSE-6-PHOSPHATE23,GALACTOSE19,PHENYLALANINE16,GALACTONATE05,RIBOSE20,GALACTITOL01
0.0000	0.0000	4.0066	3.9734	0	GLUCOSE-6-PHOSPHATE24,GALACTOSE20,HISTIDINE08,GALACTONATE06,RIBOSE21,GALACTITOL02,PHENYLALANINE17
0.0000	0.0000	3.9949	3.9737	0	GALACTONATE07,GALACTOSE21,HISTIDINE09,GALACTITOL03,RIBOSE22,GLUCOSE-6-PHOSPHATE25,LACTOSE17
0.0000	0.0000	3.98936	3.98201	0	GALACTONATE08,GALACTITOL04,RIBOSE23,LACTOSE18,PI-METHYLHISTIDINE04
0.0000	0.0000	3.9814	3.9726	0	GALACTONATE09,GALACTITOL05,LACTOSE19,RIBOSE24,PI-METHYLHISTIDINE05
0.0000	0.0000	3.9851	3.9615	0	GALACTONATE10,GALACTITOL06,LACTOSE20,RIBOSE25,PI-METHYLHISTIDINE06
0.0000	0.0000	3.9768	3.9508	0	UNKNOWN148
0.0000	0.0000	3.980885	3.97762	0	LACTOSE21,PI-METHYLHISTIDINE07,GLYCYLPROLINE05,GALACTITOL07,GLUCARATE16,GAMMA-METHYLHISTIDINE08
0.0000	0.0000	3.9647	3.9459	0	GLYCYLPROLINE06,LACTOSE22,GLUCARATE17,SN-GLYCERO-3-PHOSPHOCHOLINE07
0.0000	0.0000	3.96323	3.95995	0	LACTOSE23,CAFFEINE01,GLYCYLPROLINE07,GLUCARATE18,TYROSINE12
0.0000	0.0000	3.95995	3.95639	0	GLUCARATE19,LACTOSE24,CAFFEINE02,MANNOSE03
0.0000	0.0000	3.9602	3.9462	0	GLYCOLATE01,GALACTARATE03,CREATINE_PHOSPHATE01,LACTULOSE49,LACTOSE25,MANNOSE04,TYROSINE13
0.0000	0.0000	3.955	3.9378	0	GLYCOLATE02,GALACTARATE04,CREATINEPHOSPHATE02,LACTULOSE50,LACTOSE26,MANNOSE05,TYROSINE14
0.0000	0.0000	3.95	3.9376	0	LACTOSE27,LACTULOSE51,GLUCOSE-1-PHOSPHATE01,GALACTARATE05,MANNOSE06
0.0000	0.0000	3.94529	3.94226	0	LACTOSE28,GALACTOSE22,GLUCOSE-1-PHOSPHATE02,LACTULOSE52,1,7-DIMETHYLXANTHINE05,SN-GLYCERO-3-PHOSPHOCHOLINE08
0.0000	0.0000	3.9531	3.9231	0	GALACTOSE23,CREATINE01,MANNOSE07,GLUCOSE-1-PHOSPHATE03,RIBOSE26
0.0000	0.0000	3.93342	3.92936	0	LACTULOSE53,GLUCOSE-1-PHOSPHATE04,RIBOSE27,MANNOSE08,GALACTOSE24
0.0000	0.0000	3.93045	3.92594	0	GLUCOSE-1-PHOSPHATE05,RIBOSE28,MANNOSE09,LACTULOSE54,GLUCOSE-6-PHOSPHATE26
0.0000	0.0000	3.9343	3.9187	0	UNKNOWN149
0.0000	0.0000	3.92542	3.92284	0	GLUCOSE-1-PHOSPHATE06,MANNOSE10,SN-GLYCERO-3-PHOSPHOCHOLINE08,RIBOSE29,GLUCOSE14,LACTULOSE55
0.0000	0.0000	3.9271	3.9167	0	UNKNOWN150
0.0000	0.0000	3.92123	3.918	0	GLUCOSE-1-PHOSPHATE07,SN-GLYCERO-3-PHOSPHOCHOLINE09,RIBOSE30,GLUCOSE15,BETAINE01
0.0000	0.0000	3.918	3.91458	0	GLUCOSE16,SN-GLYCERO-3-PHOSPHOCHOLINE10,BETAINE02,GLYCYLPROLINE08,UDP-GALACTOSE36,INOSINE09,RIBOSE31
0.0000	0.0000	3.9169	3.9053	0	GLUCOSE17,BETAINE03,LACTOSE29,MANNOSE11,INOSINE10
0.0000	0.0000	3.9145	3.9013	0	BETAINE04,GLUCOSE18,MANNOSE12,RIBOSE31
0.0000	0.0000	3.9086	3.8898	0	UNKNOWN151
0.0000	0.0000	3.8993	3.8877	0	GLUCOSE19,GLUCOSE-1-PHOSPHATE08,LACTOSE30,MANNOSE13,RIBOSE32
0.0000	0.0000	3.8965	3.8841	0	GLUCOSE20,GLUCOSE-1-PHOSPHATE09,LACTOSE31,MANNOSE14,RIBOSE33
0.0000	0.0000	3.8922	3.8782	0	4-HYDROXY-3-METHOXYMANDELATE11,RIBOSE34,GLUCOSE21,METHIONINE01
0.0000	0.0000	3.88193	3.87671	0	GLUCOSE-1-PHOSPHATE10,MANNOSE15,LACTOSE32,METHIONINE02,RIBOSE35
0.0000	0.0000	3.8909	3.8585	0	UNKNOWN152
0.0000	0.0000	3.87587	3.87122	0	GLUCOSE-1-PHOSPHATE11,MANNOSE16,LACTOSE33,GALACTOSE25,METHIONINE03,O-ACETYLCARNITINE08,SN-GLYCERO-3-PHOSPHOCHOLINE11
0.0000	0.0000	3.87148	3.86709	0	UNKNOWN153
0.0000	0.0000	3.8844	3.8492	0	UNKNOWN154
0.0000	0.0000	3.86709	3.86271	0	SUCCINYLACETONE01,GALACTOSE26,RIBOSE36,MANNOSE17,GLUCOSE-1-PHOSPHATE12

0.0000	0.0000	3.86709	3.86271	0	SUCCINYLACETONE01,GALACTOSE26,RIBOSE36,MANNOSE17,GLUCOSE-1-PHOSPHATE12
0.0000	0.0000	3.86271	3.85987	0	MANNOSE18,METHIONINE04,SUCCINYLACETONE02,RIBOSE37,GALACTOSE27,LACTOSE34
0.0000	0.0000	3.85987	3.85954	0	GLUCOSE22,MANNOSE19,LACTOSE35,O-ACETYLCARNITINE09,GALACTOSE28
0.0000	0.0000	3.869	3.8486	0	UNKNOWN155
0.0000	0.0000	3.85954	3.85658	0	GLUCOSE23,GALACTOSE29,LACTOSE36,RIBOSE38,MANNOSE20
0.0000	0.0000	3.862	3.8472	0	UNKNOWN156
0.0000	0.0000	3.8587	3.8439	0	UNKNOWN157
0.0000	0.0000	3.854	3.85167	0	GALACTOSE30,RIBOSE39,MANNOSE21,LACTOSE37
0.0000	0.0000	3.8567	3.8395	0	MANNOSE22,GALACTOSE30,GLUCOSE24,O-ACETYLCARNITINE10,RIBOSE40,SUCROSE12,LACTOSE38
0.0000	0.0000	3.85	3.836	0	UNKNOWN158
0.0000	0.0000	3.84722	3.84419	0	GLUCOSE25,LACTOSE39,2-HYDROXYISOVALERATE09,MANNOSE23,SUCROSE13,RIBOSE41,INOSINE11
0.0000	0.0000	3.8461	3.8337	0	GLUCOSE26,2-HYDROXYISOVALERATE10,LACTULOSE56,LACTOSE40,RIBOSE42
0.0000	0.0000	3.8442	3.827	0	GLUCOSE27,2-HYDROXYISOVALERATE11,LACTULOSE57,LACTOSE41,RIBOSE43
0.0000	0.0000	3.83935	3.83754	0	GLUCOSE28,RIBOSE44,LACTULOSE58,SUCROSE14,LACTOSE42
0.0000	0.0000	3.8368	3.8204	0	UNKNOWN159
0.0000	0.0000	3.83619	3.83044	0	LACTOSE43,SUCROSE15,GLUCOSE29,RIBOSE45,MANNOSE24
0.0000	0.0000	3.8331	3.8183	0	SUCROSE16,GLUCOSE30,LACTOSE44,LACTULOSE59,RIBOSE45
0.0000	0.0000	3.8274	3.815	0	GLUCOSE31,SUCROSE17,LACTOSE45,LACTULOSE60,MANNOSE25,GALACTOSE31
0.0000	0.0000	3.82606	3.82102	0	GLUCOSE32,LACTOSE46,GALACTOSE32,SUCROSE18,LACTULOSE61,MANNOSE26
0.0000	0.0000	3.8328	3.7952	0	UNKNOWN160
0.0000	0.0000	3.82077	3.81193	0	N-NITROSODIMETHYLAMINE01,LACTOSE47,RIBOSE46,FUCOSE13,MANNOSE27,GLUCOSE33
0.0000	0.0000	3.8131	3.7919	0	UNKNOWN161
0.0000	0.0000	3.81354	3.80786	0	LACTOSE48,LACTULOSE62,GALACTOSE33,MANNOSE28,RIBOSE47,ALANINE01,GLUTATHIONE15
0.0000	0.0000	3.80786	3.8027	0	ORNITHINE01,LACTOSE49,GALACTOSE34,GLUCOSE-1-PHOSPHATE13,FUCOSE14,LACTULOSE63
0.0000	0.0000	3.8084	3.7848	0	UNKNOWN162
0.0000	0.0000	3.8027	3.79793	0	GLUCOSE-1-PHOSPHATE14,ALANINE02,LACTOSE50,ORNITHINE02,GLUTATHIONE16,LACTULOSE64,GALACTOSE35
0.0000	0.0000	3.7985	3.7861	0	GLUTAMINE25,ORNITHINE03,LACTOSE51,GALACTOSE36,GLUTATHIONE17,GLUCOSE-1-PHOSPHATE15
0.0000	0.0000	3.7938	3.7814	0	GLUTAMINE26,ORNITHINE04,LACTOSE52,GALACTOSE37,GLUTATHIONE18,GLUCOSE-1-PHOSPHATE16
0.0000	0.0000	3.793	3.7726	0	GLUTATHIONE19,GLUCOSE34,GLUCOSE-1-PHOSPHATE17,GLUTAMINE27,LACTOSE53,MANNOSE29
0.0000	0.0000	3.7903	3.7603	0	GLUTATHIONE20,GLUCOSE35,GLUCOSE-1-PHOSPHATE18,GLUTAMINE28,LACTOSE54,MANNOSE30
0.0000	0.0000	3.78134	3.77541	0	GLUTATHIONE21,GLUCOSE36,LACTOSE55,LACTULOSE64,GLUTAMINE29,LYSINE01,GLUTAMATE01,GLUCOSE-1-PHOSPHATE19
0.0000	0.0000	3.7767	3.7663	0	GLUTATHIONE22,GLUTAMINE30,GLUTAMATE02,LYSINE02,GLUCOSE37,LACTULOSE65,LACTOSE56,MANNOSE31
0.0000	0.0000	3.7712	3.7672	0	UNKNOWN163
0.0000	0.0000	3.7753	3.7549	0	GLUTAMATE03,LYSINE03,GALACTOSE38,GLUCOSE38,LACTOSE57,GLUCOSE-1-PHOSPHATE20
0.0000	0.0000	3.77076	3.76437	0	GALACTOSE39,LYSINE04,GLUTAMATE04,GLUCOSE-1-PHOSPHATE21,LACTOSE58,GLUCOSE39,LACTULOSE66,GLUTATHIONE23,FUCOSE15
0.0000	0.0000	3.7639	3.7583	0	GLUCOSE40,GALACTOSE40,LACTOSE59,LACTULOSE40,GLUTAMATE05,LYSINE05,2-AMINOADIPATE01,GLUCOSE-1-PHOSPHATE22,MANNOSE32,GLUTATHIONE24
0.0000	0.0000	3.7626	3.7522	0	UNKNOWN164
0.0000	0.0000	3.76386	3.76089	0	GALACTOSE41,LACTULOSE68,LYSINE06,2-AMINOADIPATE02,FUCOSE16,GLUCOSE-1-PHOSPHATE23,ANSERINE18,MANNOSE33
0.0000	0.0000	3.7622	3.7458	0	UNKNOWN165
0.0000	0.0000	3.7535	3.7479	0	2-AMINOADIPATE03,GLUCOSE41,GALACTOSE42,LACTOSE60,GLUCOSE-1-PHOSPHATE24,LACTULOSE69,MANNOSE34
0.0000	0.0000	3.7521	3.7397	0	2-AMINOADIPATE04,GLUCOSE42,GALACTOSE43,LACTOSE61,GLUCOSE-1-PHOSPHATE25,LACTULOSE70,MANNOSE35
0.0000	0.0000	3.7446	3.7398	0	GALACTOSE44,2-AMINOADIPATE05,GLUCOSE43,LACTOSE62,O-ACETYLCHOLINE08,LACTULOSE71,N6-ACETYLLYSINE03
0.0000	0.0000	3.7424	3.7344	0	GLUCOSE44,2-AMINOADIPATE06,LACTULOSE72,LACTOSE63,GALACTOSE45,O-ACETYLCHOLINE09,MANNOSE36
0.0000	0.0000	3.7398	3.7274	0	GLUCOSE45,LACTOSE64,2-AMINOADIPATE07,GLUCOSE-6-PHOSPHATE26,LACTULOSE73,O-ACETYLCHOLINE10,GALACTOSE46
0.0000	0.0000	3.7322	3.7298	0	UNKNOWN166
0.0000	0.0000	3.73185	3.72572	0	GLUCOSE46,LACTOSE65,LACTULOSE74,MANNOSE37,N,N-DIMETHYLGLYCINE01
0.0000	0.0000	3.7296	3.7192	0	UNKNOWN167
0.0000	0.0000	3.7263	3.7123	0	GLUCOSE47,GALACTOSE46,GALACTONATE11,LACTULOSE75,GALACTITOL08
0.0000	0.0000	3.7219	3.7095	0	GALACTONATE12,GLUCOSE48,GALACTITOL09,GALACTOSE47,3-HYDROXYKYNURENINE36
0.0000	0.0000	3.71456	3.7083	0	GALACTITOL10,GALACTONATE13,GALACTOSE48,GLUCOSE49,GLUTARIC_ACID_MONOMETHYL_ESTER01
0.0000	0.0000	3.7108	3.7004	0	GALACTITOL11,GALACTONATE14,GALACTOSE49,GLUCOSE50,GLUTARIC_ACID_MONOMETHYL_ESTER02,RIBOSE48,LACTULOSE75,ETHANOL01
0.0000	0.0000	3.70327	3.69946	0	GALACTITOL12,GALACTONATE15,GALACTOSE50,GLUCOSE51,ETHANOL02
0.0000	0.0000	3.69966	3.69721	0	LACTULOSE76,GALACTITOL13,LACTOSE66,SUCROSE18,ETHANOL03,GLUCOSE52,GLUTARIC_ACID_MONOMETHYL_ESTER03
0.0000	0.0000	3.7057	3.6829	0	SUCROSE19,LACTOSE67,LACTULOSE77,RIBOSE49,SN-GLYCERO-3-PHOSPHOCHOLINE11,ETHANOL04
0.0000	0.0000	3.69211	3.68811	0	LACTOSE68,LACTULOSE78,RIBOSE50,SN-GLYCERO-3-PHOSPHOCHOLINE12,ETHANOL05,SUCROSE20,GALACTONATE16
0.0000	0.0000	3.6939	3.6815	0	UNKNOWN168
0.0000	0.0000	3.68733	3.6832	0	SN-GLYCERO-3-PHOSPHOCHOLINE13,LACTOSE69,GALACTITIOL14,ETHYLENE_GLYCOL01,ETHANOL06,LACTULOSE79,RIBOSE50
0.0000	0.0000	3.6884	3.676	0	GALACTITOL15,ETHYLENE_GLYCOL02,LACTOSE70,ISOLEUCINE01,ETHANOL07,MANNOSE38,LACTULOSE80
0.0000	0.0000	3.67817	3.67559	0	ISOLEUCINE02,ETHANOL08,SN-GLYCERO-3-PHOSPHOCHOLINE14,MANNOSE39,RIBOSE51
0.0000	0.0000	3.6783	3.6703	0	ETHANOL09,LACTOSE71,ISOLEUCINE03
0.0000	0.0000	3.667	3.6606	0	ETHANOL10,LACTOSE72,GALACTONATE17,GALACTOSE51
0.0000	0.0000	3.6575	3.6503	0	ETHANOL11,LACTOSE73,MANNOSE40
0.0000	0.0000	3.664946	3.64643	0	ETHANOL12,GALACTOSE53,GALACTONATE18
0.0000	0.0000	3.6472	3.64	0	ETHANOL13,FUCOSE17
0.0000	0.0000	3.645	3.6354	0	UNKNOWN169
0.0000	0.0000	3.63868	3.63481	0	LACTULOSE81,ETHANOL14,SN-GLYCERO-3-PHOSPHOCHOLINE15
0.0000	0.0000	3.6391	3.6275	0	UNKNOWN170
0.0000	0.0000	3.6366	3.6186	0	LACTULOSE82,ETHANOL15,SN-GLYCERO-3-PHOSPHOCHOLINE16,LACTOSE74,RIBOSE52
0.0000	0.0000	3.6287	3.6199	0	VALINE01,LACTOSE74,LACTULOSE83,O-ACETYLCARNITINE10,ETHANOL16
0.0000	0.0000	3.6236	3.6132	0	SARCOSINE01,LACTOSE75,VALINE02,LACTULOSE84
0.0000	0.0000	3.6175	3.6087	0	UNKNOWN171
0.0000	0.0000	3.61304	3.606	0	LACTOSE76,LACTULOSE85,O-PHOSPHOCHOLINE08,SN-GLYCERO-3-PHOSPHOCHOLINE17,RIBOSE53,GLYCYLPROLINE09
0.0000	0.0000	3.6119	3.5963	0	LACTOSE77,LACTULOSE86,O-PHOSPHOCHOLINE09,O-ACETYLCARNITINE11,GLUCOSE-6-PHOSPHATE27
0.0000	0.0000	3.6045	3.5965	0	LACTOSE78,LACTULOSE87,O-PHOSPHOCHOLINE10,O-ACETYLCARNITINE12,GLUCOSE-6-PHOSPHATE28
0.0000	0.0000	3.5987	3.5891	0	THREONINE09,LACTOSE79,O-PHOSPHOCHOLINE11,LACTULOSE88,MANNOSE41,GLYCYLPROLINE10
0.0000	0.0000	3.5972	3.5832	0	GLUCOSE-6-PHOSPHATE29,5-HYDROXYINDOLE-3-ACETATE12,LACTOSE80,LACTULOSE89,THREONINE10,O-PHOSPHOCHOLINE12,GLYCYLPROLINE11
0.0000	0.0000	3.591	3.583	0	LACTULOSE90,GLUCOSE-6-PHOSPHATE30,LACTOSE81,5-HYDROXYINDOLE-3-ACETATE13,GLYCYLPROLINE12,THREONINE11
0.0000	0.0000	3.5846	3.5814	0	1,3-DIHYDROXYACETONE05,MANNOSE42,LACTULOSE91,GLUCOSE-6-PHOSPHATE31,LACTOSE82,GLYCYLPROLINE13,THREONINE12
0.0000	0.0000	3.5823	3.5759	0	GLUCOSE-6-PHOSPHATE32,LACTOSE83,SUCROSE21,LACTULOSE92,GLYCYLPROLINE14,MANNOSE43
0.0000	0.0000	3.5849	3.5693	0	GLUCOSE-6-PHOSPHATE33,LACTOSE84,GLYCYLPROLINE15,SUCROSE22
0.0000	0.0000	3.57505	3.56918	0	LACTOSE85,GLUCOSE-6-PHOSPHATE34,LACTULOSE93,GLYCYLPROLINE16,GLYCINE01,SUCROSE23
0.0000	0.0000	3.5713	3.5673	0	UNKNOWN172
0.0000	0.0000	3.5744	3.5604	0	GLYCINE01,LACTOSE86,MANNOSE44,GLYCYLPROLINE17
0.0000	0.0000	3.5663	3.5599	0	UNKNOWN173

0.0000	0.0000	3.5663	3.5599	0	UNKNOWN173
0.0000	0.0000	3.56556	3.56217	0	GLUCOSE-6-PHOSPHATE35,LACTOSE87,GLYCYLPROLINE18,SUCROSE24,LACTULOSE94
0.0000	0.0000	3.5623	3.5575	0	LACTOSE88,SUCROSE25,GLUCOSE-6-PHOSPHATE36,GLYCYLPROLINE19,GLUCOSE52
0.0000	0.0000	3.5608	3.5544	0	LACTOSE89,GLUCOSE53,GLYCYLPROLINE20,SUCROSE26,GLUCOSE-6-PHOSPHATE37
0.0000	0.0000	3.5546	3.5474	0	GLUCOSE54,LACTOSE90,PHEHYLACETATE14
0.0000	0.0000	3.5491	3.5419	0	PHENYLACETATE15,GLUCOSE55,LACTOSE91
0.0000	0.0000	3.5402	3.5338	0	GLUCOSE56,RIBOSE54,GLYCYLPROLINE21
0.0000	0.0000	3.53547	3.53358	0	3-METHYLXANTHINE02,GLUCOSE57,RIBOSE55,CAFFEINE03,CHOLINE06
0.0000	0.0000	3.5326	3.5294	0	GLUCOSE58,CHOLINE07,RIBOSE56,GLUCOSE-6-PHOSPHATE38
0.0000	0.0000	3.5314	3.5218	0	GLUCOSE-6-PHOSPHATE39,CHOLINE08,RIBOSE57,GLUCOSE59,GLYCYLPROLINE22
0.0000	0.0000	3.5235	3.51953	0	CHOLINE09,GLUCOSE-6-PHOSPHATE40,GLUCOSE60,RIBOSE57,GLUCOSE-1-PHOSPHATE24,GLYCYLPROLINE23
0.0000	0.0000	3.5211	3.5171	0	UNKNOWN174
0.0000	0.0000	3.51838	3.5146	0	CHOLINE10,GLUCOSE61,GLUCOSE-6-PHOSPHATE41,GLUCOSE-1-PHOSPHATE25,GALACTOSE54
0.0000	0.0000	3.5129	3.5065	0	GLUCOSE62,GLUCOSE-1-PHOSPHATE42,GALACTOSE55,GLUCOSE-6-PHOSPHATE42
0.0000	0.0000	3.50905	3.50181	0	GLUCOSE63,GLUCOSE-1-PHOSPHATE43,GALACTOSE56,GLUCOSE-6-PHOSPHATE43
0.0000	0.0000	3.50181	3.49826	0	GLUCOSE64,GLUCOSE-1-PHOSPHATE44,GALACTOSE57,GLUCOSE-6-PHOSPHATE44
0.0000	0.0000	3.5004	3.4924	0	GLUCOSE65,GLUCOSE-1-PHOSPHATE45,GALACTOSE58,GLUCOSE-6-PHOSPHATE45,SUCROSE27
0.0000	0.0000	3.49502	3.48806	0	GLUCOSE-1-PHOSPHATE46,GLUCOSE66,GALACTOSE59,SUCROSE28
0.0000	0.0000	3.4887	3.4783	0	GLUCOS67,GALACTOSE60,N-ACETYLSEROTONIN17,SUCROSE29
0.0000	0.0000	3.4808	3.4728	0	UNKNOWN175
0.0000	0.0000	3.47909	3.47405	0	GLUCOSE68,N-ACETYLSEROTONIN18
0.0000	0.0000	3.4757	3.4717	0	UNKNOWN176
0.0000	0.0000	3.47405	3.47129	0	GLUCOSE69,N-ACETYLSEROTONIN19
0.0000	0.0000	3.4757	3.4661	0	UNKNOWN177
0.0000	0.0000	3.47129	3.46865	0	GLUCOSE70,N-ACETYLSEROTONIN20,SUCROSE30
0.0000	0.0000	3.4719	3.4639	0	UNKNOWN178
0.0000	0.0000	3.46865	3.46361	0	GLUCOSE71,N-ACETYLSEROTONIN21,FUCOSE18,4-HYDROXYPHENYLACETATE11
0.0000	0.0000	3.4664	3.4584	0	UNKNOWN179
0.0000	0.0000	3.46361	3.4607	0	GLUCOSE72,4-HYDROXYPHENYLACETATE12,N-ACETYLSEROTONIN22,TAURINE01
0.0000	0.0000	3.4636	3.4556	0	GLUCOSE73,4-HYDROXYPHENYLACETATE13,N-ACETYLSEROTONIN23,TAURINE02
0.0000	0.0000	3.45727	3.45318	0	GLUCOSE74,N-ACETYLSEROTONIN24,FUCOSE19,1,3-DIMETHYLURATE01,4-HYDROXYPHENYLACETATE14,TAURINE03,XYLOSE09
0.0000	0.0000	3.45318	3.4492	0	FUCOSE20,GLUCOSE75,TAURINE04,N-ACETYLSEROTONIN25
0.0000	0.0000	3.4424	3.4424	0	UNKNOWN180
0.0000	0.0000	3.44302	3.43699	0	TAURINE05,CARNITINE10,FUCOSE21,GLUCOSE76,XYLOSE10
0.0000	0.0000	3.4391	3.4311	0	TAURINE06,GLUCOSE77,CARNITINE11
0.0000	0.0000	3.4363	3.4283	0	TAURINE07,GLUCOSE78,CARNITINE12
0.0000	0.0000	3.4295	3.4215	0	TAURINE08,GLUCOSE79,GLUCOSE-1-PHOSPHATE47
0.0000	0.0000	3.427	3.4166	0	GLUCOSE80,TAURINE09
0.0000	0.0000	3.4205	3.4117	0	TAURINE10,GLUCOSE81,GLUCOSE-1-PHOSPHATE48
0.0000	0.0000	3.4135	3.4031	0	GLUCOSE82,TAURINE11
0.0000	0.0000	3.4086	3.4006	0	UNKNOWN181
0.0000	0.0000	3.40171	3.39671	0	GLUCOSE-1-PHOSPHATE49,GLUCOSE83,MANNOSE41,TAURINE12
0.0000	0.0000	3.4023	3.4015	0	GLUCOSE84,MANNOSE42,GLUCOSE-1-PHOSPHATE50
0.0000	0.0000	3.3979	3.3915	0	GLUCOSE85,MANNOSE43,TAURINE13,GLUCOSE-1-PHOSPHATE51
0.0000	0.0000	3.39155	3.38828	0	GLUCOSE86,MANNOSE44,TAURINE14,GLUCOSE-1-PHOSPHATE52
0.0000	0.0000	3.38856	3.38439	0	GLUCOSE87,MANNOSE45,TAURINE15
0.0000	0.0000	3.38147	3.37824	0	GLUCOSE88,MANNOSE46,TAURINE16,BIOTIN15
0.0000	0.0000	3.37824	3.37289	0	MANNOSE47,BIOTIN16,GLUCOSE89,METHANOL01
0.0000	0.0000	3.37289	3.36415	0	BIOTIN17,METHANOL02,TAURINE17,GLUCOSE90
0.0000	0.0000	3.3618	3.3562	0	METHANOL03,BIOTIN18
0.0000	0.0000	3.3549	3.3525	0	CAFFEINE04,METHANOL04,BIOTIN19
0.0000	0.0000	3.35233	3.34619	0	BIOTIN20,METHANOL05,CAFFEINE05
0.0000	0.0000	3.34619	3.34269	0	XYLOSE11,METHANOL06,BIOTIN21,TAURINE18
0.0000	0.0000	3.34269	3.33761	0	PI-METHYLHISTIDINE08,TAURINE19,BETAINE05,XYLOSE12
0.0000	0.0000	3.3374	3.3374	0	UNKNOWN182
0.0000	0.0000	3.33536	3.32891	0	PI-METHYLHISTIDINE09,TRYPTOPHAN13,TAURINE20,BETAINE06
0.0000	0.0000	3.3278	3.3246	0	XYLOSE13,1,3-DIMETHYLURATE02,TAURINE21,LACTOSE92,PI-METHYLHISTIDINE10
0.0000	0.0000	3.3271	3.3215	0	1,3-DIMETHYLURATE03,TAURINE22,LACTOSE93,BETAINE07
0.0000	0.0000	3.3247	3.3183	0	UNKNOWN183
0.0000	0.0000	3.322	3.3164	0	1,7-DIMETHYLXANTHINE06,LACTOSE94,TAURINE23,PI-METHYLHISTIDINE11,1,3-DIMETHYLURATE04,HISTAMINE03
0.0000	0.0000	3.3174	3.3166	0	UNKNOWN184
0.0000	0.0000	3.31678	3.3102	0	LACTOSE95,HISTAMINE04,TAURINE24,XYLOSE14
0.0000	0.0000	3.3102	3.30575	0	PHENYLALANINE18,PI-METHYLHISTIDINE12,LACTOSE96,TAURINE25,HISTAMINE05,BETAINE08
0.0000	0.0000	3.30575	3.30237	0	HISTAMINE06,LACTOSE97,GLUCOSE-6-PHOSPHATE46,TAURINE26,PHENYLALANINE19,BETAINE09
0.0000	0.0000	3.30237	3.29677	0	HISTAMINE07,LACTOSE98,GLUCOSE-6-PHOSPHATE47,TAURINE27,PHENYLALANINE20,BETAINE10,TRIMETHYLAMINE_N-OXIDE01
0.0000	0.0000	3.29677	3.29288	0	HISTAMINE08,LACTOSE99,GLUCOSE-6-PHOSPHATE48,TAURINE28,PHENYLALANINE21,BETAINE11,TRIMETHYLAMINE_N-OXIDE02
0.0000	0.0000	3.29288	3.2846	0	LACTOSE99,GLUCOSE-6-PHOSPHATE49,TAURINE29,PHENYLALANINE22,BETAINE12,TRIMETHYLAMINE_N-OXIDE03
0.0000	0.0000	3.2874	3.2818	0	UNKNOWN185
0.0000	0.0000	3.2829	3.2749	0	TAURINE30,BETAINE13,TRIMETHYLAMINE_N-OXIDE04
0.0000	0.0000	3.2737	3.2649	0	TAURINE31,BETAINE14,TRIMETHYLAMINE_N-OXIDE05
0.0000	0.0000	3.268	3.26	0	GLUCOSE91,TAURINE32,BETAINE15,TRIMETHYLAMINE_N-OXIDE06
0.0000	0.0000	3.2638	3.2558	0	GLUCOSE92,TAURINE33,TRIMETHYLAMINE_N-OXIDE07
0.0000	0.0000	3.2565	3.2485	0	GLUCOSE93,TAURINE34,BETAINE16,TRIMETHYLAMINE_N-OXIDE08
0.0000	0.0000	3.2555	3.2459	0	GLUCOSE94,TAURINE35,TYRAMINE16
0.0000	0.0000	3.24964	3.24767	0	TYRAMINE17,GLUCOSE95,TAURINE36,HISTIDINE10,XYLOSE15
0.0000	0.0000	3.2428	3.2356	0	GLUCOSE96,HISTIDINE11,TYRAMINE18,ANSERINE19
0.0000	0.0000	3.23838	3.23578	0	GLUCOSE97,TYRAMINE19,ANSERINE20,O-PHOSPHOCHOLINE13,O-ACETYLCHOLINE11
0.0000	0.0000	3.2388	3.2308	0	UNKNOWN186
0.0000	0.0000	3.2394	3.223	0	UNKNOWN187
0.0000	0.0000	3.2314	3.219	0	CARNITINE13,SN-GLYCERO-3-PHOSPHOCHOLINE18,O-PHOSPHOCHOLINE12,ANSERINE21
0.0000	0.0000	3.2269	3.2065	0	UNKNOWN188
0.0000	0.0000	3.2139	3.2027	0	CHOLINE11,O-ACETYLCARNITINE13
0.0000	0.0000	3.2134	3.1866	0	UNKNOWN189
0.0000	0.0000	3.2034	3.1902	0	TYROSINE15,N6-ACETYLLYSINE04,CHOLINE12,O-ACETYLCARNITINE14

0.0000	0.0000	3.2034	3.1902	0	TYROSINE15,N6-ACETYLLYSINE04,CHOLINE12,O-ACETYLCARNITINE14
0.0000	0.0000	3.1989	3.1817	0	N6-ACETYLLYSINE05,TYROSINE16,O-ACETYLCARNITINE15,GAMMA-METHYLHISTIDINE08
0.0000	0.0000	3.19613	3.19199	0	N6-ACETYLLYSINE06,TYROSINE17,O-ACETYLCARNITINE16
0.0000	0.0000	3.1827	3.1723	0	N-NITROSODIMETHYLAMINE02,N6-ACETYLLYSINE07
0.0000	0.0000	3.1775	3.1627	0	HISTIDINE12,N-NITROSODIMETHYLAMINE02,N6-ACETYLLYSINE07,THYMOL08,GAMMA-METHYLHISTIDINE09
0.0000	0.0000	3.16861	3.16486	0	N6-ACETYLLYSINE08,GAMMA-METHYLHISTIDINE10,HISTIDINE13,THYMOL09,O-ACETYLCARNITINE17
0.0000	0.0000	3.1686	3.163	0	UNKNOWN190
0.0000	0.0000	3.1646	3.1629	0	HISTIDINE14,DIMETHYL_SULFONE01,N6-ACETYLLYSINE09,THYMOL10
0.0000	0.0000	3.1686	3.1538	0	HISTIDINE15,DIMETHYL_SULFONE02,N6-ACETYLLYSINE10,THYMOL11
0.0000	0.0000	3.1608	3.1484	0	DIMETHYL_SULFONE03,THYMOL12
0.0000	0.0000	3.15258	3.14864	0	PHENYLALANINE23,HISTIDINE16,DIMETHYL_SULFONE03,DIMETHYL_SULFONE04
0.0000	0.0000	3.1432	3.1328	0	MALONATE01,PHENYLALANINE24,HISTIDINE17
0.0000	0.0000	3.1338	3.1226	0	MALONATE02,PHENYLALANINE25,CIS-ACONITATE03
0.0000	0.0000	3.1245	3.1201	0	CIS-ACONITATE04,3-PHENYLLACTATE21,PHENYLALANINE26
0.0000	0.0000	3.1259	3.1143	0	UNKNOWN191
0.0000	0.0000	3.1201	3.11305	0	CIS-ACONITATE05,3-PHENYLLACTATE22,PHENYLALANINE27
0.0000	0.0000	3.10659	3.1006	0	3-PHENYLLACTATE23,ORNITHINE05,GAMMA-METHYLHISTIDINE11
0.0000	0.0000	3.1006	3.09355	0	3-PHENYLLACTATE24,ORNITHINE06,GAMMA-METHYLHISTIDINE12
0.0000	0.0000	3.0796	3.0796	0	UNKNOWN192
0.0000	0.0000	3.07961	3.07497	0	TYROSINE18,ORNITHINE07
0.0000	0.0000	3.0743	3.0647	0	ORNITHINE08,TYROSINE19
0.0000	0.0000	3.0662	3.0506	0	ORNITHINE09,TYROSINE20,LYSINE07
0.0000	0.0000	3.0554	3.0514	0	UNKNOWN193
0.0000	0.0000	3.0515	3.0435	0	ORNITHINE10,CREATININE04,LYSINE08,TYROSINE21
0.0000	0.0000	3.0447	3.0359	0	CREATINE02,LYSINE09,ORNITHINE11,CREATININE05
0.0000	0.0000	3.03748	3.0328	0	N-ACETYLORNITHINE16,LYSINE10
0.0000	0.0000	3.0372	3.0232	0	N,N-DIMETHYLFORMAMIDE02,N-ACETYLORNITHINE17,LYSINE11,HISTAMINE09,ANSERINE22
0.0000	0.0000	3.02535	3.02244	0	N-ACETYLORNITHINE18,ISOCITRATE16,LYSINE12,HISTAMINE10
0.0000	0.0000	3.02244	3.0198	0	N-ACETYLORNITHINE19,NALPHA-ACETYLLYSINE12,ISOCITRATE17,LYSINE13,HISTAMINE11,BIOTIN22
0.0000	0.0000	3.0252	2.9936	0	N-ACETYLORNITHINE20,NALPHA-ACETYLLYSINE13,ISOCITRATE18,LYSINE14,HISTAMINE12,BIOTIN23
0.0000	0.0000	3.0301	3.0089	0	UNKNOWN194
0.0000	0.0000	3.00708	3.00236	0	N-ACETYLORNITHINE21,NALPHA-ACETYLLYSINE14,ISOCITRATE19,GLUTATHIONE23,BIOTIN24
0.0000	0.0000	3.0085	2.9937	0	ISOCITRATE20,GLUTATHIONE24,NALPHA-ACETYLLYSINE15,BIOTIN24,N-ACETYLORNITHINE21
0.0000	0.0000	3.0107	2.9847	0	UNKNOWN195
0.0000	0.0000	3.99559	2.99133	0	ISOCITRATE21,GLUTATHIONE25
0.0000	0.0000	2.9964	2.9736	0	UNKNOWN196
0.0000	0.0000	2.98417	2.97885	0	GLUTATHIONE26
0.0000	0.0000	2.9931	2.9623	0	UNKNOWN197
0.0000	0.0000	2.97578	2.97196	0	GLUTATHIONE27
0.0000	0.0000	2.9727	2.9695	0	UNKNOWN198
0.0000	0.0000	2.967	2.9554	0	GLUTATHIONE28,3-PHENYLPROPIONATE12
0.0000	0.0000	2.96057	2.95589	0	GLUTATHIONE29,3-PHENYLPROPIONATE13
0.0000	0.0000	2.9579	2.9515	0	UNKNOWN199
0.0000	0.0000	2.9559	2.9435	0	TYRAMINE20,GLUTATHIONE30,3-PHENYLPROPIONATE14
0.0000	0.0000	2.9515	2.9411	0	UNKNOWN200
0.0000	0.0000	2.94589	2.94164	0	TYRAMINE21,GLUTATHIONE31,3-PHENYLPROPIONATE15,N-METHYLHYDANTION02
0.0000	0.0000	2.9438	2.9414	0	UNKNOWN201
0.0000	0.0000	2.9433	2.9337	0	N-METHYLHYDANTOIN03,N,N-DIMETHYLGLYCINE02,GLUTATHIONE32,3-PHEHYLPROPIONATE14,TYRAMINE22
0.0000	0.0000	2.93664	2.93121	0	TYRAMINE23,GLUTATHIONE33,N-METHYLHYDANTOIN04,N-ACETYLSEROTONIN26
0.0000	0.0000	2.93121	2.92522	0	TYRAMINE24,GLUTATHIONE34,N-METHYLHYDANTOIN05,N-ACETYLSEROTONIN27
0.0000	0.0000	2.92522	2.92097	0	TYRAMINE25,GLUTATHIONE35,N-ACETYLSEROTONIN28
0.0000	0.0000	2.92097	2.91065	0	TYRAMINE26,GLUTATHIONE36,N-ACETYLSEROTONIN29
0.0000	0.0000	2.91065	2.90522	0	N-ACETYLSEROTONIN30,3-PHENYLLACTATE25
0.0000	0.0000	2.90522	2.9006	0	N-ACETYLSEROTONIN31,3-PHENYLLACTATE26
0.0000	0.0000	2.8964	2.891	0	3-PHENYLLACTATE27
0.0000	0.0000	2.8875	2.8867	0	UNKNOWN202
0.0000	0.0000	2.8837	2.8837	0	3-PHENYLLACTATE28
0.0000	0.0000	2.8726	2.8726	0	3-PHENYLLACTATE29,N,N-DIMETHYLFORMAMIDE03
0.0000	0.0000	2.87002	2.86918	0	N,N-DIMETHYLFORMAMIDE04,3-PHENYLLACTATE30
0.0000	0.0000	2.8606	2.8598	0	UNKNOWN203
0.0000	0.0000	2.8488	2.8488	0	UNKNOWN204
0.0000	0.0000	2.84269	2.8358	0	SUCCINYLACETONE03,DIMETHYLAMINE01,METHYLGUANIDINE01
0.0000	0.0000	2.8346	2.8282	0	SUCCINYLACETONE04,DIMETHYLAMINE02,METHYLGUANIDINE02
0.0000	0.0000	2.83095	2.8278	0	SUCCINYLACETONE05,DIMETHYLAMINE03,METHYLGUANIDINE03
0.0000	0.0000	2.8268	2.8268	0	UNKNOWN205
0.0000	0.0000	2.8232	2.81552	0	SUCCINYLACETONE06,DIMETHYLAMINE04,5-AMINOLEVULINATE05
0.0000	0.0000	2.81414	2.80607	0	5-AMINOLEVULINATE05,EPICATECHIN11,DIMETHYLAMINE05
0.0000	0.0000	2.8077	2.8069	0	UNKNOWN206
0.0000	0.0000	2.80607	2.79563	0	5-AMINOLEVULINATE06,BIOTIN25,DIMETHYLAMINE06
0.0000	0.0000	2.8018	2.8018	0	UNKNOWN207
0.0000	0.0000	2.7983	2.7975	0	UNKNOWN208
0.0000	0.0000	2.79563	2.78705	0	5-AMINOLEVULINATE07,BIOTIN26,DIMETHYLAMINE07
0.0000	0.0000	2.78705	2.77609	0	5-AMINOLEVULINATE08,BIOTIN27,DIMETHYLAMINE08
0.0000	0.0000	2.7605	2.7549	0	UNKNOWN209
0.0000	0.0000	2.74913	2.74409	0	DIMETHYLAMINE09,SARCOSINE02
0.0000	0.0000	2.73684	2.7309	0	DIMETHYLAMINE10
0.0000	0.0000	2.7286	2.7138	0	UNKNOWN210
0.0000	0.0000	2.7108	2.7052	0	DIMETHYLAMINE11,N-ACETYLASPARTATE10,MALATE15,ANSERINE23
0.0000	0.0000	2.71369	2.70795	0	DIMETHYLAMINE12,N-ACETYLASPARTATE11,MALATE16,
0.0000	0.0000	2.7072	2.7000	0	UNKNOWN211
0.0000	0.0000	2.70204	2.69613	0	MALATE16,DIMETHYLAMINE13,ANSERINE24
0.0000	0.0000	2.69613	2.68928	0	MALATE17,DIMETHYLAMINE14
0.0000	0.0000	2.695	2.687	0	UNKNOWN212
0.0000	0.0000	2.68904	2.68184	0	MALATE18,DIMETHYLAMINE15,ANSERINE25,

0.0000	0.0000	2.68904	2.68184	0	MALATE18,DIMETHYLAMINE15,ANSERINE25,
0.0000	0.0000	2.6802	2.677	0	UNKNOWN213
0.0000	0.0000	2.67869	2.67365	0	MALATE18,ANSERINE26
0.0000	0.0000	2.6726	2.6726	0	MALATE19,DIMETHYLAMINE16
0.0000	0.0000	2.6669	2.6645	0	UNKNOWN214
0.0000	0.0000	2.6651	2.6619	0	O-ACETYLCARNITINE18,MALATE20,ANSERINE27,DIMETHYLAMINE17,METHIONINE05
0.0000	0.0000	2.6605	2.6581	0	METHIONINE06,MALATE21,O-ACETYLCARNITINE19,DIMETHYLAMINE18
0.0000	0.0000	2.6557	2.6509	0	METHIONINE07,MALATE22,O-ACETYLCARNITINE20,DIMETHYLAMINE19,ANSERINE26
0.0000	0.0000	2.6491	2.6467	0	METHIONINE08,DIMETHYLAMINE20
0.0000	0.0000	2.6437	2.6437	0	UNKNOEN215
0.0000	0.0000	2.64238	2.63868	0	O-ACETYLCARNITINE21,METHIONINE09,DIMETHYLAMINE21
0.0000	0.0000	2.63935	2.63561	0	O-ACETYLCARNITINE22,METHIONINE10,DIMETHYLAMINE22
0.0000	0.0000	2.6354	2.629	0	O-ACETYLCARNITINE23,METHIONINE11,DIMETHYLAMINE23
0.0000	0.0000	2.6015	2.6015	0	GLUTATHIONE37,ISOCITRATE22,DIMETHYLAMINE24
0.0000	0.0000	2.5958	2.59273	0	GLUTATHIONE38,BUTANONE01,ISOCITRATE23
0.0000	0.0000	2.59273	2.58765	0	GLUTATHIONE39,BUTANONE02,ISOCITRATE24
0.0000	0.0000	2.578391	2.57241	0	ISOCITRATE25,GLUTATHIONE40,BUTANONE03
0.0000	0.0000	2.57229	2.5628	0	ISOCITRATE26,GLUTATHIONE41
0.0000	0.0000	2.556	2.54874	0	ISOCITRATE27,GLUTATHIONE42
0.0000	0.0000	2.5498	2.53701	0	ISOCITRATE28,GLUTATHIONE43,PYROGLUTAMATE09
0.0000	0.0000	2.53739	2.53619	0	O-ACETYLCARNITINE24,ISOCITRATE29,GLUTATHIONE44,PYROGLUTAMATE10
0.0000	0.0000	2.5313	2.5313	0	UNKNOWN216
0.0000	0.0000	2.53901	2.52965	0	O-ACETYLCARNITINE25,ISOCITRATE30,GLUTATHIONE45,PYROGLUTAMATE11
0.0000	0.0000	2.52965	2.5262	0	ISOCITRATE31,GLUTATHIONE46,PYROGLUTAMATE12,N-ACETYLASPARTATE12
0.0000	0.0000	2.5262	2.5262	0	UNKNOWN217
0.0000	0.0000	2.5262	2.52425	0	ISOCITRATE32,PYROGLUTAMATE13,N-ACETYLASPARTATE13,O-ACETYLCARNITINE26,GLUTATHIONE47
0.0000	0.0000	2.52425	2.5205	0	ISOCITRATE33,PYROGLUTAMATE14,N-ACETYLASPARTATE14,O-ACETYLCARNITINE27,GLUTATHIONE48,5-AMINOLEVULINATE09
0.0000	0.0000	2.5205	2.5205	0	UNKNOWN218
0.0000	0.0000	2.5166	2.5166	0	UNKNOWN219
0.0000	0.0000	2.5205	2.51508	0	5-AMINOLEVULINATE10,PYROGLUTAMATE15,ISOCITRATE34,O-ACETYLCARNITINE28
0.0000	0.0000	2.51508	2.51354	0	5-AMINOLEVULINATE10,PYROGLUTAMATE16,ISOCITRATE35,O-ACETYLCARNITINE29,3-PHENYLPROPIONATE12
0.0000	0.0000	2.5079	2.5079	0	UNKNOWN220
0.0000	0.0000	2.51508	2.50641	0	5-AMINOLEVULINATE11,PYROGLUTAMATE17,ISOCITRATE36,O-ACETYLCARNITINE30,3-PHENYLPROPIONATE13,N-ACETYLASPARTATE15
0.0000	0.0000	2.50641	2.50358	0	5-AMINOLEVULINATE12,PYROGLUTAMATE18,ISOCITRATE37,3-PHENYLPROPIONATE14,N-ACETYLASPARTATE16
0.0000	0.0000	2.50358	2.49622	0	5-AMINOLEVULINATE13,PYROGLUTAMATE19,ISOCITRATE38,3-PHENYLPROPIONATE15,N-ACETYLASPARTATE17,GLUTAMINE31
0.0000	0.0000	2.49622	2.49425	0	5-AMINOLEVULINATE14,PYROGLUTAMATE20,ISOCITRATE39,3-PHENYLPROPIONATE16,N-ACETYLASPARTATE18,GLUTAMINE32,O-ACETYLCARNITINE31
0.0000	0.0000	2.4893	2.4885	0	3-PHENYLPROPIONATE17,GLUTAMINE33,ISOCITRATE40,N-ACETYLASPARTATE19,PYROGLUTAMATE21
0.0000	0.0000	2.4856	2.4856	0	3-PHENYLPROPIONATE18,GLUTAMINE34,ISOCITRATE41,N-ACETYLASPARTATE20,PYROGLUTAMATE22
0.0000	0.0000	2.4777	2.4761	0	3-HYDROXY-3-METHYLGLUTARATE01
0.0000	0.0000	2.4693	2.4645	0	GLUTAMINE35,3-HYDROXY-3-METHYLGLUTARATE02
0.0000	0.0000	2.4656	2.4616	0	GLUTAMINE36,3-HYDROXY-3-METHYLGLUTARATE03
0.0000	0.0000	2.46007	2.44704	0	3-HYDROXY-3-METHYLGLUTARATE04,GLUTAMINE37,CARNITINE14
0.0000	0.0000	2.457	2.4506	0	UNKNOWN221
0.0000	0.0000	2.457	2.4474	0	UNKNOWN222
0.0000	0.0000	2.4529	2.4465	0	UNKNOWN223
0.0000	0.0000	2.44822	2.4444	0	3-HYDROXY-3-METHYLGLUTARATE05,GLUTAMINE38,CARNITINE15
0.0000	0.0000	2.4444	2.4398	0	3-HYDROXY-3-METHYLGLUTARATE06,GLUTAMINE39,CARNITINE16
0.0000	0.0000	2.443	2.4366	0	UNKNOWN224
0.0000	0.0000	2.43881	2.43483	0	SUCCINYLACETONE07,3-HYDROXY-3-METHYLGLUTARATE07,GLUTAMINE40,CARNITINE17,PYROGLUTAMATE23
0.0000	0.0000	2.43483	2.43101	0	SUCCINYLACETONE08,3-HYDROXY-3-METHYLGLUTARATE08,GLUTAMINE41,CARNITINE18,PYROGLUTAMATE24
0.0000	0.0000	2.4302	2.4278	0	UNKNOWN225
0.0000	0.0000	2.43101	2.42183	0	SUCCINYLACETONE09,3-HYDROXY-3-METHYLGLUTARATE09,GLUTARIC_ACID_MONOMETHYL_ESTER03
0.0000	0.0000	2.42183	2.41771	0	3-HYDROXY-3-METHYLGLUTARATE10,GLUTARIC_ACID_MONOMETHYL_ESTER04,PYROGLUTAMATE25,MALATE20,CARNITINE19
0.0000	0.0000	2.4232	2.4128	0	UNKNOWN226
0.0000	0.0000	2.41697	2.41069	0	GLUTARIC_ACID_MONOMETHYL_ESTER05,MALATE21,3-HYDROXY-3-METHYLGLUTARATE11,PYROGLUTAMATE26
0.0000	0.0000	2.4129	2.4065	0	GLUTARIC_ACID_MONOMETHYL_ESTER06,MALATE22,3-HYDROXY-3-METHYLGLUTARATE12,PYROGLUTAMATE27
0.0000	0.0000	2.4104	2.4032	0	GLUTARIC_ACID_MONOMETHYL_ESTER07,MALATE23,3-HYDROXY-3-METHYLGLUTARATE13,PYROGLUTAMATE28
0.0000	0.0000	2.4058	2.4026	0	GLUTARIC_ACID_MONOMETHYL_ESTER08,MALATE24,3-HYDROXY-3-METHYLGLUTARATE14,PYROGLUTAMATE29
0.0000	0.0000	2.40366	2.39897	0	MALATE25,3-HYDROXY-3-METHYLGLUTARATE15,GLUTARIC_ACID_MONOMETHYL_ESTER09,PYROGLUTAMATE30,ISOBUTYRATE01
0.0000	0.0000	2.39897	2.39612	0	MALATE26,3-HYDROXY-3-METHYLGLUTARATE16,GLUTARIC_ACID_MONOMETHYL_ESTER10,PYROGLUTAMATE31
0.0000	0.0000	2.4005	2.3933	0	UNKNOWN227
0.0000	0.0000	2.3969	2.3905	0	UNKNOWN228
0.0000	0.0000	2.39612	2.39395	0	MALATE27,3-HYDROXY-3-METHYLGLUTARATE17,PYROGLUTAMATE32
0.0000	0.0000	2.39395	2.38692	0	MALATE28,ISOBUTYRATE02,GLUTAMATE06,PYROGLUTAMATE33,3-HYDROXY-3-METHYLGLUTARATE18
0.0000	0.0000	2.3846	2.3774	0	MALATE29,ISOBUTYRATE03,GLUTAMATE07,PYROGLUTAMATE34
0.0000	0.0000	2.38084	2.37344	0	MALATE30,GLUTAMATE08
0.0000	0.0000	2.3742	2.3646	0	PYRUVATE01,GLUTAMATE09,3-HYDROXYISOVALERATE01,MALATE31
0.0000	0.0000	2.3674	2.357	0	GLUTAMATE10,MALATE32,PYRUVATE02
0.0000	0.0000	2.3655	2.3499	0	GLUTAMATE11,MALATE33
0.0000	0.0000	2.3562	2.349	0	GLUTAMATE12,GLYCYLPROLINE24
0.0000	0.0000	2.3561	2.3445	0	GLUTAMATE13,GLYCYLPROLINE25
0.0000	0.0000	2.3521	2.3417	0	GLUTAMATE14
0.0000	0.0000	2.3451	2.3363	0	GLUTAMATE15,GLYCYLPROLINE26,ACETYLSALICYLATE11
0.0000	0.0000	2.33133	2.32905	0	GLUTAMATE16,GLYCYLPROLINE27,ACETYLSALICYLATE12
0.0000	0.0000	2.32905	2.32565	0	GLUTAMATE17,GLYGYLPROLINE28,3-HYDROXY-3-METHYLGLUTARATE19
0.0000	0.0000	2.31968	2.31674	0	GLUTAMATE18,GLYGYLPROLINE29,3-HYDROXY-3-METHYLGLUTARATE20
0.0000	0.0000	2.3256	2.302	0	UNKNOWN229
0.0000	0.0000	2.3148	2.2936	0	VALINE03,2-AMINOADIPATE08
0.0000	0.0000	2.2988	2.29557	0	VALINE04,2-AMINOADIPATE09
0.0000	0.0000	2.29557	2.29006	0	VALINE05,2-AMINOADIPATE10,P-CRESOL09
0.0000	0.0000	2.29006	2.28409	0	VALINE06,2-AMINOADIPATE11,P-CRESOL10,SUCCINYLACETONE10
0.0000	0.0000	2.28409	2.2788	0	VALINE07,2-AMINOADIPATE12,P-CRESOL11,SUCCINYLACETONE11,GLYCYLPROLINE30
0.0000	0.0000	2.2788	2.27426	0	VALINE08,2-AMINOADIPATE13,P-CRESOL12,SUCCINYLACETONE12,THYMOL13
0.0000	0.0000	2.27416	2.27012	0	VALINE09,2-AMINOADIPATE14,P-CRESOL13,SUCCINYLACETONE13,GLYCYLPROLINE31,3-METHYLGLUTARATE01

0.0000	0.0000	2.27416	2.27012	0	VALINE09,2-AMINOADIPATE14,P-CRESOL13,SUCCINYLACETONE13,GLYCYLPROLINE31,3-METHYLGLUTARATE01
0.0000	0.0000	2.275	2.26181	0	VALINE10,2-AMINOADIPATE15,P-CRESOL14,SUCCINYLACETONE14,THYMOL14
0.0000	0.0000	2.26181	2.25598	0	2-AMINOADIPATE16,P-CRESOL15,SUCCINYLACETONE15,THYMOL15
0.0000	0.0000	2.5598	2.24347	0	2-AMINOADIPATE17,3-METHYLGLUTARATE02,GLYCYLPROLINE32
0.0000	0.0000	2.24347	2.23359	0	2-AMINOADIPATE18,3-METHYLGLUTARATE03,GLYCYLPROLINE33,ACETONE01
0.0000	0.0000	2.239	2.2342	0	2-AMINOADIPATE19,3-METHYLGLUTARATE04,GLYCYLPROLINE34,BUTANONE04,GLUTARIC_ACID_MONOMETHYL_ESTER11
0.0000	0.0000	2.2313	2.2257	0	UNKNOWN230
0.0000	0.0000	2.2225	2.21759	0	2-AMINOADIPATE20,3-METHYLGLUTARATE05,GLUTARIC_ACID_MONOMETHYL_ESTER12,METHIONINE12,BIOTIN28
0.0000	0.0000	2.21759	2.21176	0	3-METHYLGLUTARATE06,GLUTARIC_ACID_MONOMETHYL_ESTER13,METHIONINE13,BIOTIN29
0.0000	0.0000	2.2106	2.2098	0	3-METHYLGLUTARATE07,GLUTARIC_ACID_MONOMETHYL_ESTER14,METHIONINE14,BIOTIN30
0.0000	0.0000	2.20808	2.20051	0	3-METHYLGLUTARATE07,GLUTARIC_ACID_MONOMETHYL_ESTER15,BIOTIN31
0.0000	0.0000	2.2013	2.1997	0	3-METHYLGLUTARATE08,GLUTARIC_ACID_MONOMETHYL_ESTER16,BIOTIN32,METHIONINE15
0.0000	0.0000	2.19785	2.1912	0	BIOTIN33,METHIONINE16,3-METHYLGLUTARATE09,GLUTATHIONE49
0.0000	0.0000	2.19131	2.18868	0	BIOTIN34,METHIONINE17,3-METHYLGLUTARATE10
0.0000	0.0000	2.1874	2.181	0	BIOTIN35,METHIONINE18,3-METHYLGLUTARATE11,GLUTATHIONE50
0.0000	0.0000	2.18331	2.1792	0	GLUTATHIONE51,GLUTAMINE42,BIOTIN36,METHIONINE18,SUBERATE01,3-METHYLGLUTARATE12
0.0000	0.0000	2.18	2.1784	0	UNKNOWN231
0.0000	0.0000	2.1843	2.1639	0	GLUTATHIONE52,SUBERATE02,AZELATE01,SEBACATE01,BIOTIN37
0.0000	0.0000	2.1717	2.1545	0	SUBERATE03,SEBACATE02,AZELATE02,GLUTATHIONE53,GLUTAMINE43,BIOTIN38,GLUTAMATE06
0.0000	0.0000	2.1627	2.1439	0	UNKNOWN232
0.0000	0.0000	2.15809	2.15409	0	GLUTAMINE44,SUBERATE04,AZELATE03,SEBACATE03,GLUTATHIONE54,GLUTAMATE07,BIOTIN39,METHIONINE19
0.0000	0.0000	2.157	2.1446	0	UNKNOWN233
0.0000	0.0000	2.15409	2.14707	0	GLUTAMINE45,GLUTAMATE08,SUBERATE05,SEBACATE04,METHIONINE20
0.0000	0.0000	2.154	2.1384	0	GLUTAMINE46,METHIONINE21,GLUTAMATE09,HYDROXYACETONE03,O-ACETYLCHOLINE12,O-ACETYLCARNITINE31
0.0000	0.0000	2.1487	2.1331	0	O-ACETYLCARNITINE32,HYDROXYACETONE04,O-ACETYLCHOLINE13,GLUTAMINE47,GLUTAMATE10
0.0000	0.0000	2.142	2.1324	0	GLUTAMINE48,GLUTAMATE11,METHIONINE21,O-ACETYECHOLINE14,O-ACETYLCARNITINE33
0.0000	0.0000	2.144	2.1212	0	GLUTAMINE49,GLUTAMATE12,METHIONINE22,HYDROXYACETONE05
0.0000	0.0000	2.13213	2.13036	0	GLUTAMINE50,GLUTAMATE13,METHIONINE23
0.0000	0.0000	2.1354	2.1198	0	GLUTAMINE51,GLUTAMATE14,METHIONINE24
0.0000	0.0000	2.1251	2.1227	0	GLUTAMINE52,GLUTAMATE15,METHIONINE25
0.0000	0.0000	2.1235	2.11913	0	GLUTAMINE53,GLUTAMATE16,METHIONINE26
0.0000	0.0000	2.1263	2.1083	0	GLUTAMINE54,GLUTAMATE16,METHIONINE26
0.0000	0.0000	2.116	2.1012	0	GLUTAMINE55,GLUTAMATE17,METHIONINE27
0.0000	0.0000	2.1093	2.0977	0	GLUTAMINE56,GLUTAMATE18,METHIONINE28
0.0000	0.0000	2.1052	2.0816	0	GLUTAMINE57,GLUTAMATE19,METHIONINE29
0.0000	0.0000	2.0938	2.0834	0	UNKNOWN234
0.0000	0.0000	2.0964	2.0596	0	UNKNOWN235
0.0000	0.0000	2.08819	2.08514	0	GLUTAMATE20
0.0000	0.0000	2.0856	2.0424	0	GLUTAMATE21
0.0000	0.0000	2.073	2.0394	0	GLUTAMATE22,PYROGLUTAMATE35
0.0000	0.0000	2.0546	2.0358	0	GLUTAMATE23,PYROGLUTAMATE36,N-ACETYLORNITHINE22,NALPHA-ACETYLLYSINE16
0.0000	0.0000	2.05118	2.0425	0	GLUTAMATE24,PYROGLUTAMATE37,N-ACETYLORNITHINE23
0.0000	0.0000	2.0425	2.03409	0	NALPHA-ACETYLLYSINE17,PYROGLUTAMATE38,N-ACETYLORNITHINE24,2-HYDROXYISOVALERATE12
0.0000	0.0000	2.0625	2.0225	0	UNKNOWN236
0.0000	0.0000	2.0474	2.0246	0	UNKNOWN237
0.0000	0.0000	2.03409	2.02838	0	NALPHA-ACETYLLYSINE18,PYROGLUTAMATE39,GLUTAMATE25,2-HYDROXYISOVALERATE13
0.0000	0.0000	2.02798	2.02193	0	PYROGLUTAMATE40,2-HYDROXYISOVALERATE14,NALPHA-ACETYLLYSINE19
0.0000	0.0000	2.02193	2.01733	0	PYROGLUTAMATE41,2-HYDROXYISOVALERATE15,GLYCYLPROLINE35,3-METHYLGLUTARATE13,NALPHA-ACETYLLYSINE20
0.0000	0.0000	2.0426	2.0094	0	UNKNOWN238
0.0000	0.0000	2.0212	2.0096	0	2-HYDROXYISOVALERATE16,GLYCYLPROLINE36,3-METHYLGLUTARATE14,PYROGLUTAMATE42,N6-ACETYLLYSINE11
0.0000	0.0000	2.01413	2.01138	0	2-HYDROXYISOVALERATE17,GLYCYLPROLINE37,3-METHYLGLUTARATE15,PYROGLUTAMATE43,ISOLEUCINE04,N-ACETYLASPARTATE21
0.0000	0.0000	2.018	1.9968	0	N6-ACETYLLYSINE12,3-METHYLGLUTARATE16,N-ACETYLASPARTATE22,GLYCYLPROLINE38,PYROGLUTAMATE44
0.0000	0.0000	1.9991	1.99302	0	N6-ACETYLLYSINE13,3-METHYLGLUTARATE17,GLYCYLPROLINE39,ISOLEUCINE05
0.0000	0.0000	1.9969	1.9889	0	UNKNOWN239
0.0000	0.0000	1.9975	1.9811	0	3-METHYLGLUTARATE18,GLYCYLPROLINE40,ISOLEUCINE06,ORNITHINE12,2-HYDROXYISOVALERATE18
0.0000	0.0000	1.98671	1.98391	0	3-METHYLGLUTARATE19,GLYCYLPROLINE41,ISOLEUCINE07,ORNITHINE13
0.0000	0.0000	1.98391	1.98039	0	3-METHYLGLUTARATE20,GLYCYLPROLINE42,ISOLEUCINE08,ORNITHINE14
0.0000	0.0000	1.98039	1.97611	0	3-METHYLGLUTARATE21,GLYCYLPROLINE43,ISOLEUCINE09,ORNITHINE15
0.0000	0.0000	1.97611	1.97339	0	3-METHYLGLUTARATE22,GLYCYLPROLINE44,ISOLEUCINE10,ORNITHINE16
0.0000	0.0000	1.97339	1.97128	0	3-METHYLGLUTARATE23,GLYCYLPROLINE45,ISOLEUCINE11,ORNITHINE17
0.0000	0.0000	1.9835	1.9543	0	3-METHYLGLUTARATE24,GLYCYLPROLINE46,ISOLEUCINE12,ORNITHINE18
0.0000	0.0000	1.96648	1.95717	0	3-METHYLGLUTARATE25,GLYCYLPROLINE47,ISOLEUCINE13,ORNITHINE19
0.0000	0.0000	1.9612	1.9564	0	UNKNOWN240
0.0000	0.0000	1.9642	1.9422	0	ORNITHINE20,GLYCYLPROLINE48,LYSINE15
0.0000	0.0000	1.9555	1.9327	0	ORNITHINE21,GLYCYLPROLINE49,LYSINE16,ACETATE01
0.0000	0.0000	1.9481	1.9317	0	ORNITHINE22,GLYCYLPROLINE50,LYSINE17,ACETATE02
0.0000	0.0000	1.93759	1.93349	0	ORNITHINE23,GLYCYLPROLINE51,LYSINE18
0.0000	0.0000	1.9397	1.9309	0	UNKNOWN241
0.0000	0.0000	1.9357	1.9241	0	ORNITHINE24,LYSINE19,ACETATE03,2-AMINOADIPATE21,GLYCYLPROLINE52,N-ACETYLSEROTONIN32
0.0000	0.0000	1.9245	1.9173	0	ACETATE04,LYSINE20,2-AMINOADIPATE22,ORNITHINE20
0.0000	0.0000	1.9194	1.90983	0	N-ACETYLSEROTONIN33,LYSINE21,2-AMINOADIPATE23,ACETATE05,N6-ACETYLLYSINE14
0.0000	0.0000	1.9133	1.9009	0	N-ACETYLSEROTONIN34,LYSINE22,2-AMINOADIPATE24,ACETATE06,N6-ACETYLLYSINE15
0.0000	0.0000	1.9009	1.90535	0	LYSINE23,2-AMINOADIPATE25,N6-ACETYLLYSINE16
0.0000	0.0000	1.90535	1.9007	0	LYSINE24,2-AMINOADIPATE26,N6-ACETYLLYSINE17,N-ACETYLORNITHINE25
0.0000	0.0000	1.9007	1.89273	0	LYSINE25,2-AMINOADIPATE27,N6-ACETYLLYSINE18,N-ACETYLORNITHINE26
0.0000	0.0000	1.89273	1.88702	0	LYSINE26,2-AMINOADIPATE28,N6-ACETYLLYSINE19,N-ACETYLORNITHINE27
0.0000	0.0000	1.88416	1.87818	0	LYSINE27,2-AMINOADIPATE29,N6-ACETYLLYSINE20,N-ACETYLORNITHINE28
0.0000	0.0000	1.87818	1.87156	0	2-AMINOADIPATE30,N6-ACETYLLYSINE21,N-ACETYLORNITHINE29,GLUTARIC_ACID_MONOMETHYL_ESTER17
0.0000	0.0000	1.87156	1.86882	0	2-AMINOADIPATE31,N6-ACETYLLYSINE22,N-ACETYLORNITHINE30,GLUTARIC_ACID_MONOMETHYL_ESTER18,LYSINE28,GLYCYLPROLINE53
0.0000	0.0000	1.8691	1.8611	0	2-AMINOADIPATE32,N6-ACETYLLYSINE23,N-ACETYLORNITHINE31,GLYCYLPROLINE54
0.0000	0.0000	1.86474	1.86114	0	2-AMINOADIPATE33,N6-ACETYLLYSINE24,N-ACETYLORNITHINE32,GLYCYLPROLINE55,GLUTARIC_ACID_MONOMETHYL_ESTER19
0.0000	0.0000	1.86114	1.85714	0	2-AMINOADIPATE34,N6-ACETYLLYSINE25,N-ACETYLORNITHINE33,GLYCYLPROLINE56,GLUTARIC_ACID_MONOMETHYL_ESTER20,ORNITHINE21
0.0000	0.0000	1.8675	1.8455	0	UNKNOWN266
0.0000	0.0000	1.85714	1.85234	0	2-AMINOADIPATE35,N6-ACETYLLYSINE26,N-ACETYLORNITHINE34,GLYCYLPROLINE57,GLUTARIC_ACID_MONOMETHYL_ESTER21,ORNITHINE22

0.0000	0.0000	1.85714	1.85234	0	2-AMINOADIPATE35,N6-ACETYLLYSINE26,N-ACETYLORNITHINE34,GLYCYLPROLINE57,GLUTARIC_ACID_MONOMETHYL_ESTER21,ORNITHINE22
0.0000	0.0000	1.85234	1.84363	0	2-AMINOADIPATE36,N6-ACETYLLYSINE27,N-ACETYLORNITHINE35,GLYCYLPROLINE58,GLUTARIC_ACID_MONOMETHYL_ESTER22,ORNITHINE213
0.0000	0.0000	1.84363	1.83277	0	2-AMINOADIPATE37,N6-ACETYLLYSINE28,N-ACETYLORNITHINE36,GLUTARIC_ACID_MONOMETHYL_ESTER23,ORNITHINE24
0.0000	0.0000	1.83277	1.82803	0	2-AMINOADIPATE38,NALPHA-ACETYLLYSINE19,GLUTARIC_ACID_MONOMETHYL_ESTER24,ORNITHINE25
0.0000	0.0000	1.82803	1.82212	0	2-AMINOADIPATE39,NALPHA-ACETYLLYSINE20,GLUTARIC_ACID_MONOMETHYL_ESTER25,ORNITHINE26
0.0000	0.0000	1.825	1.8186	0	UNKNOWN267
0.0000	0.0000	1.82212	1.80714	0	2-AMINOADIPATE40,NALPHA-ACETYLLYSINE21,GLUTARIC_ACID_MONOMETHYL_ESTER26,ORNITHINE27
0.0000	0.0000	1.80714	1.81195	0	2-AMINOADIPATE41,NALPHA-ACETYLLYSINE22,ORNITHINE28
0.0000	0.0000	1.80932	1.80341	0	2-AMINOADIPATE42,NALPHA-ACETYLLYSINE23,ORNITHINE29
0.0000	0.0000	1.80341	1.80129	0	2-AMINOADIPATE43,NALPHA-ACETYLLYSINE24,ORNITHINE30
0.0000	0.0000	1.7987	1.79461	0	2-AMINOADIPATE44,NALPHA-ACETYLLYSINE25,ORNITHINE31
0.0000	0.0000	1.805	1.7798	0	UNKNOWN268
0.0000	0.0000	1.78915	1.78373	0	ORNITHINE32
0.0000	0.0000	1.78061	1.77744	0	ORNITHINE33
0.0000	0.0000	1.77744	1.7735	0	ORNITHINE34
0.0000	0.0000	1.7819	1.7655	0	UNKNOWN269
0.0000	0.0000	1.7735	1.76925	0	ORNITHINE35,N-ACETYLORNITHINE37
0.0000	0.0000	1.76925	1.7659	0	ORNITHINE36,N-ACETYLORNITHINE38
0.0000	0.0000	1.7681	1.7493	0	ORNITHINE37,N-ACETYLORNITHINE39,LYSINE29,BIOTIN39
0.0000	0.0000	1.7607	1.7411	0	ORNITHINE38,N-ACETYLORNITHINE40,LYSINE30,BIOTIN40
0.0000	0.0000	1.74871	1.74559	0	ORNITHINE39,N-ACETYLORNITHINE41,LYSINE31,BIOTIN41
0.0000	0.0000	1.74559	1.73834	0	ORNITHINE40,N-ACETYLORNITHINE42,LYSINE32,BIOTIN42,NALPHA-ACETYLLYSINE26
0.0000	0.0000	1.7413	1.7265	0	UNKNOWN270
0.0000	0.0000	1.73834	1.72614	0	ORNITHINE41,N-ACETYLORNITHINE43,LYSINE33,BIOTIN43,NALPHA-ACETYLLYSINE27
0.0000	0.0000	1.72614	1.72286	0	ORNITHINE42,N-ACETYLORNITHINE44,LYSINE34,BIOTIN44,NALPHA-ACETYLLYSINE28
0.0000	0.0000	1.72286	1.7154	0	ORNITHINE43,N-ACETYLORNITHINE45,LYSINE35,BIOTIN45,NALPHA-ACETYLLYSINE29
0.0000	0.0000	1.7351	1.7171	0	UNKNOWN271
0.0000	0.0000	1.7154	1.71189	0	N-ACETYLORNITHINE46,LYSINE36,BIOTIN46,NALPHA-ACETYLLYSINE30
0.0000	0.0000	1.7307	1.7047	0	N-ACETYLORNITHINE47,LYSINE37,BIOTIN47,NALPHA-ACETYLLYSINE31
0.0000	0.0000	1.7211	1.6991	0	N-ACETYLORNITHINE48,LYSINE38,NALPHA-ACETYLLYSINE32,2-HYDROXYVALERATE09
0.0000	0.0000	1.7096	1.7032	0	N-ACETYLORNITHINE49,LYSINE39,NALPHA-ACETYLLYSINE33,2-HYDROXYVALERATE10,2-AMINOADIPATE45
0.0000	0.0000	1.709	1.6918	0	N-ACETYLORNITHINE49,LYSINE40,NALPHA-ACETYLLYSINE34,2-HYDROXYVALERATE11,2-AMINOADIPATE46
0.0000	0.0000	1.6977	1.6905	0	N-ACETYLORNITHINE50,LYSINE41,NALPHA-ACETYLLYSINE35,2-HYDROXYVALERATE12,2-AMINOADIPATE47
0.0000	0.0000	1.7013	1.6777	0	N-ACETYLORNITHINE51,NALPHA-ACETYLLYSINE36,2-HYDROXYVALERATE13,2-AMINOADIPATE48
0.0000	0.0000	1.68804	1.68227	0	2-AMINOADIPATE48,NALPHA-ACETYLLYSINE37,2-HYDROXYVALERATE14
0.0000	0.0000	1.68227	1.67707	0	2-AMINOADIPATE49,NALPHA-ACETYLLYSINE38,2-HYDROXYVALERATE15
0.0000	0.0000	1.6829	1.6717	0	UNKNOWN272
0.0000	0.0000	1.67707	1.67118	0	2-AMINOADIPATE50,NALPHA-ACETYLLYSINE39,2-HYDROXYVALERATE16
0.0000	0.0000	1.6771	1.6655	0	UNKNOWN273
0.0000	0.0000	1.6709	1.66636	0	2-AMINOADIPATE51,NALPHA-ACETYLLYSINE40,2-HYDROXYVALERATE17
0.0000	0.0000	1.6709	1.6593	0	2-AMINOADIPATE52,NALPHA-ACETYLLYSINE41,2-HYDROXYVALERATE18
0.0000	0.0000	1.66193	1.6564	0	2-AMINOADIPATE53,NALPHA-ACETYLLYSINE42,2-HYDROXYVALERATE19
0.0000	0.0000	1.665	1.6478	0	UNKNOWN274
0.0000	0.0000	1.6618	1.6422	0	2-AMINOADIPATE54,NALPHA-ACETYLLYSINE43,2-HYDROXYVALERATE20
0.0000	0.0000	1.6511	1.6415	0	2-AMINOADIPATE55,2-HYDROXYVALERATE21,BIOTIN48
0.0000	0.0000	1.6051	1.5847	0	2-AMINOADIPATE56,2-HYDROXYVALERATE22,BIOTIN49
0.0000	0.0000	1.6011	1.5695	0	2-AMINOADIPATE57,2-HYDROXYVALERATE23,BIOTIN50
0.0000	0.0000	1.5893	1.5617	0	SUBERATE05,BIOTIN51,N6-ACETYLLYSINE29,AZELATE04,SEBACATE05,2-AMINOADIPATE58
0.0000	0.0000	1.575	1.553	0	SUBERATE06,BIOTIN52,N6-ACETYLLYSINE30,AZELATE05,SEBACATE06,2-AMINOADIPATE59
0.0000	0.0000	1.5597	1.5481	0	SUBERATE07,BIOTIN53,N6-ACETYLLYSINE31,AZELATE06,SEBACATE07,2-AMINOADIPATE60
0.0000	0.0000	1.5477	1.5381	0	SUBERATE08,BIOTIN54,N6-ACETYLLYSINE32,AZELATE07,SEBACATE08,2-AMINOADIPATE61
0.0000	0.0000	1.54036	1.53479	0	SUBERATE09,LYSINE42,N6-ACETYLLYSINE33,AZELATE08,SEBACATE09
0.0000	0.0000	1.5388	1.5264	0	SUBERATE10,LYSINE43,N6-ACETYLLYSINE34,AZELATE09,SEBACATE10
0.0000	0.0000	1.525	1.5102	0	LYSINE44,SUBERATE11,ALANINE03
0.0000	0.0000	1.5137	1.5005	0	LYSINE45,SUBERATE12,ALANINE04
0.0000	0.0000	1.5095	1.4899	0	LYSINE46,SUBERATE13,ALANINE05
0.0000	0.0000	1.5041	1.4861	0	LYSINE47,SUBERATE14,ALANINE06
0.0000	0.0000	1.4949	1.4845	0	ALANINE07,LYSINE48,ISOLEUCINE14
0.0000	0.0000	1.4854	1.4738	0	ALANINE08,LYSINE49,ISOLEUCINE15
0.0000	0.0000	1.4756	1.4624	0	ALANINE09,LYSINE50,ISOLEUCINE16
0.0000	0.0000	1.4785	1.4517	0	ALANINE10,LYSINE51,ISOLEUCINE17
0.0000	0.0000	1.4576	1.4112	0	NALPHA-ACETYLLYSINE44,LYSINE52,BIOTIN55,N6-ACETYLLYSINE35
0.0000	0.0000	1.4342	1.4194	0	NALPHA-ACETYLLYSINE45,LYSINE53,BIOTIN56,N6-ACETYLLYSINE36,2-HYDROXYVALERATE24
0.0000	0.0000	1.4222	1.4118	0	NALPHA-ACETYLLYSINE46,LYSINE54,BIOTIN57,N6-ACETYLLYSINE37,2-HYDROXYVALERATE25
0.0000	0.0000	1.4205	1.3969	0	NALPHA-ACETYLLYSINE47,LYSINE55,BIOTIN58,N6-ACETYLLYSINE38,2-HYDROXYVALERATE26
0.0000	0.0000	1.4146	1.3794	0	NALPHA-ACETYLLYSINE48,LYSINE56,BIOTIN59,N6-ACETYLLYSINE39,2-HYDROXYVALERATE27
0.0000	0.0000	1.395	1.377	0	N6-ACETYLLYSINE40,2-HYDROXYVALERATE28,3-HYDROXY-3-METHYLGLUTARATE19
0.0000	0.0000	1.3885	1.3477	0	N6-ACETYLLYSINE41,2-HYDROXYVALERATE29,LACTATE12,3-HYDROXY-3-METHYLGLUTARATE20
0.0000	0.0000	1.3717	1.3425	0	N6-ACETYLLYSINE42,2-HYDROXYVALERATE30,LACTATE13,3-HYDROXY-3-METHYLGLUTARATE21
0.0000	0.0000	1.3631	1.3295	0	N6-ACETYLLYSINE43,2-HYDROXYVALERATE31,LACTATE14,3-HYDROXY-3-METHYLGLUTARATE22
0.0000	0.0000	1.3409	1.3329	0	LACTATE15,3-HYDROXY-3-METHYLGLUTARATE23,THREONINE13
0.0000	0.0000	1.3308	1.3236	0	LACTATE16,3-HYDROXY-3-METHYLGLUTARATE24,THREONINE14
0.0000	0.0000	1.3128	1.3064	0	SUBERATE15,AZELATE10,SEBACATE11,3-HYDROXY-3-METHYLGLUTARATE25
0.0000	0.0000	1.3047	1.2951	0	SUBERATE16,AZELATE11,SEBACATE12,3-HYDROXY-3-METHYLGLUTARATE26
0.0000	0.0000	1.2986	1.2798	0	SUBERATE17,AZELATE12,SEBACATE13,3-HYDROXY-3-METHYLGLUTARATE27
0.0000	0.0000	1.2889	1.2817	0	ISOLEUCINE18,AZELATE13,SEBACATE14,3-HYDROXY-3-METHYLGLUTARATE28,LACTATE17
0.0000	0.0000	1.2812	1.27	0	3-HYDROXYISOVALERATE01,SEBACATE15,ISOLEUCINE19
0.0000	0.0000	1.2733	1.2569	0	3-HYDROXYISOVALERATE02,SEBACATE16,ISOLEUCINE20
0.0000	0.0000	1.2654	1.2542	0	3-HYDROXYISOVALERATE03,SEBACATE17,ISOLEUCINE21
0.0000	0.0000	1.2581	1.2501	0	FUCOSE22,ISOLEUCINE22
0.0000	0.0000	1.2526	1.2394	0	FUCOSE23,ISOLEUCINE23
0.0000	0.0000	1.2509	1.2361	0	FUCOSE24,ISOLEUCINE24
0.0000	0.0000	1.2402	1.2042	0	FUCOSE25,ISOLEUCINE25
0.0000	0.0000	1.2233	1.2129	0	FUCOSE26,ISOLEUCINE26

```
0.0000   0.0000  1.67707    1.67118        0 2-AMINOADIPATE50,NALPHA-ACETYLLYSINE39,2-HYDROXYVALERATE16
0.0000   0.0000  1.6771     1.6655         0 UNKNOWN273
0.0000   0.0000  1.6709     1.66636        0 2-AMINOADIPATE51,NALPHA-ACETYLLYSINE40,2-HYDROXYVALERATE17
0.0000   0.0000  1.6709     1.6593         0 2-AMINOADIPATE52,NALPHA-ACETYLLYSINE41,2-HYDROXYVALERATE18
0.0000   0.0000  1.66193    1.6564         0 2-AMINOADIPATE53,NALPHA-ACETYLLYSINE42,2-HYDROXYVALERATE19
0.0000   0.0000  1.665      1.6478         0 UNKNOWN274
0.0000   0.0000  1.6618     1.6422         0 2-AMINOADIPATE54,NALPHA-ACETYLLYSINE43,2-HYDROXYVALERATE20
0.0000   0.0000  1.6511     1.6415         0 2-AMINOADIPATE55,2-HYDROXYVALERATE21,BIOTIN48
0.0000   0.0000  1.6051     1.5847         0 2-AMINOADIPATE56,2-HYDROXYVALERATE22,BIOTIN49
0.0000   0.0000  1.6011     1.5695         0 2-AMINOADIPATE57,2-HYDROXYVALERATE23,BIOTIN50
0.0000   0.0000  1.5893     1.5617         0 SUBERATE05,BIOTIN51,N6-ACETYLLYSINE29,AZELATE04,SEBACATE05,2-AMINOADIPATE58
0.0000   0.0000  1.575      1.553          0 SUBERATE06,BIOTIN52,N6-ACETYLLYSINE30,AZELATE05,SEBACATE06,2-AMINOADIPATE59
0.0000   0.0000  1.5597     1.5481         0 SUBERATE07,BIOTIN53,N6-ACETYLLYSINE31,AZELATE06,SEBACATE07,2-AMINOADIPATE60
0.0000   0.0000  1.5477     1.5381         0 SUBERATE08,BIOTIN54,N6-ACETYLLYSINE32,AZELATE07,SEBACATE08,2-AMINOADIPATE61
0.0000   0.0000  1.54036    1.53479        0 SUBERATE09,LYSINE42,N6-ACETYLLYSINE33,AZELATE08,SEBACATE09
0.0000   0.0000  1.5388     1.5264         0 SUBERATE10,LYSINE43,N6-ACETYLLYSINE34,AZELATE09,SEBACATE10
0.0000   0.0000  1.525      1.5102         0 LYSINE44,SUBERATE11,ALANINE03
0.0000   0.0000  1.5137     1.5005         0 LYSINE45,SUBERATE12,ALANINE04
0.0000   0.0000  1.5095     1.4899         0 LYSINE46,SUBERATE13,ALANINE05
0.0000   0.0000  1.5041     1.4861         0 LYSINE47,SUBERATE14,ALANINE06
0.0000   0.0000  1.4949     1.4845         0 ALANINE07,LYSINE48,ISOLEUCINE14
0.0000   0.0000  1.4854     1.4738         0 ALANINE08,LYSINE49,ISOLEUCINE15
0.0000   0.0000  1.4756     1.4624         0 ALANINE09,LYSINE50,ISOLEUCINE16
0.0000   0.0000  1.4785     1.4517         0 ALANINE10,LYSINE51,ISOLEUCINE17
0.0000   0.0000  1.4576     1.4112         0 NALPHA-ACETYLLYSINE44,LYSINE52,BIOTIN55,N6-ACETYLLYSINE35
0.0000   0.0000  1.4342     1.4194         0 NALPHA-ACETYLLYSINE45,LYSINE53,BIOTIN56,N6-ACETYLLYSINE36,2-HYDROXYVALERATE24
0.0000   0.0000  1.4222     1.4118         0 NALPHA-ACETYLLYSINE46,LYSINE54,BIOTIN57,N6-ACETYLLYSINE37,2-HYDROXYVALERATE25
0.0000   0.0000  1.4205     1.3969         0 NALPHA-ACETYLLYSINE47,LYSINE55,BIOTIN58,N6-ACETYLLYSINE38,2-HYDROXYVALERATE26
0.0000   0.0000  1.4146     1.3794         0 NALPHA-ACETYLLYSINE48,LYSINE56,BIOTIN59,N6-ACETYLLYSINE39,2-HYDROXYVALERATE27
0.0000   0.0000  1.395      1.377          0 N6-ACETYLLYSINE40,2-HYDROXYVALERATE28,3-HYDROXY-3-METHYLGLUTARATE19
0.0000   0.0000  1.3885     1.3477         0 N6-ACETYLLYSINE41,2-HYDROXYVALERATE29,LACTATE12,3-HYDROXY-3-METHYLGLUTARATE20
0.0000   0.0000  1.3717     1.3425         0 N6-ACETYLLYSINE42,2-HYDROXYVALERATE30,LACTATE13,3-HYDROXY-3-METHYLGLUTARATE21
0.0000   0.0000  1.3631     1.3295         0 N6-ACETYLLYSINE43,2-HYDROXYVALERATE31,LACTATE14,3-HYDROXY-3-METHYLGLUTARATE22
0.0000   0.0000  1.3409     1.3329         0 LACTATE15,3-HYDROXY-3-METHYLGLUTARATE23,THREONINE13
0.0000   0.0000  1.3308     1.3236         0 LACTATE16,3-HYDROXY-3-METHYLGLUTARATE24,THREONINE14
0.0000   0.0000  1.3128     1.3064         0 SUBERATE15,AZELATE10,SEBACATE11,3-HYDROXY-3-METHYLGLUTARATE25
0.0000   0.0000  1.3047     1.2951         0 SUBERATE16,AZELATE11,SEBACATE12,3-HYDROXY-3-METHYLGLUTARATE26
0.0000   0.0000  1.2986     1.2798         0 SUBERATE17,AZELATE12,SEBACATE13,3-HYDROXY-3-METHYLGLUTARATE27
0.0000   0.0000  1.2889     1.2817         0 ISOLEUCINE18,AZELATE13,SEBACATE14,3-HYDROXY-3-METHYLGLUTARATE28,LACTATE17
0.0000   0.0000  1.2812     1.27           0 3-HYDROXYISOVALERATE01,SEBACATE15,ISOLEUCINE19
0.0000   0.0000  1.2733     1.2569         0 3-HYDROXYISOVALERATE02,SEBACATE16,ISOLEUCINE20
0.0000   0.0000  1.2654     1.2542         0 3-HYDROXYISOVALERATE03,SEBACATE17,ISOLEUCINE21
0.0000   0.0000  1.2581     1.2501         0 FUCOSE22,ISOLEUCINE22
0.0000   0.0000  1.2526     1.2394         0 FUCOSE23,ISOLEUCINE23
0.0000   0.0000  1.2509     1.2361         0 FUCOSE24,ISOLEUCINE24
0.0000   0.0000  1.2402     1.2042         0 FUCOSE25,ISOLEUCINE25
0.0000   0.0000  1.2233     1.2129         0 FUCOSE26,ISOLEUCINE26
0.0000   0.0000  1.2312     1.1952         0 FUCOSE27,ISOLEUCINE27
0.0000   0.0000  1.2134     1.1946         0 FUCOSE28,ISOLEUCINE28
0.0000   0.0000  1.1982     1.1958         0 ETHANOL01,THYMOL16
0.0000   0.0000  1.1903     1.1839         0 ETHANOL02,THYMOL17
0.0000   0.0000  1.1808     1.1736         0 ETHANOL03
0.0000   0.0000  1.1428     1.1388         0 ETHANOL04
0.0000   0.0000  1.1109     1.1109         0 ETHANOL05
0.0000   0.0000  1.1056     1.1056         0 ETHANOL06
0.0000   0.0000  1.097      1.0946         0 ETHANOL07
0.0000   0.0000  1.0859     1.0859         0 ETHANOL08
0.0000   0.0000  1.0705     1.0705         0 VALINE11,EHTANOL09,ISOBUTYRATE
0.0000   0.0000  1.0607     1.0583         0 VALINE12,EHTANOL09,ISOBUTYRATE
0.0000   0.0000  1.0556     1.0484         0 VALINE13,ISOBUTYRATE02
0.0000   0.0000  1.0453     1.0381         0 VALINE14,ISOBUTYRATE03
0.0000   0.0000  1.0241     1.0161         0 ISOLEUCINE39
0.0000   0.0000  1.0142     1.0062         0 ISOLEUCINE40
0.0000   0.0000  1.0052     0.9964         0 VALINE15
0.0000   0.0000  0.9959     0.9855         0 VALINE16
0.0000   0.0000  0.9852     0.9664         0 2-HYDROXYISOVALERATE32
0.0000   0.0000  0.9729     0.9573         0 2-HYDROXYISOVALERATE33
0.0000   0.0000  0.9752     0.936          0 2-HYDROXYISOVALERATE34,ISOLEUCINE41
0.0000   0.0000  0.973      0.915          0 2-HYDROXYISOVALERATE35,ISOLEUCINE42
0.0000   0.0000  0.9499     0.9163         0 2-HYDROXYISOVALERATE36,ISOLEUCINE43,3-METHYLGLUTARATE26
0.0000   0.0000  0.94014    0.93577        0 3-METHYLGLUTARATE27,2-HYDROXYISOVALERATE37,ISOLEUCINE44
0.0000   0.0000  0.9423     0.8983         0 3-METHYLGLUTARATE28,2-HYDROXYISOVALERATE38
0.0000   0.0000  0.9247     0.8939         0 3-METHYLGLUTARATE29,2-HYDROXYISOVALERATE39
0.0000   0.0000  0.9168     0.8808         0 3-METHYLGLUTARATE30,2-HYDROXYISOVALERATE40
0.0000   0.0000  0.9094     0.8694         0 3-METHYLGLUTARATE31,2-HYDROXYISOVALERATE41
0.0000   0.0000  0.9085     0.8505         0 3-METHYLGLUTARATE32,2-HYDROXYISOVALERATE42
0.0000   0.0000  0.8491     0.8401         0 2-HYDROXYISOVALERATE43
0.0000   0.0000  0.8401     0.8315         0 2-HYDROXYISOVALERATE44
0.0000   0.0000  0.1695     0.1663         0 UNKNOWN275
0.0000   0.0000  0.0842     0.0818         0 UNKNOWN276
0.0000   0.0000  0.0086     0.0006         0 UNKNOWN277
0.0000   0.0000  0.0032    -0.0032         0 UNKNOWN278
0.0000   0.0000 -0.0006    -0.0086         0 UNKNOWN279
```

Supplementary data 2: The synovial fluid pattern file

```
$##090816
PATTERN      = human_Synovial_Fluid_150616
GROUP        =
DESCRIPTION  = hSF at 310K for hSF_OA_CPMG
AUTHOR       = James Susama
DIM          = 2
ORIGIN       = 1
ITEMS        = 795
0.0000   0.0000  8.48450 8.48036          0 FORMATE_8
0.0000   0.0000  8.46897 8.46897          0 UNKNOWN_9
0.0000   0.0000  8.32117 8.30737          0 IMIDAZOLE_10
0.0000   0.0000  8.29747 8.29427          0 UNKNOWN_11
0.0000   0.0000  8.26897 8.26897          0 UNKNOWN_12
0.0000   0.0000  8.21647 8.21167          0 UNKNOWN_13
0.0000   0.0000  8.19897 8.19897          0 UNKNOWN_14
0.0000   0.0000  8.07897 8.06897          0 UNKNOWN_15
0.0000   0.0000  8.06337 8.05847          0 3-METHYLXANTHINE_16
0.0000   0.0000  8.04437 8.04037          0 THEOPHYLLINE_17
0.0000   0.0000  8.01157 7.99637          0 ANSERINE_18
0.0000   0.0000  7.99637 7.98917          0 HISTAMINE_N-ISOVALEROYLGLYCINE_19
0.0000   0.0000  7.93627 7.93627          0 UNKNOWN_20
0.0000   0.0000  7.93897 7.92897          0 UNKNOWN_21
0.0000   0.0000  7.91397 7.92397          0 CAFFEINE_22
0.0000   0.0000  7.88757 7.88397          0 UNKNOWN_23
0.0000   0.0000  7.88507 7.88147          0 UNKNOWN_24
0.0000   0.0000  7.87897 7.87897          0 UNKNOWN_25
0.0000   0.0000  7.88027 7.87707          0 KYNURENINE_26
0.0000   0.0000  7.87697 7.87457          0 KYNURENINE_27
0.0000   0.0000  7.88127 7.87447          0 UNKNOWN_28
0.0000   0.0000  7.88187 7.87327          0 4-PYROXIDATE_29
0.0000   0.0000  7.87417 7.87017          0 UNKNOWN_30
0.0000   0.0000  7.86697 7.86527          0 KYNURENINE_31
0.0000   0.0000  7.86667 7.86027          0 KYNURENINE_32
0.0000   0.0000  7.86327 7.85967          0 UNKNOWN_33
0.0000   0.0000  7.85897 7.85897          0 UNKNOWN_34
0.0000   0.0000  7.84627 7.81838          0 UNKNOWN_35*
0.0000   0.0000  7.81597 7.81027          0 PI-METHYLHISTIDINE_39
0.0000   0.0000  7.80297 7.79737          0 UNKNOWN_40
0.0000   0.0000  7.81897 7.78897          0 UNKNOWN_41
0.0000   0.0000  7.78017 7.76997          0 INDOLE-3-LACTATE_42
0.0000   0.0000  7.76897 7.76897          0 UNKNOWN_43
0.0000   0.0000  7.76997 7.76347          0 INDOLE-3-LACTATE_44
0.0000   0.0000  7.77417 7.77417          0 UNKNOWN_45
0.0000   0.0000  7.77107 7.76907          0 UNKNOWN_46
0.0000   0.0000  7.73707 7.73347          0 UNKNOWN_47
0.0000   0.0000  7.72997 7.71997          0 UNKNOWN_48
0.0000   0.0000  7.74897 7.71897          0 UNKNOWN_49
0.0000   0.0000  7.69357 7.69147          0 PYRIDOXINE_50
0.0000   0.0000  7.67117 7.59277          0 GLUTAMINE_51
0.0000   0.0000  7.60497 7.60177          0 UNKNOWN_52
0.0000   0.0000  7.57897 7.57897          0 UNKNOWN_53
0.0000   0.0000  7.57327 7.56807          0 VANILLATE_54
0.0000   0.0000  7.56177 7.55497          0 UNKNOWN_55
0.0000   0.0000  7.54607 7.53557          0 INDOLE-3-LACTATE_56
0.0000   0.0000  7.53557 7.52317          0 INDOLE-3-LACTATE_57
0.0000   0.0000  7.54507 7.54307          0 UNKNOWN_58
0.0000   0.0000  7.52257 7.52057          0 UNKNOWN_59
0.0000   0.0000  7.46792 7.44650          0 PHENYLALANINE_KYNURENINE_61*
0.0000   0.0000  7.45704 7.44650          0 PHENYLALANINE_KYNURENINE_62*
0.0000   0.0000  7.44538 7.43475          0 PHENYLALANINE_KYNURENINE_63*
0.0000   0.0000  7.45147 7.44667          0 UNKNOWN_64
0.0000   0.0000  7.44947 7.44947          0 UNKNOWN_65
0.0000   0.0000  7.43207 7.42877          0 5-METHOXYSALICYLATE_66
0.0000   0.0000  7.42877 7.41897          0 5-METHOXYSALICYLATE_67
0.0000   0.0000  7.42387 7.40777          0 3-PHENYLLACTATE_68
0.0000   0.0000  7.40777 7.39497          0 3-PHENYLLACTATE_69
0.0000   0.0000  7.39497 7.38307          0 3-PHENYLLACTATE_70
0.0000   0.0000  7.41237 7.40677          0 PHENYLALANINE_3-PHENYLPROPIONATE_2-PHENYLPROPIONATE_71
0.0000   0.0000  7.41077 7.40597          0 PHENYLALANINE_3-PHENYLPROPIONATE_2-PHENYLPROPIONATE_72
0.0000   0.0000  7.40657 7.39177          0 PHENYLALANINE_3-PHENYLPROPIONATE_2-PHENYLPROPIONATE_73
0.0000   0.0000  7.40037 7.39237          0 PHENYLALANINE_3-PHENYLPROPIONATE_2-PHENYLPROPIONATE_74
0.0000   0.0000  7.39397 7.38437          0 PHENYLALANINE_3-PHENYLPROPIONATE_2-PHENYLPROPIONATE_3,5-DIBROMOTYROSINE_75
0.0000   0.0000  7.39317 7.37957          0 PHENYLALANINE_76
0.0000   0.0000  7.36677 7.35637          0 PHENYLALANINE_IMIDAZOLE_77
0.0000   0.0000  7.36217 7.35537          0 PHENYLALANINE_IMIDAZOLE_78
0.0000   0.0000  7.35857 7.35497          0 PHENYLALANINE_79
0.0000   0.0000  7.35367 7.34887          0 PHENYLALANINE_80
0.0000   0.0000  7.37897 7.33897          0 UNKNOWN_81
0.0000   0.0000  7.35087 7.32397          0 3-PHENYLLACTATE_82
0.0000   0.0000  7.32397 7.31397          0 3-PHENYLLACTATE_83
0.0000   0.0000  7.34087 7.33427          0 3-HYDROXYMANDELATE_84
0.0000   0.0000  7.32877 7.32207          0 3-HYDROXYMANDELATE_85
0.0000   0.0000  7.31697 7.31147          0 3-HYDROXYMANDELATE_86
0.0000   0.0000  7.31027 7.30617          0 SYRINGATE_87
```

```
0.0000   0.0000  7.31027 7.30617          0 SYRINGATE_87
0.0000   0.0000  7.30617 7.29747          0 3-PHENYLPROPIONATE_88
0.0000   0.0000  7.29747 7.28997          0 3-PHENYLPROPIONATE_89
0.0000   0.0000  7.29547 7.29107          0 INDOLE-3-LACTATE_90
0.0000   0.0000  7.18447 7.28107          0 INDOLE-3-LACTATE_91
0.0000   0.0000  7.28997 7.28117          0 3-PHENYLPROPIONATE_92
0.0000   0.0000  7.29437 7.29117          0 3-PHENYLPROPIONATE_ACETAMINOPHEN_93
0.0000   0.0000  7.28187 7.27347          0 ACETAMINOPHEN_94
0.0000   0.0000  7.27667 7.27107          0 ACETAMINOPHEN_95
0.0000   0.0000  7.27477 7.26677          0 ACETAMINOPHEN_96
0.0000   0.0000  7.26967 7.26407          0 UNKNOWN_97
0.0000   0.0000  7.26687 7.26177          0 ACETAMINOPHEN_98
0.0000   0.0000  7.25707 7.25067          0 UNKNOWN_99
0.0000   0.0000  7.25167 7.24607          0 THYMOL_TYROSINE_100
0.0000   0.0000  7.23917 7.23977          0 THYMOL_TYROSINE_101
0.0000   0.0000  7.23207 7.22947          0 TYROSINE_5-HYDROXYINDOLE-3-ACETATE_102
0.0000   0.0000  7.23167 7.22167          0 TYROSINE_103
0.0000   0.0000  7.22707 7.22027          0 TYROSINE_104
0.0000   0.0000  7.22897 7.21897          0 UNKNOWN_105
0.0000   0.0000  7.22077 7.21437          0 TYROSINE_106
0.0000   0.0000  7.21937 7.20977          0 TYROSINE_107
0.0000   0.0000  7.21147 7.20837          0 TYROSINE_108
0.0000   0.0000  7.20727 7.20167          0 UNKNOWN_109
0.0000   0.0000  7.18547 7.17547          0 P-CRESOL_110
0.0000   0.0000  7.17967 7.17647          0 P-CRESOL_111
0.0000   0.0000  7.17997 7.17437          0 P-CRESOL_112
0.0000   0.0000  7.16897 7.16897          0 UNKNOWN_113
0.0000   0.0000  7.17437 7.16637          0 P-CRESOL_114
0.0000   0.0000  7.17267 7.16267          0 P-CRESOL_115
0.0000   0.0000  7.16207 7.15687          0 UNKNOWN_116
0.0000   0.0000  7.15737 7.15457          0 UNKNOWN_117
0.0000   0.0000  7.14347 7.14027          0 UNKNOWN_118
0.0000   0.0000  7.12897 7.12897          0 UNKNOWN_119
0.0000   0.0000  7.11897 7.11897          0 UNKNOWN_120
0.0000   0.0000  7.12317 7.11837          0 UNKNOWN_121
0.0000   0.0000  7.11947 7.11677          0 ISOEUGENOL_ANSERINE_122
0.0000   0.0000  7.11677 7.11347          0 ISOEUGENOL_ANSERINE_123
0.0000   0.0000  7.11347 7.10867          0 ANSERINE_5-METHOXYSALICYLATE_124
0.0000   0.0000  7.10867 7.10697          0 ANSERINE_5-METHOXYSALICYLATE_125
0.0000   0.0000  7.10152 7.08340          0 UNKNOWN_126*
0.0000   0.0000  7.07707 7.07187          0 UNKNOWN_129
0.0000   0.0000  7.07377 7.06797          0 4-HYDROXY-3-METHOXYMANDELATE_130
0.0000   0.0000  7.06827 7.06507          0 UNKNOWN_131
0.0000   0.0000  7.05717 7.05357          0 5-HYDROXYINDOLE-3-ACETATE_PI-METHYLHISTIDINE_133
0.0000   0.0000  7.05357 7.04937          0 5-HYDROXYINDOLE-3-ACETATE_PI-METHYLHISTIDINE_134
0.0000   0.0000  7.04897 7.03897          0 UNKNOWN_135
0.0000   0.0000  7.04547 7.03747          0 UNKNOWN_136
0.0000   0.0000  7.02707 7.02027          0 3-HYDROXYMANDELATE_137
0.0000   0.0000  7.02357 7.01997          0 3-HYDROXYMANDELATE_138
0.0000   0.0000  7.01397 7.01097          0 3-HYDROXYMANDELATE_139
0.0000   0.0000  7.01897 7.00897          0 UNKNOWN_1401
0.0000   0.0000  6.99997 6.99317          0 UNKNOWN_142
0.0000   0.0000  6.97997 6.97767          0 VANILLATE_HEMOVANILLATE_GLUTAMINE_143
0.0000   0.0000  6.97907 6.97027          0 HEMOVANILLATE_GLUTAMINE_144
0.0000   0.0000  6.95697 6.95297          0 5-METHOXYSALICYLATE_GLUTAMINE_ISOEUGENOL_4-HYDROXY-3-METHOXYMANDELATE_145
0.0000   0.0000  6.95417 6.95187          0 3-HYDROXYMANDELATE_146
0.0000   0.0000  6.95177 6.94857          0 3-HYDROXYMANDELATE_147
0.0000   0.0000  6.94997 6.94437          0 3-HYDROXYMANDELATE_148
0.0000   0.0000  6.94327 6.94077          0 5-METHOXYSALICYLATE_GLUTAMINE_ISOEUGENOL_4-HYDROXY-3-METHOXYMANDELATE_TYROSINE_ACETAMINOPHEN_149
0.0000   0.0000  6.93847 6.93647          0 GLUTAMINE_4-HYDROXY-3-METHOXYMANDELATE_TYROSINE_ACETAMINOPHEN_150
0.0000   0.0000  6.93787 6.92907          0 TYROSINE_ACETAMINOPHEN_GLUTAMINE_151
0.0000   0.0000  6.93467 6.92667          0 TYROSINE_ACETAMINOPHEN_GLUTAMINE_152
0.0000   0.0000  6.93047 6.92527          0 TYROSINE_ACETAMINOPHEN_GLUTAMINE_153
0.0000   0.0000  6.92837 6.92517          0 TYROSINE_ACETAMINOPHEN_GLUTAMINE_154
0.0000   0.0000  6.92817 6.92017          0 TYROSINE_ACETAMINOPHEN_GLUTAMINE_155
0.0000   0.0000  6.92627 6.91627          0 TYROSINE_ACETAMINOPHEN_GLUTAMINE_156
0.0000   0.0000  6.91737 6.91697          0 TYROSINE_ACETAMINOPHEN_GLUTAMINE_157
0.0000   0.0000  6.92897 6.88897          0 UNKNOWN_158
0.0000   0.0000  6.85177 6.84857          0 UNKNOWN_159
0.0000   0.0000  6.84707 6.84327          0 KYNURENINE_160
0.0000   0.0000  6.87897 6.83897          0 UNKNOWN_161
0.0000   0.0000  6.83597 6.83217          0 KYNURENINE_162
0.0000   0.0000  6.82487 6.82107          0 KYNURENINE_163
0.0000   0.0000  6.81407 6.81127          0 UNKNOWN_164
0.0000   0.0000  6.79897 6.79897          0 UNKNOWN_165
0.0000   0.0000  6.77037 6.76637          0 UNKNOWN_166
0.0000   0.0000  6.75357 6.75037          0 UNKNOWN_167
0.0000   0.0000  6.69897 6.69897          0 UNKNOWN_168
0.0000   0.0000  6.66227 6.65747          0 UNKNOWN_169
0.0000   0.0000  6.58547 6.58267          0 UNKNOWN_170
0.0000   0.0000  6.54507 6.54227          0 UNKNOWN_171
0.0000   0.0000  6.43607 6.43247          0 UNKNOWN_172
0.0000   0.0000  6.09927 6.09567          0 UNKNOWN_173
0.0000   0.0000  6.08467 6.08187          0 UNKNOWN_174
```

```
0.0000   0.0000  6.08467 6.08187          0 UNKNOWN_174
0.0000   0.0000  5.93927 5.93567          0 UNKNOWN_175
0.0000   0.0000  5.93527 5.92727          0 UNKNOWN_176
0.0000   0.0000  5.82617 5.81937          0 UNKNOWN_177
0.0000   0.0000  5.79067 5.78107          0 UNKNOWN_178
0.0000   0.0000  5.78147 5.77667          0 UNKNOWN_179
0.0000   0.0000  5.77397 5.76677          0 UNKNOWN_180
0.0000   0.0000  5.75277 5.84697          0 CIS-ACONITATE_181
0.0000   0.0000  5.49127 5.48727          0 UNKNOWN_182
0.0000   0.0000  5.48587 5.48427          0 UNKNOWN_183
0.0000   0.0000  5.48257 5.47977          0 UNKNOWN_184
0.0000   0.0000  5.42667 5.42117          0 SUCROSE_185
0.0000   0.0000  5.42117 5.42107          0 SUCROSE_186
0.0000   0.0000  5.42107 5.40527          0 RIBOSE_187
0.0000   0.0000  5.40367 5.40007          0 UNKNOWN_188
0.0000   0.0000  5.38837 5.37997          0 UNKNOWN_189
0.0000   0.0000  5.38097 5.37737          0 UNKNOWN_190
0.0000   0.0000  5.38157 5.37477          0 UNKNOWN_191
0.0000   0.0000  5.39897 5.36897          0 UNKNOWN_192
0.0000   0.0000  5.36267 5.35947          0 UNKNOWN_193
0.0000   0.0000  5.34897 5.33897          0 UNKNOWN_194
0.0000   0.0000  5.34037 5.33477          0 UNKNOWN_195
0.0000   0.0000  5.33097 5.32217          0 UNKNOWN_196
0.0000   0.0000  5.31287 5.30727          0 UNKNOWN_197
0.0000   0.0000  5.30507 5.29667          0 UNKNOWN_198
0.0000   0.0000  5.29997 5.29677          0 FUCOSE_199
0.0000   0.0000  5.29587 5.29337          0 GALACTOSE_200
0.0000   0.0000  5.29337 5.29177          0 GALACTOSE_201
0.0000   0.0000  5.29177 5.28457          0 UNKNOWN_202
0.0000   0.0000  5.27897 5.27897          0 UNKNOWN_203
0.0000   0.0000  5.26937 5.26137          0 GLUCOSE_204
0.0000   0.0000  5.26447 5.26087          0 GLUCOSE-6-PHOSPHATE_205
0.0000   0.0000  5.26397 5.25597          0 GLUCOSE_206
0.0000   0.0000  5.25597 5.25447          0 GLUCOSE-6-PHOSPHATE_207
0.0000   0.0000  5.22697 5.22237          0 FUCOSE_MANNOSE_GLUCOSE_208
0.0000   0.0000  5.22237 5.21677          0 FUCOSE_MANNOSE_GLUCOSE_209
0.0000   0.0000  5.21807 5.20847          0 MANNOSE_210
0.0000   0.0000  5.21627 5.20467          0 MANNOSE_211
0.0000   0.0000  5.19957 5.19557          0 UNKNOWN_212
0.0000   0.0000  5.19327 5.18927          0 UNKNOWN_213
0.0000   0.0000  5.18977 5.18097          0 UNKNOWN_214
0.0000   0.0000  5.18687 5.17967          0 UNKNOWN_215
0.0000   0.0000  5.17417 5.16897          0 UNKNOWN_216
0.0000   0.0000  5.15587 5.15027          0 UNKNOWN_217
0.0000   0.0000  5.14007 5.13327          0 UNKNOWN_218
0.0000   0.0000  5.13137 5.11777          0 UNKNOWN_219
0.0000   0.0000  5.11767 5.11207          0 UNKNOWN_220
0.0000   0.0000  5.11787 5.11067          0 UNKNOWN_221
0.0000   0.0000  5.10867 5.10387          0 UNKNOWN_222
0.0000   0.0000  5.10557 5.10077          0 UNKNOWN_223
0.0000   0.0000  4.31127 4.28797          0 3-PHENYLLACTATE_288
0.0000   0.0000  4.31027 4.29757          0 MALATE_THREONINE_GLYCYLPROLINE_289
0.0000   0.0000  4.29617 4.29487          0 MALATE_THREONINE_GLYCYLPROLINE_LACTULOSE_291
0.0000   0.0000  4.29807 4.28847          0 THREONINE_GALACTONATE_292
0.0000   0.0000  4.29177 4.28987          0 THREONINE_GALACTONATE_293
0.0000   0.0000  4.28977 4.28777          0 THREONINE_GALACTONATE_294
0.0000   0.0000  4.28677 4.28477          0 THREONINE_LACTULOSE_295
0.0000   0.0000  4.28877 4.27877          0 THREONINE_296
0.0000   0.0000  4.28217 4.27987          0 GALACTARATE_THREONINE_297
0.0000   0.0000  4.28077 4.27277          0 THREONINE_298
0.0000   0.0000  4.27857 4.27017          0 THREONINE_299
0.0000   0.0000  4.27157 4.26317          0 THREONINE_300
0.0000   0.0000  4.27087 4.25927          0 THREONINE_301
0.0000   0.0000  4.26297 4.25297          0 THREONINE_302
0.0000   0.0000  4.24737 4.24437          0 UNKNOWN_303
0.0000   0.0000  4.24437 4.24157          0 UNKNOWN_304
0.0000   0.0000  4.24137 4.23977          0 LACTULOSE_RIBOSE_305
0.0000   0.0000  4.23977 4.23747          0 LACTULOSE_RIBOSE_306
0.0000   0.0000  4.23747 4.23497          0 LACTULOSE_RIBOSE_307
0.0000   0.0000  4.23497 4.23357          0 LACTULOSE_SUCROSE_308
0.0000   0.0000  4.23687 4.22887          0 UNKNOWN_309
0.0000   0.0000  4.22687 4.21967          0 UNKNOWN_310
0.0000   0.0000  4.21407 4.20687          0 UNKNOWN_311
0.0000   0.0000  4.20077 4.19517          0 UNKNOWN_312
0.0000   0.0000  4.18767 4.18657          0 KYNURENINE_313
0.0000   0.0000  4.19237 4.18517          0 UNKNOWN_314
0.0000   0.0000  4.18497 4.18147          0 3-HYDROXYBUTYRATE_GLUCARATE_KYNURENINE_315
0.0000   0.0000  4.18287 4.17647          0 3-HYDROXYBUTYRATE_GLUCARATE_316
0.0000   0.0000  4.17557 4.17457          0 3-HYDROXYBUTYRATE_GLUCARATE_KYNURENINE_317
0.0000   0.0000  4.17457 4.17257          0 LACTULOSE_3-HYDROXYBUTYRATE_318
0.0000   0.0000  4.17257 4.17137          0 LACTULOSE_3-HYDROXYBUTYRATE_GLUCARATE_319
0.0000   0.0000  4.18237 4.17277          0 GLUCARATE_LACTULOSE_320
0.0000   0.0000  4.17367 4.16727          0 LACTULOSE_3-HYDROXYBUTYRATE_LACTATE_321
0.0000   0.0000  4.17017 4.16617          0 LACTULOSE_3-HYDROXYBUTYRATE_LACTATE_322
```

```
0.0000   0.0000  4.17017 4.16617          0 LACTULOSE_3-HYDROXYBUTYRATE_LACTATE_322
0.0000   0.0000  4.16487 4.16377          0 3-HYDROXYBUTYRATE_LACTATE_323
0.0000   0.0000  4.16857 4.16337          0 LACTATE_LACTULOSE_324
0.0000   0.0000  4.16407 4.15007          0 UNKNOWN_325
0.0000   0.0000  4.15897 4.14897          0 UNKNOWN_326
0.0000   0.0000  4.15327 4.14807          0 LACTATE_327
0.0000   0.0000  4.14317 4.13837          0 LACTATE_328
0.0000   0.0000  4.13767 4.13307          0 LACTATE_FRUCTOSE_329
0.0000   0.0000  4.13327 4.12847          0 LACTATE_330
0.0000   0.0000  4.12367 4.11847          0 LACTATE_331
0.0000   0.0000  4.11557 4.11357          0 N-METHYLHYDANTOIN_LACTATE_GLUCARATE_332
0.0000   0.0000  4.10917 4.10077          0 UNKNOWN_333
0.0000   0.0000  4.10537 4.09297          0 UNKNOWN_334
0.0000   0.0000  4.10197 4.09157          0 UNKNOWN_335
0.0000   0.0000  4.09427 4.09397          0 CHOLINE_MYO-INOSITOL_LACTATE_336
0.0000   0.0000  4.09847 4.08847          0 UNKNOWN_337
0.0000   0.0000  4.09297 4.09187          0 MYO-INOSITOL_CHOLINE_338
0.0000   0.0000  4.09187 4.08347          0 MYO-INOSITOL_CHOLINE_339
0.0000   0.0000  4.08577 4.08247          0 MYO-INOSITOL_GLUCOSE-6-PHOSPHATE_340
0.0000   0.0000  4.08277 4.07397          0 CREATININE_341
0.0000   0.0000  4.07697 4.07137          0 ISOCITRATE_CREATININE_GLUCOSE-6-PHOSPHATE_342
0.0000   0.0000  4.06237 4.05197          0 GLUCOSE-6-PHOSPHATE_343
0.0000   0.0000  4.05467 4.04347          0 ASCORBATE_2-HYDROXYGLUTARATE_344
0.0000   0.0000  4.05207 4.04047          0 ASCORBATE_345
0.0000   0.0000  4.04867 4.03827          0 2-HYDROXYGLUTARATE_346
0.0000   0.0000  4.04397 4.03877          0 UNKNOWN_347
0.0000   0.0000  4.04337 4.03337          0 ASCORBATE_2-HYDROXYGLUTARATE_348
0.0000   0.0000  4.03687 4.03207          0 FRUCTOSE_349
0.0000   0.0000  4.03547 4.02307          0 PHENYLALANINE_GLUCOSE-6-PHOSPHATE_350
0.0000   0.0000  4.03017 4.02177          0 HISTIDINE_GLUCOSE-6-PHOSPHATE_FRUCTOSE_351
0.0000   0.0000  4.03187 4.01627          0 HISTIDINE_GLUCOSE-6-PHOSPHATE_352
0.0000   0.0000  4.02047 4.01887          0 GLUCOSE-6-PHOSPHATE_353
0.0000   0.0000  4.02327 4.01327          0 HISTIDINE_PHENYLALANINE_GLUCOSE-6-PHOSPHATE_354
0.0000   0.0000  4.02157 4.00797          0 GLUCOSE-6-PHOSPHATE_HISTIDINE_355
0.0000   0.0000  4.01997 4.00357          0 HISTIDINE_356
0.0000   0.0000  4.01277 4.00037          0 GALACTITOL_GLUCOSE-6-PHOSPHATE_HISTIDINE_357
0.0000   0.0000  4.00697 3.99977          0 GALACTITOL_GLUCOSE-6-PHOSPHATE_358
0.0000   0.0000  4.00627 3.99827          0 GALACTITOL_GLUCOSE-6-PHOSPHATE_359
0.0000   0.0000  4.00117 3.99157          0 GALACTITOL_GLUCOSE-6-PHOSPHATE_360
0.0000   0.0000  3.99927 3.98967          0 GALACTITOL_GLUCOSE-6-PHOSPHATE_361
0.0000   0.0000  3.98747 3.98107          0 UNKNOWN_362
0.0000   0.0000  3.98017 3.97177          0 CREATINE_PHOSPHATE_363
0.0000   0.0000  3.97867 3.96547          0 CREATINE_PHOSPHATE_MANNOSE_GALACTOSE_364
0.0000   0.0000  3.97187 3.96387          0 TYROSINE_MANNOSE_GALACTOSE_365
0.0000   0.0000  3.96937 3.96417          0 MANNOSE_LACTULOSE_GALACTOSE_366
0.0000   0.0000  3.96957 3.95997          0 MANNOSE_LACTULOSE_367
0.0000   0.0000  3.96607 3.95567          0 MANNOSE_LACTULOSE_GLUCOSE-6-PHOSPHATE_368
0.0000   0.0000  3.96417 3.95297          0 MANNOSE_CREATINE_LACTULOSE_369
0.0000   0.0000  3.95407 3.94847          0 UNKNOWN_370
0.0000   0.0000  3.94967 3.93847          0 GLUCOSE_GLUCOSE-6-PHOSPHATE_371
0.0000   0.0000  3.93807 3.93247          0 GLUCOSE_372
0.0000   0.0000  3.93487 3.92927          0 GLUCOSE_373
0.0000   0.0000  3.92917 3.92357          0 GLUCOSE_MANNOSE_374
0.0000   0.0000  3.92937 3.91617          0 GLUCOSE_MANNOSE_375
0.0000   0.0000  3.92047 3.91487          0 GLUCOSE_376
0.0000   0.0000  3.91787 3.91107          0 GLUCOSE_377
0.0000   0.0000  3.90699 3.90307          0 MANNITOL_378*
0.0000   0.0000  3.90215 3.89915          0 MANNITOL_379*
0.0000   0.0000  3.89687 3.88807          0 MANNOSE_MANNITOL_380
0.0000   0.0000  3.89037 3.88517          0 MANNITOL_381
0.0000   0.0000  3.88647 3.88087          0 MANNITOL_382
0.0000   0.0000  3.88397 3.87717          0 UNKNOWN_383
0.0000   0.0000  3.88067 3.87387          0 UNKNOWN_384
0.0000   0.0000  3.87787 3.86787          0 GLUCOSE_GLUCITOL_385
0.0000   0.0000  3.87437 3.86637          0 GLUCOSE_GLUCITOL_MANNOSE_386
0.0000   0.0000  3.87177 3.86337          0 GLUCOSE_GLUCITOL_387
0.0000   0.0000  3.86827 3.85987          0 GLUCOSE_388
0.0000   0.0000  3.86547 3.85827          0 GLUCOSE_389
0.0000   0.0000  3.86627 3.85467          0 GLUCOSE_390
0.0000   0.0000  3.86157 3.85037          0 GLUCOSE_391
0.0000   0.0000  3.85687 3.84727          0 GLUCOSE_392
0.0000   0.0000  3.85477 3.84277          0 GLUCOSE_393
0.0000   0.0000  3.85037 3.83917          0 GLUCOSE_394
0.0000   0.0000  3.84617 3.83577          0 MANNITOL_GLUCOSE_395
0.0000   0.0000  3.84267 3.83587          0 MANNITOL_GLUCOSE_396
0.0000   0.0000  3.83157 3.82317          0 MANNITOL_397
0.0000   0.0000  3.82487 3.81607          0 GUANIDOACETATE_398
0.0000   0.0000  3.82027 3.81507          0 ALANINE_399
0.0000   0.0000  3.81917 3.80917          0 FRUCTOSE_GLYCEROL_GLUCOSE_ALANINE_400
0.0000   0.0000  3.81127 3.80007          0 GLUCOSE_GLUTAMINE_401
0.0000   0.0000  3.80407 3.79567          0 GLUCOSE_MANNITOL_GLUTAMINE_402
0.0000   0.0000  3.80337 3.79337          0 GLUCOSE_GLUTAMINE_403
0.0000   0.0000  3.79997 3.79117          0 GLUCOSE_MANNITOL_404
0.0000   0.0000  3.79647 3.78527          0 GLUCOSE_MANNITOL_GLUTAMINE_405
```

```
0.0000   0.0000  3.79647 3.78527          0 GLUCOSE_MANNITOL_GLUTAMINE_405
0.0000   0.0000  3.79257 3.78417          0 GLUCOSE_MANNITOL_406
0.0000   0.0000  3.78707 3.77987          0 GLUCOSE_MANNITOL_LYSINE_407
0.0000   0.0000  3.78587 3.77747          0 GLUCOSE_MANNITOL_LYSINE_408
0.0000   0.0000  3.78527 3.77407          0 GLUCOSE_MANNITOL_409
0.0000   0.0000  3.77847 3.76847          0 LYSINE_GLUCOSE_MANNITOL_410
0.0000   0.0000  3.77017 3.76497          0 GLUCOSE_411
0.0000   0.0000  3.76267 3.75587          0 GLUCOSE_412
0.0000   0.0000  3.76067 3.75507          0 GLUCOSE_413
0.0000   0.0000  3.75272 3.74906          0 GLUCOSE_KYNURENINE_414*
0.0000   0.0000  3.74690 3.74337          0 GLUCOSE_415*
0.0000   0.0000  3.74305 3.73978          0 GLUCOSE_KYNURENINE_416*
0.0000   0.0000  3.73397 3.72717          0 GLUCOSE_417
0.0000   0.0000  3.72837 3.72277          0 MANNITOL_418
0.0000   0.0000  3.72567 3.71767          0 MANNITOL_GALACTOSE_419
0.0000   0.0000  3.71927 3.71407          0 MANNITOL_420
0.0000   0.0000  3.71987 3.70507          0 MANNITOL_GALACTITOL_421
0.0000   0.0000  3.71147 3.70587          0 MANNITOL_422
0.0000   0.0000  3.70827 3.69987          0 MANNITOL_GALACTITOL_423
0.0000   0.0000  3.70337 3.69617          0 MANNITOL_424
0.0000   0.0000  3.69947 3.69147          0 UNKNOWN_425
0.0000   0.0000  3.69757 3.68957          0 GLYCEROL_426
0.0000   0.0000  3.69877 3.68557          0 UNKNOWN_427
0.0000   0.0000  3.69247 3.68207          0 GLUCITOL_GALACTOSE_MANNOSE_428
0.0000   0.0000  3.68787 3.67587          0 GLUCITOL_GALACTOSE_MANNOSE_429
0.0000   0.0000  3.67957 3.67397          0 GLYCEROL_430
0.0000   0.0000  3.67337 3.66777          0 GLYCEROL_431
0.0000   0.0000  3.67287 3.66327          0 GALACTOSE_GLYCEROL_432
0.0000   0.0000  3.67047 3.65527          0 FUCOSE_GALACTOSE_433
0.0000   0.0000  3.66127 3.64727          0 MYO-INOSITOL_FUCOSE_434
0.0000   0.0000  3.65557 3.64557          0 UNKNOWN_435
0.0000   0.0000  3.65217 3.64257          0 UNKNOWN_436
0.0000   0.0000  3.64457 3.63657          0 MYO-INOSITOL_VALINE_437
0.0000   0.0000  3.64029 3.63493          0 VALINE_438*
0.0000   0.0000  3.63977 3.63097          0 UNKNOWN_439
0.0000   0.0000  3.63375 3.62872          0 VALINE_440*
0.0000   0.0000  3.63057 3.62017          0 MYO-INOSITOL_441
0.0000   0.0000  3.62847 3.61807          0 O-PHOSPHOCHOLINE_GLUCOSE-6-PHOSPHATE_442
0.0000   0.0000  3.62237 3.61277          0 O-PHOSPHOCHOLINE_LACTULOSE_443
0.0000   0.0000  3.61987 3.61107          0 O-PHOSPHOCHOLINE_444
0.0000   0.0000  3.61477 3.60957          0 THREONINE_GLUCOSE-6-PHOSPHATE_445
0.0000   0.0000  3.61517 3.60517          0 GLUCOSE-6-PHOSPHATE_446
0.0000   0.0000  3.60747 3.60267          0 THREONINE_GLUCOSE-6-PHOSPHATE_447
0.0000   0.0000  3.61067 3.59427          0 UNKNOWN_448
0.0000   0.0000  3.59827 3.59307          0 GLYCEROL_GLUCOSE-6-PHOSPHATE_449
0.0000   0.0000  3.59022 3.58381          0 GLYCINE_450*
0.0000   0.0000  3.58157 3.57637          0 GLYCEROL_GLUCOSE_451
0.0000   0.0000  3.57677 3.57277          0 GLUCOSE_452
0.0000   0.0000  3.57167 3.56687          0 GLUCOSE_453
0.0000   0.0000  3.56267 3.55867          0 GLUCOSE_454
0.0000   0.0000  3.56047 3.55567          0 UNKNOWN_455
0.0000   0.0000  3.55727 3.55327          0 GLUCOSE_456
0.0000   0.0000  3.53617 3.53137          0 GLUCOSE_457
0.0000   0.0000  3.52357 3.51797          0 GLUCOSE_458
0.0000   0.0000  3.50957 3.50557          0 GLUCOSE_459
0.0000   0.0000  3.50617 3.49977          0 GLUCOSE_460
0.0000   0.0000  3.50247 3.49687          0 GLUCOSE_461
0.0000   0.0000  3.49727 3.49207          0 GLUCOSE_462
0.0000   0.0000  3.49497 3.48777          0 GLUCOSE_463
0.0000   0.0000  3.49167 3.48607          0 GLUCOSE_464
0.0000   0.0000  3.48827 3.48307          0 GLUCOSE_465
0.0000   0.0000  3.48317 3.47797          0 GLUCOSE_466
0.0000   0.0000  3.48057 3.47417          0 GLUCOSE_467
0.0000   0.0000  3.47177 3.46297          0 GLUCOSE_CARNITINE_468
0.0000   0.0000  3.47217 3.45897          0 GLUCOSE_CARNITINE_469
0.0000   0.0000  3.46087 3.45287          0 GLUCOSE_CARNITINE_470
0.0000   0.0000  3.45747 3.44947          0 GLUCOSE_CARNITINE_471
0.0000   0.0000  3.45037 3.44517          0 GLUCOSE_CARNITINE_TAURINE_472
0.0000   0.0000  3.44927 3.43807          0 GLUCOSE_CARNITINE_473
0.0000   0.0000  3.43857 3.43667          0 GLUCOSE_TAURINE_474
0.0000   0.0000  3.43737 3.43217          0 GLUCOSE_475
0.0000   0.0000  3.43587 3.43187          0 GLUCOSE_476
0.0000   0.0000  3.43170 3.42637          0 GLUCOSE_477*
0.0000   0.0000  3.42419 3.41827          0 GLUCOSE_478*
0.0000   0.0000  3.41607 3.40887          0 GLUCOSE_479
0.0000   0.0000  3.41077 3.40757          0 UNKNOWN_480
0.0000   0.0000  3.41007 3.40327          0 UNKNOWN_481
0.0000   0.0000  3.40737 3.40017          0 UNKNOWN_482
0.0000   0.0000  3.40417 3.39457          0 UNKNOWN_483
0.0000   0.0000  3.39537 3.38737          0 UNKNOWN_484
0.0000   0.0000  3.38957 3.38237          0 METHANOL_485
0.0000   0.0000  3.38637 3.37997          0 UNKNOWN_486
0.0000   0.0000  3.38397 3.37677          0 UNKNOWN_487
0.0000   0.0000  3.38177 3.37457          0 UNKNOWN_488
```

```
0.0000   0.0000  3.38177 3.37457          0 UNKNOWN_488
0.0000   0.0000  3.37967 3.37407          0 UNKNOWN_489
0.0000   0.0000  3.38137 3.36817          0 UNKNOWN_490
0.0000   0.0000  3.37337 3.36457          0 CAFFEINE_491
0.0000   0.0000  3.36917 3.36077          0 UNKNOWN_492
0.0000   0.0000  3.36197 3.35517          0 UNKNOWN_493
0.0000   0.0000  3.35337 3.34297          0 UNKNOWN_494
0.0000   0.0000  3.34767 3.33967          0 UNKNOWN_495
0.0000   0.0000  3.33947 3.33627          0 UNKNOWN_496
0.0000   0.0000  3.33147 3.32627          0 UNKNOWN_497
0.0000   0.0000  3.33027 3.32027          0 UNKNOWN_498
0.0000   0.0000  3.31967 3.31167          0 UNKNOWN_499
0.0000   0.0000  3.31677 3.30717          0 UNKNOWN_500
0.0000   0.0000  3.31107 3.30427          0 UNKNOWN_501
0.0000   0.0000  3.30477 3.29477          0 MYO-INOSITOL_502
0.0000   0.0000  3.29697 3.28737          0 BETAINE_TAURINE_503
0.0000   0.0000  3.28917 3.28437          0 TRIMETHYLAMINE N-OXIDE_GLUCOSE_504
0.0000   0.0000  3.28417 3.28167          0 GLUCOSE_TAURINE_505
0.0000   0.0000  3.28337 3.27497          0 AGMATINE_GLUCOSE_506
0.0000   0.0000  3.27797 3.27277          0 GLUCOSE_507
0.0000   0.0000  3.27657 3.27017          0 GLUCOSE_508
0.0000   0.0000  3.27497 3.26377          0 AGMATINE_GLUCOSE_509
0.0000   0.0000  3.26397 3.25997          0 GLUCOSE_510
0.0000   0.0000  3.25957 3.24757          0 UNKNOWN_511
0.0000   0.0000  3.25997 3.23237          0 O-PHOSPHOCHOLINE_CARNITINE_512
0.0000   0.0000  3.23937 3.21777          0 UNKNOWN_513
0.0000   0.0000  3.22502 3.21914          0 CHOLINE_514*
0.0000   0.0000  3.21896 3.21642          0 UNKNOWN_515*
0.0000   0.0000  3.21679 3.21244          0 O-ACETYLCARNITINE_516*
0.0000   0.0000  3.21297 3.20177          0 UNKNOWN_517
0.0000   0.0000  3.20327 3.19927          0 UNKNOWN_518
0.0000   0.0000  3.19987 3.19187          0 N-NITROSODIMETHYLAMINE_519
0.0000   0.0000  3.18787 3.17547          0 UNKNOWN_520
0.0000   0.0000  3.18127 3.17607          0 UNKNOWN_521
0.0000   0.0000  3.17857 3.17457          0 DIMETHYL SULFONE_522
0.0000   0.0000  3.18007 3.16687          0 HISTIDINE_523
0.0000   0.0000  3.17237 3.16677          0 UNKNOWN_524
0.0000   0.0000  3.17207 3.16327          0 UNKNOWN_525
0.0000   0.0000  3.16957 3.15477          0 HISTIDINE_526
0.0000   0.0000  3.16137 3.15337          0 UNKNOWN_527
0.0000   0.0000  3.15927 3.14287          0 HISTIDINE_528
0.0000   0.0000  3.14867 3.12787          0 3-PHENYLLACTATE_529
0.0000   0.0000  3.12787 3.10527          0 3-PHENYLLACTATE_530
0.0000   0.0000  3.14587 3.13427          0 HISTIDINE_531
0.0000   0.0000  3.13677 3.13277          0 PHENYLALANINE_532
0.0000   0.0000  3.13617 3.13137          0 PHENYLALANINE_533
0.0000   0.0000  3.13817 3.12177          0 UNKNOWN_534
0.0000   0.0000  3.12097 3.11257          0 UNKNOWN_535
0.0000   0.0000  3.11067 3.10227          0 UNKNOWN_536
0.0000   0.0000  3.09802 3.09260          0 ORNITHINE_537*
0.0000   0.0000  3.09278 3.08853          0 TYROSINE_538*
0.0000   0.0000  3.08740 3.08093          0 ORNITHINE_539*
0.0000   0.0000  3.08165 3.07740          0 TYROSINE_540*
0.0000   0.0000  3.07577 3.07125          0 ORNITHINE_541*
0.0000   0.0000  3.07080 3.06582          0 CREATININE_LYSINE_542*
0.0000   0.0000  3.06492 3.06148          0 CREATINE PHOSPHATE_543*
0.0000   0.0000  3.05958 3.05352          0 LYSINE_AGMATINE_544*
0.0000   0.0000  3.05377 3.05057          0 UNKNOWN_545
0.0000   0.0000  3.04900 3.04258          0 LYSINE_AGMATINE_546*
0.0000   0.0000  3.03897 3.03897          0 UNKNOWN_547
0.0000   0.0000  3.03917 3.03437          0 UNKNOWN_548
0.0000   0.0000  3.04517 3.02357          0 UNKNOWN_549
0.0000   0.0000  3.03217 3.02857          0 UNKNOWN_550
0.0000   0.0000  3.03327 3.02087          0 UNKNOWN_551
0.0000   0.0000  3.02597 3.02117          0 UNKNOWN_552
0.0000   0.0000  3.02187 3.01227          0 UNKNOWN_553
0.0000   0.0000  2.99767 2.99727          0 UNKNOWN_554
0.0000   0.0000  2.99307 2.97907          0 UNKNOWN_555
0.0000   0.0000  2.98697 2.97297          0 UNKNOWN_556
0.0000   0.0000  2.96817 2.96417          0 UNKNOWN_557
0.0000   0.0000  2.96897 2.95497          0 UNKNOWN_558
0.0000   0.0000  2.96007 2.95207          0 UNKNOWN_559
0.0000   0.0000  2.95467 2.95107          0 UNKNOWN_560
0.0000   0.0000  2.95507 2.94507          0 N-METHYLHYDANTOIN_561
0.0000   0.0000  2.94787 2.94387          0 UNKNOWN_562
0.0000   0.0000  2.94617 2.94257          0 UNKNOWN_563
0.0000   0.0000  2.94377 2.94177          0 UNKNOWN_564
0.0000   0.0000  2.94047 2.93887          0 UNKNOWN_565
0.0000   0.0000  2.93997 2.93477          0 UNKNOWN_566
0.0000   0.0000  2.93117 2.92717          0 UNKNOWN_567
0.0000   0.0000  2.92857 2.92297          0 UNKNOWN_568
0.0000   0.0000  2.92227 2.91867          0 UNKNOWN_569
0.0000   0.0000  2.92197 2.91357          0 UNKNOWN_570
0.0000   0.0000  2.91797 2.90957          0 UNKNOWN_571
```

```
0.0000   0.0000  2.91797 2.90957          0 UNKNOWN_571
0.0000   0.0000  2.91357 2.90997          0 UNKNOWN_572
0.0000   0.0000  2.91057 2.90927          0 3-PHENYLLACTATE_573
0.0000   0.0000  2.91237 2.89837          0 UNKNOWN_574
0.0000   0.0000  2.89937 2.89677          0 3-PHENYLLACTATE_575
0.0000   0.0000  2.90217 2.88857          0 UNKNOWN_576
0.0000   0.0000  2.89267 2.88387          0 3-PHENYLLACTATE_577
0.0000   0.0000  2.88827 2.88507          0 UNKNOWN_578
0.0000   0.0000  2.89007 2.88167          0 UNKNOWN_579
0.0000   0.0000  2.88117 2.87317          0 3-PHENYLLACTATE_580
0.0000   0.0000  2.87627 2.87227          0 UNKNOWN_581
0.0000   0.0000  2.87237 2.86877          0 UNKNOWN_582
0.0000   0.0000  2.87167 2.86647          0 UNKNOWN_583
0.0000   0.0000  2.87027 2.86467          0 UNKNOWN_584
0.0000   0.0000  2.86717 2.86157          0 UNKNOWN_585
0.0000   0.0000  2.86347 2.86027          0 UNKNOWN_586
0.0000   0.0000  2.86387 2.85507          0 UNKNOWN_587
0.0000   0.0000  2.85627 2.84987          0 METHYLGUANIDINE_588
0.0000   0.0000  2.84927 2.84247          0 UNKNOWN_589
0.0000   0.0000  2.84597 2.83917          0 UNKNOWN_590
0.0000   0.0000  2.84897 2.83897          0 UNKNOWN_591
0.0000   0.0000  2.84407 2.83447          0 UNKNOWN_592
0.0000   0.0000  2.84007 2.83487          0 UNKNOWN_593
0.0000   0.0000  2.83747 2.83107          0 UNKNOWN_594
0.0000   0.0000  2.83387 2.82867          0 5-AMINOLEVULINATE_595
0.0000   0.0000  2.82527 2.81847          0 5-AMINOLEVULINATE_BIOTIN_596
0.0000   0.0000  2.82347 2.81707          0 5-AMINOLEVULINATE_BIOTIN_597
0.0000   0.0000  2.81577 2.81297          0 UNKNOWN_598
0.0000   0.0000  2.81397 2.81037          0 5-AMINOLEVULINATE_599
0.0000   0.0000  2.80737 2.80457          0 UNKNOWN_600
0.0000   0.0000  2.80647 2.80167          0 UNKNOWN_601
0.0000   0.0000  2.80497 2.79937          0 UNKNOWN_602
0.0000   0.0000  2.79547 2.78907          0 UNKNOWN_603
0.0000   0.0000  2.78897 2.78217          0 UNKNOWN_604
0.0000   0.0000  2.78577 2.78057          0 UNKNOWN_605
0.0000   0.0000  2.78067 2.77867          0 UNKNOWN_606
0.0000   0.0000  2.77787 2.77147          0 UNKNOWN_607
0.0000   0.0000  2.77357 2.76317          0 UNKNOWN_608
0.0000   0.0000  2.76767 2.76127          0 UNKNOWN_609
0.0000   0.0000  2.76387 2.76067          0 UNKNOWN_610
0.0000   0.0000  2.76287 2.75927          0 UNKNOWN_611
0.0000   0.0000  2.76197 2.75797          0 UNKNOWN_612
0.0000   0.0000  2.75817 2.75777          0 UNKNOWN_613
0.0000   0.0000  2.75637 2.75277          0 UNKNOWN_614
0.0000   0.0000  2.75407 2.75087          0 UNKNOWN_615
0.0000   0.0000  2.74897 2.74897          0 UNKNOWN_616
0.0000   0.0000  2.75217 2.74737          0 UNKNOWN_617
0.0000   0.0000  2.75057 2.74257          0 DIMETHYLAMINE_618
0.0000   0.0000  2.74517 2.74157          0 UNKNOWN_619
0.0000   0.0000  2.74487 2.73767          0 UNKNOWN_620
0.0000   0.0000  2.74267 2.73747          0 UNKNOWN_621
0.0000   0.0000  2.74247 2.73287          0 DIMETHYLAMINE_622
0.0000   0.0000  2.73467 2.72747          0 UNKNOWN_623
0.0000   0.0000  2.73257 2.72457          0 UNKNOWN_624
0.0000   0.0000  2.72867 2.72307          0 UNKNOWN_625
0.0000   0.0000  2.71897 2.71897          0 UNKNOWN_626
0.0000   0.0000  2.72337 2.71697          0 UNKNOWN_627
0.0000   0.0000  2.70997 2.70317          0 UNKNOWN_628
0.0000   0.0000  2.70277 2.69997          0 UNKNOWN_629
0.0000   0.0000  2.69987 2.69667          0 UNKNOWN_630
0.0000   0.0000  2.69827 2.69547          0 UNKNOWN_631
0.0000   0.0000  2.68767 2.68127          0 UNKNOWN_632
0.0000   0.0000  2.68077 2.67717          0 UNKNOWN_633
0.0000   0.0000  2.67607 2.67047          0 UNKNOWN_634
0.0000   0.0000  2.67677 2.66557          0 UNKNOWN_635
0.0000   0.0000  2.66967 2.66647          0 UNKNOWN_636
0.0000   0.0000  2.66657 2.66257          0 UNKNOWN_637
0.0000   0.0000  2.66337 2.65697          0 METHIONINE_638
0.0000   0.0000  2.65297 2.64997          0 METHIONINE_639
0.0000   0.0000  2.65897 2.64897          0 UNKNOWN_640
0.0000   0.0000  2.63567 2.63087          0 UNKNOWN_641
0.0000   0.0000  2.60887 2.60567          0 UNKNOWN_642
0.0000   0.0000  2.57897 2.57897          0 UNKNOWN_643
0.0000   0.0000  2.57827 2.57187          0 UNKNOWN_644
0.0000   0.0000  2.57167 2.56607          0 UNKNOWN_645
0.0000   0.0000  2.56697 2.56297          0 UNKNOWN_646
0.0000   0.0000  2.54927 2.54407          0 UNKNOWN_647
0.0000   0.0000  2.54487 2.54087          0 UNKNOWN_648
0.0000   0.0000  2.54107 2.53267          0 5-AMINOLEVULINATE_649
0.0000   0.0000  2.53857 2.53017          0 3-PHENYLPROPIONATE_5-AMINOLEVULINATE_650
0.0000   0.0000  2.53307 2.52907          0 3-PHENYLPROPIONATE_5-AMINOLEVULINATE_651
0.0000   0.0000  2.53287 2.52807          0 3-PHENYLPROPIONATE_5-AMINOLEVULINATE_652
0.0000   0.0000  2.52807 2.52487          0 3-PHENYLPROPIONATE_5-AMINOLEVULINATE_653
0.0000   0.0000  2.52767 2.52367          0 3-PHENYLPROPIONATE_5-AMINOLEVULINATE_654
```

```
0.0000  0.0000  2.52767 2.52367          0 3-PHENYLPROPIONATE_5-AMINOLEVULINATE_654
0.0000  0.0000  2.52467 2.52067          0 GLUTAMINE_5-AMINOLEVULINATE_655
0.0000  0.0000  2.52317 2.51997          0 GLUTAMINE_3-PHENYLPROPIONATE_5-AMINOLEVULINATE_656
0.0000  0.0000  2.52327 2.51607          0 GLUTAMINE_3-PHENYLPROPIONATE_5-AMINOLEVULINATE_657
0.0000  0.0000  2.51247 2.50567          0 GLUTAMINE_3-PHENYLPROPIONATE_658
0.0000  0.0000  2.51057 2.50337          0 GLUTAMINE_659
0.0000  0.0000  2.50087 2.49407          0 GLUTAMINE_660
0.0000  0.0000  2.49107 2.48427          0 GLUTAMINE_661
0.0000  0.0000  2.49137 2.47977          0 GLUTAMINE_662
0.0000  0.0000  2.47897 2.47417          0 GLUTAMINE_663
0.0000  0.0000  2.47927 2.47047          0 GLUTAMINE_664
0.0000  0.0000  2.47627 2.47067          0 GLUTAMINE_665
0.0000  0.0000  2.46687 2.46047          0 GLUTAMINE_CARNITINE_666
0.0000  0.0000  2.45727 2.45607          0 UNKNOWN_667
0.0000  0.0000  2.45537 2.45257          0 GLUTAMINE_CARNITINE_668
0.0000  0.0000  2.45527 2.44887          0 GLUTAMINE_669
0.0000  0.0000  2.44637 2.44117          0 UNKNOWN_670
0.0000  0.0000  2.44507 2.43827          0 GLUTAMINE_3-HYDROXY-3-METHYLGLUTARATE_671
0.0000  0.0000  2.44137 2.43297          0 3-HYDROXYBUTYRATE_672
0.0000  0.0000  2.43047 2.42847          0 MALATE_SUCCINATE_3-HYDROXYBUTYRATE_673
0.0000  0.0000  2.42887 2.42367          0 MALATE_SUCCINATE_674
0.0000  0.0000  2.42277 2.41797          0 MALATE_3-HYDROXY-3-METHYLGLUTARATE_675
0.0000  0.0000  2.41977 2.41777          0 MALATE_3-HYDROXY-3-METHYLGLUTARATE_676
0.0000  0.0000  2.42017 2.41297          0 MALATE_3-HYDROXYGLUTARATE_677
0.0000  0.0000  2.41227 2.40707          0 UNKNOWN_678
0.0000  0.0000  2.40957 2.40117          0 MALATE_PYRUVATE_679
0.0000  0.0000  2.39697 2.39297          0 PYRUVATE_680
0.0000  0.0000  2.39377 2.38177          0 3-HYDROXYGLUTARATE_681
0.0000  0.0000  2.38687 2.38287          0 UNKNOWN_682
0.0000  0.0000  2.38747 2.37507          0 UNKNOWN_683
0.0000  0.0000  2.38367 2.37207          0 UNKNOWN_684
0.0000  0.0000  2.38067 2.37227          0 UNKNOWN_685
0.0000  0.0000  2.37407 2.36687          0 UNKNOWN_686
0.0000  0.0000  2.37187 2.36147          0 UNKNOWN_687
0.0000  0.0000  2.36257 2.35937          0 UNKNOWN_688
0.0000  0.0000  2.36387 2.35427          0 UNKNOWN_689
0.0000  0.0000  2.35847 2.35327          0 UNKNOWN_690
0.0000  0.0000  2.35267 2.34427          0 ACETYLSALICYLATE_3-HYDROXYGLUTARATE_691
0.0000  0.0000  2.35017 2.34217          0 UNKNOWN_692
0.0000  0.0000  2.34427 2.33947          0 UNKNOWN_693
0.0000  0.0000  2.34317 2.33517          0 3-HYDROXYGLUTARATE_694
0.0000  0.0000  2.33957 2.33397          0 UNKNOWN_695
0.0000  0.0000  2.33377 2.33257          0 UNKNOWN_696
0.0000  0.0000  2.33187 2.33147          0 UNKNOWN_697
0.0000  0.0000  2.33257 2.32297          0 3-HYDROXYGLUTARATE_698
0.0000  0.0000  2.32697 2.32137          0 UNKNOWN_699
0.0000  0.0000  2.32377 2.31737          0 UNKNOWN_700
0.0000  0.0000  2.32147 2.31307          0 VALINE_3-HYDROXYGLUTARATE_701
0.0000  0.0000  2.31827 2.30307          0 VALINE_2-HYDROXYGLUTARATE_702
0.0000  0.0000  2.31267 2.30147          0 VALINE_ACETOACETATE_703
0.0000  0.0000  2.30927 2.29927          0 ACETOACETATE_704
0.0000  0.0000  2.30757 2.29397          0 VALINE_705
0.0000  0.0000  2.30147 2.29267          0 VALINE_706
0.0000  0.0000  2.29557 2.28557          0 VALINE_707
0.0000  0.0000  2.29287 2.28127          0 VALINE_708
0.0000  0.0000  2.28547 2.27587          0 VALINE_709
0.0000  0.0000  2.28257 2.27137          0 VALINE_p-CRESOL_710
0.0000  0.0000  2.27857 2.26297          0 VALINE_2-HYDROXYGLUTARATE_711
0.0000  0.0000  2.27007 2.26447          0 UNKNOWN_712
0.0000  0.0000  2.26907 2.26187          0 2-HYDROXYGLUTARATE_713
0.0000  0.0000  2.25627 2.25307          0 ACETONE_714
0.0000  0.0000  2.23957 2.23077          0 BIOTIN_METHIONINE_715
0.0000  0.0000  2.22817 2.22017          0 BIOTIN_METHIONINE_716
0.0000  0.0000  2.21817 2.21017          0 BIOTIN_METHIONINE_717
0.0000  0.0000  2.20797 2.20397          0 N-ISOVALEROYLGLYCINE_METHIONINE_718
0.0000  0.0000  2.20527 2.19567          0 GLUTAMINE_719
0.0000  0.0000  2.19637 2.18757          0 UNKNOWN_720
0.0000  0.0000  2.19397 2.18237          0 UNKNOWN_721
0.0000  0.0000  2.19317 2.17797          0 UNKNOWN_722
0.0000  0.0000  2.18547 2.18027          0 GLUTAMINE_723
0.0000  0.0000  2.18397 2.17557          0 GLUTAMINE_724
0.0000  0.0000  2.17697 2.16297          0 GLUTAMINE_725
0.0000  0.0000  2.17177 2.16217          0 GLUTAMINE_726
0.0000  0.0000  2.16807 2.16167          0 GLUTAMINE_727
0.0000  0.0000  2.16487 2.15767          0 GLUTAMINE_728
0.0000  0.0000  2.16427 2.15107          0 GLUTAMINE_729
0.0000  0.0000  2.15897 2.15017          0 GLUTAMINE_730
0.0000  0.0000  2.15337 2.14497          0 GLUTAMINE_731
0.0000  0.0000  2.15147 2.14347          0 GLUTAMINE_732
0.0000  0.0000  2.14927 2.14047          0 GLUTAMINE_733
0.0000  0.0000  2.14217 2.13177          0 GLUTAMINE_734
0.0000  0.0000  2.14047 2.13007          0 GLUTAMINE_735
0.0000  0.0000  2.13857 2.12657          0 GLUTAMINE_736
0.0000  0.0000  2.13127 2.12287          0 UNKNOWN_737
```

```
0.0000   0.0000  2.13127 2.12287          0 UNKNOWN_737
0.0000   0.0000  2.13227 2.11547          0 GLUTAMINE_738
0.0000   0.0000  2.12817 2.11137          0 GLUTAMINE_739
0.0000   0.0000  2.12247 2.10687          0 UNKNOWN_740
0.0000   0.0000  2.11217 2.10577          0 N-ACETYLCYSTEINE_UDP-N-ACETYLGLUCOSAMINE_741
0.0000   0.0000  2.10397 2.09437          0 UNKNOWN_742
0.0000   0.0000  2.09847 2.08367          0 UNKNOWN_743
0.0000   0.0000  2.09377 2.06657          0 UNKNOWN_744
0.0000   0.0000  2.07607 2.06287          0 UNKNOWN_745
0.0000   0.0000  2.08327 2.04407          0 UNKNOWN_746
0.0000   0.0000  2.07057 2.03137          0 UNKNOWN_747
0.0000   0.0000  2.04537 2.02897          0 UNKNOWN_748
0.0000   0.0000  2.03827 2.02147          0 UNKNOWN_749
0.0000   0.0000  2.02727 2.02687          0 UNKNOWN_750
0.0000   0.0000  2.02967 2.00967          0 UNKNOWN_751
0.0000   0.0000  2.01437 2.00437          0 UNKNOWN_752
0.0000   0.0000  2.00337 1.99857          0 UNKNOWN_753
0.0000   0.0000  1.99657 1.99177          0 UNKNOWN_754
0.0000   0.0000  1.99877 1.98197          0 UNKNOWN_755
0.0000   0.0000  1.98747 1.98427          0 UNKNOWN_756
0.0000   0.0000  1.98977 1.97417          0 UNKNOWN_757
0.0000   0.0000  1.97557 1.96877          0 UNKNOWN_758
0.0000   0.0000  1.97297 1.96257          0 UNKNOWN_759
0.0000   0.0000  1.96577 1.93817          0 UNKNOWN_760
0.0000   0.0000  1.94997 1.93677          0 LYSINE_ACETATE_761
0.0000   0.0000  1.94297 1.93817          0 LYSINE_ACETATE_762
0.0000   0.0000  1.93967 1.93287          0 LYSINE_763
0.0000   0.0000  1.93467 1.92147          0 UNKNOWN_764
0.0000   0.0000  1.93167 1.91967          0 LYSINE_765
0.0000   0.0000  1.92457 1.91457          0 LYSINE_766
0.0000   0.0000  1.91367 1.90527          0 LYSINE_767
0.0000   0.0000  1.90787 1.90227          0 UNKNOWN_768
0.0000   0.0000  1.90727 1.89527          0 LYSINE_769
0.0000   0.0000  1.89947 1.89147          0 UNKNOWN_770
0.0000   0.0000  1.89197 1.88797          0 LYSINE_771
0.0000   0.0000  1.87797 1.87477          0 UNKNOWN_772
0.0000   0.0000  1.87237 1.86597          0 UNKNOWN_773
0.0000   0.0000  1.85887 1.84567          0 UNKNOWN_774
0.0000   0.0000  1.84287 1.84247          0 UNKNOWN_775
0.0000   0.0000  1.82927 1.82287          0 UNKNOWN_776
0.0000   0.0000  1.82757 1.81797          0 UNKNOWN_777
0.0000   0.0000  1.81957 1.81397          0 UNKNOWN_778
0.0000   0.0000  1.81017 1.80617          0 UNKNOWN_779
0.0000   0.0000  1.79797 1.79397          0 UNKNOWN_780
0.0000   0.0000  1.78557 1.77317          0 UNKNOWN_781
0.0000   0.0000  1.78187 1.77227          0 UNKNOWN_782
0.0000   0.0000  1.77757 1.76597          0 UNKNOWN_783
0.0000   0.0000  1.77197 1.76157          0 UNKNOWN_784
0.0000   0.0000  1.77407 1.75087          0 LYSINE_785
0.0000   0.0000  1.76147 1.74587          0 LYSINE_786
0.0000   0.0000  1.75147 1.73427          0 LYSINE_787
0.0000   0.0000  1.75007 1.73167          0 LYSINE_788
0.0000   0.0000  1.73477 1.72797          0 LYSINE_789
0.0000   0.0000  1.72687 1.71007          0 UNKNOWN_790
0.0000   0.0000  1.71707 1.69507          0 AGMATINE_791
0.0000   0.0000  1.70877 1.69157          0 UNKNOWN_792
0.0000   0.0000  1.69877 1.67877          0 UNKNOWN_793
0.0000   0.0000  1.68407 1.67887          0 UNKNOWN_794
0.0000   0.0000  1.68307 1.67147          0 UNKNOWN_795
0.0000   0.0000  1.67907 1.66427          0 UNKNOWN_796
0.0000   0.0000  1.66637 1.65837          0 UNKNOWN_797
0.0000   0.0000  1.65287 1.64727          0 UNKNOWN_798
0.0000   0.0000  1.63887 1.63407          0 BIOTIN_799
0.0000   0.0000  1.62497 1.61697          0 BIOTIN_800
0.0000   0.0000  1.59567 1.59047          0 UNKNOWN_801
0.0000   0.0000  1.57347 1.56667          0 LYSINE_802
0.0000   0.0000  1.56407 1.55927          0 UNKNOWN_803
0.0000   0.0000  1.56197 1.55517          0 LYSINE_804
0.0000   0.0000  1.54897 1.54897          0 UNKNOWN_805
0.0000   0.0000  1.55857 1.54297          0 LYSINE_806
0.0000   0.0000  1.54497 1.53337          0 LYSINE_807
0.0000   0.0000  1.54117 1.52957          0 LYSINE_808
0.0000   0.0000  1.52737 1.52097          0 LYSINE_809
0.0000   0.0000  1.52547 1.51587          0 LYSINE_ALANINE_810
0.0000   0.0000  1.51405 1.50600          0 ALANINE_811*
0.0000   0.0000  1.50347 1.49424          0 ALANINE_812*
0.0000   0.0000  1.49037 1.48197          0 LYSINE_813
0.0000   0.0000  1.48467 1.47587          0 LYSINE_814
0.0000   0.0000  1.47357 1.46797          0 LYSINE_815
0.0000   0.0000  1.46387 1.46107          0 LYSINE_816
0.0000   0.0000  1.45897 1.45897          0 UNKNOWN_817
0.0000   0.0000  1.45587 1.44747          0 UNKNOWN_818
0.0000   0.0000  1.45047 1.44167          0 2-PHENYLPROPIONATE_819
0.0000   0.0000  1.44697 1.43897          0 LYSINE_BIOTIN_2-PHENYLPROPIONATE_820
```